Tuber development in potato (*Solanum tuberosum* L.): molecular cloning, sequence analyses and expression patterns of some crucial genes

A

Thesis submitted

In the partial fulfilment of the requirements for the award of degree of

DOCTOR OF PHILOSOPHY

IN

BIOTECHNOLOGY

Submitted By

Gurpreet Kaur

(Reg. No. 901400003)

Under the supervision of

Dr. N. Das

Professor

Department of Biotechnology

Thapar Institute of Engineering & Technology

Patiala-147004, Punjab, INDIA

July 2022

DEDICATED TO …

MY HUSBAND,

(Mr. Hardeep Singh Saini "NAHAR")

CERTIFICATE

Certified that the thesis entitled **"Tuber development in potato (*Solanum tuberosum* L.): molecular cloning, sequence analyses and expression patterns of some crucial genes"** submitted by Mrs. Gurpreet Kaur, Reg. No. 901400003 in the partial fulfilment of the requirements for the award of the degree of Doctor of Philosophy in the Department of Biotechnology, Thapar Institute of Engineering & Technology, Patiala, Punjab is a record of candidate's own independent and original research work carried out by herself under my supervision and guidance. The materials embodied in this thesis have not been submitted in part or full to any other University or Institute for the award of any degree.

Prof. N. Das
(Supervisor)
Department of Biotechnology
TIET, Patiala, Punjab

Place: TIET, Patiala

Date: 21 July 2022

CANDIDATE'S DECLARATION

I, hereby declare that the work presented in the thesis entitled **"Tuber development in potato (*Solanum tuberosum* L.): molecular cloning, sequence analyses and expression patterns of some crucial genes"** in the partial fulfilment of the requirements for the award of the degree of Doctor of Philosophy at Department of Biotechnology, Thapar Institute of Engineering & Technology, Patiala is an authentic record of my work during the period from July 2014 to July 2022, under the supervision of Prof. N. Das, Professor, Department of Biotechnology, Thapar Institute of Engineering & Technology, Patiala, Punjab. This report has not been submitted for the award of any degree or certificate in this or any other university.

Gurpreet Kaur

Gurpreet Kaur

(Reg. No. 901400003)

Place: Patiala, Punjab

Date: 21st July. 2022

Acknowledgment

It is my pleasure and privilege to acknowledge my supervisor ***Dr. Niranjan Das****, Professor, Department of Biotechnology, Thapar Institute of Engineering& Technology (T.I.ET), Patiala for providing me an opportunity to work under his guidance and supervision, assisting with all kinds of support and inspiration, wide counsel, constant encouragement, prudent advice, valuable suggestions and comments and expertise throughout this preparation of the thesis. I extend my heartfelt thanks to him forever. It's a great privilege to experience sustained enthusiasm and involved interest, constructive criticism, and meticulous supervision from his side throughout my work.*

I would like to express my sincere thanks to my Doctoral Committee members, Dr. M.S. Reddy (Head & Chairperson, Doctoral Committee of the Department), Dr. Anil Kumar Dutta, Dr. Vikas Handa and Dr. B.N. Chudamsama (Ph.D. committee members) for their constant motivation, insightful comments, and ideas. I express my gratitude to Dr. Rafat Siddique, Dean (Research and Sponsored Projects), T.I.ET, Patiala, for his encouragement and support during my research work at the Institute. I wish to express my thanks to our respected Director, ***Prof. Prakash Gopalan****, T.I.ET, Patiala, for providing infrastructure facilities and help during my research work.*

My sincere thanks are to all the faculty members of DBT, T.I.ET Patiala, for their constant motivation, invaluable suggestions, and support during my research work. I would like to acknowledge the Department of Biotechnology (DBT), TIFAC-CORE, and Science & Technology Entrepreneur's Park (STEP) at T.I.ET, Patiala, for providing infrastructural support, assistance, and co-operation.

I would like to acknowledge my colleagues ***Rajneesh****,* ***Yadveer, Vagish, Sahil, Shweta Lawania, Divya Mittal, Parul, Purnima, Anuja, Arkodeep and Lakhwinder Singh*** *for their co-operation and help. I pay my sincere thanks to the non-teaching staff members of the department,* ***Mr. Ram Newal Yadav, Phool Chand****, for their technical assistance and help. I am also thankful to* ***Surinder, Lallan Yadav, Iqbal, Phoolchand, and Mohinder*** *for their help and co-operation. I owe a word of thanks to all research scholars at the Department of Biotechnology for providing constant support, encouragement, and an excellent working atmosphere that has given me the necessary time to relax from my work.*

I feel a deep sense of gratitude for my parents ***(God on Earth)****, (Charanjeet Singh and Satwinder Kaur, Gifted by biology, Shalinder Kaur and Gurbax Kaur by the soul and Baljeet Kaur by the law) and Dr. Surinder Kumar (uncle;* ***Gift of heaven****). They formed a part of my vision and taught me the good things that matter in life. Along with them, I would like to mention the name of my siblings* ***Amanpreet Singh (biological) , Dr. Rakhi Chawla****,* ***Happy and Navi (soul gift)*** *who encouraged me to complete the work. My special thanks to my Next family my friends* ***Shivani, Anjali, Poonam****, my dearest, and the nearest ones for their moral support during the course of my thesis work and life. I express my gratitude to my wonderful life partner*

Mr. Hardeep Singh Saini *for the development of courage and complimenting me in every aspect to go ahead throughout this journey. My very special acknowledgment goes to my only Daughter* ***Navraj Kaur Saini*** *whose fortunate steps in my life have turned my life through. Above all, I'm grateful to Almighty God and MY* ***Babag (Mahant BALWANT SINGH JI)*** *for his divine grace that enabled me to pursue my thesis work successfully.*

(Gurpreet Kaur)

Table of Contents

List of Figures

List of Tables

List of Abbreviations

µL: micro litre

3-D : Three-dimensional

ADP: Adenine dinucleotide phosphate

AI : Aliphatic index

Amp: Ampicillin

ANOVA: Analysis of variance

BLAST: Basic Local Alignment Search Tool

bp: Base pair

BSA: Bovine serum albumin

Ca^{2+} : Calcium

CaM-LD : calmodulin-like domain

CaMLs : Calmodulin-like proteins

CaMs,: Calmodulins

CAT: Catalase

CBLs : Calcineurin B-like proteins

cDNA : Complementary Deoxyribonucleic acid

CDPKs : Ca^{2+}-dependent protein kinases

CPRI : Central Potato Research Institute

DEPC: Diethyl pyrocarbonate

DNA: Deoxyribonucleic acid

dNTP: 2'-deoxynucleoside-5'-triphosphate

DOPE : Discrete Optimized Protein Energy

DTT: Dithiothreitol

EBI : European Bioinformatics Institute

EDTA : Ethylenediamine-tetra acetic acid

ExPASy : Expert Protein Analysis System

FLN: Fructokinase- like

FRK : Fructokinase

Fru: Fructose

FW: Fresh weight

GA_3: Gibberillic acid

gm: Gram

h : Hour

H_2O_2: Hydrogen peroxide

HXK : Hexokinase

I-TASSER : Iterative Threading Assembly Refinement

KC-I : Kufri Chipsona-1

L: Litre

m : Metre

MEGA : Molecular Evolutionary Genetic Analysis

mg/L: Milligram per litre

min: Minute

mL: Millilitre

mM: Milli molar

MS: Murashige and Skoog medium

MSA : Multiple sequence alignments

MW : Molecular weight

NaCl : Sodium chloride

NCBI: National Center for Biotechnology Information

ORF: Open reading frame

PGRs: Plant growth regulators

pH: Potential of Hydrogen

Pi : Isoelectric point

RH: Relative humidity

RNA : Ribonucleic Acid

ROS: Reactive oxygen species

RT-PCR: Reverse transcription polymerase chain reaction

SAVES : Structural Analysis and Verification Server

SD: Standard deviation

Sec: Second

SFP: Spectral flux photon

SIB : Swiss Institute of Bioinformatics

SPSS: Statistical product and services

SUS/ SuSy : Sucrose synthase

TRXz : Thioredoxins

v/v: Volume per volume

w/w: Weight/weight

Abstract

Potato (*Solanum tuberosum* L.) is a major non-grain food crop grown all over the world and belongs to the *Solanaceae* family. Currently, the major objectives of global potato research include optimization of production by producing resistant varieties towards various challenging biotic and abiotic stresses to ensure both high yield and improvement of the nutritional values. In potato life cycle, tuberization is developmentally-regulated and depends on the activities of several interdependent complex processes. Considerable progress has been made towards understanding the multiple signaling pathways that lead to activation of many proteins/enzymes along with expression of many genes which are crucial at the different stages of tuber development. Tuberization is associated with sucrose, fructose and starch metabolism, calcium (Ca^{2+}) signaling and reactive oxygen species (ROS). Tuberization in potato involves many constitutive and developmentally-regulated genes with multiple forms which still remain unknown. Likewise, an enzyme or protein could exist in different forms in a plant; therefore, we need to understand the corresponding genes/allelic variants and their expression patterns/regulations particularly at different stages of tuber development. Keeping in view, the focus was on molecular and biochemical studies on a few crucial enzymes namely Sucrose synthase (SuSy), Fructokinase (FRK), Calcium-dependent protein kinases (CDPK) and Catalase (CAT) in an Indian potato cultivar. *In silico* approaches were also adopted for sequence analyses. Sucrose synthase (SuSy, EC 2.4.1.13) refers to a glycosyltranferase (GT) that plays a crucial role in sugar metabolism mainly in the sink tissues of plants. Here, we report isolation and characterization of a 2,668-bp cDNA encoding a distinct full-length SuSy4 form, corresponding to *SUS I* group gene family, from a commercially important Indian potato (*Solanum tuberosum* L.) cultivar, Kufri Chipsona-1 by RT-PCR using tuber total RNA. The predicted protein, designated as KC-SuSy, consisted of 805 amino acids (protein_id QWW18611). Fructokinase (FRK) (ATP: D-fructose 6-phosphotransferase; EC 2.7.1.4) is a key enzyme in fructose metabolism in the sink organs of plants. In developing potato (*Solanum tuberosum* L.) tubers, fructose released by sucrose synthase (SuSy)-mediated sucrolytic pathway is converted to fructose-6-phosphate by FRKs. We report isolation of a 1110-bp cDNA clone encoding a 319-aa FRK2 isoform (designated St-FRK2, QIS79145) from tuber total RNA along with two more cDNAs encoding a 256-aa FRK2 variant (QIV66775) and a 266-aa FRK-like protein (designated StFLN,

QIV66777) using total RNA from tuber and leaf, respectively. Calcium-dependent protein kinases (CDPK) act as sensor-transducers in decoding the calcium (Ca^{2+}) ions associated with multiple signal transduction pathways. In this study, a 1560-bp cDNA clone encoding 515-aa CDPK2 isoform (designated StCDPK2, QIS79146) was isolated and characterized using tuber total RNA. Catalase (CAT; EC 1.11.1.6) is regarded as one of the major enzymatic antioxidants in plants and plays a crucial role in regulation of growth and stress metabolism. Through RT-PCR using tuber RNA, a 1600-bp cDNA clone was isolated which encoded a novel 492-aa CAT1 isoform designated KC-CAT1 (QWW18612).

Apart from the cDNA cloning studies, more members corresponding to the above genes were retrieved from the published reports and other genome databases. Genome wide characterization of the gene families, prediction of the crucial catalytic motifs, chromosomal localization of the genes and phylogenetic analyses were carried out. This thesis work constitutes a comprehensive report providing an insight into the gene families and their classification in potato. Multiple sequence alignments with the catalytic motifs, crucial amino acids and secondary structures were presented; 3-D structures were predicted. Gene-specific expression patterns were shown. Significantly higher level of SuSy, FRK and CAT activities were noticed during the early stages of tuber development implicating their crucial roles in the process of tuberization i,e., from initial swelling of underground stolon to the mature tuber. Protein-protein interaction studies could provide clues of the cross talk between these signalling pathways. Significantly higher expression levels of *Susy4*, *FRK2*, *CDPK2* and *CAT1* genes in the developing tubers indicated that Suc, Fru and starch metabolism, Ca^{2+} signaling and ROS metabolism are important in the process of tuberization. These results would be quite useful in improving not only the potato crops but the other members of the *Solanaceae* family as well.

Key words: Potato (*Solanum tuberosum* L.) cultivar Kufri Chipsona-1; Field condition; Tuberization; Sucrose synthase (SuSy/SUS); Fructokinase (FRK); Calcium-dependent protein kinase (CDPK); Catalase (CAT); cDNA cloning; Sequence and Phylogenetic analyses; Protein motifs/domains; 3-D structures; Gene expression; Enzyme assay, Protein-protein interactions

Chapter 1

Introduction

1.1 Potato Crop

Potato (*Solanum tuberosum* L.) is a major non-grain food crop grown all over the world. It ranks third, and comes only after wheat and rice. Worldwide production of this crop was more than 350 million metric tonnes in 2021 (https://faostat.fao.org/). Potato belongs to the *Solanaceae* family which consists of more than 3,000 members. Apart from potato some other economically important members of this family are tomato, eggplant, tobacco, pepper and capsicum. Among the various tuber crops such as cassava, sweet potato, yams, and taro, potato is the most important in terms of production, accounting for about 45% of the total global production of all tuber crops. Potato tubers are important dietary sources of starch, protein, antioxidants and vitamins. This crop is quite promising with regard to global food security i.e., in fighting hunger and malnutrition. Currently, the major objectives of global potato and other crop breeding programs are optimization of production levels by producing resistant varieties towards various challenging biotic and abiotic stresses (Visser et al. 2009; Hazarika and Rajam 2011; Verma et al. 2012; Gleadow et al. 2013; Singh et al. 2014). In fact, both root and tuber crops are now considered to play pivotal role in feeding the developing world in near future. Recent trend indicates that the growth rates of potato tuber production are particularly high with an annual average increase of 4.5 million tonnes per year which is significantly higher in comparison to rice and wheat. Recent increases of potato production in the Asian continent have been noteworthy. The recent potato production in some countries is shown in Table 1.1.

Table 1.1 Top potato producing countries (Source: FAO Statistical Corporate Database, 2021)

Country	**Production (tonnes)**
China	91818950
India	50190000
Russian federation	22074874
Ukraine	20269190
United States	19181970
Bangladesh	9655082
Netherlands	6961230
Poland	6481620
Belarus	6414760
United Kingdom	6218000
Iran	5102340
Belgium	5035000
Turkey	4800000

About 190 wild tuber-bearing species have been recognized in the section **Petota** of the genus *Solanum* reflecting very rich genetic resources of the potato crop. However, the taxonomy is currently being revised because of the occurrence of highly diverse landraces (Spooner and Hijmans 2001; Spooner et al. 2007). The cultivated *Solanum tuberosum* subsp. *tuberosum* is considered to be originated from Andean and Chilean landraces. But, the tuber-bearing *Solanum* species are widely distributed from the South Western USA to Southern Chile and Argentina, and also from the sea level to the Andes Mountains. Many wild species possess various valuable traits, such as a wide range of resistance to pests and diseases and tolerance to frost and drought. As these species can be crossed directly with the common potato, therefore, they have become useful resources for breeding new cultivars (Visser et al. 2009). During the second half of the 16^{th} century, the Spanish introduced the potato in Europe. Subsequently, this crop was introduced to many parts of Europe and throughout the world by European mariners. In India, potato was introduced by Europeans in the early 17^{th} century.

In India, the importance of this tuber crop was realized soon after independence in 1947. The Central Potato Research Institute (CPRI), Shimla, established in 1949, adopted conventional breeding programmes for the improvement of potato crop, and released a number of high-yielding commercially important cultivars including some processing varieties suitable to different agro-climatic zones of the Indian subcontinent. Now India ranks third in terms of area of potato cultivation, and the second position (only after China) with regard to annual production of potato (approx. 50.19 million tons). Potato is regarded as a short-duration crop with an average maturation time of 90–100 days. There are many potato varieties which are routinely grown in different regions of India. Only top ten potato producing Indian states are listed in Table 1.2.

Table 1.2 Top ten potato producing Indian states (Source: FAOSTAT, 2021)

State	**Production (tonnes)**
Uttar Pradesh	1532355
West Bengal	1378300
Bihar	810141
Gujarat	370769
Madhya Pradesh	327750
Punjab	272444
Assam	111657
Haryana	82809
Jharkhand	69357
Chhattisgarh	65966

1.1.1 Morphology of Potato Plant

The potato, an herbaceous annual plant can grow up to 20–40 inches (50 to 100 cm) high (Fig. 1.1). Plant bears alternate and irregularly pinnate compound leaves. Flowers are pentamerous, actinomorphic, perfect and have sympetalous coloured corollas (white, pink, red, blue, or purple). Usually, potato plant is propagated through tubers (vegetative or asexual propagation), known as “seed tubers” or “seed potatoes”. The tubers bear lateral buds (eyes) that grow into new plants when the conditions are favourable for growth. Under certain conditions, potato plants can produce flowers and small green fruits that contain seeds, solan also called "true seeds" or "botanical seeds". These fruits contain large amounts of solanine, a toxic colourless glycoalkaloid with bitter taste, and therefore not suitable for consumption. Potato plants can be propagated through botanical seeds, which are known as True Potato Seeds (TPS). Such type of agricultural practice is not popular for usual cultivation but very useful in conventional breeding.

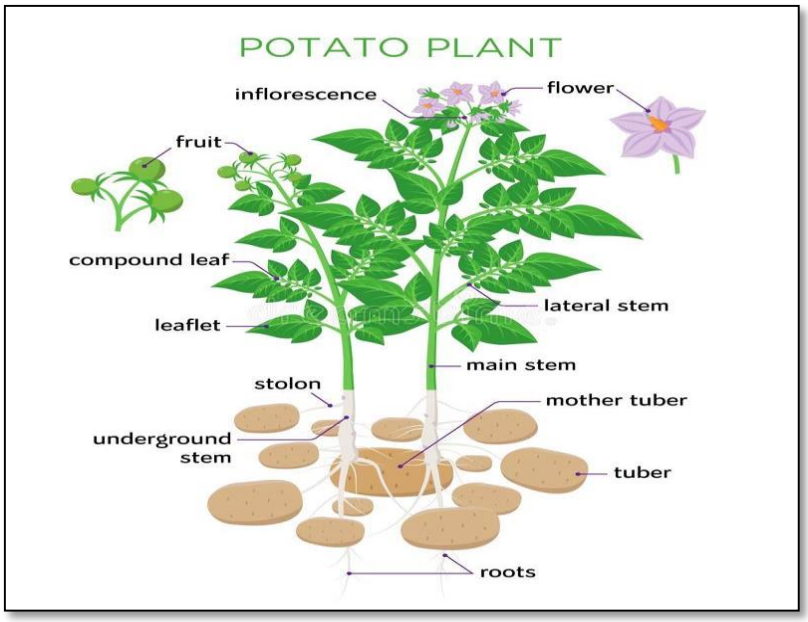

Fig. 1.1 Various organs of a potato plant, a schematic view (https://www.vectorstock.com/royalty-free-vector/potato-plant-in-flat-design-vector-23602588)

1.1.2 Potato Tuber-a Modified Stem

Potato tubers are the somatic storage tissues which develop by the modification of tips of the underground stems or stolons. Tuberization requires short days (small photoperiod) and long cool nights. In India, it is a winter crop except some varieties which can grow during summers in hilly regions. Tuberization is the result of several complex interdependent processes; for example, stolon initiation and elongation, subapical swelling, cell division and

induction of the specific proteins are some of the contributing processes. The potato skin colour can vary from brownish white to deep purple. In mature tubers, cortical and pith cells accumulate large amount of starch and storage proteins. Starch is the predominant storage material in potato tubers. In addition, there are also high quality proteins, substantial amounts of essential vitamins particularly vitamin C, minerals and trace elements present in potato tubers (Fig. 1.2).

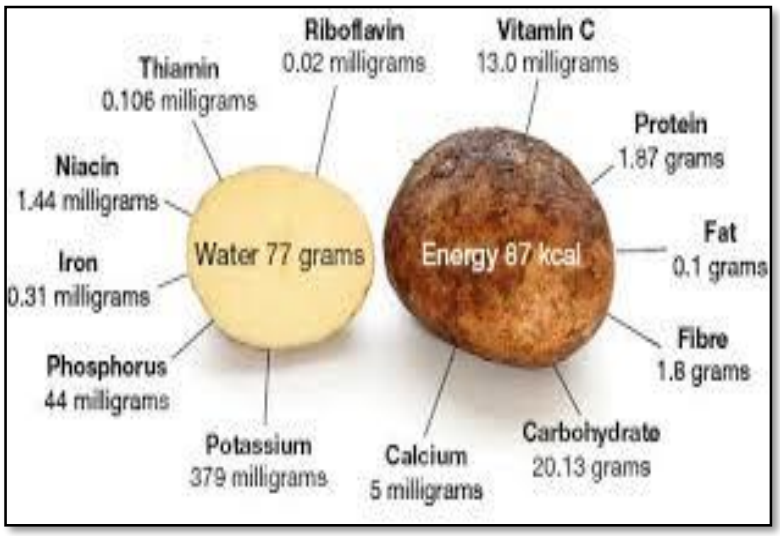

Fig. 1.2 Nutritional aspects of potato tuber (https://healthjade.com/potato-nutrition-facts/). The amounts of the individual nutrients as shown in the figure are on the basis of 100 g fresh tuber weight.

1.2 Potato: An Important System for Basic and Applied Research

Currently, efforts are being made to produce disease-free and high-yielding potato varieties which can withstand a host of various biotic and abiotic stresses. In order to introduce these desirable traits, many countries initiated the strategic potato breeding programmes which are now being continued. The primary focus of applied research on potato and other priority crops is mainly on disease control, starch metabolism, protein metabolism, nutritional aspects, post-harvest preservation at low temperatures, improving the yield and other processing attributes through identifying the target genes, and transgene expression/ inhibition of gene function, and importantly cultivation of this crop under different agro-climatic conditions (Bevan 1991; Liu et al. 2008; Bandopadhyay et al. 2010; Taylor 2018). Potato plants suffer from a variety of viral (such as potato viruses X and Y), bacterial (*Streptomyces scabies* and *Erwinia carotovora*), and fungal diseases (*Phythophthora infestans*) that cause serious loss of tuber yield. Various laboratories are involved in

addressing such challenges using various molecular and genetic approaches. In-depth studies on biochemical, molecular, cellular and morphological aspects of tuber development in potato have become the areas active research to understand growth and development of the sink organ (i.e., somatic storage tissue). Many laboratories are involved in identifying different tuber-specific genes involved in this complex process of tuberization. Studies on starch and protein biosynthesis are important areas of tuber research. As starch is a valuable storage macromolecule in potato, efforts are being made for manipulations of starch metabolism for both quality and quantity improvement. Potato contains high amount of proteins, so the biological values of such proteins could be improved by altering amino acid compositions through genetic manipulations. Developing potato tubers could serve as "factories" for the production of novel proteins and metabolites having commercial and therapeutic importance. Therefore, in the area of 'molecular farming' potato systems are significantly gaining importance. Extent of accumulation of various soluble sugars such as sucrose, glucose and fructose along with their hexose-phosphate intermediates determine the quality of the tubers particularly under storage conditions. Moreover, interconversion between these sugars and starch, sugar-based signalling, interactions between the reducing sugars with free amino acids and proteins are interesting areas of research at biochemical level. Recently, understanding various signals, signal transduction pathways, and particularly sugar-based signalling and other plants are important research areas in potato (Koch 1996; Koch 2004; Halford et al. 2010; Swain et al. 2011; Gangappa et al. 2013).

Many desirable potato traits, such as the traits involved in tuber quality (Li et al. 2005; Menendez et al. 2002) and horizontal disease resistance (reviewed by Gebhardt and Valkonen 2001), are known to be under polygenic control. For improvement through marker-assisted breeding/genetic approaches or any other biotechnological means of a potato variety, we need to identify and characterize the target genes that control the desirable traits. The allelic variations of the individual genes/members of the multigene families are also known to considerably influence the phenotypic traits (Visser et al. 2009; van de Wal et al. 2001; Draffehn et al. 2010). All these studies were mainly based on the availability of a large number of Expressed Sequence Tags (ESTs) (Bachem et al. 2000; Rensink et al. 2005; Ronning et al. 2003) and some full-length gene sequences from potato. However, many more important gene functions involved in potato life cycle, particularly during various stages of tuber development are yet to be isolated and functionally characterized. This is only possible by exploring the rich genetic resources of different potato cultivars/clones. Despite the global importance of the potato crop, the genetics and inheritance of many important qualitative and

quantitative agronomic traits are relatively poorly understood. We have limited knowledge with regard to compositional and processing traits of the potato tuber because of a) tetraploid nature of the genome, b) the high degree of heterozygosity, c) the absence of homozygous inbred lines or d) a poor collection of genetically well-defined marker stocks. It is very likely that high genetic load in potato leads to the distorted segregation ratios as observed frequently causing hindrance to the classical genetic research. However, a profound understanding of genetic composition of potato is still a basic requirement to develop efficient breeding methods. In this context, the major potato genome sequence projects are quite relevant and important (Visser et al. 2009, Genova et al. 2011).

1.3 Tuberization-a Complex Process in Potato Life Cycle

In potato life cycle, tuberization is a complex developmental process which depends on the activities of several interdependent processes, under the influence of various external cues and intrinsic factors and their interactions. Phytochrome B (PHYB)-mediated multiple signal transduction pathways could trigger the physiochemical responses and induce tuberization (Sarkar 2008). This process is also influenced by a number of factors such as photoperiod, temperature, nitrogen nutrition, and endogenous levels of the phytohormones (Sarkar 2008; Aksenova et al. 2012). The salient aspects of tuberization include the induction, initiation and growth of an underground shoot and the cessation of longitudinal growth of the stolon followed by the development of a storage organ i.e., tuber. Two distinct processes at both morphological and biochemical levels are associated with the formation of potato tubers. Tuber induction and subsequent swelling in the stolon tip refer to the morphological changes; whereas both cell division and cell enlargement, and change in orientation of cell growth in the subapical region of stolon tip are clearly the characteristics of cellular growth and development (Xu et al. 1998). High level accumulation of starch (consisting of amylose and amylopectin) and different proteins are due to the distinct biochemical activities associated with tuberization in potato. All these processes of tuberization are associated with expression of a large number of both constitutive and developmentally regulated genes which eventually control the crucial sucrose and starch metabolism, accumulation of different soluble proteins including patatins, various housekeeping functions, signaling pathways and reactive oxygen species (ROS) metabolism (Prat et al. 1990; Bevan 1991; Aggrawal et al 2008). Some of the relevant biochemical and signaling aspects associated with tuberization are precisely depicted below.

1.3.1 Sucrose and Starch Metabolism

In plants, sucrose and starch are the major photoassimilates produced during photosynthesis. Photosynthesis provides energy and carbon to both photosynthetic and non-photosynthetic tissues for their growth and development. Therefore, translocation and partitioning of the photoassimilates are basic processes in plants where sucrose plays a pivotal role. Sucrose (Suc), the most common naturally occurring disaccharide i.e., glucose (Glc) ($\alpha 1 \leftrightarrow 2\beta$) fructose (Fru) or Fru ($2\beta \leftrightarrow \alpha 1$) Glc, is synthesized in the cytosol and acts as the main form of reduced carbon translocated from source leaves to the developing sink tissues. In potato, tuber is a major sink tissue. Sink strength of the growing potato tubers largely depends on sucrose and starch metabolism. Suc is not only an important component of tuber-inducing signal in the terms of energy source, but also regulates the expression of a number of constitutive and other genes involved in tuberization (Fernie and Willmitzer 2002; Raíces et al. 2003). Suc is also considered to positively influence tuberization by regulating the levels of bioactive giberrellins (GAs) (Xu et al. 1998), and above a threshold level controls the developmental switch between shoot and tuber formation (Fischer et al. 2008). Suc along with GAs is thought to trigger the calcium signaling pathhways involved in tuberization by inducing the release of calcium (Ca^{2+}) ions into cytoplasm (Gargantini et al. 2009). Viola et al. (2001) made a significant contribution with regard to sucrose metabolism during tuber development. They showed that during tuber induction, the apoplastic phloem unloading of Suc was predominantly replaced by symplastic phloem unloading, which in turn may be responsible for the up regulation of several genes involved in sucrose metabolism. In other words, SuSy-mediated sucrolytic pathway becomes predominant as compared to invertase-mediated Suc breakdown in the apical region of swollen tip. Since, volume of flow is necessary for the proper mobility of signal molecules in phloem, it is very likely that the Suc may act as mobile signal and have distinct roles in the various stages of tuber development (Thomas 2006).

The enzymes related to sucrose biosynthesis and metabolism are referred to as sucrose-biosynthesis-related proteins (SBRPs) which include Sucrose-phosphate synthase (SPS), Sucrose synthase (SuSy) and Sucrose-phosphate phosphatase (SPP) (Salerno and Curatti 2003; Taneja and Das 2014). The committed pathway of sucrose synthesis involves the sequential action of following enzymes: SPS (EC 2.4.1.14) catalyzes the synthesis of sucrose-6-phosphate (Suc-6-P) by transferring the glycosyl group from uridine diphosphate glucose (UDP-Glc) to fructose-6-phosphate (Fru-6-P). Suc-6-P is then hydrolyzed to sucrose by SPP (EC 3.1.3.24). This high-activity phosphatase catalyzed reaction is essentially irreversible and

displaces the reversible SPS reaction from equilibrium into the direction of net sucrose synthesis. Under most physiological conditions, SuSy (EC 2.4.1.13) catalyzes reversible cleavage of Suc using UDP with formation of UDP-Glc and Fru. SuSy activity can undergo feedback inhibition by free Fru. Fructokinase (FRK; EC 2.7.1.4) catalyses the phosphorylation of the Fru released by SuSy-mediated cleavage to yield Fru-6-P. The latter can then be used to support starch synthesis following further metabolism in the cytosol and amyloplast. Therefore, FRK potentially plays an important role in maintaining the flux of carbon toward starch biosynthesis in the amyloplast, and SuSy is regarded as a key player in determining the sink strength of the potato tuber; hence called as fruit of the labour (Zrenner 1995). Starch biosynthesis in the tubers are developmentally regulated, and involves various enzymes namely ADP-glucose pyrophosphorylase, Granule-bound starch synthases (GBSS) soluble Starch synthases (SS), Starch-branching enzymes (SBEs), and Starch debranching enzymes (DBEs) (Han et al. 2007; Zeeman et al. 2010; Tetlow 2018). The above metabolic aspects clearly portray that SuSy and FRK are the two key enzymes in both sucrose and starch metabolism particularly during tuber development in potato shown in Fig. 2.3.

1.3.2 Multiple Signaling Pathways Associated with Tuberization

Considerable progress has been made during the last few decades with regard to understanding of tuberization in potato. Based on the growing body of evidences as depicted in Fig. 1.3, it is now known that the complex tuberization process is controlled by phytochrome B (phyB)-mediated multiple signaling pathways such as phytohormone signaling, RNA signaling, Ca^{2+} signaling, lipoxygenase (LOX) cascade (Sarkar 2008, Dutt et al. 2017, Niu et al. 2022). Moreover, aquaporins are also believed to contribute to the tuberization process. Some of the factors namely high irradiance, cool and long nights and short day photoperiods are known to influence this process in potato. After the perception of an appropriate environmental signal mediated by the GAs and phyB in the leaves, the systemic signal is produced and transmitted to the underground stolons for the initiation of tubers (Jackson 1999). Several transcription factors such as POTM1, POTH1, StBEL5 are known to regulate tuberization at various stages either independently or in concert with others. Apart from these regulatory factors, cycling DOF (DNA-binding One Zinc Finger) factor (CDF1), MADS box and ABFs (ABA responsive element-binding factors) also act as central regulators involved in plant maturity and initiation of tuberization in potato. They also control the circadian rhythms of plants by interacting with StSP6A (FT protein)-a mobile tuberization signal (Sarkar 2008; Niu et al. 2022). Ca^{2+} and Ca-binding modulator proteins (calmodulins) are considered to be important signal molecules for tuber induction (Jena et al. 1989, Nookaraju et al. 2012). For example, Raices et al. (2001) demonstrated the transient

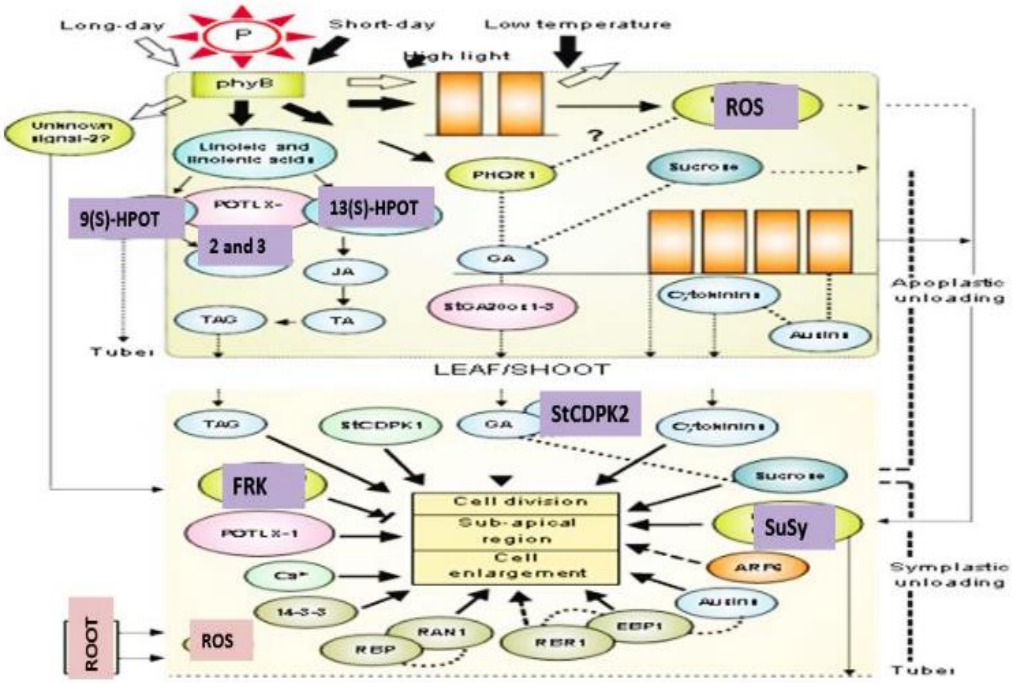

Fig. 1.3 Multiple signaling pathways associated with tuberization in potato (Sarkar 2008, reproduced with minor modifications)

expression of a Ca^{2+}-dependent protein kinase (CDPK), namely StCDPK1 in tuberizing stolons. Tuberization is also characterized by an enhanced activity of lipoxygenase (LOX) cascade (Kolomiets et al. 2001). The role of CDPKs is also well-recognized in the complex tuberization process in potato (Raices et al. 2003). CDPK activities with different substrate and cellular specificity are known to play important role in potato life cycle. For example, StCDPK3 is expressed predominantly during early initiation of stolon elongation, while StCDPK1 is expressed during apical swelling in the stolon tip, StCDPK2 is expressed during tuberization and also in leaves (Raices et al. 2003). Also, StCDPK2 was found to play a crucial role in light sensing and stress metabolism (Grossi et al. 2021). Since cytosolic concentration of Ca^{2+} ion regulates the oxidative burst via CDPKs, therefore, it is considered that an oxidative burst-mediated redox signaling pathway could be involved in tuberization (Sarkar 2008). The possibility of cross-talks between redox signaling pathways and PHYB mediated signalling still remains an enigma.

1.3.3. ROS Signaling Pathways Influence Tuberization

An oxidative burst results in the generation of ROS, which are known to induce an intracellular signaling pathway (Vogel et al 2011). Currently, ROS are being viewed as cellular indicators of stress, and also as signals and secondary messengers involved in the activation of stress-response and defense pathways. Apart from their role in the basic biological processes like cellular proliferation, expansion and differentiation, being integral

part of plant growth and development ROS are also believed to trigger the pathways that lead to programmed cell death (PCD), an alternative perception to the 'direct killing via oxidative stress' (Gapper and Dolan 2006; Mittler 2017). Plant cells have evolved different enzymatic and non-enzymatic antioxidants to get rid of such ROS-mediated deleterious effects. Some of the major enzymatic antioxidants include Superoxide dismutase (SOD), Catalase (CAT), Ascorbate peroxidase (APX) which determine the steady-state cellular level of superoxide radicals and hydrogen peroxide (Bowler et al. 1991). Ascorbic acid (AA), reduced glutathione (GSH), α-tocopherol, carotenoids, phenolics, flavonoids, and proline are the common examples of non-enzymatic components of antioxidant machinery (Foyer and Noctor 2005; Das and Roychoudhury 2014; Choudhury et al. 2017). Despite a possible role of an oxidative burst in the signaling network of the tuberization process, a direct evidence for the involvement of ROS molecules in tuberization process is rather recent.

H_2O_2, most frequently occurring ROS, plays some crucial role in plant cells that include signal transduction, cell wall lignification, and defence against pathogens. Several oxidases in the peroxisomes and glyoxysomes i.e., specialized peroxisomes catalyze the production of H_2O_2. With the help of catalases, these organelles essentially eliminate H_2O_2 if produced in excess into water and molecular oxygen. Hence, the role of CAT is indispensable in a plant's life under stressed conditions as it effectively removes this ROS in order to keep at a basal non-toxic level. During tuberization there are multiple changes-a sea of stress is due to various molecular, biochemical and morphological processes resulting in the significant increase of H_2O_2 production. To scavenge H_2O_2, catalases play a significant role whereas other enzymes like APX, SOD are responsible for fine tuning only. Therefore, CAT is important not only in potato growth but also in tuberization as supported by its high activity during the initial stages of tuberization (Agrawal et al. 2008). In order to gain an insight of oxidative burst mechanism and the cross talks between different signaling pathways during tuberization, CAT expression patterns at various stages of tuber development need to be understood.

Keeping in view the importance of Suc metabolism, calcium signalling and ROS metabolism during tuberization, the major focus of this thesis work was on molecular and biochemical studies on the following enzymes: Sucrose synthase (SuSy), Fructokinase (FRK), Calcium-dependent protein kinase (CDPK), Catalase (CAT). The overall advances on these aspects precisely depicted in the following Review of Literature section.

Chapter 2

Review of Literature & Objectives

2.1 Tuberization in Potato

Tuberization in potato is a complex developmental process influenced by a number of factors such as photoperiod, temperature, nitrogen nutrition, and endogenous levels of the phytohormones (Aksenova et al. 2012). This process is accompanied with the expression of a large number of both constitutive and developmentally regulated genes which are involved in various housekeeping functions, sucrose metabolism, storage starch biosynthesis, and accumulation of large amounts of different soluble proteins (Prat et al. 1990; Bevan 1991; Kloosterman et al. 2005; Agrawal et al. 2008). Potato tuber refers to a major sink tissue. It is commonly believed that sink strength of growing potato tubers largely depend on sucrose metabolism and/or starch synthesis. Tuberization is the result of the activities of several interdependent processes which culminate in tuberization: e.g., stolon initiation, elongation, subapical swelling, cell division, starch biosynthesis and the induction of specific proteins are a few of the contributing processes. It indicates the photoassimilative capacity of the potato plant, which is somewhat lower as compared with other C3 plants. In addition to this, tuberization process mainly involves the carbon assimilation and calcium signaling for the growth. An efficient antioxidative machinery to curb the stresses associated with tuber development.

In carbon assimilation, biosynthesis of large amount of storage starch (consists of approximately 25-30% amylose and 70-80% amylopectin), and the accumulation of a set of relatively abundant proteins are two major biochemical changes during tuber formation unlike other somatic tissues of the potato. As starch is the predominant storage molecule in tubers, the activities of enzymes involved in the carbohydrate metabolism are crucial to study. Since, the Suc is only the transport form of sugar, energy source and acts as a signal for other metabolic pathways; therefore, the Suc metabolism is of primary importance to study the process of tuberization. Keeping in view, current advances on Suc metabolism and associated two key enzymes namely SuSy and FRK are precisely described here with the supporting evidences as reported in the literature.

Among the multiple signaling pathways, Ca^{2+} ion signaling is crucial in potato tuberization. Jena et al. (1989) proposed the involvement of Ca^{2+} and Ca^{2+}-binding modulator proteins (calmodulins) in tuber development as calmodulin inhibitors were known to inhibit tuberization. Ca^{2+} influx into the cytoplasm is induced by Suc and GAs, and the expression of *CDPKs* especially *StCDPK1* was noticed with high Suc concentration (Gargantini et al. 2009). As the cytosolic Ca^{2+} regulates oxidative burst through CDPKs, therefore, oxidative burst mediated

redox signaling pathway are believed to be involved in tuberization. The broad spectrum expressions studies of some isoforms of CDPKs suggest that they act as a guard of calcium cues, participate in numerous signaling pathways resulting into various physiological processes such as tuberization, light signaling, biotic and abiotic stresses, biosynthesis of phytohormones, confer immunity and resistance against pathogen attack (Giammaria et al. 2011; Grossi et al. 2021). Recent advances on the CDPKs are described in this section.

An oxidative burst leads to the generation of ROS, and associated signaling pathways profoundly influence tuberization via gibberellin acid biosynthesis pathway (Grant 2000; Kim et al. 2007 b; Bae et al. 2011). The process of GA biosynthesis depends on the Suc and Ca^{2+} concentration in cytoplasm. It becomes necessary to alleviate the harmful H_2O_2 for proper functioning of a cell. For defense, plants have developed molecular antioxidant machinery comprising both enzymatic and non-enzymatic components. The crucial enzymes such as superoxide dismutase (SOD), peroxidases (POD) and catalases (CAT) scavenge the free radicals. CAT is crucial as it acts above threshold level, and dismutates H_2O_2 into water and oxygen (Kaur et al. 2020). In the context of the ROS metabolism, the recent advances on CAT are described.

2.2 Sucrose Metabolism in Plants

In plants, sucrose and starch are the major photoassimilates produced during photosynthesis which provides both energy and carbon to both photosynthetic and nonphotosynthetic tissues for growth and development. Translocation and partitioning of the photoassimilates are basic processes in plants where Suc plays a very pivotal role. It is the most common naturally occurring disaccharide i.e. glucose (Glc) ($\alpha 1 \leftrightarrow 2\beta$) fructose (Fru) or Fru ($2\beta \leftrightarrow \alpha 1$) Glc. Suc is synthesized in the cytosol and is the main form of reduced carbon translocated from source leaves to developing tissues. Suc metabolism is schematically presented in Fig. 2.1.

In plants, sucrose fulfils many roles such as storage reserve, compatible solute under stress conditions, signal transduction, and regulation of gene expression (Huber and Huber 1996; Winter and Huber 2000; Halford et al. 2011). It could be involved in regulating photosynthesis and other metabolic aspects in the plastids. Sucrose biosynthesis-related proteins (SBRPs) usually include sucrose-phosphate synthase (SPS), sucrose synthase (SuSy/*SUS)* and sucrose-phosphate phosphatase (SPP) (Cumino et al. 2002; Salerno and Curatti 2003; Taneja and Das 2014). The

committed pathway of sucrose synthesis involves the sequential action of following enzymes: SPS (EC 2.4.1.14) catalyzes the synthesis of sucrose-6-phosphate (Suc-6-P) by transferring the

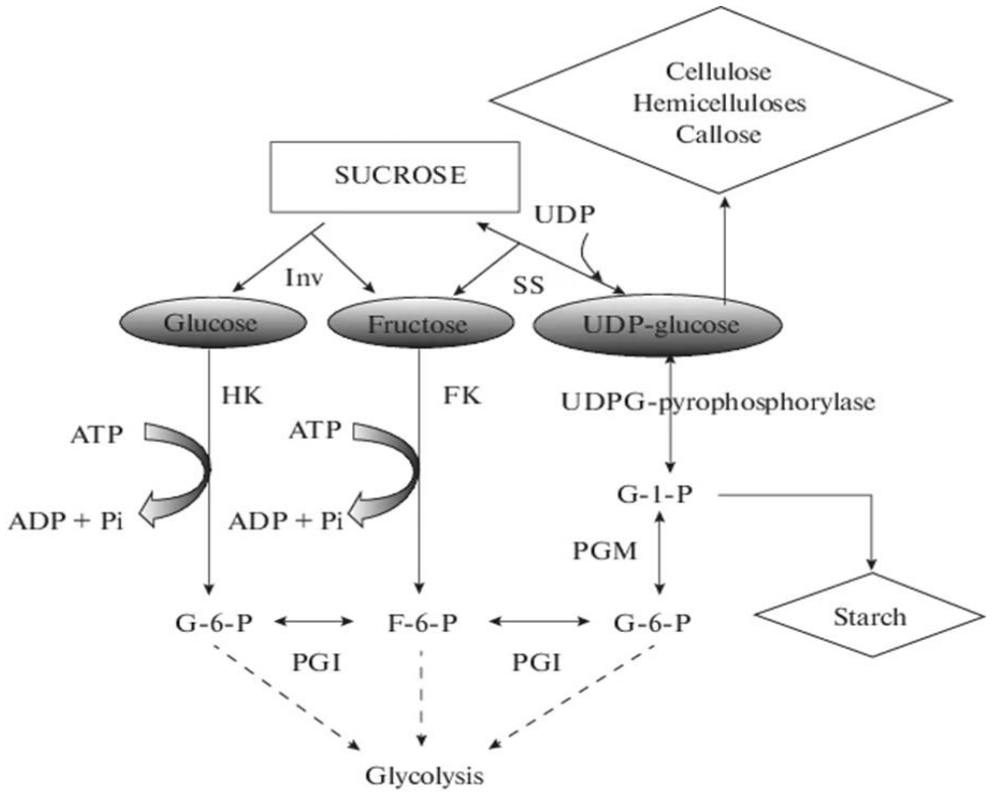

Fig. 2.1 Modes of sucrose metabolism and the main pathways of carbon partitioning in sink tissues of woody plants. SS sucrose synthase; Inv invertase; HK hexokinase; FK fructokinase; PGM phosphoglucomutase; PGI phosphogluco-isomerase; G-6-P glucose-6-phosphate; F-6-P fructose-6-phosphate; G-1-P glucose-1-phosphate; ADP adenosine diphosphate; ATP adenosine triphosphate*;* UD uridine diphosphate; PP_i pyrophosphate (Moshchenskaya et al. 2019)

glycosyl group from uridine diphospate glucose (UDPGlc) to fructose-6-phosphate (Fru-6-P). Suc-6-P is then hydrolyzed to sucrose by SPP (EC 3.1.3.24). This high-activity phosphatase catalyzed reaction is essentially irreversible and displaces the reversible SPS reaction from equilibrium into the direction of net sucrose synthesis (Stitt et al. 1987). Under most physiological conditions, SuSy (EC 2.4.1.13) catalyzes reversible cleavage of Suc using UDP with formation of UDP-Glc and Fru. This free Fru must be phosphorylated to Fru-6-phosphate, prior to its utilization in any metabolic process, which is done by the fructokinase (FRK).

2.2.1 Sucrose Synthases (SuSy/SUS)

Suc is a nonreducing sugar transported from the source tissues to the non-photosynthetic tissues i.e., sink tissues through the phloem. The transported Suc is crucial in regard to providing energy, many metabolic pathways, synthesis of different organic molecules for growth and development, and also for sugar signalling (Huber and Huber 1996; Winter and Huber 2000). In the sink tissues, Suc can be hydrolyzed into Glc and Fru by the cell-wall invertase (cwINV) and vacuolar/cytosolic invertases; whereas, with the help of uridine diphosphate (UDP) the enzyme SuSy reversibly and efficiently hydrolyzes Suc into UDP-Glc and Fru as depicted in Fig. 2.2 (Salerno and Curatti 2003; Ruan 2014).

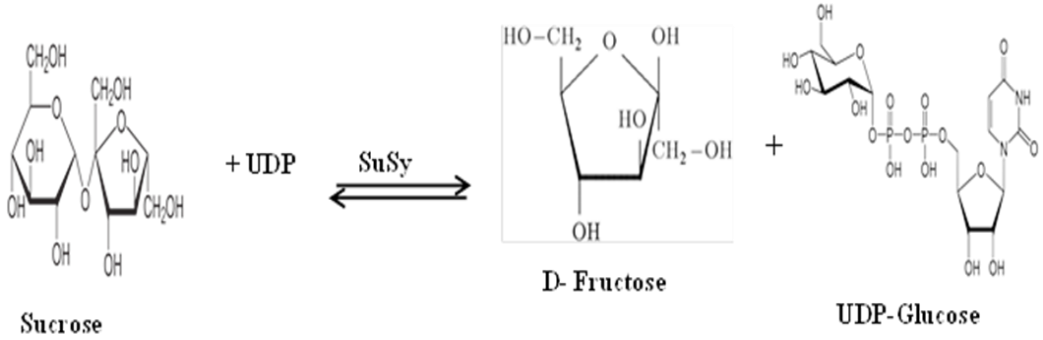

Fig. 2.2 Suc hydrolysis by SuSy (Sucrose synthase)

Structure and enzymatic activity of SuSy: SuSy, a glycosyltransferase (GT), is commonly found in plants and has recently been reported in bacteria. In cereal endosperm and potato tuber, SuSy is regarded as the predominant sucrose cleavage enzyme, and provides substrates for starch synthesis (Winter and Huber 2000). It meets the increased glycolytic demand under anaerobic condition and cold stress, and provides UDP-Glc for cell wall biosynthesis; also plays a crucial role by providing substrate for respiration by supplying energy during loading and unloading in phloem (Fu and Park 1995). SuSy proteins are typically homotetrameric, and the monomer is around 90 kDa consisting of 800 amino acids. The monomers may vary between 53 to 110 kDa in different plants. SuSy could act as a heterotetramer as reported in some plant species namely maize, barley, rice and bird cherry. The activity of SuSy was known to be regulated by pH. It showed Suc-synthesis activity at pH 7.5–9.5; whereas for Suc degradation, the optimal pH values were between 5.5–7.5. SuSy requires UDP for the cleavage of Suc. ADP can also be utilized at a

lower affinity for the same reaction (Guerin and Carbonero 1997; Duncan et al. 2006; Sytykiewicz et al. 2008; Schmölzer et al. 2016). The two major domains of a SuSy monomer are approx..250-amino acid N-terminal domain for cellular targeting, and 500-amino acid C-terminal GT-B domain having the enzyme's glycosyl transferase activity (Zheng et al. 2011). SuSy proteins contain two phosphorylation sites. The first site is a serine phosphorylation site at position 11 to 15, which is thought to play a role in membrane association (see section "Subcellular Localization of SuSy"). The second site is also a serine, at around position 170, and is thought to regulate protein degradation (Hardin et al. 2003). *In vitro* phosphorylation of rice SuSy proteins, Rsus1-3 may promote SuSy activity (Takehara et al. 2018).The tetrameric structure of plant SuSy was confirmed by the determination of the structure of Arabidopsis AtSUS1 by X-ray crystallography (Zheng et al. 2011). Site-directed mutagenesis of an E-X7-E motif of the GT-B domain of rice SuSy, RSuS3, revealed two glutamate residues (E678 and E686) and a phenylalanine residue (680^{th} position) are essential for enzymatic activity (Huang et al. 2016).

Subcellular localization of SuSy: The SuSy proteins were first reported to be present in the cyotosol only but recent studies showed their presence in other cell organelles namely, vacuoles, plastid, mitochondria, golgi apparatus, cytoskeleton and tonoplasts where they could play different roles such as carbon allocation to plastid for starch synthesis, solute regulation between the cytosol and mitochondria, and cytoskeleton functioning (Morell and Copeland 1985; Winter et al. 1998; Buckeridge et al. 1999; Konishi et al. 2004; Subbaiah et al. 2006). Amor et al. (1995) provided the first evidence of non-cytosolic SuSy in cotton. A year later, Carlson and Chourey (1996) detected the SuSy associated with plasma membrane in maize by the activity assay and monoclonal antibody studies. Further, Persia et al. (2008) revealed the presence of two SUS isoforms in tobacco; one membrane associated and other cytosolic one. Cai et al. (2011) studied the co-localisation of SuSy with callose synthase and cellulose synthase in tobacco pollen tubes pointing out the enzyme's dual role in callose and cellulose synthesis.

SUS gene families: SuSy is encoded by a multigene family ranging from two to thirty genes (Avigad 1982; Stein and Granot, 2019). Two SuSy genes in *Amborella trichopoda*, five from grape and sugarcane, six from Arabidopsis, rice, tomato, rubber tree and peach, seven from cotton, bamboo and tobacco while from apple, tobacco species, popular and chinese pear 11, 14, 15 and 30 genes have been identified (Zhang et al. 2013; Zhu et al. 2017; Baud et al. 2004;

Hirose et al. 2008, Goren et al. 2017; Xiao et al. 2014; Wang et al. 2015; Chen et al. 2012; Huang et al. 2018; Tong et al. 2018; Wang et al. 2015; An et al. 2014 ; Abdullah et al. 2018). Recent advances in plant genome sequencing, assembly and the publication of new draft genomes have allowed the *SUS* gene family to be characterized in many plant species in a more comprehensive manner. According to the earlier published reports, SuSy has been divided into three different separate clades: *SUS I, SUS II,* and *SUS III*. It was reported that only the *SUS I* clade was clearly distinguished between eudicots and monocots whereas in the cases of SUS II and III there was no clear distinction (Zhang et al. 2015; Zhu et al. 2017). This unique trait of phylogenetic analysis poses a question on constraints in the evolution of the enzyme.

The first *SUS* gene to be cloned and sequenced was the *Shrunken* (*Sh*) gene from maize (Werr et al. 1985). Since then, many other *SUS* genes have been cloned from different plants, including another maize *SUS* (McCarty et al. 1986; Shaw et al. 1994) and genes from *Arabidopsis* (Chopra et al. 1992; Martin et al. 1993), rice (Wang et al. 1992; Yu et al. 1992), potato (*S.tuberosum*) (Fu et al. 1991; Fu and Park 1995) and tomato (*S.lycopersicum*) (Goren et al. 2011).

SuSy, a crucial enzyme for sink strength: In addition to Suc metabolism, SuSy is considered to play other roles in plants. It determines sink strength defined as the ability of an organ to import photoassimi lates which depends on two parameters: sink organ size as a physical constraint and activity as a physiological constraint (Ho 1988). The catalytic role of SuSy is shown in Fig. 2.3. Extent of phloem loading and breakdown of Suc are considered in determining the sink strength. This was supported with the detection of high *SUS* promoter strength in phloem tissues by GUS fusion assays in different plant species like potato, *Arabidopsis*, maize, rice and tomato work with promoter-GUS fusions has revealed *SUS* promoter activity in the phloem (Fu and Park 1995; Martin et al. 1993; Bieniawska et al. 2007; Yang and Russell 1990; Shi et al. 1994; Goren et al.2017). Also, the high abundance of the SuSy isoforms was noticed in phloem by the isoform-specific antibodies assay in *Arabidopsis* where *AtSUS5* and *AtSUS6* were found to be phloem specific (Barratt et al. 2009). In citrus and maize, phloem-specific SuSy was studied by immunohistological analysis (Nolte and Koch 1993). Apart from phloem unloading zones, SuSy was found to be localized in loading zones in the mature leaves of some plants like popular, rice, maize, *Arabidopsis,* citrus and maize leading to the hypothesis that SuSy plays a crucial role in maintaining the equilibrium between the Suc and its breakdown products and allocating carbon resources for energy production in companion cells (Nolte and Koch 1993; Regmi et al. 2016).

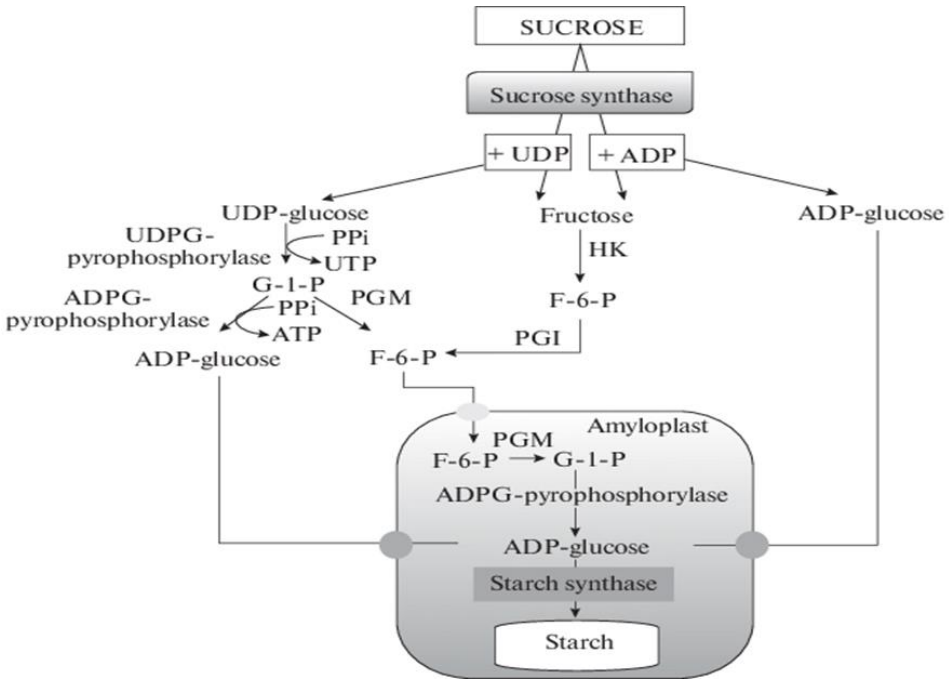

Fig. 2.3 The role of Sucrose synthase in sink organs of plants (Moshchenskaya et al. 2019)

Apart from this, there is plethora of evidence that it is SuSy and not INV, which breaks Suc in the sink tissues of various plants like tubers of potato, roots of cassava, seeds of mung and fruit of tomato (Morrell and Rees 1986; Sung et al. 1989; Sun et al. 1992; Wang et al. 1993). Studies on altered SuSy expression resulted into varied growth and significant loss in dry weight, embryos and produced shrunken–seed phenotype in maize, rice, pea and dry weight in potato tubers. These findings supports the correlation between SuSy activity and sink strength (Chourey and Nelson 1976; Counce and Gravois 2006 ; Craig et al. 1999; Zrenner et al.1995),

SuSy in regulating carbon flux: The function of SuSy largely depends on its location inside the cell. The mitochondrial SuSy was found to interact with the anion channels and plays a role in determining and regulating the transport of ions and other solutes between the cytosol and mitochondria. Thus, it aids in maintaining the homeostasis of the cell (Subbaiah et al. 2006).

SuSy in symbiotic associations: SuSy was found to be associated with the mutualism process in symbiotic organisms like *Rhizobium.* Gordon et al. (1999) reported approx. 90% reduced SUS

activity in root nodules of the *SUS* mutant (*rug4*) pea. It was proposed that in the low oxygen environment, SuSy activity was indispensable for nitrogen fixation. Surprisingly, the mutation did not have any effect on plant's relationship with mycorrhizae but impacted the nitrogenase activity (Yarnes and Sengupta-Gopalan 2009).

SuSy in heat stress: The possible role of SuSy in conferring heat resistance was studied in many plants. In rice, a *SUS3* allele was found to express during the seed ripening and was thought to prevent chalky phenotype due to heat stress. In the transgenic heat sensitive commercial plants, the chalky grain formation was only reduced by the transfer of both the promoter and cDNA of the heat resistant lines expressing high *SUS3* gene portraying the importance of SUS in conferring the heat resistance (Takehara et al. 2018). In wheat, a thermostable SUS was purified from heat-tolerant line wh-1021 which was found to be stable till 50º C unlike other SUS proteins which are stable up to 30ºC (Verma et al.2018; Schmolzer et al. 2016). In strawberry, SuSy was found to be associated with fruit ripening. Delayed fruit ripening, anothycyanin accumulation and increased firmness were observed in the fruits with RNAi suppression of *FaSUS1* gene by virus-induced gene silencing method (Zhao et al. 2017). Despite being the subject of intensive study, understanding of *SUS* genes still have lacunae which need to be figured out such as regulation, intracellular localization and functional specializations of the individual SuSy isoforms; co-evolution of SUS and INV and interactions of SuSy with other proteins.

Advances on SuSy in potato: Salanoubat and Belliard (1987) first isolated and characterized a *SuSy* cDNA clone from potato and showed relatively higher levels of its transcripts in developing tubers as compared to other organs. It was demonstrated that SuSy activity was regulated by wounding and anaerobiosis (Salanoubat and Belliard 1989). Two classes of *SUS* genes namely *Sus3* and *Sus4* were isolated and characterized from a potato cultivar (FL1607), and found to be differentially expressed (Fu and Park 1995). Zrenner et al. (1995) demonstrated that SuSy but not invertases was responsible for Suc cleavage in tuber (a sink organ). In potato, the crucial role of SuSy was established with regard to carbon partitioning and determining the sink strength. Later, two more SuSy isoforms were characterized from potato (Baroja-Fernandez et al. 2003) which revealed that eenhanced SuSy activity in transgenic potato tubers grown under both green house and field condition resulted in increased levels of starch, ADP-glucose and UDP-glucose and total yield. Their studies also revealed an inverse relationship between the expression of INV and SuSy coding genes clearly indicating that SuSy-mediated sucrolytic pathway played a major role

in determining the sink capacity of tubers rather than invertases. Till date, there is no comprehensive studies with regard to the *SUS* gene family members in potato, crucial protein motifs/domains and expression patterns at various stages of tuber development.

2.2.2 Fructokinases (FRKs)

In plants, the hexose sugars namely glucose (Glc) and fructose (Fru), products of photosynthesis, serve as starting materials in various metabolic pathways leading to the synthesis of various organic matters. The source organs determine the carbon fixation capacity and a series of sinks compete for the available photo-assimilates mostly in the form of Suc, a primary end product of photosynthesis and a major transport form of sugar. An overall growth and development of a plant depend on environmental factors, source-sink relationships and sugar allocation between the organs (Granot et al. 2013). Presumably, the cellular sugar levels coordinate the absorption and uptake of various components such as the minerals, carbon dioxide, water and sunlight, the essentials for the photosynthesis, having influence on metabolism, physiology and development (Granot et al. 2014). Therefore, translocation and partitioning of the photoassimilates are basic processes in plants where Suc plays a very pivotal role. In plants, Suc fulfils many roles such as storage reserve, compatible solute under stress conditions, signal transduction, and regulation of gene expression (Huber and Huber 1996; Winter and Huber 2000; Halford et al. 2011). It could be metabolized in the photosynthetic tissues or exported to other non-photosynthetic tissues, where it acts as a substrate for all the pathways involved in the plant metabolism. But it has to be cleaved in to its monomeric hexose units i.e., Glu and Fruc for its transport and assimilation (Chia et al. 2004; Smith et al. 2005). These hexoses further must be phosphorylated by the phosphorylating enzymes i.e., hexokinase (HXK, EC 2.7.1.1) or fructokinase (FRK, EC2.7.1.4) in order to yield G6P and F6P prior to their entry into other metabolic pathways. For all the essential aspects of plant metabolism hexose phosphorylating enzymes also play crucial and indispensable role in sugar sensing (Claeyssen and Rivoal, 2007; Granot et al. 2013). Glu can be phosphorylated by HXK; whereas Fru can be phosphorylated by both HXK and FRK. Primarily, FRKs phosphorylate fructose with the help of ATP and magnesium ion (Mg^{2+}) as depicted in Fig. 2.4 (Stein and Granot 2018). Apart from this, some of the proteins are found in the plants, show substantial sequence similarity with FRKs but they do not possess any kinase activity; rather, play an important role in redox signaling and gene expression as found in chloroplast. These proteins

are called FRK-like enzymes (FLNs) (Gilkerson et al. 2012). In *Arabidopsis*, interactions of two FRK-like enzymes namely FLN1 and FLN2 with thioredoxin z were found to influence plastidic gene expression (Arosva et al. 2010). Like FRKs, some FLNs were also studied.

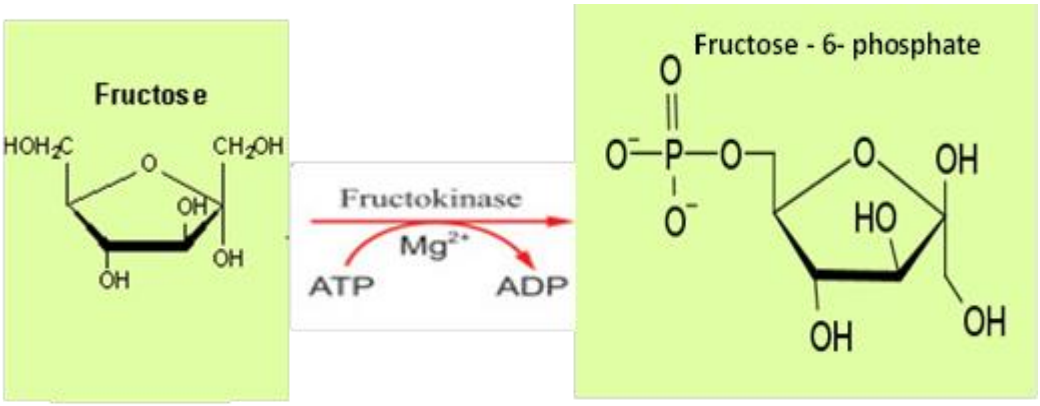

Fig. 2.4 Fructose phosphoyrlation by Fructokinase (FRK)

Enzymatic activities of plant FRKs: Plant FRKs usually act as homodimers with a monomer mass of about 34–37 kDa and generally utilize ATP as the phosphate donor for the phosphorylation of fructose, due to their high affinities for ATP, but may use other nucleotides such as GTP and UTP in the absence of ATP (Pego and Smeekens 2000). Some FRKs have higher levels of activity with GTP (Doehlert, 1990; Gardner et al. 1992; Hoepfner and Botha 2004) or CTP (Doehlert 1990). They usually have pH optima of about 8.0 (Pego and Smeekens 2000) and require magnesium ions (Mg^{2+}) as a cofactor for activity (Turner et al. 1977; Renz and Stitt 1993; Schaffer and Petreikov 1997a; Gonzali et al. 2001; Karni and Aloni 2002), but those ions can sometimes be partially replaced by manganese ions (Mn^{2+}) (Turner et al. 1977; Copeland and Morell 1985). Potassium ions (K^{+}) could stimulate plant FRK activity (Turner et al. 1977; Copeland et al. 1978; Copeland and Morell 1985; Baysdorfer et al. 1989; Gardner et al. 1992). FRKs have a wide range of affinities for fructose ranging from K_m = 0.006 mM for FRKIb of barley (Baysdorfer et al. 1989) to K_m = 3.3 mM for OsFKI of rice (Jiang et al. 2003). Only a few plant FRKs have Km values >1 mM and the affinity of most plant FRKs for fructose is about two orders of magnitude greater than the affinity of plant HXKs for fructose (Granot et al. 2013).

Another important aspect of plant FRK activity is its inhibition by its own substrate, Fru. Many plant FRKs, including plastidic FRKs, have been reported to be inhibited by Fru concentrations

above 1–2 mM, with Ki values of 1–6 mM (Pego and Smeekens 2000). It appears that FRKs with higher affinities for Fru are usually more susceptible to substrate inhibition than FRKs with lower affinities (Pego and Smeekens 2000). Because Fru also inhibits the cleavage of Suc by SUS in a product-inhibition manner, it has been suggested as a mechanism for the regulation of carbohydrate flux into starch synthesis in young tomato fruits (Schaffer and Petreikov, 1997b) and during vascular development (German et al. 2003; Damari-Weissler et al. 2009). Fru substrate inhibition might play a role in directing carbon to different metabolic pathways.

Structural features of FRKs: PfkB proteins share two main signature motifs: a pair of glycines (di-gly (GG)) motif in the N-terminal region and a G/AXGD motif in the C-terminal region. The role of each motif has been identified through mutational and structural analyses. The GG motif provides flexibility in the hinge region that connects the lid and the large domain, while the second domain is responsible for catalysis. In the *Leishmania donovani* pfkB member ADK, it was observed that activity of the enzyme substantially reduced to 1% as that of the wild-type enzyme by substitution of the second glycine to aspartate in the GG motif and substrate binding affinity was also reduced, presumably due to the inability of the mutant protein to adopt the closed conformation that supports catalysis (Datta et al. 2005). The aspartate in the G/AXGD motif acts as a base during catalysis and activates the C6 fructose hydroxyl group for nucleophilic attack on the γ-phosphate in ATP (Sigrell et al. 1998; Carbera et al. 2010). Some of the pfkB proteins which do not possess any kinase activity but show substantial resemblance with FRKs and are important for redox and cell signalling and some regulatory roles as opposed to direct catalytic function are found in choloroplast (Gilkerson et al. 2012). Majority of active FRKs in plants possess GAGD as second motifs, whereas in FLN1 it is GSGD and in FLN2 it is A/QSGD. Moreover, FLN has longer N-terminus (Stein and Granot 2018).

FRK gene families: FRKs belongs to family of diverse kinases known as the phosphofructokinase B (pfkB) sub family, a large group within the ribokinase family based on their sequence similarity with first pfkB gene, a minor fructokinase isoform in *E. coli*. Plant and bacterial FRKs phosphorylate Fru to Fru-6-P (F6P) on the other hand Fru is phoshporylated to Fru-1-P (F1P) by mammalian FRKs. The pfkB family of enzymes across kingdoms includes kinases (ADKs) and several others with diverse substrate specificities (Stein and Granot 2018). Typical PfkB protein comprises of two main domains, large active site consisting of a β-sheet positioned between two α-helices, and a smaller domain in the periphery, known as the lid domain, comprised of another

β-sheet attached to the larger domain by short loops that act as a hinge (Carberra et al. 2010). Many protein kinases are homodimers and during the catalysis substrate binding induces a conformational change in which the lid closes over the substrates. (Riggs and Callis 2017). After catalysis, the protein returns to an open state and the products are released. Binding of substrates to pfkB proteins follows ordered bi-bi kinetics where the carbohydrate enters first, followed by ATP (Campus et al.1984).

Molecular studies on plant FRKs: Despite of renewed interest in understanding regulation of carbon flux within the plant and overall plant biomass accumulation for energy purposes, molecular and biochemical studies on FRK activities were carried out only in some plant species. Turner et al. (1977) first reported the isolation of FRK gene from pea. Afterwards, a number of cDNA/genomic sequences encoding different FRK isoforms were reported from different plant species namely soybean (Copeland and Morell 1985), potato (Z12823, JX576230; Smith et al. 1993), tomato (U64817, U64818, AY323226, AY099454), and a number of other plant species such as citrus fruit, rice, sugarcane, *Arabidopsis thaliana,* maize spinach. All these studies significantly contributed in understanding the structure-function and phylogenetic relationships of FRKs along with their expression patterns in plants. Molecular studies showed the presence of three to seven FRK genes in different plant species (Granot et al. 2014). In tomato, four genes were cloned and designated SlFRK1-4. As GFP fusions, tomato FRK3 localizes to plastid stroma and the other three FRKs localize to the cytosol. Tomato plants with antisense RNAs targeting FRK1 or FRK2 had markedly less FRK activity than control plants. Surprisingly, Fru levels were lower in all FRK knock-down (KD) plant lines compared to control plants. While the growth of all FRK KD plant lines were stunted, KD of FRK2 affected plant size more than FRK1. FRK2 was shown to be involved with both xylem and phloem development. Vascular cells were smaller in FRK2 KD plants than control plants and vessels in the stems were thinner, leading to impaired water conductance. RNAi-mediated KD of tomato FRK3 correlated with diminished stem xylem and reduced water conductance. Simultaneous KD of both FRK2–3 led to severe defects in plant growth that were more drastic than seen in FRK2 KD plants alone. The differences in tissue-specific expression and the differential phenotypes seen upon KD of different FRKs suggests non-overlapping roles for different FRKs in tomato. Interestingly, a probable fifth FRK gene (Solyc11g042850) was revealed by the tomato genome sequencing, whose expression was very low (Sato et al. 2012; Koeing et al. 2013). Riggs et al. (2017) studied seven FRK genes in

Arabidopsis by protein purification and comprehensive enzymatic and biochemical characterization. In developing tomato fruit, potato tuber and sugar beet root, the size of FRK was found to be around 36 kDa which is in close agreement with the deduced amino acid sequences. Native gel assays revealed the presence of two distinct FRK forms i.e., FRK 1 and FRK 2.

FRKs were found to be mainly dimeric in nature as revealed by gel filtration assay (Pego and Smeekeens 2000). Similarly, in cassava seven FRK genes were also identified through bioinformatic approaches (Yao et al. 2017). However, the bioinformatic tools were less successful in the case of sugar cane (Chen et al. 2017). Therefore, more genes encoding the FRK forms are yet to be identified from plants which would help to know their expression patterns and functional specializations. Apart from FRKs, some FLNs forms have also been reported in the plant species namely potato (JX576279, DQ235199), *Nicotiana sylvestries* (XM_009764513), Glycine *max* (XP_003546905), and *Arabidopsis thaliana* (AAM64445). The expression patterns and functional significance of these FLNs forms is yet to be understood in plants.

FRKs in plant growth and development: The role FRKs in various developmental processes is known to be less as compared with HXKs hypothesized from the transgenics and expression profile under different conditions. Schaffer and Petreikov (1997b) demonstrated that FRKs play key role in starch accumulation in plants like tomato (Odanaka et al. 2002). Davies et al. (2005) through examination of FRK antisense lines proposed the role of FRK2 in vasculature development. German et al. (2003) and Damari-Weissler et al. (2009), proposed that FRK is essential for the vascular development as the transgenic plant lines with antisense FRK showed deformed vasculature with reduced cambium activity and low callose deposition. The development of xylem and phloem depends on Suc metabolism; therefore, Suc must be first cleaved by either INV or SUS so that it can be metabolized. In the vascular tissues of tomato stems *SUS1*, *SUS2* and *FRK2* are highly expressed (German et al. 2003; Goren et al. 2011). Fru and UDP-G are the products of sucrose cleavage by SUS and both are believed to be central for development of vascular system. In cellulose and cell wall synthesis UDP-G is used, while Fru is phosphorylated so that it can be either utilized in energy production or fed into other metabolic pathways. Increase of Fru concentration from 0.5 to 1 mM led to feedback inhibition of SUS (Schaffer and Petreikov 1997a). Thus the phosphorylation of Fru by FRK2 might be necessary for the Suc cleavage, sugar metabolism, and cell wall synthesis that are essential for proper development of the vascular tissues (German et al. 2003 and Damari-Weissler et al. 2009). The

FRK plant mutants suggested that *FRK* genes are either essential or have highly redundant functions under normal growth conditions. Low tuber yield in potato was noticed by Davies et al. (2005) when the FRK activity was reduced by antisense suppression of *StFRK1*. In anther development, it was shown that FRKs played crucial role as developing anther was not photosyntheically active suggesting the requirement of Suc as energy source for development. FRK provides F6P and facilitates UDP-G in cellulose synthesis for elongation of cell wall as feedback inhibition of SUS by Fru could be insignificant (Karni and Aloni 2002). All these studies suggest that FRKs are crucial for carbon assimilation particularly in the sink tissues, and in development of vascular systems and seeds.

FRKs in potato: Potato (*Solanum tuberosum* L.) is a major non-grain food crop grown in many countries all over the world. It is autotetraploid and highly heterozygous so, a gene may exist in multiple forms. Tuberization is a complex process where a number of enzymes are involved. FRKs play a crucial role in potato tuber. Metabolic pathways of hexose sugars were considerably studied in developing potato tubers (Davies et al. 1985). Gardner et al. (1992) purified FRK from developing potato tubers and studied its catalytic and other biochemical properties. Smith et al. (1993) isolated and characterized a cDNA clone encoding FRK, and studied its expression in potato. Features of the *FRK* cDNAs, G+C content and structural features of the deduced proteins were reported by Taylor et al. (1995). Modulation of FRK activity in potato tuber metabolism, phenotypes of the FRK antisense lines and effects of *FRK* gene overexpression were examined in potato (Davies et al. 2005). In potato, high INV and HXK activities are associated at subapical region of non-tuberizing stolon during the early stage of tuberization; during the later stages of tuberization, FRK exhibits most of the hexose phosphorylating activity due to predominant SuSy-mediated Suc cleavage (Renz et al. 1993; Appeldoorn et al. 2002; Davies et al. 2005). Moreover, the catalytic role of FRK in sugar metabolism is required for the development of vascular tissues in potato tubers and other sink tissues (Granot et al. 2014).

2.3 Calcium ion (Ca^{2+}) Signaling in Plants

In plants, Ca^{2+} plays important physiological role such as growth, development and stress responses. Transient increase in cyotosolic Ca^{2+} concentrations is involved in cell signaling pathways which lead to the cellular changes like stomatal movement, increased water retention, defense from microbial attacks (DeFalco et al. 2010). Plant Ca^{2+} signatures are understood by

some calcium sensors such as calmodulins (CaMs), calmodulin-like proteins (CaMLs), calcineurin B-like proteins (CBLs) and Ca^{2+}-dependent protein kinases (CDPKs). Upon binding with Ca^{2+} ions these proteins undergo conformational changes, thus activating many downstream proteins. Among all these sensors, CDPKs are unique as they act Ca^{2+} ion responders (Patra et al. 2021). The role of CDPKs is recognized in the complex tuberization process. Some of the CDPKs are known to regulate the oxidative burst by activating NADPH oxidase. This explains the possibility of a cross-talk with an oxidative burst-mediated redox signalling pathway during tuberization. Recent advances on the CDPKs are precisely described below.

2.3.1 Calcium-dependent Protein Kinases (CDPKs)

The stress signals in plants are transduced by various primary and secondary messengers. Calcium (Ca^{2+}) acts as a universal secondary messenger in signalling pathways and regulates growth and development (Boudsocq and Sheen 2013). Several stimuli including hormones, elicitors (Romeis et al. 2001), light (Frattini et al. 1999), and different abiotic stresses change the intracellular Ca^{2+} concentration (Sanders et al. 2002) Calcium binding proteins and/or calcium sensors as mentioned earlier recognize changes in the intracellular Ca^{2+} concentration resulting in downstream expression events (Sarkar and Sharma 2010). CDPKs serve as special sensors as they can directly convert upstream Ca^{2+} signals into downstream protein phosphorylation events as they have both sensing and responding behaviour due to the presence of CaM-like and protein kinase domains (Poovaiah et al. 2013). CDPKs have been identified all over plant kingdom including some protozoans (Harper et al. 2004).

Structural aspects and activation of CDPKs: CDPKs (M_r: 40 to 90 kDa) are encoded by the multigene family in plants. They possess five distinct domains: N-terminal variable domain, kinase domain, auto-inhibitory domain, regulatory domain i.e., calmodulin-like domain (CaM-LD), and a C-terminal domain of variable length (Harmon et al. 2001). At the N-terminus region, the CDPK protein contains the variable N-terminal domain (VNTD) which is thought to be involved in substrate recognition. It also contains two another important sites i.e., N-myristoylation and N-palmitoylation that promote protein targeting towards the membrane i.e., localization of protein (Harmon et al. 2000). However, in response to various stresses the membrane targeted CDPKs can move away from membranes (Dammann et al. 2003; Benetka et al. 2008). Whereas the C-terminal region is responsible for binding Ca^{2+} ion (even at low

concentration), thus aiding in maintaining the ROS basal level. The C-terminal region also acts as stabilising region by triggering intramolecular binding between auto inhibitory domain (AID) and kinase domain. The calmodulin-like regulatory domain (CBD) contains the elongation factors (EF) hands, the calcium binding motifs. These features enable CDPKs to shuttle between various subcellular compartments as a way to accomplish a broader array of cellular functions. The catalytic domains along with the EF hands in CBD domain are shown in Fig.2.5.

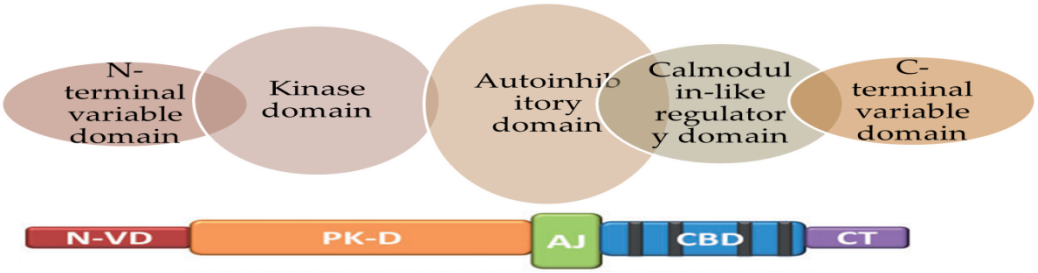

Fig. 2.5 Schematic view of the domains of Calcium dependent protein kinases (CDPKs)

The auto-inhibitory domain (AID) acts as pseudo-substrate and keeps the protein in inactive state in absence of Ca^{2+}. But after perception of environment cues in the form of calcium ions, CDPKs undergo conformational changes to make enzyme active by making enzyme free from pseudo substrate to promote phoshphorylation, thus regulating the activities of many of downstream proteins/enzymes (Harper et al. 2004). In the CDPKs, nearly conserved 24-aa protein kinase ATP binding signature (LGRGQFGVTYYCTENSTENPYACK) towards the N-terminal region and a 13-aa (VMHRDLKPENFLL) serine/threonine protein kinase-like domain containing Asp in the active site help in positioning the ligand-binding domain into the extracellular space (Kaur and Das 2022). The CDPK multigene family consists of at least 12 subfamilies which are derived from a common ancestor for both monocot and eudicots. CDPKs occur in both soluble and membrane bound forms, and found in multiple locations such as cyotosol, nucleus, ER, peroxisomes, mitochondria (Harper et al. 2004).

Localization CDPKs in plants: In plants, CDPKs exhibit distinct spatio-temporal expression patterns which might be responsible for their functional specificities (Zhang et al. 2015). They are found to be localized in the cytosol and various organelles like mitochondria, ER, tonoplast and chloroplast. Multiple localizations of CDPKs suggesting their variable affinities for different

substrates in a cell required for various cellular functions like stress response, signalling, and development (Schulz et al. 2013).

CDPK gene family: The modern molecular techniques unravelled the presence of CDPK multigene family in different plant species. Analyses of the genes, protein domain structures along with phylogenetic features and chromosomal localizations provided insights into the evolution and expansion of the CDPKs (Deepika et al. 2022). Genome sequencing and expressed sequence tags (ESTs) indicated the presence of multigene families of CDPKs in plants such as 34 genes for CDPKs in *Arabidopsis* (Cheng et al. 2002), 31 genes in rice (Ray et al. 2007), 29 genes in tomato (Hu et al. 2016 ; Wang et al. 2015), 40 in maize (Kong et al. 2013), 23 in potato (Gromadka et al. 2018; Kaur and Das 2022). Phylogenetic analyses in the earlier reports revealed that CDPKs from bryophytes to highly evolved angiosperms belong to four distinct groups i.e., I−IV (Hamel et al. 2014). Group I CDPKs are highest in number and found to be associated with pathogen resistance through convergent MAMP signalling; Group II members in membrane targeting and signal transduction pathways in response to environmental stresses; Group III members with ABF4 gene regulation, salt tolerance and stomatal opening and Group IV has lowest members involved in jasmonate pathway (Gargantini et al. 2009; Grandellis et al. 2012; Asano et al. 2012; Liese and Romeis 2013; Hu et al. 2016; Gromadka et al. 2018; Bi et al. 2021). The major motifs and domains were found to be conserved in plant species ranging from early land plant to modern plants. From the evolutionary analyses in some plants, it was predicted that gene duplication had played a central role in the expansion of CDPK gene family across the plants. For example, in *Arabidopsis* 8 and in rice 9 pairs of genes have underwent segmental gene duplication (Ray et al. 2007). Recent studies in Chinese cabbage, cotton, grapevine also supported the family expansion through segmental duplication (Wu et al. 2017; Liu et al. 2014; Chen et al. 2013). In mosses, the gene duplication was found to be a pivotal dragging force of duplication of CDPK gene family (Hamel et al. 2014). However in early plants like pteridophytes, gene duplication of CDPK genes was not observed, possibly explained their low numbers (Banks et al. 2011). Very likely, gene duplication events contributed to the expansion of CDPK gene family across the plant species resulting in high number of genes in the genome.

CDPKs in abiotic stresses: In plants, CDPKs are involved in responses to both abiotic and biotic stresses, ROS generation and homeostasis As an adaptive mechanism, plants undergo osmotic adjustments and accumulate one or more types of compatible solutes, such as proline or glycine

betaine, in response to low water potential, freezing, salinity, and other stresses that alter water status (Verslues et al. 2006). A few CDPKs were known to mediate abiotic stress responses through osmotic adjustment. Overexpression of *AtCPK6* resulted in drought tolerance via enhanced gene expression and accumulation of the compatible osmolyte proline (Xu et al. 2010). In contrast, AtCPK21 acts as a negative regulator of osmotic response, and inhibits proline accumulation (Franz et al. 2011). *OsCPK9* transcripts were induced by ABA, drought, and salt treatments. Overexpression and RNAi mutant analysis showed that OsCPK9 improved drought stress tolerance through increased stomata closure and osmotic adjustment (Wei et al. 2014).

ROS homeostasis and stress metabolism: CDPKs were found to regulate ROS homeostasis and acted as a shielding agent for plants against stress. In rice, CPK12 triggered the induction of ROS alleviating genes *OsAPX2/OsAPX8* and suppressed NADPH oxidase gene (Asano et al. 2012). Constitutive expression of OsCPK10 was found to be crucial in removing the excess of H_2O_2 through CAT (Bund´o and Coca 2017). In ginger, CDPK12 was found to induce exponentially in order to maintain homeostasis and combating the stress situations (Vivek et al. 2013). In *Arabidopsis* CDPKs, CPK3 and CPK27 regulated the sodium toxicity and calcium uptake through salt stress response and tolerance (Mehlmer et al. 2010; Zhao et al. 2015). Sajo et al. (2000) reported the role of CDPK7 in rice in providing enhanced cold tolerance. Plants tend to accumulate some amino acids like proline, glycine in response to the water deficit and stress conditions that changes the water potential (Verslues et al. 2006). Some of the CDPKs in various plants such as *Arabidopsis* AtCPK6 and rice OsCPK9 are considered to be important in the process of accumulation of the osmolytes (Xu et al. 2010; Wei et al. 2014).

ROS generation and cell death: In plant cell, CDPKs regulate ROS production when attacked by pathogens. NtCDPK2 and AtCPK1 from tobacco and *Arabidopsis*, respectively trigger ROS generation and hyper sensitive response such as cell death elicited by pathogens (Xing et al. 2001; Ludwig et al. 2005). Two isoforms in potato belonging to Group I namely StCDPK4 and StCDPK5 were found to phosphorylate NADPH oxidase and induce ROS production when attacked by *Phytopthora infestans* (Kobayashi et al. 2007). Transgenic plants overexpressing *StCDPK5* showed augmentation in ROS generation, and conferred resistance to late blight pathogen *P. infestans*, but remained susceptive to other pathogens (Kobayashi et al. 2012). Boudsocq et al. (2010) demonstrated that transformants of multiple mutants of *Arabidopsis* subgroup I showed ROS generation at low level in response to fungal elicitor Flg 22 suggesting

the importance of CDPK subgroup I members in ROS generation. However, the members of subgroup II appeared to be antagonist in defense responses, as hypothesized from the studies in rice, where overexpression of CPK12, a member of subgroup II, led to impairing of ROS generation became more sensitive towards viral and fungal pathogens (Asano et al. 2012). Likewise, in barley crop, HvCDPK3 led to decreased resistance towards powdery mildew fungus (Freymark et al. 2007).

Response to pathogen attack and immunity: The calcium influx into the cytoplasm was augmented when the pattern recognition receptors (PRRs) on plant cells recognized some pathogen associated molecular patterns (PAMPs) (Akira et al. 2006). The calcium signals were then decoded by the CDPKs into defense responses by phosphorylating various enzymes leading to accumulation of phytohormones and expression of defense-related genes. In tobacco, NtCDPK2 was involved in plant defense reaction and activated by fungal effector (Avr9) in leaves which led to activation of jasmonate and ethylene regulated defense system (Romeis et al. 2001; Ludwig et al. 2005). Tomato LeCDPK2, a homologue to tobacco CDPK2, was known to be involved in ethylene production and defense response (Kamiyoshihara et al. 2010).

CDPKs and plant development: Apart from stress signaling and responses, CDPKs are thought to play a central role in various physiological process of plant growth and development. In *Arabidopsis*, the growth of pollen tube is directly related to the expression of multiple CDPK forms. Some CDPK isoforms are involved in growth of pollen tube as double mutants of these forms drastically affected the development of pollen tubes (Myers et al. 2009). Ion flux is crucial for pollen elongation, where CPK 11 and 24 worked together to facilitate the influx of ions for pollen tube elongation (Zhao et al. 2013). Another ion channel namely SLAH3 was found to be regulated by CDPKS namely CPK 2 and 20, indispensable for pollen tube growth (Gutermuth et al. 2013). CDPKs are also considered to modulate the plant growth regulators. In rice CDPK isoform (OsCPK13) was found to induce plant hormone gibberellin (Abbasi et al. 2004). Likewise, in tobacco NtCDPK1 was found to phosphyorylate bZIP transcription factor involved in GA biosynthesis (Ishida et al. 2008). In model plant *Arabidopsis*, a CDPK isoform (AtCPK28*)* was also found to be crucial in development of stem, petiole and secondary growth as the mutants lacking the function of ATCPK8 showed developmental defects (Matschi et al. 2013). Such defects could be due to the disturbance in balance between the phytohormones, particularly Jasmonate and GAs (Matschi et al. 2015). In *Arabidopsis*, CDPKs were found to play a

significant role in floral transition and flower development (Kawamoto et al. 2015). *Arabidopsis* CDPK-related kinase 5, was found to be associated with root elongation through auxin signaling (Rig´o et al. 2013). CDPKs were found to be key players in plant immune signalling, nitrogen-deficiency induced oil accumulation and protein-protein interaction networks (Bredow and Monaghan 2019; Li et al. 2019; Ahmed et al. 2020; Marques et al. 2022).

CDPKs in potato: The role of CDPKs is well-recognized in the complex tuberization process in potato (Raices et al. 2003). CDPK activities with different substrate and cellular specificities are known to play important role in potato life cycle. StCDPK3 was predominantly expressed during early initiation of stolon elongation, while StCDPK1 was expressed during apical swelling in the stolon tip and acted as a mediator in Suc synthesis during tuber growth and development; StCDPK2 was expressed during tuberization and in leaves (Raices et al. 2003). StCDPK2 was crucial role in light sensing and stress metabolism (Grossi et al. 2022). StCDPK1 has conserved myristoylation sites, and found to trigger the signal cascades and initiate the apical swelling in the stolon leading to tuberization (Raices et al. 2001). StCDPK4 and StCDPK5 were identified as modulators of early defense reactions in response to the challenges from *Phytophthora infestans* in potato (Kobayashi et al 2007). Fantino et al. (2017) characterized StCDPK7, a CDPK isoform which was induced upon infection with fungal pathogen *P. infestans*. The analysis of CDPK gene family and an insight into potato genome was done by Gromadka et al. (2018). A total of 26 CDPKs, belonging to four CDPK groups were proposed in this study. Apart from these forms, other CDPK isoforms were known to be crucial in stress metabolism (Bi et al. 2021). Sciorria et al. (2021) reported two CDPK isoforms from potato namely StCDPK22 and StCDPK24, belonging to CDPK group III which conferred resistance towards heat stress.

2.4 ROS Signaling

Aerobic metabolism and various stresses are considered to be the major contributory factor for generation of the reactive oxygen species (ROS) in all the living systems. In plants, various ROS that include species of active oxygen, H_2O_2 ((hydrogen peroxide), O_2^- (superoxide), $OH^\bullet$ (hydroxyl radical) and $^1O_2$ (singlet oxygen) are produced at varying degrees depending on the cell or tissue types. The generation of ROS is a common cellular process; however, their damaging effects are usually eliminated by different enzymatic and non-enzymatic antioxidant mechanisms. Plant cells have evolved enzymatic and non-enzymatic defence pathways to overcome the hazard

caused by the presence of ROS. The enzymatic components comprising the superoxide dismutase (SOD), ascorbate peroxidise (APX), guaiacol peroxidise (GPX), glutathione-S-transferase (GST), and catalase (CAT); the non-enzymatic low molecular compounds like ascorbic acid (AA), reduced glutathione (GSH), α-tocopherol, carotenoids, phenolics, flavonoids, and proline (Das and Roychoudhury 2014; Verma et al. 2022). In plants, different types of stresses such as salinity, drought, extreme temperatures, heavy metals, pollutants, high irradiance, infection by pathogens lead to an imbalance situation between ROS generation and their scavenging referred to as oxidative stress (Foyer and Noctor 2005; Lee et al. 2012; Das and Roychoudhury 2014). According to Jones (2006), oxidative stress could be regarded as disruption of redox signalling and control mechanisms in a cell. ROS are known to be toxic as they cause damage to various cellular components; however, they play role in redox signalling involved in plant growth and development. H_2O_2 is considered to be the most frequently occurring ROS in the biosphere. Certain oxidases catalyze the production of H_2O_2 directly by a process of two-electron reduction of O_2. Different oxidases and peroxidases catalyse the production of O_2^- during photosynthetic and respiratory electron transport which is in turn converted to H_2O_2 via reduction or dismutation (Foyer and Noctor 2000; Mittler et al. 2004; Bindschedler et al. 2006; Sagi and Fluhr 2006). In unicellular organisms, H_2O_2 is known to stimulate production of antioxidants along with ROS removing and repairing enzymes; whereas in multicellular organisms it is involved in activation of the signalling pathways related to developmental processes (Melov et al. 2000). H_2O_2 in excess leads to formation of harmful $OH^{\bullet}$ radical through decomposition by fenton type of reaction (Cabiscol et al. 2003). Therefore, rapid and efficient removal of H_2O_2 by cellular antioxidant machinery is essential for normal metabolism.

2.4.1 Catalases (CATs)

Catalase (CAT H_2O_2:H_2O_2 oxidoreductase; EC 1.11.1.6) is known to be the first antioxidant enzyme which was discovered and characterized in the living organisms. The metabolic importance of this enzyme is reflected from its widespread occurrence in the animals, plants, bacteria and the other forms of life including some anaerobes (Kirkman and Gaetani 2007; Zamocky et al. 2008). Extremely rapid dismutation of two molecules of H_2O_2 to water and O_2 is a distinct catalytic reaction in which H_2O_2 acts as both acceptor and donor of hydrogen molecules (Scandalios et al. 1997) as depicted in Fig. 2.6. Catalase along with superoxide dismutase and

hydroperoxidase constitute a major defense system involved in scavenging superoxide radicals and hydroperoxides.

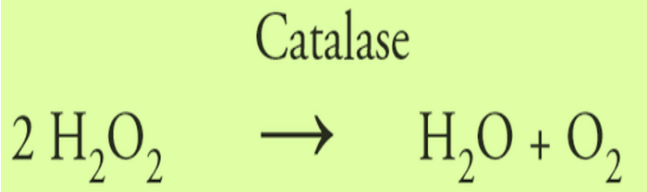

Fig. 2.6 Dismutation of H_2O_2 by Catalase (CAT)

Structural and biochemical properties of CAT: Except some bacterial nonheme manganese-containing catalases (Mn-catalases), typically most of the well-known prokaryotic and eukaryotic catalases are haem-based i.e., bearing a haem prosthetic group, monofunctional consisting of polypeptides of M_r~50–70 kDa, and organized into tetramers (Regelsberger et al. 2002; Chelikani et al. 2004; Zamocky et al. 2008). In some fungi and prokaryotes, a second type of bifunctional haem-dependent catalase i.e., catalase-peroxidases are present. Sometimes it is difficult to distinguish between the aforesaid types as the monofunctional type is able to catalyse H_2O_2-dependent peroxidation of the organic compounds (Zamocky et al. 2008). Bifunctional catalase-peroxidases differ distinctly with monofunctional catalases with regard to the following attributes: closer to the haem-containing peroxidases e.g., APX and fungal cytochrome c peroxidise, higher affinities for H_2O_2 and relatively insensitive to the inhibitor 3-amino-1,2,4-triazole (3-AT) (Regelsberger et al. 2001; Mhamdi et al. 2010). Growing body of evidences clearly suggest that various plant catalase genes differ with regard to spatio-temporal nature of expression, and their responsiveness to developmental and environmental stimuli (Guan and Scandalios 1996; Zimmermann et al. 2006; Du et al. 2008). In tobacco, several types of *CAT* mRNA transcripts namely *CAT1*, *CAT2*, and *CAT3* were found to be expressed differentially; the former two transcripts were detected in non-senescent leaves whereas the latter one was found in both non-senescent and senescing leaves (Niewiadomska et al. 2009). In maize, *CAT1*, *CAT2* and *CAT3* transcripts were detected at various stages of seed kernel development (Acevedo and Scandalios 1990; Acevedo et al. 1991). Catalases were intensely investigated in *Arabidopsis* at biochemical, molecular and genetic levels.

CAT gene family: As evident from several genetic and molecular studies, catalase in plants has multiple forms encoded by a relatively small gene family e.g., four candidate *CAT* genes were found in cucumber; three members of this family were reported in each of the following species namely *Arabidopsis*, tobacco, maize, and pumpkins, whereas cottonseed and barley contain only two members (Hu et al. 2016). On the basis of their expression, catalases were categorised into different classes namely; Class I, Class II and Class III. Class I is found to be expressed in photosynthetic tissues, Class II in vascular tissues and Class III in reproductive tissues (Willekens et al. 1995). Various plant catalase genes differ with regard to spatio-temporal nature of expression, and their responsiveness to developmental and environmental stimuli (Scandalios 1992; Guan and Scandalios 1996; Zimmermann et al. 2006; Du et al. 2008). In tobacco, several types of CAT mRNA transcripts namely *CAT1*, *CAT2*, and *CAT3* were found to be expressed differentially; the former two transcripts were detected in non-senescent leaves, whereas the latter one was found in both non-senescent and senescing leaves (Niewiadomska et al. 2009). In maize, *CAT1, CAT2* and *CAT3* transcripts were detected at various stages of seed kernel development (Acevedo and Scandalios 1990; Acevedo et al. 1991).

Role of Catalases: Catalase plays a crucial role in the various processes of the plant life cycle such as development, defense, and senescence. Some processes of aerobic metabolism like mitochondrial electron transport, β-oxidation of fatty acids, photorespiratory oxidation are inherently associated with the generation of H_2O_2 which in turn is scavenged by catalases (Yang and Poovaiah 2002). This explains why the plant mutants lacking catalase activity are unable to sustain under such conditions. Drought conditions are known to trigger oxidative stress in plants resulting in more accumulation of H_2O_2. Under such situation, transgenic tobacco overexpressing the *E. coli* katE gene appeared to be tolerant to high irradiance as compared to the control wild plants affected severely by photosynthesis induced damages (Shikanai et al. 1998). Transgenic tobacco *CAT1* antisense lines showed markedly reduced level of CAT activity along with necrotic lesions in some of the lower leaves (Takahashi et al. 1997). Arabidopsis catalase 2 knock-out mutants (*cat2*) were found to have elevated level of H_2O_2 and associated with the widespread necrotic lesions (Queval et al. 2007). Exogenous application of sweet potato CAT i.e., SPCAT1 fusion protein was found to be effective against ethephon-mediated leaf senescence and H_2O_2 accumulation elevation clearly suggesting the crucial role of catalase role in H_2O_2 homeostasis in leaves (Chen et al. 2012).

Organ-specific expression patterns of the three genes were demonstrated, and their expression patterns were differentially affected by the exogenous factors like light, ozone, UV irradiation, and SO_2 (McClung, 1997; Zhong and McClung, 1996). Differential expression of the *CAT* genes was intensely investigated in Arabidopsis as evident from several reports. For example, *CAT1* and *CAT2* are expressed in leaves and siliques, whereas *CAT3* expression was noticed in stem and root. Circadian rhythms had impact on the expression of *CAT2* and *CAT3*. Under cold and drought stresses, CAT2 was activated; abscisic acid, oxidative treatments, and senescence could trigger the activation of CAT3 (Du et al. 2008; Hackenberg et al. 2013; Li et al. 2013; Zou et al. 2015). In hot pepper, several forms of CAT namely, CaCAT1- CaCAT3 were found to differ with regard to organ-specific expression patterns and also responsive to the circadian rhythms and stress treatments (Lee and An 2005). CAT activity was found to be crucial in some physiological processes such as embryogenesis and cell death in *Pinus sylvestris* (Vuosku et al. 2015).

In tobacco, out of four *CAT* genes three showed differential spatio-temporal expression patterns. The abiotic factors like ozone, SO_2, irradiation, light and temperature influenced their expression (Willekens et al. 1994, 1997). Several stresses such as heavy metals, osmotic agents, plant hormones and high light irradiances were found to show differential response of a *CAT* gene, namely *PgCAT1* expression in ginseng (Purev et al. 2010). In banana, *MaCat2* transcript level was elevated by cold treatment and physical damage (Figueroa-Yáñez et al. 2012). Various abiotic stresses such as oxidative, heavy metal (Cu^{2+}), hyperosmotic (PEG and NaCl) and some other stresses like treatment with plant hormones such as salicylic acid (SA), methyl jasmonate (MeJA), and ABA, and threat from the fungal pathogen namely *S. scitamineum* could trigger the expression of *CAT* gene in sugarcane (Su et al.2014). Two catalase genes from *Erianthus arundinaceus* and *Saccharum officinarum* namely *EaCAT-1b* and *SoCAT-1c* were reported recently. Under drought situation, the former was up-regulated and the latter was down-regulated (Liu et al. 2016). The spatio-temporal expression patterns of the CAT isoforms under the abiotic stresses clearly suggested their protective role in plant defence (Su et al.2014). This explains why over expression of *CAT* genes are important in generating stress tolerant plants.

Studies on CAT in potato: Considerable progress has been made on CAT and other antioxidants in potato to date. Appleman (1910) proposed that CAT activity was influenced by the structural aspects, and in potato it was dependent on respiratory activity. At low temperatures, the respiration is low and CAT activity was also low. Beaumont et al. (1990) isolated and purified

CAT, a tetramer of 56 kDa subunits and devoid of NADPH, from peroxisomal fraction of mature potato tubers. Cyanide, azide and thiols were found to act as inhibitors of this enzyme. Cultivar-dependent differences of antioxidative capacity in terms of SOD, CAT and α-Tocopherol content under stresses were also reported in potato tubers (Spychalla and Desborough 1990). Wu and Shah (1995) isolated and characterized a 1772-bp *CAT1* cDNA clone from the mature root of potato cultivar, Russet Burbank. The distinct expression patterns of various antioxidant enzymes were noticed during tuber dormancy and oxidative stress due to soil drought (Rojas-Beltran et al. 2000; Boguszewska et al. 2010). Enhanced activities of some antioxidant enzymes including CAT along with the changes in isoenzyme composition were reported in the potato cultivars under salt stress (Rahnama and Ebrahimzadeh 2005). Santos et al. (2006) studied the differential expression pattern of two isoforms CAT1 and CAT2 in non-photosynthetic organs and during the development of photosynthetic organ (leaf). CAT1 was associated with photorespiration whereas CAT2 was found to fulfill multiple physiological roles.

Boguszewska et al. (2010) carried out experiments with ten potato cultivars which differed in dehydration tolerance. They were grown in a vegetation house under natural condition with optimal water supply till maturity except some of the plants were subjected to soil drought conditions for 2 weeks. Water deficit even for such brief period of time grossly compromised the desirable attributes of potato tubers including yield losses. Apart from the diminished relative water content (RWC), enhanced accumulation of ROS as noticed under stresses had deleterious effects on structure and function of different biomolecules in the growing tubers. As evident from the experimental data, significantly increased activities of some antioxidative enzymes like peroxidase, superoxide dismutase and CAT could protect the plants from oxidative stress. CAT activities at different stages of tuberization and in the leaves and stems were estimated in some Indian potato cultivars having varying genetic makeup and maturation time. CAT expression patterns clearly suggested its protective role in combating stress during tuberization. Three phase partitioning was found to be efficient in purification of CAT (Kaur et al. 2020).

2.5 Our National Scenario of Potato Research

Currently, food security and nutritional aspects are the major concerns all over the world, mostly in the developing nations. India is an emerging and fast developing nation with exponentially expanding population, and facing burgeoning issues of meeting the food demand and challenges

due to changing climate. Potato is a promising non-grain food crop to meet the nutritional demand to fight both hunger and malnutrition. Moreover, demand for the commercial processed potato products has significantly increased due to rapid urbanization, modernization along with expansion in tourist trades. Potato is a major vegetable in India; so there is an urgent requirement to supply adequate amounts quality potatoes as raw materials round the year.

Since, after independence of India in 1947, a large number of potato cultivars have been released by CPRI (Central Potato Research Institute, Shimla) mostly through conventional breeding programmes. These cultivars considerably vary with regard to the processing attributes, crop yield, genetic makeups, disease resistance and suitability to different agro-climatic conditions in the Indian subcontinent. Although many potato varieties are available in our country but not all of them are suitable for processing industries. For example, the potatoes required for processing need to have 21-23% tuber dry matter and reducing sugars below 150 mg per 100 g fresh weight of tubers. Because the texture and quality of processed potato products largely depend upon the two most important parameters, the tuber dry matter and reducing sugar content. Some of the processing varieties include Kufri Chipsona-1, Kufri Chipsona-2, Kufri Chipsona-3 along with a few other notable medium-maturing varieties. Several morphological and biochemical attributes of Chipsona varieties are oblong fleet creamish white tubers, high starch content. Apart from consumer acceptance, these attributes are desirable for making fries and other processed products. Some other salient features of the Indian cultivar varieties include resistance to late blight, ability to give high yields under short days, less duration growing periods suitable for the plains, tolerance to several pathogenic viruses, immunity to wart disease and resistance to nematodes. All these important attributes in potato clearly reflect the success of our conventional breeding programmes. Some laboratories are also involved in improving the nutritive quality of potato tubers (Chakraborty et al. 2000). Apart from this, efforts are being made to develop the varieties that accumulate low levels of the soluble sugars during storage at low temperatures.

2.6 Origin of the Problem & Objectives of the Thesis Work

Potato is the most important non-grain food crop in many countries including India. Potato is an example of C3 plants having a low assimilative power and dependent upon the environmental conditions (Powell et al. 2012). Apart from improving the yield, tuber quality and increasing resistance to pathogen infection, research efforts of many laboratories are directed towards

improving the nutritional aspects of the tuber. Currently, plant molecular farming is gaining importance where potato system plays a crucial role. Many commercially important proteins/enzymes, novel organic compounds could be produced by using potato as a 'natural bioreactor'. Therefore, in-depth studies on the developmentally-regulated tuberization i.e., initiation to formation mature tubers could help for possible manipulation of these processes though modern biotechnological approaches and state-of-the-art molecular techniques.

Various environmental, physiological and hormonal control mechanisms are known to be crucial at different physiological stages of potato life cycle; still the underlying molecular orchestrations remain to be elucidated. Developmentally-regulated Suc and starch metabolism, Ca^{2+} signalling, ROS metabolism with enzymatic/non-enzymatic antioxidants, and many other factors are inherently associated with the complex tuberization process at various stages of growth and development under normal and stress conditions. For example, apoplastic phloem loading during initiation of tuberization is related with Suc metabolism which leads to molecular and biochemical changes that activate Ca^{2+}-signaling and ROS-driven gene expression (Sarkar and Sharma 2010). Many investigators pay attention to understand their role at various stages of potato life cycle, particularly during tuberization as multiple signaling pathways influence this complex process where a cascade of various signaling molecules, number of transcription factors and enzymes are involved. Literature survey and database search clearly indicated that in potato, there is ample scope of in-depth studies on multiple enzymes such as Sucrose synthases, Fructokinases, Calcium-dependent protein kinases and Catalases at both biochemical and molecular levels. Genome wide identification and characterization of the corresponding genes, predicted proteins and their crucial motifs/ domains, 3-D structures, expression patterns in various organs and different stages of tuberization still remain fascinating areas of investigation in potato in comparison to tomato system. Such studies are required for crop improvement.

Most of the potato cultivars are autotetraploid (*2n=4x=48*), and highly heterozygous. High level of DNA polymorphism and multiple allelism and natural allelic variations because of cumulative mutations in the potato genome are well known (van de Wal et al. 2001; Draffehn et al. 2010). Multiple forms of the individual genes are common in potato. Literature search clearly indicated that there is no comprehensive report available till date on the various aspects of tuber development with regard to the Indian potato cultivars. These potato cultivars vary with regard to genetic makeup, maturation time, tuber dry matter, starch quality (i.e., amylose to amylopectin

ratio, glucan chain lengths) and sugar contents. Some of them are processing varieties such as Kufri Chipsona-1, Kufri Chipsona-2. Therefore, the rich genetic resources of the Indian potato cultivars could be explored for isolation, characterization and studying expression patterns of different allelic variants of the genes expressed at various stages of tuberization.

Keeping in view with the importance of Suc/starch metabolism, Ca^{2+} and ROS signaling as described earlier, this thesis focused mainly on the molecular, biochemical and *in silico* studies on a few crucial enzymes namely SuSy, FRK, CDPK, and CAT in a commercially important Indian potato cultivar, Kufri Chipsona-1 (KC-1) with the following Objectives.

❖ Objectives of the Thesis Work

- Molecular cloning and characterization of cDNAs encoding Sucrose synthase, Fructokinase, Calcium-dependent protein kinase and Catalase from an Indian potato cultivar
- Sequence analyses of the enzymes for identifying the characteristic sequence features
- To study the expression patterns of the enzymes in different potato organs including various stages of tuber development

Chapter 3

Materials & Methods

3.1 Materials

3.1.1 Procurement of Plant and Other Materials

The germplasm of high-yielding, commercially important Indian potato cultivar Kufri Chipsona-1 (KC-1) was procured from Central Potato Research Institute (CPRI), Shimla, India. Short name of this potato cultivar is shown within parenthesis.

Chemicals/biochemicals: Various chemicals/biochemicals/molecular biology items were procured from different vendors. The chemicals were purchased from Sisco Research Laboratory Pvt. Ltd., Mumbai, Qualigens Fine Chemicals, Merck, CDH Pvt. Ltd., New Delhi, and HiMedia Laboratories, Mumbai. Various enzymes used were purchased from Bangalore Genei Pvt. Ltd., Bangalore and Amersham Biosciences Ltd., Hongkong. The oligonucleotide primers used in the study were synthesized from Bangalore Genei Pvt. Ltd., Bangalore. All salts and additives were purchased from HiMedia Labs Ltd. and plant growth regulators from Sigma chemicals, USA. The gel extraction Qiagen Kit was purchased from Genetix. Glasswares and Plasticwares were from Borosil and Tarsons Products Pvt. Ltd.

3.1.2 Maintenance of Potato Germplasm

The potato cultivar KC-1 is a medium maturing cultivar bred by CPRI, Shimla in 1998 suitable for Indo-Gangetic plains of India which produces oblong fleet tubers. Apart from consumption as a vegetable, this is suitable for the commercial potato processing sectors (Kumar, 1998). It was routinely micropropagated in our laboratory under controlled conditions (25–27 ºC, ~70 % relative humidity under 16 h photoperiod with a light intensity of 40−42 μmol m^{-2} s^{-1} spectral flux photon of photo-synthetically active i.e., 460−700 nm radiations) on MS-basal medium with 2.5 % sucrose at 4–5 wk intervals.

3.1.3 Bacterial Strains and Vectors

Cloning host: E. coli DH5α: supE44 ΔlacU169 (Φ80 lacZΔM15) hsdR17 recA1 endA1 gyrA96 thi-1 *rel*A1. *E. coli* DH5α strain was maintained on Luria agar medium. *E. coli* transformed with pUC19 plasmid was maintained on Luria agar medium containing 50 μg mL^{-1} of ampicillin.

Cloning vector: pUC19 Vector: pUC19 (GenBank Acc. No: X02514; 2686 bp) is a commonly used high copy number plasmid vector in *E. coli* (Yanisch-Perron et al. 1985). This plasmid vector contains a 54-bp multiple cloning site (MCS) having unique sites for a number of different hexanucleotide-specific restriction endonucleases. The salient genetic features along with some restriction sites are shown in Fig. 3.1.

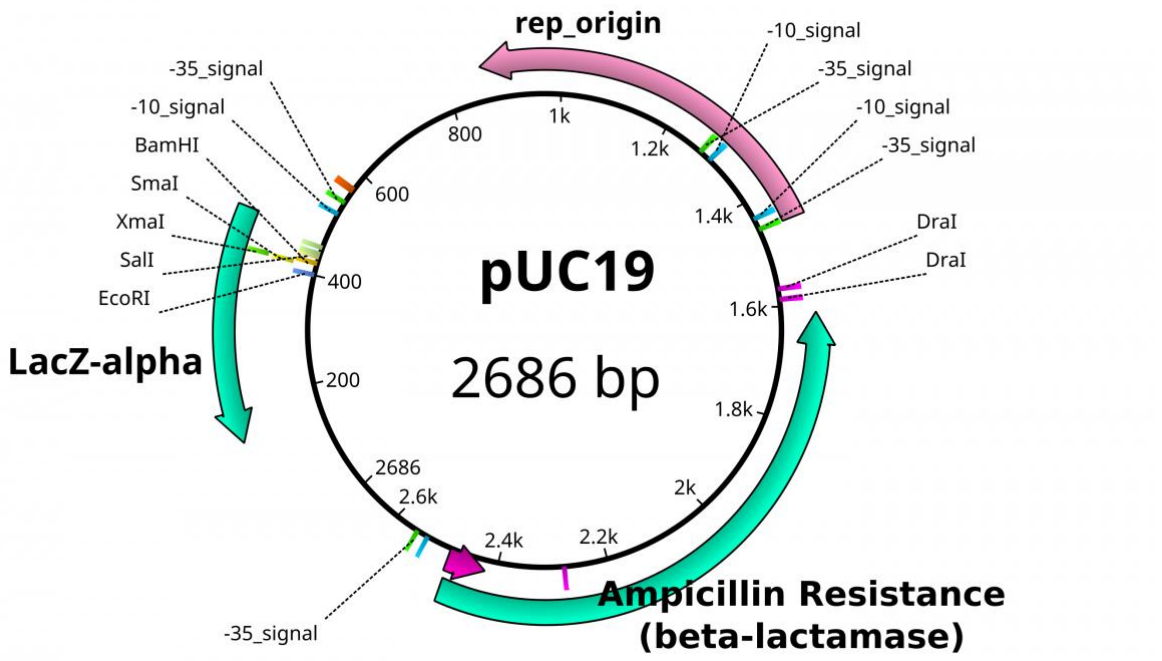

Fig. 3.1 Feature map of pUC19 including the locations of some restriction enzymes (Source: https://openlab.citytech.cuny.edu/bio-oer/files/2015/07/pUC19.png)

3.2 Methods for cDNA Cloning Studies

To obtain different full length cDNA clones, the following steps remained common:

- Gene-specific primers were designed based on the reference sequences.
- Total RNA was isolated from the field-grown potato organs.
- Oligo $(dT)_{18}$ -mediated first strand cDNA synthesis
- Polymerase chain reaction (PCR) using gene-specific forward and reverse primers
- Processing and purification of the PCR-amplified DNAs
- Ligation of the individual PCR-amplified DNAs into the plasmid vector
- Transformation of the *E. coli* strain with the ligation products and screening
- Identification of the cDNA clones, sequencing and submission to GenBank, NCBI

The details of the above steps are described below:

3.2.1 Designing of Oligonucleotide Primers

To minimize non-specific amplifications, the following points were considered for designing the gene-specific primers:

- G+C content was kept around 40–60%.
- The length of oligonucleotides was kept around 20 mers, neither too short or long.
- Self-complementarity or complementarity between the primers to be avoided.
- Primers with melting temperatures should be in the range of 52–58°C.

The details of the gene-specific oligonucleotide primers are described below:

Sucrose synthase (SuSy)-specific primers: The following oligonucleotide primers were designed based on a potato *SuSy* cDNA sequence reported earlier (M18745; Salanoubat and Belliard 1987): a forward primer SSF1-0025, 5′-TCTCAAAGTTGAACTTTGTC-3′ (corresponding to the bases 25–44); and two reverse primers namely SSR1–0986, 5′-ACA ACCTGGCCACCG GTGTC-3′ (complementary to the bases 967–986), and SSR3-2693, 5′-ATCTCTTATTC ATACCAACAG-3′ (complementary to the bases 2673–2693).

Fructokinase (FRK)-specific primers: The following oligonucleotides were designed based on a potato *FRK* cDNA sequence corresponding to FRK2 form (Z12823; Smith et al. 1993): a forward primer F1-FK0001, 5′-CATCGTCGCCATGGCAGTTA-3′ (corresponding to the bases 1–20); and two reverse primers namely R1-FK0606, 5′-TCGAGTTCCACATCGC TGAC-3′ (complementary to the bases 587–606), and R2-FK1110, 5′-TGATGGACCGTAT CACAACA-3′ (complementary to the bases 1091–1110).

To investigate the role of FRK forms in stress metabolism, a few more primers were designed based on a *FRK2* allele (i.e., *FRK2A*) and Fructokinase-like (FLN) protein. The following oligonucleotide primers were based on the potato *FRK* cDNA sequence (JX576230; Gangadhar et al. 2014): a forward primer F2B-FK01, 5′-GATGCTCGCCGGGATTCTGA -3′ (corresponding to the bases 1–20); and two reverse primers namely RU-FK373, 5′-ATAGT TCCAGATGCTCTTGA-3′ (complementary to the bases 354–373), and R1-FK784, 5′-AA CATGATGTTTCTATGCTC-3′ (complementary to the bases 765–784). With regard to the FLN form (JX576279; Gangadhar et al. 2014), a forward primer FLF1-0001, 5′-GCTCCT CCTCTTCTCTCT-3′ (corresponding to the bases 1-20); and the two reverse primers namely FLR1-500, 5′-TCCGTAGTGGAACACCTTAG-3′ (complementary to the bases 481–500), and FLR2-876, 5′-AGAATCACCAGCTCAGTG-3′ (complementary to the bases 858–876) were designed.

Calcium-dependent protein kinase2 (CDPK2)-specific primers: On the basis of a potato *CDPK2* (AF418563, Raices et al. 2003), the following oligonucleotides were designed: a forward primer, SC2F1-0001; 5′-ATGGGTATTTGTGCTAGTA-3′ (bases 1–19) and two

reverse primers namely SC2R1-0920 (complementary to the bases 901–920, 5′-AGGTC CTTGGCACTACTTGA-3′) and SC2R2–1560 (complementary to the bases 1541–1560), 5′-GACCTTGCCTGGTTATTTGG-3′).

Catalase (CAT)-specific primers:: To study ROS metabolic aspects in potato, the following oligonucleotides were designed based on a potato CAT cDNA (U27082): a forward primer F1-CT0001, 5′-CCATGGATCCGTCTAAGTAT-3′ (corresponding to the bases 1–20); and two reverse primers namely R1-CT403, 5′-TCAAAGTTACCACCTCTGTTG-3′ (complementary to the bases 383–403), and R2-CT1600, 5′-GTACAAATACAACATTACGAT-3′ (complementary to the bases 1580–1600) (Wu and Shah 1995).

Constitutive gene Actin-specific primers: Actin (M_r~41.8 kDa) is widely expressed in eukaryotic cells, often being the most abundant protein and commonly making up of 10% of the total cell protein: For internal control, the following primers were designed based on a potato actin gene i.e., *S. tuberosum* actin-65 (XM_006348930): a forward (F1-AC0591, 5′-CCACATGCTATCCTTCGTCTC-3′) and a reverse (R1-AC1149, 5′-TCCACATCTGTTG GAAGGTAC-3′) primers.

3.2.2 Isolation of total RNA from the Potato Organs

Plant tissues contain high amount of polysaccharides, phenolics, nucleases and other storage materials. Therefore, isolation of total RNA from different plant materials in terms of intactness and quality is relatively difficult. A number of methods are reported in the literature. Here, we used SDS-Phenol method described by Gilman (1987) with some modifications depending upon the nature of plant material.

The individual plant materials (0.2 to 1.0 g) were frozen and pulverized in the liquid nitrogen to a fine powder. The contents were mixed in a buffer containing lithium chloride (LiCl) and SDS (the composition of RNA extraction buffer: 100 mM LiCl, 100 mM Tris-HCl pH 8.0, 10 mM EDTA pH 8.0, 1.0% SDS, 0.2% β-mercaptoethanol) followed by direct extraction with phenol:chloroform (1:1). Under ice-cold condition, one-third volume of 8.0 M LiCl was added to the supernatant, and incubated for minimum of 2 h for selective precipitation of RNA. The crude RNA was further purified by RNase-free DNase treatment followed by solvent extraction and ethanol precipitation. RNA was then dissolved in RNase-free deionized water, and kept in aliquots at -70^{0}C for further use. The quality of the total RNA preparations was checked by regular and formaldehyde agarose gel electrophoresis along

with RT-PCR using different potato gene-specific primers. The analysis, A_{260}/A_{280} ratio of the RNA samples were also measured spectrophotometrically to check the quality.

3.2.3 Formaldehyde Agarose Gel Eectrophoresis

Total RNA samples were denatured by the treatment with formamide and separated by electrophoresis through agarose gel containing formaldehyde (Sambrook et al. 1989). For 100 mL agarose gel (1.5%) : 1.5 g of agarose in 62 mL of sterile water was boiled and cooled up to 55ºC. 20 mL of 5X MOPS buffer and 18 mL of deionized formaldehyde was added. The gel was cast in gel apparatus and was allowed to set for 1 h at room temperature. The gel was submerged in the 1X MOPS electrophoresis buffer. RNA samples were prepared as follows: 10.0 µL of RNA, 2.0 µL of 5X MOPS electrophoresis buffer, 3.0 µL of formaldehyde, 7.0 µL formamide and 1.0 µL ethidium bromide (200 µg mL^{-1}) were mixed. The samples were incubated at 65ºC for 15 min and immediately chilled on ice. 3.0 µL of formaldehyde gel loading buffer was added and loaded in the gel and electrophoresis was carried out at 4–5 V cm^{-1}. Composition of 5X MOPS Buffer: 0.1 M MOPS (pH 7.0), 40 mM sodium acetate, 5 mM EDTA (pH 8.0); formaldehyde gel loading buffer: 50% glycerol, 1.0 mM EDTA (pH 7.5), 0.25% Bromophenol Blue.

3.2.4 Reverse Transcription (RT)

Reverse transcription (RT) was carried out using the RevertAid^{TM} H Minus First Strand cDNA Synthesis Kit with Moloney Murine Leukemia Virus (M-MuLV) Reverse Transcriptase (Fermentas Life Sciences). The enzyme lacks Ribonuclease H activity specific to RNA in RNA:DNA hybrids. Therefore, degradation of RNA does not occur during first strand cDNA synthesis, resulting in higher yields of full-length cDNA from long templates up to 13 kb. In the reaction mixture, 1.0–2.0 µg of total RNA was mixed with 1.0 µL of oligo $(dT)_{18}$ or gene specific reverse primer and made the reaction volume 10.0 µL in ice. Then the mixture was incubated at 70ºC for 5 min and quickly chilled on ice. 4.0 µL of reaction buffer (5X), 1.0 µL of RiboLock Ribonuclease inhibitor and 2.0 µL of 10 mM dNTPs mix were added and mixed well. Then reaction mixture was incubated at 37ºC for 5 min. 1.0 µL of Revert Aid H Minus M-MuLV reverse transcriptase was added and incubated at 39ºC for 60 min. The reaction was stopped by heating at 70ºC for 10 min and then quickly chilled on ice.

3.2.5 Polymerase Chain Reaction (PCR)

PCR consists of three cycling parameters, heat denaturation of DNA template to open the two strands of DNA, and annealing of the oligonucleotide primers to single stranded DNA templates, and extension of the primers to replicate DNA by DNA polymerase.

The PCR was usually set in 50 µL reaction volume as: 5µL of 10X PCR buffer, 0.5–1.0 µg template DNA, around 10 pmoles of each forward and reverse primer, 2.5 µL of 2.5 mM dNTPs mix, 1.0 µL (1U μL^{-1}) *Taq* DNA polymerase and finally the volume was made up to 50 µL with sterile water. After initial denaturation at 94ºC for 1 min 30 s, the thermal cycling parameters were set according to the different genes: for *SuSy*, denaturation at 94ºC for 1 min 30 s, annealing at 55ºC for 2 min; polymerization at 72ºC for 3 min for 30 cycles followed by final extension at 72ºC for 5 min; for *FRK* and *FLN*, denaturation at 94ºC for 1 min, annealing at 55ºC for 2 min; polymerization at 72ºC for 1 min for 30 cycles followed by final extension at 72ºC for 5 min; for *CDPK*, denaturation at 94ºC for 1 min, annealing at 50ºC for 2 min, polymerization at 72ºC for 2 min for 30 cycles followed by final extension at 72ºC for 5 min; and for *CAT* denaturation at 94ºC for 1 min, annealing at 50ºC for 2 min; polymerization at 72ºC for 1 min 30 s for 30 cycles, and final extension at 72ºC for 5 min.

Klenow treatment of the PCR products: The PCR-amplified DNA products are not truly blunt-ended as the enzyme *Taq* DNA polymerase has a tendency to add an extra 'A' residue at the 3' end of both the strands. Klenow treatment polished the DNA by removing the extra 'A' residue at the 3' ends and filling up the recessed 3' termini. For this purpose, 25 µL of the amplified DNA products were first precipitated, then dissolved in minimum volume of deionized water. In the same tube, a reaction volume of 40 µL was set by adding required amounts of 10X Klenow enzyme buffer, dNTPs-mix and 1–2 units of Klenow enzyme. The reaction was kept at 28°C for 40 min and terminated by incubating at 65°C for 5–7 min.

3.2.6 Purification of the DNA Fragments

Silica bead DNA gel extraction kit was used to elute the Klenow-treated DNA bands for further cloning into a plasmid vector. According to manufacturer's instructions, the gel extraction protocol was followed for elution of the DNA bands. The individual DNA samples were resolved in 0.8% agarose gel using 1X TAE buffer. In one lane, DNA sample was loaded as control. This control lane was excised with a clean scalpel and visualized under UV-trans illuminator to mark the position of the DNA band. The corresponding DNA bands were excised from the gel (without UV exposure) by matching the position of bands in the control lane. The gel slices containing the DNA bands were weighed in 1.5 mL microfuge

tubes. Three volumes of binding buffer was added to one volume of gel and incubated at 55°C, till the gel was completely solubilized followed by addition of 7 µL of silica gel suspension beads, mixed properly by vortexing for 30 s. The tubes were then incubated at 55°C in water bath for 5 minutes with intermittent gentle vortexing after every 1 min for 10 s in order to allow adsorption of DNA on the beads. The samples were then centrifuged at 6,000 rpm for 30 s and supernatant was removed very carefully with the help of a pipette. The pellet was washed with 500 µL of washing buffer and then centrifuging at high speed for 30 s followed by removal of supernatant. The pellet was washed twice with 500 µL of washing buffer, properly air dried in the laminar air flow until it attained a white powdery form. 7 µL of DEPC treated water and 7 µL of TE buffer was added to the dried pellet. Pellet was suspended in TE buffer by vortexing for 15-20 s. It was incubated at 55°C water bath for 5 minutes. Then centrifuged at 6,000 rpm for 30 s. The supernatant containing the purified DNA was carefully transferred to a fresh sterile microfuge tube. The last two steps were repeated to increase the yield of DNA. Intactness and yield of the eluted DNA was checked by 0.8% agarose gel electrophoresis.

3.2.7 Preparation of the Linearized Vector

pUC19 was digested with the enzyme *Sma*I that produced blunt ends at 5′-CCC/GGG-3′ site. 1–2 µg of the plasmid vector was digested in a reaction volume of 20 µL at 30ºC for 2 h then the reaction was terminated by incubating at 60 ºC for 5 min. The complete digestion was checked by resolving in agarose gel electrophoresis.

3.2.8 Ligation Reaction

A ligation reaction was set up in order to ligate the individual purified DNA fragments into the vector, using the enzyme T4 DNA ligase. It catalyses the formation of phosphodiester bond between the juxtaposed 5'-phosphate and 3'-OH termini in the duplex DNA. The main components of a ligation reaction were: vector (~0.5 µg), insert i.e., RT-PCR mediated cDNA (~0.5 to 1.0 µg) and T4 DNA Ligase enzyme (1–10 units). PEG 8000 was used in the cases of blunt end ligation. The reaction volume was made up to 15 µL and incubated ~15°C for cohesive end ligation, and at ~20°C for blunt end ligation. Usually, ligation reactions were carried out for a period of 10–12 h.

3.2.9 Genetic transformation of E. coli DH5α with Plasmid Vector

E. coli DH5α was transformed with the ligation products using the $CaCl_2$ method (Mandel and Higa 1970) as depicted by a schematic view in Fig. 3.2. *E. coli* culture was inoculated in

25 mL of Luria broth and incubated with shaking at 37°C. A fresh 25 mL of LB was re-inoculated with 100 µL of the overnight-grown culture and then incubated at 37°C with shaking for 2–3 h (O.D. 0.4–0.6 at 560 nm). The culture was kept on ice to minimize the metabolic activities of cells. The cells were washed with ice-cold 25 mM $CaCl_2$. The cells were resuspended in 1.0 mL of ice-cold 100 mM $CaCl_2$ and kept in ice for 2½ hrs in order to develop competence. The ligation mix (~5 µL) was added to 100 µL of competent cell suspension, mixed well and kept at 4°C for 30 min. Heat shock was given at 42°C for 2 min, followed by the addition of fresh LB (~1.0 mL) and incubation at 37°C for 1½ hrs. *E. coli* transformants were screened by spreading the cell suspension on selective LA medium containing 50 µg mL^{-1} ampicillin. The plates were incubated overnight at 37°C. Recombinant pUC19 clones were screened based on blue/white selection.

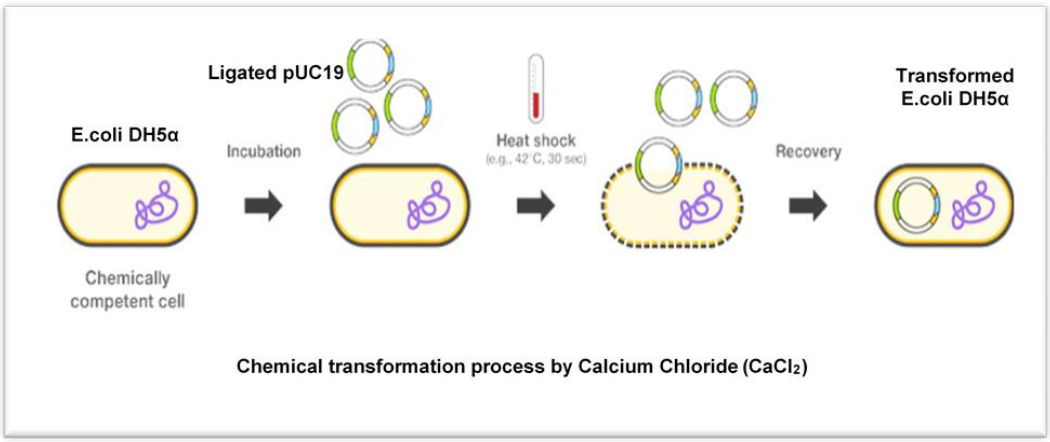

Fig. 3.2 A **s**chematic view of induction of artificial competency in *E. coli* cells by chemical transformation (source:https://www.thermofisher.com/in/en/home/life-science/cloning/cloning-learning-center/invitrogen-school-of-molecular-biology/molecular-cloning/transformation/competent-cell-basics.html) and modification

3.2.10 Plasmid Isolation

Two methods were followed for plasmid isolation: alkali lysis and boiling methods. These are described briefly, below.

Alkali lysis method (Birnboim and Doly 1979): This method allows the fast annealing followed by rapid denaturation of intact plamid DNA leading to its separation from the bacterial genetic DNA without triggering the activation of enzymes responsible for DNA digestion. 1.5 mL overnight grown culture of transformant *E. coli* was centrifuged. The cells were mixed with 200 µL of Solution I and 30 µL lysozyme (stock 10 mg mL^{-1}). Then 400 µL

of Solution II was added and mixed followed by addition of 300 µL of Solution III (a curdy white precipitate was formed). The microfuge tubes were kept in ice for 30 min and centrifuged at high speed for 15 min. The supernatants were treated with 2.0 µL of DNase free RNAse (10 mg mL^{-1}) followed by phenol and chloroform mixture (1:1) extraction. To the aqueous layer, equal volume of isopropanol was added and kept at 4ºC for 20 min. The DNA was pelleted at 8000 g for 15 min, washed with 70% ethanol, air-dried and dissolved in 30 µL of TE buffer and stored at –20ºC.

Boiling method (Holmes and Quigley 1981): 1.5 mL overnight grown culture of the *E. coli* transformant was harvested in microfuge tube. The cells were finely resuspended in 800 µL of STET buffer, and 30 µL of lysozyme was added to the suspension. The microfuge tube was kept in boiling water bath for 90 s. After cooling down to room temperature, centrifugation at 10,000 g was carried out for 15 min. The supernatants were treated with 2.0 µL of DNase free RNAse (10 mg mL^{-1}) followed extraction with a mixture of phenol and chloroform (1:1). To the aqueous layer, $1/10^{th}$ volume of 3 M sodium acetate (CH_3COONa) and equal volume of isopropanol was added and kept at 4ºC for 30 min. The DNA was precipitated, washed with 70% ethanol, air-dried and dissolved in 30 µL of TE buffer and stored at –20ºC.

3.2.11 Sequencing and Submission to GenBank Database of NCBI

The RT-PCR mediated individual cDNA clones were first checked by restriction digestion and PCR as well using the same set of primer primers. The cloned cDNAs were sequenced in both directions by the commercial company Bangalore Genei, Bangalore. The nucleotide sequences of the individual clones were analysed by National Center for Biotechnology Information (NCBI; http://www.ncbi.nlm.nih.gov/) Blast tools. The amino acid sequence was predicted by the open reading frame (ORF) finder available at the NCBI. Each sequence information was submitted to the GenBank database and assigned with an Accession No.

3.1.12 Semi-quantitative RT-PCR

For semi-quantitative RT-PCR, reverse transcription was carried out in a reaction volume of 20 µL using 2.0 µg of total RNA (prior treated with RNase-free DNase), oligo $(dT)_{18}$ primer and cDNA Synthesis Kit from Fermentas Life Sciences. 3.0 µL of each RT mixture was used as template in PCR (50 µL reaction volume) using the gene specific forward and reverse primers, and 1.0 unit of *Taq* DNA polymerase (Bangalore Genei). During PCR, the thermal cycling parameters were kept same as mentioned earlier except polymerization at 72ºC for 2 min. As control, the primers, Actin-FW and Actin-RV were used to amplify ~650 bp

fragment using the same 3.0 µL individual RT mixture as template. Polymerization step at 72ºC was kept 1 min in each thermal cycle in this case. The aforesaid selected genes specific and actin-specific RT-PCR products were resolved in 1% agarose gel electrophoresis, respectively. The relative expression levels between the potato organs were assessed by the quantification tool of the gel documentation system (Bio-Rad, USA).

3.3 Enzyme Assays

The potato tubers were harvested from different stages of tuberization in potato i.e., from initial apical swelling to maturation of tuber. To know about gene expression at translation level, we need to determine the corresponding gene product in the form of protein content and/or enzyme assay. Several enzyme assays were carried out based on the protocols as reported earlier usually with some modifications wherever required.

3.3.1 Fructokinase (FRK)

Preparation of crude tissue extracts: Protein extraction and FRK assay were carried out according to the protocols reported earlier (Appeldoorn et al. 1999; Petreikov et al. 2001; Jammer et al. 2015). Briefly, ~500 mg of the freshly-harvested maturing potato tubers (cultivar KC-1) at different stages of growth were homogenized in liquid nitrogen with 0.1% Polyvinylpolypyrrolidone (PVPP). All the extraction steps were performed on ice and/or in cold room (4°C) using pre-cooled liquids. The ground plant material was extracted with 1.0 mL of extraction buffer (40 mM Tris-HCl pH 7.6, 3 mM $MgCl_2$, 1 mM EDTA, 0.1 mM PMSF, 1 mM benzamidine, 14 mM β-mercaptoethanol, 24 µM $NADP^+$). The homogenate was centrifuged at 4 °C and 20,000 g for 35 min until a solid pellet was obtained and the particles were removed from the supernatant. The supernatant i.e., clarified crude extract was dialysed overnight against 20 mM potassium phosphate buffer (pH 7.4) at 4°C. In this step, highly abundant substrates of FRK and a few other enzymes as well were removed. The extracts were frozen in liquid nitrogen, stored at –20 °C in small aliquots for further use.

FRK assay: For FRK assay, aliquots of the dialysed crude extracts were incubated with 5 mM $MgCl_2$, 5 mM Fructose, 2.5 mM ATP, 1mM NAD^+, 0.8 U of Phosphoglucose Isomerase (PGI), and 0.8 U of Glucose-6-phosphate dehydrogenase (G6PDH) in 50 mM Bis-Tris at pH 8.0. Fructose was omitted in the control. The progress of the reaction was monitored by measuring the increase in absorbance at 340 nm due to conversion of NAD^+ to NADH. FRK activity i.e., the total fructose phosphorylating capacity was measured and expressed in nmol/min/g FW.

3.3.2 Sucrose Synthase (SuSy)

Preparation of crude tissue extracts: For SuSy assay, the crude tuber extracts were prepared by adopting same procedure as described above for FRK (Jammer et al. 2015).

SuSy assay: The SuSy activity was determined by two types of reactions: (a) including 1 mM UDP detecting both Susy and cytInv background activity, and (b) without 1 mM UDP to detect only the cytInv background activity. The Susy activity was then calculated by subtracting cytInv background activity (b) from total activity (a). For both the reactions, aliquots of dialysed crude extracts were incubated with 1 mM EDTA, 2 mM $MgCl_2$, 5 mM DTT, 250 mM sucrose, 1 mM UDP (omitted in the reaction (b), 1.3 mM ATP, 0.5 mM NAD^+, 0.672 U of HXK, 0.56 U of PGI, and 0.32 U of G6PDH in 50 mM HEPES/NaOH at pH 7.0. In the control, sucrose was omitted. The increase in absorbance at 340 nm due to conversion of NAD^+ to NADH was monitored. the total extractable enzyme was measured and expressed in nmol/min/g FW.

3.3.3 Catalase (CAT)

Preparation of crude tissue extracts: The crude tissue extracts were made from different potato tissues following the protocol as described earlier (Kandukuri et al. 2012; Duman and Kaya 2013). Briefly, approx. 3.0 g of the potato tissues namely tubers (skins removed), leaves, and stems were cut into small pieces and pulverized to fine powder in liquid nitrogen; then homogenized in 10 mL of 50 mM phosphate buffer, pH 7.0 with 8 % PVP, 10 mM PMSF, 0.1 mM EDTA, and 30 mM KCl into a fine paste using pestle and mortar. The homogenate was filtered through three layers of cheesecloth, and then centrifuged at 10,000 g for 20 min at 4 °C and the clear supernatant was collected and used for quantification of total protein, followed by CAT assay as well. Each of these biochemical experiments was carried out in triplicate, and the data are presented as means of the results.

CAT Assay: CAT activity was determined by measuring a decrease in the absorbance of H_2O_2 at 240 nm as described earlier (Aebi 1984; Miyagawa et al. 2000). The catalase activity is measured based on the difference in absorbance (ΔA_{240}) per unit time. 30 µL of crude enzyme extract was taken in a total reaction volume of 3.0 mL having the following composition: 10 mM H_2O_2 in 50 mM phosphate buffer (pH 7.0). One unit of activity is defined as the amount of enzyme which catalyses the decomposition of 1.0 µmol of H_2O_2 per min at pH 7.0 and 25°C as calculated from the extinction coefficient for H_2O_2 at 240 nm of 39.4 M^{-1} cm^{-1}.

3.3.4 Protein Estimation by Folin-Lowry Method

Under alkaline conditions, the divalent copper ion forms a complex with peptide bonds and reduced to a monovalent ion. Monovalent copper ion and the radical groups of tyrosine, tryptophan, and cysteine react with Folin reagent to produce an unstable product that becomes reduced to molybdenum/tungsten blue. The following solutions were used: Solution A i.e., alkaline sodium carbonate solution having 2% sodium carbonate in 0.1 N NaOH; Solution B i.e., copper sulphate-sodium potassium tartrate solution-2% of sodium potassium tartrate in 1% copper sulphate; BSA stock (0.2 mg mL^{-1}), Folin-ciocalteu reagent (diluted with water in 1:1). 5.0 mL of alkaline solution (mixture of 50 mL solution A and 1.0 mL of solution B freshly prepared) was added to 1.0 mL of test solution (protein sample) and volume made up with water, mixed well and kept at room temperature for 10 min, then 0.5 mL of diluted Folin-ciocalteu reagent was added and mixed immediately. Samples were kept at room temperature for 30 min and absorbance was taken at 750 nm. Standard curve was made using BSA stock solution.

3.3.5 Statistical Analysis

Each of these assays in different tuber extracts and other biochemical experiments was carried out in triplicate and the data were presented as the Mean ± SD of n=3 independent experiments. Standard deviation and mean values were calculated using SPSS software of IBM. One-Way ANOVA ("analysis of variance") analysis was done to find the significance.

3.4 *In silico* analysis

3.4.1 Sequence Analyses and Phylogenetic Tree

The nucleotide sequences of the cDNAs were analysed by the NCBI Blast tools. The amino acid sequence was predicted by the open reading frame (ORF) finder available at the National Center for Biotechnology Information website (http://www.ncbi.nlm.nih.gov). For calculating the theoretical molecular weight, isoelectric point (p*I*), and amino acid composition of the predicted protein, the ProtParam tool of ExPASy (Expert Protein Analysis System) proteomics server of the Swiss Institute of Bioinformatics (SIB; URL:http://expasy.org/ tools/) was used. The different ProtScale tools of ExPASy were used for prediction of the hydrophobic character (Kyte and Doolittle 1982), and the various secondary structures such as α-helix, β-sheet, α-turn, and random coil. G+C content analysis was carried out by PSIPRED. For multiple sequence alignment, the *MultAlin* software (http://www.multalin.toul-ouse.inra.fr/multalin/; Corpet 1988) was used. In order to construct phylogenetic tree,

multiple sequence alignment was done by the *MultAlin* software, followed by the neighbor-joining method (with bootstrap consensus) using MEGA 10.0 software (Saitou and Nei 1987; Tamura et al. 2011) using the protein sequences belonging to different forms of the individual genes from potato, other *solanceae* family members and *A. thaliana.*

A flowchart of the strategies for identification and characterization of the multiple forms of SuSy, FRK, CDPK, and CAT in potato by genome wide analyses:

- Data mining for identification of the multiple forms corresponding to individual genes in the potato genome databases including Spud DB and Ensembl Plants

↓

- BLASTp at NCBI (http://www.ncbi.nlm.nih.gov) search

↓

- Retrieval of the sequences for further analyses

↓

- Sequence analysis, chromosomal localization of the genes, prediction of the motifs/domains and 3-dimensional (3-D) structures

Biochemical attributes: The theoretical pI, amino acid composition, aliphaticity and mol. weight were determined by using EXPASY tools (http://web.expasy.org/protparam/). The relationships between the protein sequences and motifs were investigated by MyHits tool of ExPASy (https://myhits.sib.swiss/cgi-bin/motif_scan). Phyre2 tool (http://www.sbg.bio.ic.ac.uk/~phyre/) was used for secondary structure prediction and protein fold recognition. Many pdb files of the protein having homology were generated out of which one best model was selected and uploaded on ProSA.

3.4.2 Data Mining and Sequence Retrieval

To study each gene family and the respective gene products in potato, the specific keywords were used as queries in the latest version of Spud DB Potato Genomics Resource with tetraploid sequences http://spuddb.uga.edu/; the earlier version was at http://solanaceae.plantbiology.msu.edu/), along with other databases namely EnsemblPlants (https://plants.ensembl.org/index.html), Uniprot (https://www.uniprot.org/) and Expression Atlas (www.ebi.ac.uk/gxa/home); the home pages are shown in Fig. 3.3. The specific genes, transcripts and protein IDs were mostly verified using Ensembl Plants. The amino acid sequences were retrieved from Uniprot followed by BLASTp analyses at NCBI site.

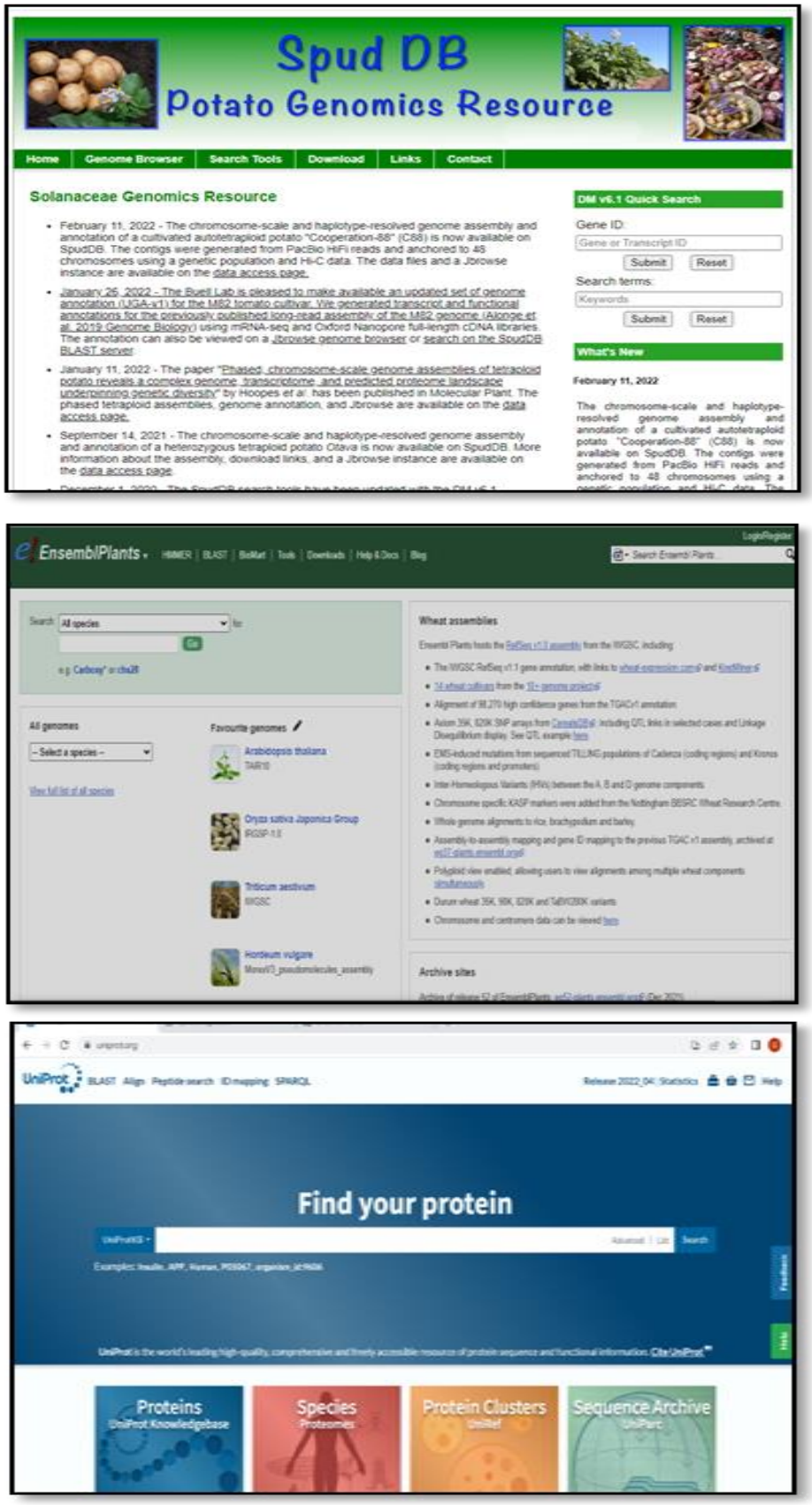

Fig. 3.3 The latest version of Spud DB Potato Genomics Resource with tetraploid sequences, Ensembl Plants, UniProt

3.4.3 Secondary Structure Prediction

The secondary structures like α-helix, β-strand and coil were examined by the PSIPRED secondary structure prediction method of Jones (1999) (http://bioinf.cs.ucl.ac.uk/psipred/). The PSIPRED Protein Analysis Workbench unites many available analysis tools into a single web based framework, thus it is an excellent tool for prediction of secondary structure, with access to GenTHREADER for protein fold recognition and MEMSAT-2 transmembrane topology prediction.

3.4.4 Identification of the Conserved Domains

To investigate the relationships between the protein sequences and motifs, MyHits tool of ExPASy (https://myhits.sib.swiss/cgi-bin/motif_scan) was used. It is a freely avaiable database of ExPASy, a new interactive resource for protein annotation and domain identification. It includes a multiple collection of tools to investigate the relationships between protein sequences and motifs described on them as shown by the interface picture of it in Fig. 3.4. The amino acid stretch called "motif" is defined by an variable collection of predictors like, HAMAP profiles, PROSITE patterns PROSITE profiles, Pfam HMMs (local models), Pfam HMMs (global models) (Pagni et al. 2004).

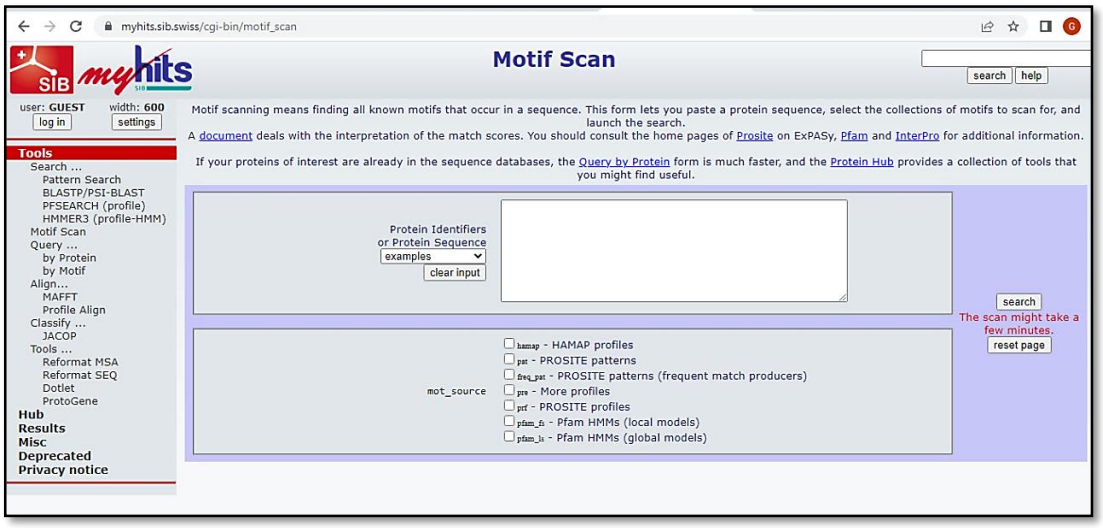

Fig. 3.4 The home page of MyHits Motif Scan

3.4.5 Chromosomal Localization of the Genes

For chromosal localization of the genes, the size of the individual chromosomes and the respective position of the centromeres were depicted according to Potato Genome Consortium, (2011). Further the specific positions multiple forms of each gene were

predicted based on the spud DB database, and further checked by EnsemblPlants prior to presenting the data.

3.4.6 3-D Structure Prediction and Validation of the Model

The 3-D models were constructed using a bioinformatics method i.e., I-TASSER (Iterative Threading Assembly Refinement; https://zhanglab.ccmb.med. umich.edu/I-TASSER/) (Zhang, 2008). The models were validated using the Structural Analysis and Verification Server (http://nihserver.mbi.ucla.edu/SAVES/; Cheatham *et al*. 1995). The predicted structures were visualized in the form of ribbons by PyMol software (https://www. pymol.org). The transmembrane helices were also predicted using Phyre2 tools of a protein fold recognition server to know the transmembrane topology of the protein (http://www.sbg.bio.ic. ac.uk/phyre2/). The predicted 3-D models were displayed using an open source molecular visualization system PyMOL (https://pymol.org/2/). Stereochemical quality and accuracy of the newly modelled structures were evaluated with PROCHECK by Ramachandran plot analyses.

3.4.7 Gene Expression Patterns

The expression values in different organs were examined and retrieved from the large scales of RNA-Seq and Microarray studies, and protein expression datasets in Expression Atlas, a database maintained by the European Bioinformatics Institute (www.ebi.ac.uk/gxa/home) and the potato genomic resource spud DB (http://solanaceae.plantbiology. msu.edu/). It provides the average signal intensity values of a gene from a high diversity of experiments covering different organs, developmental stages, and treatments.

3.4.8 Protein-Protein Interaction Network Studies

Functional interacting network of proteins was performed for the protein sequences obtained from the corresponding cDNA clones using STRING 10.0 software (Franceschini et al. 2013). The STRING database (https://string-db.org/)-a repository of known and predicted protein interactions, was used to know the functional networks of the proteins to understand their role in metabolic pathways in a better way. String software contains nearly 25 million proteins from more than 5000 organisms, and registers approximately 20 billion interactions. The database was searched for the selected genes at the high confidence level (0.700) for the protein interactions to avoid less significant results.

M&M: Appendix-I

Sr. No.	**Chemicals/Biochemicals**	**Stock conc.** (mg mL^{-1})	**Working conc.** (µg mL-1)	**Solvent used**
1.	Ethidium bromide	5	0.5-1.0	Sterile water
2.	X-gal (5-Bromo-4-chloro-3-indolyl-β-D-galactoside)	20	20 (30µL per plate)	N,N-dimethyl-formamide
3.	IPTG (Isopropyl thio-β-D-galactoside)	100	100 (8µL per plate)	Sterile water
4.	Ampicillin	50	50	Sterile water

M&M: Appendix-II

Sr. No.	Buffers	Composition and preparation
1.	0.5 M Tris-HCl (pH 8.0)	For 100 mL stock, 6.05 g of Tris base was dissolved in 50 mL water and pH was adjusted with 6.0 N HCl and made up volume with water and autoclaved.
2.	0.5 M EDTA (pH 8.0)	For 100 mL stock, 18.6 g of sodium salt of EDTA was dissolved in 50 mL water and pH was adjusted with concentrated NaOH and made up volume with water and then autoclaved.
3.	3.0 M Sodium acetate (pH 5.5)	For 50 mL stock, 12.3 g of Sodium acetate was dissolved in water and pH was adjusted with glacial acetic acid and volume made upto 50 mL.
4.	0.5 M Sodium acetate (pH 4.7)	For 50 mL stock, 2.05 g of Sodium acetate was dissolved in water and adjust the pH with glacial acetic acid and final volume 50 mL.
5.	5 M Potassium acetate	49 g of potassium acetate was dissolved in water and made final volume 100 mL and autoclaved.
5.	3 M Potassium acetate (pH4.8)	29.4 g of potassium acetate was dissolved in water and 11.5 mL of glacial acetate was added and made final volume 100 mL and autoclaved.
7.	0.2 M MOPS (pH 7.5)	4.2 g of MOPS was dissolved in water and pH adjusted to 7.5 using NaOH and volume made to 100 mL.
8.	0.5 M $MgCl_2$	10.2 g of $MgCl_2$ was dissolved in sterile water to a final volume of 100 mL
9.	1.0 M Sorbitol	18.2 g of sorbitol was dissolved in sterile water to a final volume of 100 mL
10.	0.5 M KCl	3.73 g of KCl was dissolved in sterile water to a final volume of 100 mL
11.	0.5 M Sucrose	17.1 g of sucrose was dissolved in sterile water to a final volume of 100 mL
12.	*Solutions used for plasmid isolation by alkali lysis method* :	
	Solution I:	Glucose 50 mM; Tris-HCl 25 mM (pH 8.0); EDTA 10 mM (pH 8.0)
	Solution II:	NaOH 0.2 N; SDS 1.0%
	Solution III:	Potassium acetate (3M)
13.	*The buffer for plasmid isolation by boiling method (STET)*	8.0 % (w/v) Sucrose, 0.5 % (w/v) Triton X 100, 50 mM EDTA (pH 8.0), 10 mM Tris-HCl (pH 8.0) Volume was made up by water and autoclaved.
14.	STE Buffer	0.3 M NaCl, 50 mM Tris-HCl (pH 8.0), 5 mM EDTA (pH 8.0)
15.	Saline EDTA	0.15 M Sodium chloride, 0.1 M EDTA (pH 8.0)
16.	TE Buffer (1X)	10.0 mM Tris-HCl (pH 8.0), 1.0 mM EDTA (pH 8.0) Volume was made up with water and autoclaved.
17.	TBE Buffer (5X)	54 g L^{-1} Tris base, 28 g L^{-1} Boric acid, 3.8 g L^{-1} EDTA The pH of the buffer was set at 8.0. Volume was made up with water and autoclaved.

18.	TAE Buffer (5X)	24.2 g L^{-1} Tris-base, 5.7 mL L^{-1} Glacial acetic acid, 10 mL L^{-1} 0.5M EDTA (pH 8.0). Volume was made up by water and autoclaved.
19.	DNA Gel Loading Buffer (5X)	35 % (w/v) Sucrose or 40% glycerol, 20.0 mM EDTA (pH 8.0), 0.1 % (w/v) Bromophenol blue Volume was made up with sterile water.
20.	DNA extraction buffer	50 mM Tris-HCl pH 8.0, 50 mM EDTA (pH 8.0), 250 mM NaCl, 15% sucrose
21.	REX buffer for RNA extraction	100 mM LiCl, 100 mM Tris-HCl (pH~8.0), 1.0 % SDS, 10 mM EDTA (pH~ 7.3), 0.2% ß- Mercaptoethanol
22.	Protein extraction buffer	50 mM MOPS-NaOH (pH 7.5), 10 mM $MgCl_2$, 1.0 mM EDTA, 5.0 mM DTT or 0.2% β Mercaptoethanol, 0.1%(v/v) Triton X 100
23.	*Formaldehyde gel buffers:*	
	5X Formaldehyde Gel running buffer	0.1 M MOPS, 40 mM sodium acetate, 5 mM EDTA (pH 8.0)
	Formaldehyde Gel loading buffer	50% glycerol, 1 mM EDTA (pH 7.5), 0.25% bromophenol blue
24.	Solutions for Folin Lowry protein estimation:	*Solution I*: Alkaline Sodium carbonate (20 g of sodium carbonate was dissolved in final volume of 0.1 N NaOH) *Solution II*: Copper sulphate-sodium potassium tartrate solution (5g L^{-1} $CuSO4.5H_2O$ was dissolved in 10 g L^{-1} of Sodium potassium tartrate) (Mix solution I 50 mL with 1 mL solution II for use)

Note: Deionized water was used for all the solutions as mentioned above.

Chapter 4

Results & Discussion

4.1 *Objective 1:* Molecular cloning and characterization of cDNAs encoding Sucrose synthase, Fructokinase, Calcium-dependent protein kinase and Catalase from an Indian potato cultivar

Considerable progress has been made on molecular and biochemical studies on the genes encoding enzymes/transcription factors involved in tuberization during the last few decades. A number of cDNA/genomic clones encoding these enzymes have been reported from different plant species including commercially important *Solanaceae* family members. Apart from molecular cloning studies, it is crucial to have an insight into the expression patterns and the attributes of the genes involved in carbohydrate, Ca^{2+} signalling and ROS metabolism. Multiple forms of the genes encoding SuSy, FRK, CDPK and CAT were reported from tomato, tobacco and other plant species. earlier. According to Objective 1, the cDNA cloning studies were carried out to explore the genetic resources of an Indian potato cultivar. Using total RNA from growing tubers, RT-PCR approaches were adopted to obtain full-length cDNAs encoding the distinct forms of SuSy, FRK, CDPK and CAT from a processing Indian potato cultivar, Kufri Chipsona-1. These enzymes remained focus areas of research in the recent decades as they were crucial in the developmentally-regulated tuberization process. The potato plantlets were routinely maintained in laboratory, acclimatized and grown under field condition. Different potato organs were harvested and stored by snap-freezing in liquid nitrogen. Total RNA was extracted and purified from some potato organs. For the cDNA cloning studies, the common steps are precisely described below.

Plant materials and growth conditions: Pathogen-free germplasm of an Indian potato cultivar Kufri Chipsona-1 (KC-1), was routinely maintained in our laboratory under controlled conditions as mentioned earlier. The micropropagated plantlets were properly hardened and acclimatized for cultivation in the field (Fig. 4.1). The purpose was to produce mini tubers (5–25 mm in diameter). Different potato organs including growing tubers at various stages of development such as stolons, tuberizing stolons, growing tubers from the field-grown plants were collected and frozen in liquid nitrogen, and then stored at -70^{o}C for further use.

Isolation of total RNA from different organs of potato: Total RNA was isolated from different organs of potato, i.e., leaf, stem, tuberising stolon, tuber and flower. The crude RNA samples were checked by agarose gel electrophoresis shown in Fig. 4.2. Ribosomal RNA bands were

distinct indicating the intactness of total RNA preparations. Some of the RNA samples had trace amounts of genomic DNA as impurities.

Fig. 4.1 Potato plants (cv. KC-1) at various stages of growth. **a** micropropagated plantlets, **b** and **c** hardening and acclimatization, **d** plants growing under field condition, **e** fully grown plant, and **f** an uprooted mature plant with stolons and tubers

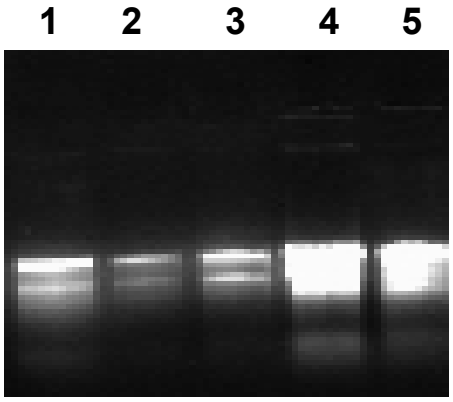

Fig. 4.2 Total RNA from different Potato organs. Lane 1- leaf, Lane 2-stem, Lane 3-flower, Lane 4-tuberising stolon, Lane 5-growing tuber

Purification of total RNA: Total RNA was purified by RNase-free DNase treatment followed by solvent extraction. Purified RNA samples were checked by agarose gel electrophoresis.

The distinct bands showed the quality of the purified RNA preparations (not shown). Nanodrop spectrophotometer was used to find A_{260}/A_{280} ratio to assess the quality and quantity of the prepared RNA samples as shown in Table 4.1.

Table 4.1 Quantification and quality checking of total RNA from different potato organs

Organ	RNA concentration (µg/mL)	A_{260}/A_{280} Ratio
Leaf	780	1.95
Stem	770	1.91
Flower	710	1.83
Tuberising stolon	910	2.00
Growing tuber	980	2.00

After purification of the RNA, synthesis of first strand cDNAs was done by the process of oligo $(dT)_{18}$ mediated reverse transcription, followed by PCR using gene-specific primers using variable thermal cycling parameters. The results of the cDNA cloning studies, sequence analyses, *in silico* approaches and enzyme assays corresponding to SuSy, FRK, CDPK and CAT are sequentially presented here.

4.1.1 Cloning and Characterization of a cDNA Encoding SuSy

A cDNA clone (2.668 kb, designated *St-CSS01*) specific to the potato cultivar KC-1 was obtained through RT-PCR (Fig. 4.3). The nucleotide sequence of the cDNA was analysed by NCBI BLAST tool, and found to encode a distinct form of SuSy4; the sequence information was submitted to GenBank database (MT731684). The 2668-bp *St-CSS01* consisted of 51-bp 5′-UTR, 2418-bp ORF (bases 52-2469), and 199-bp 3′-UTR. The G+C content the 5′-UTR, coding region, and 3′-UTR of SuSy were found to be 48, 43 and 34 %, respectively. NCBI BLAST search revealed that the cDNA shared 99% sequence identity with a full-length SuSy cDNA clone from a potato cultivar Sirtema (M18745). At nucleotide level, the coding region of *St-CSS01* showed significant sequence identities with some other plant SuSy cDNAs: XM_006345182.2, NM_001288357.1, XM_015204139.2, NM_001247726.2, L19762.1,

KF977579.1, NM_001313910.1, EU908020.1, DQ834312.1, AM087674.1 belonging to different forms of SuSy in *Solanceae* and other families.

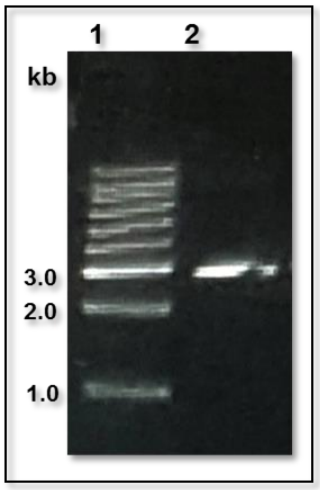

Fig. 4.3 RT-PCR amplification of SuSy cDNA. *Lane 1* 1 kb DNA ladder; *Lane 2* RT-PCR product (~2.7 kb) using total RNA from the growing potato tuber of the cultivar KC-1 and the SuSy cDNA-specific primers, SSF1-0025 and SSR3-2693

The predicted protein, designated as KC-SuSy, consisted of 805 amino acids (protein_id QWW18611). Based on the ProtParam tool, the calculated molecular weight (MW) of KC-SuSy was found to be 92.4 kDa with a predicted isoelectric point (pI) of 8.63. Out of its total 805 amino acids, 94 were strongly basic (+) (Lys, Arg), 114 were strongly acidic (-) (Asp, Glu), 298 are hydrophobic (Ala, Ile, Leu, Phe, Trp, Val), and 168 were polar (Asn, Cys, Gln, Ser, Thr, Tyr). The instability index of KC-SuSy was computed as 34.69, which classified the protein as stable. The amino acid composition data revealed that some of the amino acids such as Gln (4.2 %), Ser (4.6 %), Glu (9.4%) and Leu (11.1 %) occurred more frequently as compared to their average occurrence; whereas, the amino acids, namely Cys (0.9 %), Ser (4.6%), Asn (3.7%) occurred less frequently (Doolittle 1989). As revealed by BLAST search, KC-SuSy represented SUS4 isoform belonging to group I *SUS* gene family in plants (Fig. 4.7)

4.1.2 Cloning and Characterization of cDNAs Encoding FRKs and FLN

Cloning of FRK cDNAs: A cDNA clone (1110 bp, designated *St-CFK21*) corresponding to *FRK2* allele was obtained through RT-PCR using total RNA from the potato (cultivar KC-1)

tubers shown in Fig. 4.4; sequenced and submitted to GenBank database (MN420513). This cDNA consisted of 10-bp 5'-UTR, 960-bp ORF (bases 11–970), and 140-bp 3'-UTR.

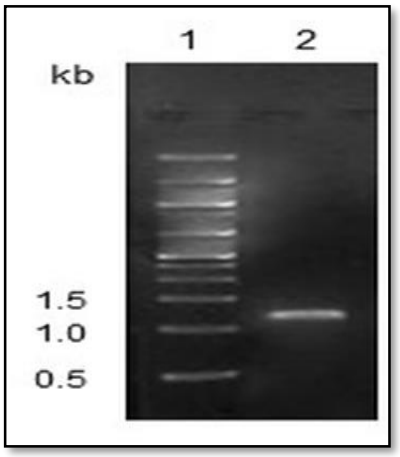

Fig. 4.4 RT-PCR amplification of FRK cDNA. *Lane 1* 500 bp DNA ladder; *Lane 2* RT-PCR product (~1.1 kb) using total RNA from the growing potato tuber of the cultivar KC-1 and the FRK cDNA-specific primers, F1-FK0001 and R2-FK1110.

The deduced protein, designated St-FRK2, consisted of 319 amino acids (QIS79145). As revealed by MyHits tool of ExPASy, the PfkB family carbohydrate kinase region of St-FRK2 consisted of 299 amino acids i.e., 10–308. NCBI BLAST search revealed that *St-CFK21* shared 99% sequence identity at nucleotide level with a 1143-bp full-length cDNA clone (Z12823) corresponding to a FRK2 isoform (CAA78283) from the potato cultivar record, with amino acid substitutions at three places. Based on the ProtParam tool, the approximate molecular weight (MW) of St-FRK2 was found to be 34 kDa with a predicted isoelectric point (pI) of 5.47. Out of its total 319 amino acids, 32 were strongly basic (+) (Lys, Arg), 39 were strongly acidic (–) (Asp, Glu), 129 were hydrophobic (Ala, Ile, Leu, Phe, Trp, Val), and 61 were polar (Asn, Cys, Gln, Ser, Thr, Tyr). Aliphatic index was found to be 97.30. The instability index (II) of St-FRK2 was found to be 20.90, which classified it as a stable protein. The amino acid composition data revealed that occurrence of some of the amino acids namely Ala (11.3%), Gly (10.3%), Leu (12.5%) was notably very high as compared to their average occurrence; whereas, the amino acids, namely Arg (3.4%), Gln (0.6%), Asn (2.8%), Pro (3.8%), Trp (0.6%) and Tyr (1.6%) occurred relatively less frequently (Doolittle 1989).

The nucleotide sequence of another cDNA clone specific to Kufri Chipsona-1 (784 bp, designated *St-CFK23*) was also analysed by NCBI BLAST tool, and found to encode a distinct form of *StFRK2* gene; the sequence information was submitted to GenBank database (MN401256). The 784-bp FRK consisted of 1-bp 5′-UTR, 771-bp ORF (bases 2–771), and 12-bp 3′-UTR). NCBI BLAST search revealed that *St-CFK23* shared 99% sequence identity with FRK, a full-length cDNA clone from potato (JX576230). The coding region of FRK showed significant sequence identities with some other FRK and FLN cDNAs: potato (MN401257, XM_006347240, DQ235181, JX576279, JX576230), tomato (NM_001246959, AK326357, AY325501, U64818) tobacco (XM_019397605, XM_016643248), coffee (XM_0272761675), populus (XM_035036621), jatropha (XM_0376635540) belonging to *Solanceae* and other families. The corresponding predicted protein, designated St-FRK2A, consisted of 256 amino acids (protein_id QIV66775). Based on the ProtParam tool, the calculated molecular weight (MW) of deduced amino acid sequence *of St-CFK23* was found to be 27.89kDa with a predicted isoelectric point (pI) of 5.61. Out of its total 256 amino acids, 28 were strongly basic (+) (Lys, Arg), 33 were strongly acidic (-) (Asp, Glu), 100 are hydrophobic (Ala, Ile, Leu, Phe, Trp, Val), and 55 were polar (Asn, Cys, Gln, Ser, Thr, Tyr). The instability indexof KC-FRK was computed as 26.79, which classified the protein as stable. The amino acid composition data revealed that some of the amino acids such as Lys (7.0 %), Asp (6.2 %), Ala (9.8 %), and Leu (12.5 %) occurred more frequently as compared to their average occurrence; whereas, the amino acids, namely Thr (3.7 %), Gln (1.2 %), Arg (3.9%), Phe (2.7 %), and Tyr (2.3 %), occurred less frequently, enabling the protein to undergo post translational modification more frequently (Doolittle 1989, Azevedo and Saiardi 2016).

Cloning of FLN cDNA: A cDNA clone (839 nts, designated *St-CFL27;* MN401258) was isolated using leaf total RNA from KC-1 and found to encode a distinct form of FLN consisting of 266 amino acids designated StFLN (protein_id QIV66777). *St-CFL27* shared 99% similarity with JX576279 and considerable similarity with the nucleotide sequences from potato (XM_006347240, DQ235181, DQ294257, Z12823), tomato (NM_001246959, AK326357, U62329, NM_001246959), tobacco (XM_016643248, XM_0162722598), populus (EF146912, XM_066372799), lotus (AK339576). As calculated by ProtParam tool, molecular weight of deduced amino acids encoded by St-FLN was found to be 28.88 kDa with a predicted isoelectric point (pI) of 5.9. Out of its total 266 amino acids, 27 were strongly basic

(+) (Lys, Arg), 31 were strongly acidic (-) (Asp, Glu), 107 are hydrophobic (Ala, Ile, Leu, Phe, Trp, Val), and 52 were polar (Asn, Cys, Gln, Ser, Thr, Tyr). The instability index of KC-FLN was computed as 25.38, which classified the protein as stable. The amino acid composition data revealed that some of the amino acids such as Gly (9.0 %), Ala (9.8 %), Ser (7.9), Phe (4.9), and Leu (12.4 %) occurred more frequently as compared to their average occurrence; whereas, the amino acids, namely Thr (3.8 %), Gln (0.8 %), Cys (0.8%), Arg (4.1%), Phe (2.7 %), and Tyr (2.3 %), occurred less frequently which could destabilize alpha chains in a protein and allowing the protein to be in its native state (Doolittle 1989, Dong et al. 2012).

4.1.3 Cloning and Characterization of a cDNA Encoding CDPK2

The nucleotide sequence of a cDNA clone (1560 bp, designated *CDPK2-A*) obtained through RT-PCR using total tuber RNA from the cultivar KC-1 shown in Fig. 4.5; analyzed by NCBI BLAST tool, and found to be a distinct form of *CDPK2* gene family. The sequence information was submitted to GenBank database (MN420514).

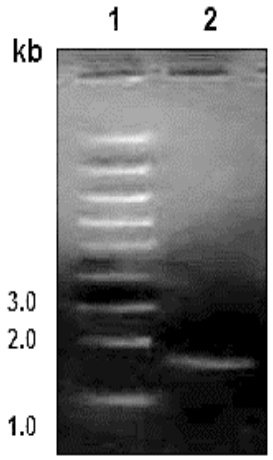

Fig. 4.5 RT-PCR amplification of CDPK2 cDNA. *Lane 1* 1 kb DNA ladder; *Lane 2* RT-PCR product (~1.6 kb) using total RNA from the growing potato tuber of the cultivar KC-1 and the CDPK cDNA-specific primers, SC2F1-0001 and SC2R2-1560

The 1560-bp *CDPK2-A* lacking 5′-UTR consisted of 1548-bp ORF, and 12-bp 3′-UTR ; the G+C content of the coding region and 3′-UTR were found to be 41.4% and 66.7%, respectively. Nucleotide BLAST search revealed that *CDPK2-A* shared 99% sequence identity with AF418563, a full-length *CDPK2* cDNA clone from the potato cultivar spunta (Raices *et*

al. 2003). The coding region of *CDPK2-A* also showed significant sequence identities with some other plant cDNAs having the following Accession Numbers: NM_001288442.1, XM_006346152.2, XM_015226573.1, NM_001247653.2, BT013334.1, AF363784.1, LC156099.1, AF115406.3, JN662020.1, XM_016701298.1, XM_016631157.1 belonging to different forms of CDPK and CDPK-like proteins in the *Solanaceae* family.

The predicted protein, designated StCDPK2, consisted of 515 amino acids (protein_id QIS79146). Based on the ProtParam tool, the calculated molecular weight (MW) of StCDPK2 was found to be 57.14 kDa with a predicted isoelectric point (p*I*) of 6.59. Out of total 515 amino acids, 67 were strongly basic (+) (Lys, Arg), 70 were strongly acidic (–) (Asp, Glu), 163 were hydrophobic (Ala, Ile, Leu, Phe, Trp, Val), and 118 were polar (Asn, Cys, Gln, Ser, Thr, Tyr). The instability index of StCDPK2 was computed as 28.35, which classified the protein as stable. The amino acid composition data revealed that some of the amino acids such as Gly (8.7%), Lys (8.9%), Glu (7.8%), and Ile (6.4%) occurred more frequently as compared to their average occurrence; whereas, the amino acids, namely Thr (4.9%), Gln (2.7%), Arg (4.1%), Phe (2.7%), and Trp (0.8%), occurred less frequently (Doolittle 1989).

4.1.4 Cloning and Characterization of a cDNA Encoding CAT1

A 1600-bp cDNA clone corresponding to *CAT1* allele was obtained through RT-PCR using total tuber RNA from the cultivar KC-1) shown in Fig. 4.6; sequenced and submitted to the GenBank database (MT731685). This cDNA consisted of 2-bp 5'-UTR, 1482-bp ORF (bases 3–1481), and 116-bp 3'-UTR. NCBI BLAST search revealed that KC-CAT1 shared 99% sequence identity with CAT1, a full-length cDNA clone from a potato cultivar ‘Russet Burbank’ (U27082). The coding region of CAT showed significant sequence identities with CAT and CAT-like cDNAs of some plants of *solanceae* family and others namely: NM_001287934, DQ2944281, AY500290 from potato; AK320529, NM_001247898, KU933832 from tomato; X71653, AF227952 from capsicum; NM_001324674, XM_019397890, XM_009592432 from tobacco; XR_0034533160, XM_027234995 from coffee and XM_0305755531 from populus.

The deduced protein, designated KC-CAT1, consisted of 492 amino acids (QWW18612). Based on the ProtParam tool, the approximate molecular weight (MW) of KC-CAT1 was found to be 56.42 kDa with a predicted isoelectric point (pI) of 6.56. Out of its total 492 amino

acids , 59 were strongly basic (+) (Lys, Arg), 63 were strongly acidic (–) (Asp, Glu), 153 were hydrophobic (Ala, Ile, Leu, Phe, Trp, Val), and 127 were polar (Asn, Cys, Gln, Ser, Thr, Tyr).

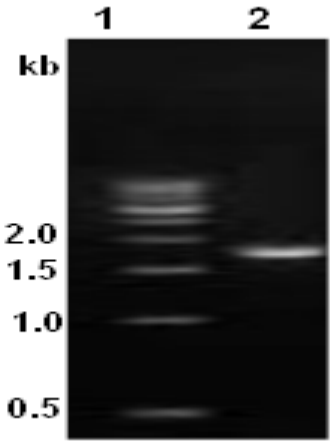

Fig. 4. 6 RT-PCR amplification of CAT1 cDNA. *Lane 1* 1 kb DNA ladder; *Lane 2* RT-PCR product (~1.6 kb) using otal RNA from the growing potato tuber of the cultivar KC-1 and the CAT cDNA-specific primers, F1-CT 0001 and R2-CT1600

Aliphatic index was found to be 68.56. The instability index (II) of KC-CAT1 was found to be 40.36, which classified it as an unstable protein. The amino acid composition data revealed that occurrence of some of the amino acids namely Pro (7.3%), Phe(5.9%), His (3.9%) was notably very high as compared to their average occurrence; whereas, the amino acids, namely Leu (5.9%), Gln (2.6%), Gly (5.2) occurred relatively less frequently (Doolittle 1989).

According to Objective 1 of the thesis work, all the aforesaid distinct individual cDNA clones corresponding to SuSy, FRKs, FLN, CDPK and CAT were isolated, sequenced, characterized and assigned with GenBank Accession Numbers. Such cDNA cloning studies were carried out for the first time from an Indian potato cultivar.

4.2 ***Objective 2:*** Sequence analyses of the enzymes for identifying the characteristic sequence features

In order to fulfill this Objective, multiple approaches were adopted to analyze the full-length deduced amino acid sequences of the individual enzymes under study. The major approaches were multiple sequence alignment (MSA), genome wide characterization of the genes and their localizations, phylogenetic analyses, prediction of secondary/3-D structures, finding the crucial domains/motifs including the catalytic/substrate binding sites. Several commonly used and reliable software tools were employed for the *in silico* studies with some manual adjustments wherever required. The details of the analyzed data are presented here.

4.2.1 Sequence Analyses of Sucrose Synthase (SuSy/SUS)

Multiple sequence alignment, regulatory/binding motifs and other sequence features: Six potato SuSy sequences representing three different *SUS* gene groups were used for alignment to identify the sequence relatedness and divergence. The crucial domains/motifs involved in the catalysis and regulation under various biotic and abiotic stresses include ATP/GTP-binding site motif A (P-loop) (RAHHYKGKT), bipartite nuclear localization signal (RRYLEMF YALKYRKM) , CodY helix-turn-helix domain (SEGNLAASLLAHKLGVTQCTIAHALEK), glycosyl transferase domain (558–725) and cAMP- and cGMP-dependent protein kinase phosphorylation sites; their relative locations and functions are presented in Fig. 4.7 and Table 4.2 as well. ATP/GTP-binding site motif A (P-loop) contains a glycine rich sequence followed by lysine rich thus helping in ATP binding while, bipartite nuclear localization signal profile helps in targeting the protein localization and CodY helix-turn-helix domain; a DNA helix which help in binding of protein to DNA grooves, thus aiding in protein functioning. In addition to this, the SuSy proteins are known to contain two main regulatory domains namely; 250 amino acids long N-terminal domain responsible for cellular targeting; including the cellular targeting domain (CTD), an early nodulin 40 (ENOD40) peptide-binding domain (EPBD) and almost double C- terminal GT-B domain of 500 amino acids playing a role in the glycosyl transferase activity. The active sites in the GT-B domains are found to be conserved, both within and among the three SuSy subgroups, hence they are subjected to more evolutionary constraints than the "regulatory" domains which are responsible for the cellular localization of SUS genes (Zheng et al. 2011; Xu et al. 2019). Also, two important serine phosphorlyation sites at position 11–15 and at position 170 are found to be responsible for

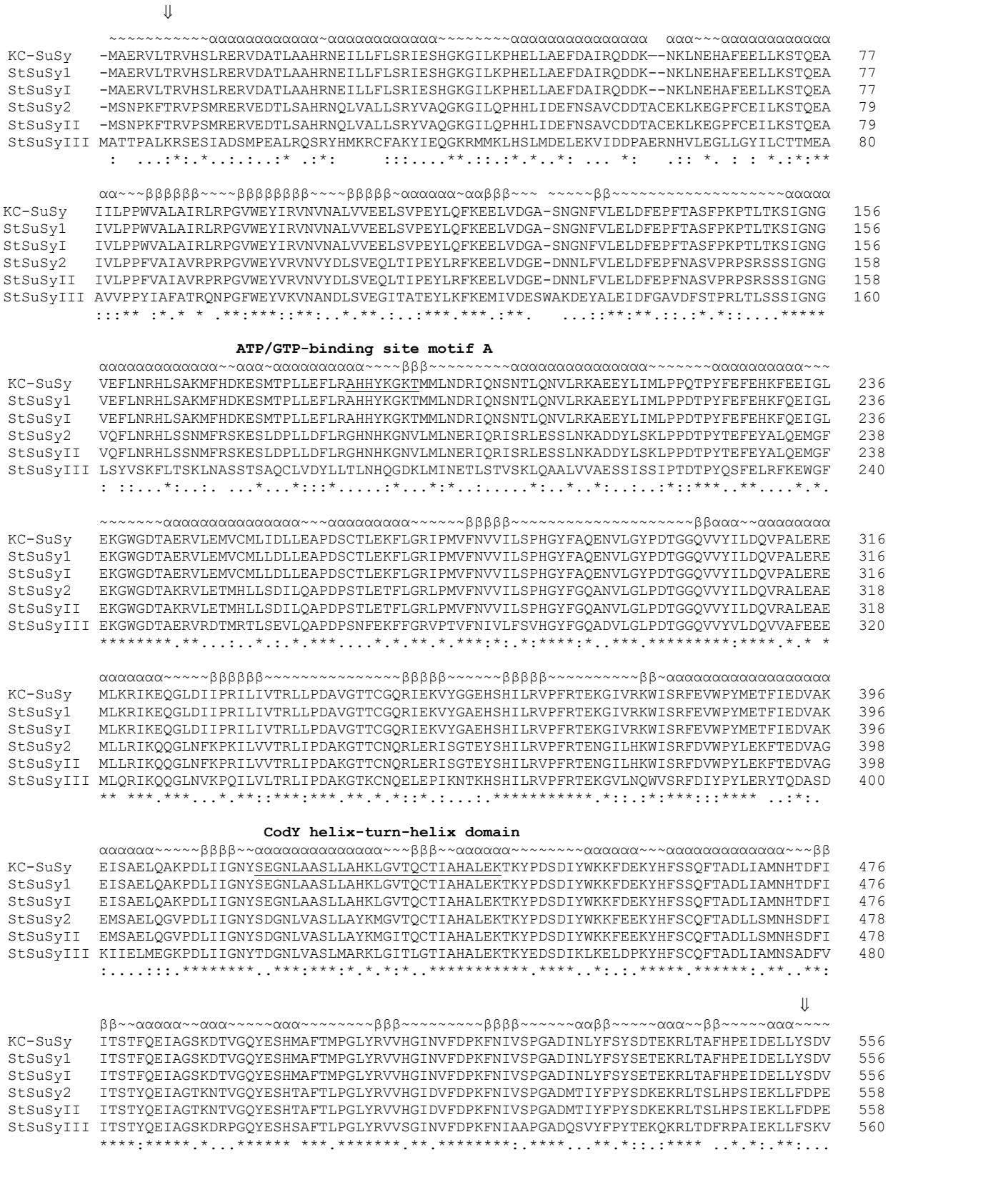
ATP/GTP-binding site motif A
CodY helix-turn-helix domain

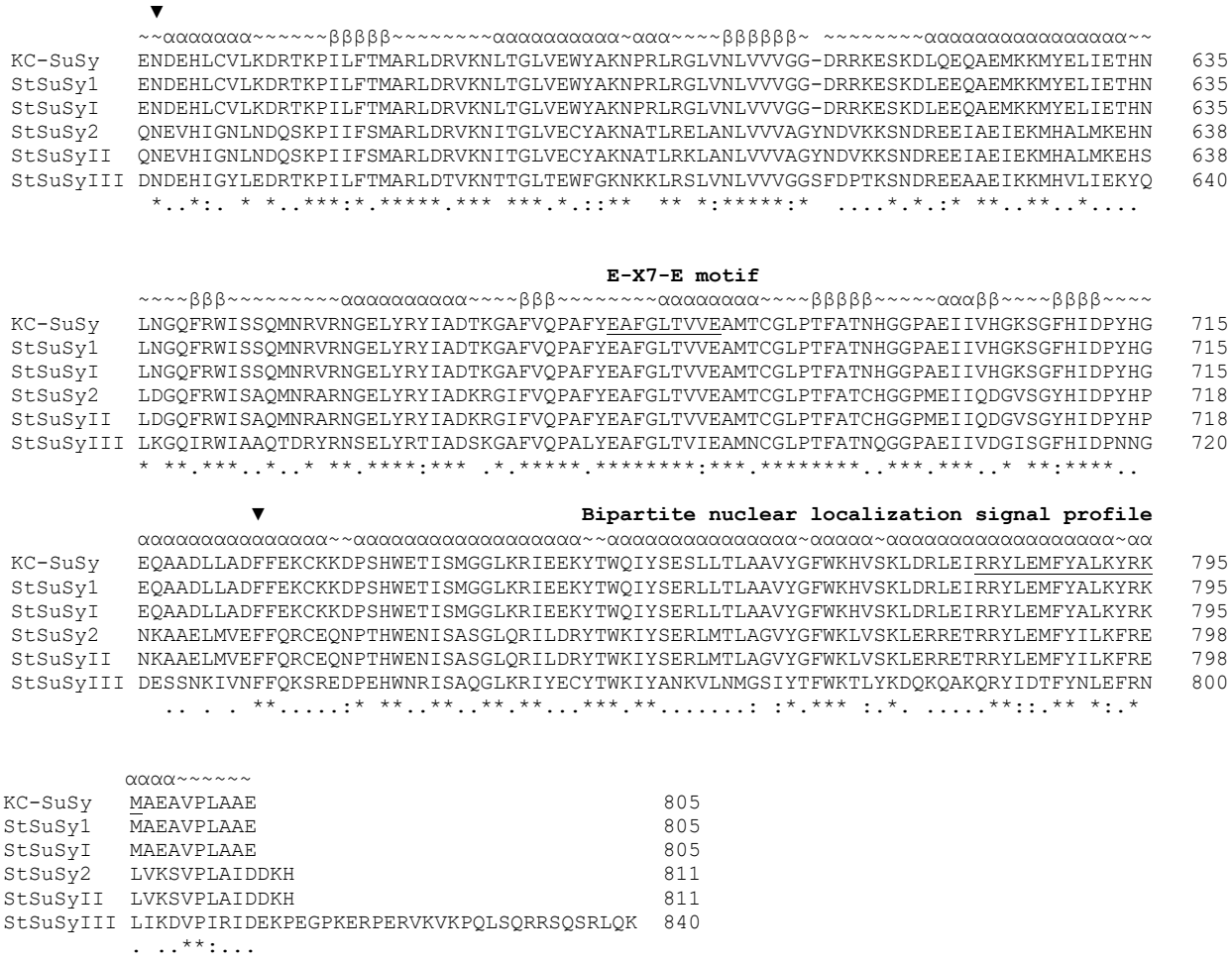

Fig. 4.7 Comparison of the predicted 6 full-length SuSy sequences corresponding to the three major active isoform groups from the potato. SuSy groupI includes KC-SuSy (QWW18611), StSuSy1 (AAA33841), StSuSyI (A7Y137); SuSy groupII includes StSuSy2 (AAO67719), StSuSyII (M1A8J5); SuSy groupIII includes StSuSyIII (M1BE45). Multiple sequence alignment was done based on *MultAlin* software along with some minor manual adjustments. Dashes indicate gaps that arise during alignment. Asterisks '*' indicate the conserved amino acids; ':' refers to the almost conserved or conservative substitutions; '.' refers to conserved amino acids in at least two SuSy groups. The downward arrow '⇓' indicates the entire sucrose synthase domain (from 7-554 aa) and '▼' denotes the glycoysltransferase Group I region (from 558-725 aa). The crucial regulatory/binding motifs are underlined in KC-SuSy. 'α', 'β' and '~' denote the propensity of the individual amino acids of KC-SuSy towards alpha helix, beta-sheet and random coil formation, respectively.

membrane association and regulation of protein breakdown or degradation (Hardin et al. 2003). Another most important conserved motif is E-X7-E found in the region from F671 to E699 of KC-SuSy, a member of GT4 proteins. The first E residue in the E-X7-E motif is invariant in all the glycosyltranferase (GT) subfamilies, while the other E residue is substituted by Gln (Q) or Tyr (Y) in the GT5 proteins. These two Glu (E) are known to play a role in the enzyme

catalysis. Their role and effect on enzyme activity was studied by mutational and structural analysis (Huang et al. 2016).

Table 4.2 Catalytic domains/motifs of KC-SuSy and their predicted functions

Catalytic domain	Position	Function
ATP/GTP-binding site motif A (P-loop)	184−191	consist of glycine rich sequence followed by a conserved lysine and a serine or threonine to help the binding of ATP and GTP for enzyme activity
Glycosyl transferase Group I	558−725	catalyzes the transfer of glycosyl groups to a nucleophilic acceptor with either retention or inversion of configuration at the anomeric centre
Bipartite nuclear localization signal profile	782−796	aids transfer of protein from nucleus to cytoplasm and other cell organelles, for the appropriate protein functioning
CodY helix-turn-helix domain	414−440	A DNA-binding motif (recognition helix) binds to the major groove of DNA
cAMP- and cGMP-dependent protein kinase phosphorylation site	539−542 612−615	phosphorylates proteins with exposed motif of arginine-arginine-X-serine to gain biological activity

SUS gene family in potato and phylogenetic analysis: By screening the potato whole genome and transcriptome databases, Spud DB, and *EnsemblPlants* (https://plants.ensembl.org/index.html), six *SUS* genes encoding sucrose synthase designated *SuS*, *SUS4* and *SuSy2* were retrieved, and categorised into three *SUS* groups (I–III) on the basis of phylogenetic analysis as reported earlier (Table 4.3, Fig. 4.8). Some of the *SUS* genes except PGSC0003DMG4000 31046 and PGSC0003DMG400013547 (which encodes only a single transcript) were found to encode multiple transcripts: e.g., PGSC0003DMG400002895, PGSC0003DMG400031046, PGSC0 003DMG400016730 encode two transcripts each, PGSC0003DMG400013546 encodes four while PGSC0003DMG4000006672 encodes five transcripts. The number of exons varied from 1 to 15, and the ORF size in these transcripts ranged from 372 to 3537 base pairs. These differences in the exon-intron structure were also reported in some other plants (Xu et al. 2019), which could the possible reason for the evolution, spatio- temporal expression and functional characterization of the *SUS* gene. The predicted proteins encoded by the transcripts consisted of 55–840 amino acids (6.13–95.57 kDa). The SuSy proteins significantly vary in terms of size, suggesting their roles in diverse biological processes such as sugar sensing and stress response (Stein and Granot 2019). The presence of multiple transcripts may be due to

Table 4.3 Features of *SUS* genes in potato extracted from genomic databases (Spud DB and Ensembl Plants)

Gene Group	PGSC Gene ID	Ch local	PGSC Transcript ID	Uniprot ID	Base pairs	Exons	Amino acids	Mol. Wt.	pI	Instability Index	Aliphatic Index	Gravy
SUSI	PGSC0003DMG400002895	12	PGSC0003DMT400007505	A7Y137	2821	13	805	92.47	5.87	33.36	92.42	-0.246
			PGSC0003DMT400007506	M0ZT40	2746	13	805	92.47	5.87	33.96	92.42	-0.246
SUSIII	PGSC0003DMG400031046	3	PGSC0003DMT400079728	M1D2C2	1017	1	176	19.91	5.79	39.78	77.76	-0.428
SUSII	PGSC0003DMG4000006672	9	PGSC0003DMT400017087	M1A8J5	2915	15	811	92.79	6.01	40.32	89.42	-0.288
			PGSC0003DMT400017088	M1A8J6	3537	11	436	49.87	6.44	41.87	97.18	-0.191
			PGSC0003DMT400017093	M1A8J8	1290	1	55	6.13	4.78	31.84	102.91	0.324
			PGSC0003DMT400017094	M1A8J9	952	1	93	10.83	6.39	40.15	86.99	-0.146
			PGSC0003DMT400017092	M1A8J7	372	1	80	8.63	6.01	38.40	93.75	0.154
SUSIII	PGSC0003DMG400016730	2	PGSC0003DMT400043117	M1BE45	2697	14	840	95.57	6.95	35.21	84.27	-0.392
			PGSC0003DMT400043118	M1BE46	1785	10	566	63.85	5.48	30.22	87.60	-0.256
SUSI	PGSC0003DMG400013546	7	PGSC0003DMT400035262	M1B217	2922	12	808	92.95	6.07	34.97	93.38	-0.225
			PGSC0003DMT400035261	M1B216	2828	14	805	92.60	6.03	34.61	93.85	-0.240
			PGSC0003DMT400035260	P49039	2809	14	805	92.57	5.98	34.28	93.85	-0.240
			PGSC0003DMT400035263	M1B218	2534	10	641	73.88	6.17	35.21	90.03	-0.237
SUSI	PGSC0003DMG400013547	7	PGSC0003DMT400035264	M1B219	2698	11	803	91.43	5.83	37.35	88.51	-0.287

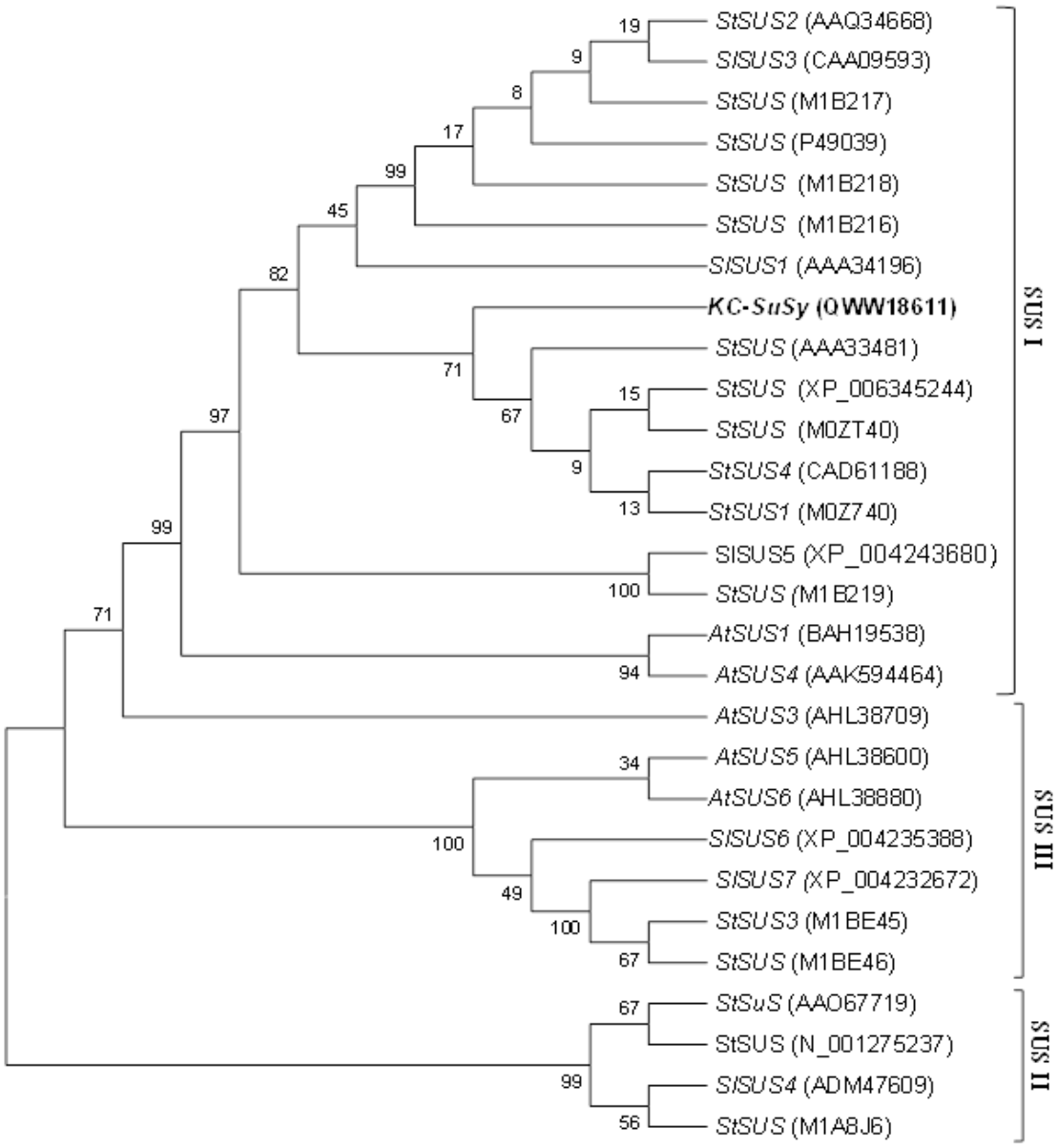

Fig. 4.8 The phylogenetic tree was generated by the MEGA X software using the Neighbor-Joining method with the bootstrap test (1000 replicates) shown next to the branches and computing the evolutionary distances computed by the Poisson correction method. The analyses involved 28 SuSy protein sequences; 17 from the potato (*StSUS*), 6 from tomato (*SlSUS*) and 5 from *A. thaliana (AtSUS)* as available in the published reports and/or databases (the plant species and the GenBank/ Uniprot accession numbers are indicated at each branch). The 805-aa KC-1 specific SuSy (QWW18611) corresponding to the culivar KC-1 of this study occupied distinct positions in the phylogenetic tree (shown in bold cases). The three *SUS* groups are also indicated.

existence of the allelic variants of the gene-a common feature of the polyploid potato plants. Interestingly, the smaller transcripts are found to be variants of the SuSy proteins, which might be involved in other physiological processes that still remain an enigma. The instability index of the functional SuSy proteins ranged from 30.22 to 41.87, which classified them as relatively stable proteins. The aliphatic index of the SuSy proteins ranged from 77.76 to 102.91 and indicated that they are thermostable. The GRAVY values of these proteins ranged from –0.428 to 0.324 indicating their segment-wise hydrophilic and hydrophobic characteristics. The p*I* values ranged from 4.78 to 6.95 and indicated their slightly acidic nature. Phylogenetic analysis of the 28 SuSy proteins from potato, tomato and Arabidopsis indicated that the SUS gene family was clearly divided into three major groups in potato also like its closest homolog tomato (Fig 4.8). From the phylogenetic tree, it was deduced that SUS I is the largest group containing many isoforms and appeared to be more evolved as compared to other two groups.

The biological characteristics of the published SuSy isoforms available in the NCBI database were also studied (Table 4.4). Although the number of amino acids were the same in some isoforms, they could differ in other biochemical parameters such as theoretical p*I* and molecular weight. Like tomato and *Arabidopsis* and other plants, the *SuS* genes could be divided into three groups in potato (Duan et al. 2021). Thus, implicating that these isoforms could be allelic variants of the individual *SUS* genes. Hence leading to the expansion and evolution of the gene family. As mentioned earlier, the size of the *SUS* gene family significantly varies between the plant species ranging from two to thirty, suggesting gene duplication events might have led to the expansion of this gene family (Abdullah et al. 2018; Stein and Granot, 2019; Xu et al. 2019).

Table 4.4 Biochemical information of the potato SuSys extracted from the NCBI database

Gene Name	Accession No. (Nucleotide)	Accession No. (Protein)	ORF (bp)	Coding Region	Protein (aa)	Mol. Wt. (kDa)	pI
Sucrose synthase (SS16)	XM_006345182	XP_006345244	2813	156.. 2573	805	92.47	5.87
Sucrose synthase	M18745	AAA33841	2711	76.. 2493	805	92.41	5.83
Sucrose synthase 2	AY205084	AAO34668	2701	122.. 2539	805	92.61	5.98
Sucrose synthase 4	AJ537575	CAD61188	2429	6.. 2423	805	92.44	5.91
Sucrose synthase 2	AY205302	AAO67719	2679	22.. 2457	811	92.77	5.99
Sucrose synthase 3	NM_001288308	NP_001275237	2679	22.. 2457	811	92.77	5.99

Chromosomal localization: The *SUS* genes were localised on five chromosomes: briefly, PGSC0003DMG400002895 at 30.85 Mb on Ch12, PGSC0003DMG400031046 on Ch3 at 44.88 Mb, PGSC0003DMG4000006672 on Ch9 at 61.46 Mb, PGSC0003DMG400016730 on Ch2 at 36.93 Mb and PGSC0003DMG400013546 at 40.64 Mb, PGSC0003DMG400013547 at 40.61 on Ch7 (Fig. 4.9).

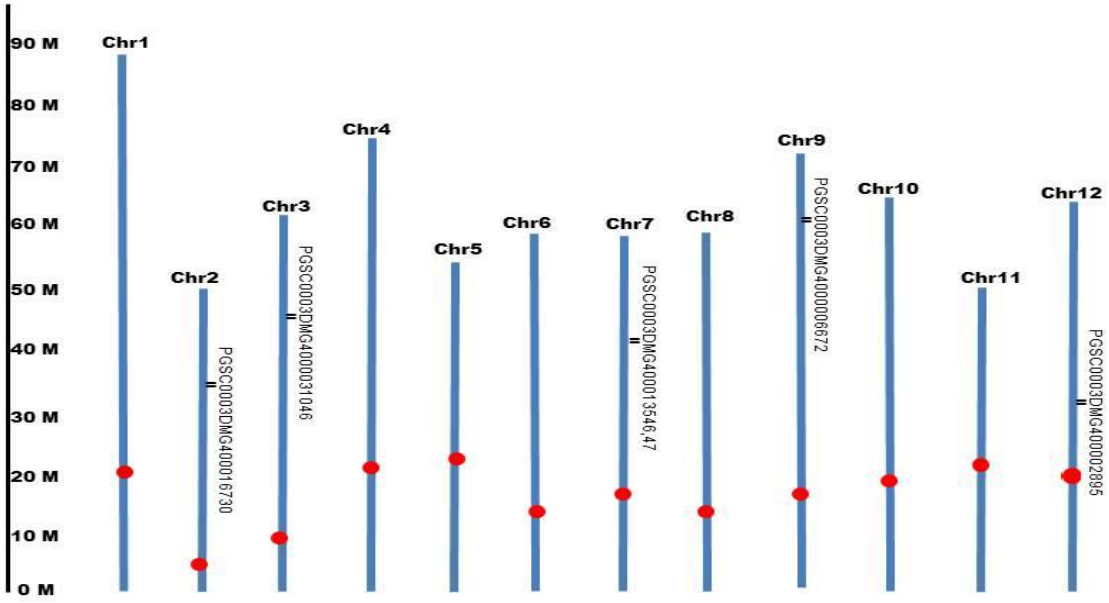

Fig. 4.9 A schematic presentation of chromosomal localization of the potato *SUS* genes retrieved from Potato Genome Sequencing Consortium (PGSC) and *Ensembl Plants* database. The chromosomes are shown in blue, while the centromeres are shown in red.

Model structure, active site prediction and validation: In order to annotate biological function of any protein it is essential to know its structure first. So, the model generated by I-TASSER (through the combination of threading and *ab initio* prediction) was taken for the study. I-TASSER, a meta server implements different threading programmes and its quality is asssed on the basis of Z-score (the energy score in standard deviation units relative to statistical mean of alignments). For confident alignment Z-score should be greater than 1. The model with minimized energy was used to show the specific glycosyl transfer signature domain. The active site and the crucial features and domains as reported earlier were also studied and shown in the 3-D structure visualized in the form of ribbons by PyMol shown in Fig.4.10 (Zheng et al. 2011; Huang et al. 2016). It was observed that in 3-D structure, the catalytically active domains i.e., CTD domain in blue, EPBD domain in cyan, the GTB-N domain in wheat, GTB-C domain in yellow and linker domain in green colour were present in close proximity thus could trigger the enzymatic activity which need to be elucidated.

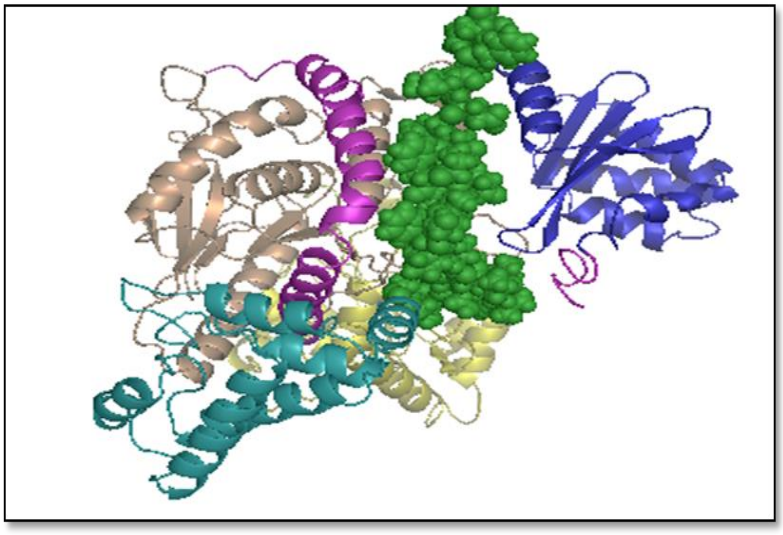

Fig. 4.10 Illustrated representation and catalytic domains of the predicted three-dimensional structure model of the KC- SuSy. The CTD domain is depicted in blue, EPBD domain in cyan, the GTB-N domain in wheat, GTB-C domain in yellow and the extra N and C terminal regions in magenta colour in the form of cartoon. The other important linker region between CTD and EPBD domain is shown as sphere in green colour. The images were generated using the PyMol program (Schrödinger, Inc., New York, NY, USA)

The modelled structure was validated using the Structural Analysis and Verification Server (http://nihserver.mbi.ucla.edu/SAVES) (Fig.4.11). Backbone conformation evaluation by the inspection of the Psi/Phi Ramachandran plot of the proteins model indicated that very few generally one or two amino acids were in disallowed regions. As these residues were considerably distant from the important domains, so their influence on the inferences derived here can be considered negligible. The details of residues in derived protein models in the various regions like, the most favoured, additional allowed, generously allowed and disallowed regions, in Ramachandran plot.

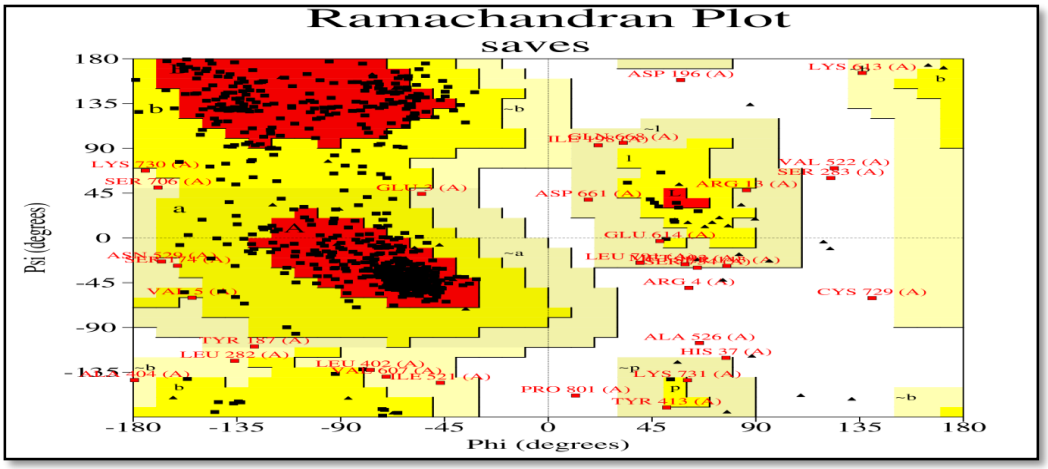

Fig. 4. 11 Ramachandran plot of the KC- SuSy model. The most favoured regions are colored red, additional allowed, generously allowed and disallowed regions are indicated as yellow, light yellow and white fields, respectively.

Thus from the Ramachandran analysis, it could be hypothesised that generated 3-D model is highly plausible. The transmembrane helices prediction (Fig.4.12) was done using Phyre2, a protein fold recognition server (sbg.bio.ic.ac.uk). The transmembrane helices help to predict the protein topology in the membrane. From the figure it could be deduced that the SuSy protein is cytoplasmic or in other words it is localized in the cytosol of cell. For this Phyre2 uses memsat-svm which has demonstrated an average accuracy of approximately 90% on large number of data set. Hence, it has proved to be beneficial in order to know the topology of any protein thus understanding its structure and function.

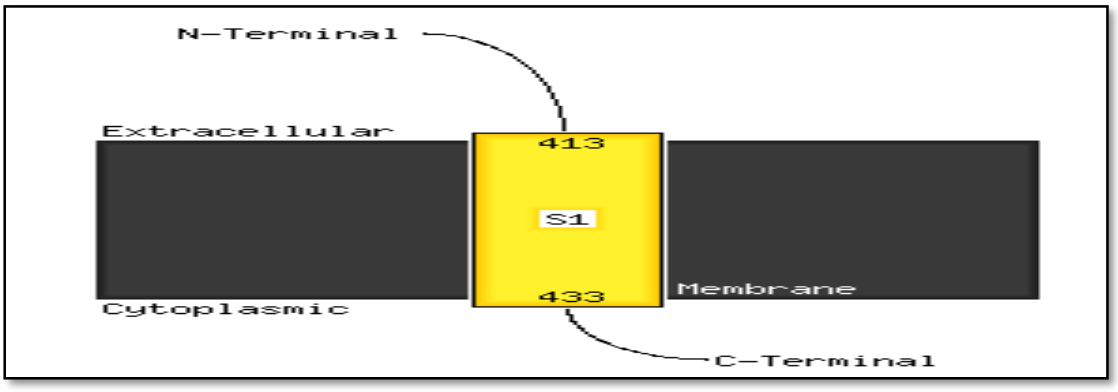

Fig. 4.12 Illustrated representation of transmembrane helix prediction of KC- SuSy by Phyre2. The extracellular and cytoplasmic sides of the membrane are labelled and the beginning and of each transmembrane helix illustrated with a number indicating the residue index

4.2.2 Sequence Analyses of Fructokinases (FRKs)

Multiple sequence alignment, protein motifs and structural features: Using the MultAlin software, multiple sequence alignment was done using a total of eighteen FRK sequences corresponding to the four major active forms (FRK1–4) from the five *Solanaceae* family members (Fig.4.13): seven FRK2 forms (three from potato, one each from tomato, tobacco, petunia and capsicum); four FRK1 forms (one each from potato, tomato, capsicum and tobacco); three FRK3 forms (one from potato, two from tomato), and four FRK4 forms (two from potato, one each from tomato and tobacco). The purpose was to closely inspect the sequence similarities and divergences, nature and location of the amino acid substitutions, deletions/insertions within and between the FRK isoforms of different plant species. Different members of the individual FRK isoforms became visibly distinct because of their nearly common N-terminal regions. Alignment of the PfkB family carbohydrate kinase regions of

```
                                                                                                    ~~~~~~~~~~~~~ββββ~~~βββ
St-FRK2                                                                                     MAVNGSALSSGLIVSFGEMLID   22
St-FRK2A                                                                                    MAVNGSALSSGLIVSFGEMLID   22
SlFRK2                                                                                      MAVNG-ASSSGLIVSFGEMLID   21
St-FRK2B                                                                                    MAVNGSAPSSGLIVSFGEMLID   22
NtFRK2                                                                                      MAANG-V-SSGLIVSFGEMLID   20
PiFRK2                                                                                      MAVNG-VSSGGLIVSFGEMLID   21
CbFRK2                                                                                      MAVNGSA-SSGLIVSFGEMLID   21
St-FRK1                                                                 MADESISGNLKDLSLNRNGDVSKKSHLVVCFGEMLID   37
SlFRK1                                                                  MAGESISGNLKDLSLNRNGAVSKKSHLVVCFGEMLID   37
CbFRK1                                                                  MADESISGNLKDLCLNRNGVASNNSHLVVCFGEMLID   37
NsFRK1                                                                  MADESISGNLKDLSLNTNGAATKKSHLVVCFGEMLID   37
St-FRK3   MALHVTAFSFTGVSTSSKASRSSLLSVFPAPRRCTVKAASQYPPSIPRCKIQGRALPSDNGPLEKDESSLVVCFGEMLID   80
SlFRK3    MALHATAFSFTGVSTSSKSSRSALLSVFPLPRRCTVKATSQYPHSFPRCKIQGRALPSDNGLVEKDESSLVVCFGEMLID   80
LeFRK3    MALHATAFSFTGVSTSSKSSRSALLS---LPRRCAVKATSQYPHSFPRCKIQGRALPSDNGLVEKDESSLVVCFGEMLID   77
St-FRK4A        MDRSSKKGSKMACCFPVILDRSMRSSFKLSKSSSSNKLNKSKSSICSPTSLSMKKKSVQENDHLVVCFGELLID   74
St-FRK4B                MACCFPVILDRSMRSSFKLSKSSSSNKLNKSKSSICSPTSLSMKKKSVQENDHLVVCFGELLID   64
LeFRK4                  MACCFPVILDRSMRSSFKLSKSSSSSKLDKSKSSICSPTSLSTKKKSIQENDNLVVCFGELLID   64
NtFRK4          MDRSSKKGSKLACCFPVILDRSMKSSFKLSKSSSSDKLNKSKSSICSPTSLSMKKRD-QENNHLVVCFGELLID   73
                                                                                                    . *:*:***:***

                                PfkB Kinase(Signature 1)/(ATP binding motif)
                                          ▼  ▼  ==========                                        ▼
                βββ~~~~~~~~~~~~~ββββ~~~ααααααααααα~~~βββββββββ~~ααααααααααα~~~~~ββββββ~~~~βββββββ
St-FRK2   FVPTVSAVSLGEAPGFLKAPGGAPANVAIAVTRLGGKSAFVGKLGDDEFGHMLGGILKTNGVQADGINFDKGARTALAFV  102
St-FRK2A  FVPTVSGVSLAEAPGFLKAPGGAPANVAIAVTRLGGKSAFVGKLGDDEFGHMLAGILKTNGVQADGINFDKGARTALAFV  102
SlFRK2    FVPTVSGVSLAEAPGFLKAPGGAPANVAIAVTRLGGKSAFVGKLGDDEFGHMLAGILKTNGVQAEGINFDKGARTALAFV  101
St-FRK2B  FVPTVSGVSLAEAPGFLKAPGGAPANVAIAVTRLGGKSAFVGKLGDDEFGHMLAGILKTNGVQADGINFDKGARTALAFV  102
NtFRK2    FVPTVSGVSLAEAPGFLKAPGGAPANVPIAVTRLGGKSAFVGKLGDDEFGHMLPGILKQNGVQADGINFHKGARTALAFL  100
PiFRK2    FVPTVSGVSLAEAPGFLKAPGGAPANVAIAVTRLGGNSAFVGKLGDDEFGHMLAGILKENGVKAEGINFDTGARTALAFV  101
CbFRK2    FVPTVSGVSLAEAPGFLKAPGGAPANVAIAVTRLGGKSAFVGKLGDDEFGHMLAGILKQNGVQADGINFDTGARTALAFV  101
St-FRK1   FIPTLAGVSLAEAPAFEKAPGGAPANVAVCISKLGGSSAFIGKVGDDEFGRMLADILKQNNVDNSGMRFDHDARTALAFI  117
SlFRK1    FIPTVAGVSLAEAPAFEKAPGGAPANVAVCISKLGGSSAFIGKVGDDEFGRMLADILKQNNVDNSGMRFDHDARTALAFI  117
CbFRK1    FIPTVGGVSLAEAPSFEKAPGGAPANVAVCVSKLGGSSAFIGKVGDDEFGRMLADILKQHNVDNSGMRFDHDARTALAFV  117
NsFRK1    FVPTVGGVSLAEAPAFEKAPGGAPANVAVCIANLGGSSAFIGKVGEDDFGRMLADILKQHNVDNSGMRFDHDARTALAFV  117
St-FRK3   FVPTISGLSLAEAPAFKKAPGGAPANVAVGISRLGGSSAFIGKVGEDEFGYMLAEILKENNVNSDGMRFDPGARTALAFV  160
SlFRK3    FVPTTSGLSLAEAPAFKKAPGGAPANVAVGISRLGGSSAFIGKVGEDEFGYMLAEILKENNVNSDGMRFDPGARTALAFV  160
LeFRK3    FVPTTSGLSLAEAPAFKKAPGGAPANVAVGISRLGGSSAFIGKVGEDEFGYMLAEILKENNVNSDGMRFDPGARTALAFV  157
St-FRK4A  FVPTVSGVSLAEAPGFKKAPGGAPANVAVGIARLGGSSAFIGKVGADEFGYMLADILKQNNVDNSGMRFDTHARTALAFV  154
St-FRK4B  FVPTVSGVSLAEAPGFKKAPGGAPANVAVGIARLGGSSAFIGKVGADEFGYMLADILKQNNVDNSGMRFDTHARTALAFV  144
LeFRK4    FVPTVSGVSLAEAPGFKKAPGGAPANVAVGIARLGGSSAFIGKVGADEFGYMLADILKQNNVDNSGMRFDTHARTALAFV  144
NtFRK4    FVPTVSEVSLAEAPGFKKAPGGAPANVAVGIARLGGSSAFIGKVGADEFGYMLSDILKQNHVDNSGMRFDTHARTALAFV  153
          *:**...:**:***.* ***********:.: .***.***:**:* ****.**..***...* ..*:.**  *******:

                                                                  Substrate recognition domain
                                                                                          ▼
          ββ~~~~~βββββββ~~~~ααα~~~ααα~~αααααα~~ββββ~~~αα~~αααααααααααααααααα~~~~~~~~~~~~~~~~
St-FRK2   TLRADGEREFMFYRNPSADMLLTPDELNLDLIRSAKVFHYGSISLIVEPCRSAHLKAMEVAKEAGALLSYDPNLRLPLWS  182
St-FRK2A  TLRADGEREFMFYRNPSADMLLTPDELNLDLIRSAKVFHYGSISLIVEPCRSAHLKAMEVAKEAGALLSYDPNLRLPLWS  182
SlFRK2    TLRADGEREFMFYRNPSADMLLTPAELNLDLIRSAKVFHYGSISLIVEPCRAAHMKAMEVAKEAGALLSYDPNLRLPLWP  181
St-FRK2B  TLRADGEREFMFYRNPSADMLLTPDELNLDLIRSAKVFHYGSISLIVEPCRSAHLKAMEVAKEAGALLSYDPNLRLPLWS  182
NtFRK2    TLRADGKREFMFYRNPSADMLLTPDELNLEVIKSAKVFHYGSINLIVEPCRSAHLKAMEVAKEARALLSYDPNLRLPLWP  180
PiFRK2    TLRADGEREFMFYRNPSADMLLTPDELNLDVIRSAKIFHYGSISLIVEPCRSAHLKAMEVAKEAGALLSYDPNLRLPLWP  181
CbFRK2    TLRADGEREFMFYRNPSADMLLKPEELNLDLIRSAKVFHYGSISLIVEPCRSAHLKAMEVAKEAGALLSYDPNLRLPLWP  181
St-FRK1   TLTAEGEREFVFFRNPSADMLLRESELDVDLIKKATIFHYGSISLIDEPCRSAHLAAMDIAKRSGSILSYDPNLRLPLWP  197
SlFRK1    TLTAEGEREFVFFRNPSADMLLRESELDVDLIKKATIFHYGSISLIDEPCRSTHLAAMDIAKRSGSILSYDPNLRLPLWP  197
CbFRK1    TLTAEGEREFVFFRNPSADMLLRESELDVNLIKKATIFHYGSISLIDEPCRSTHLAAMDIAKRSGSILSYDPNLRLPLWP  197
NsFRK1    TLTAEGEREFVFFRNPSADMFLRESELDVNLVKKATIFHYGSISLIEEPCRSTQLAAMDIAKRSGSILSYDPNLRLPLWP  197
St-FRK3   TLRKDGEREFMFYRNPSADMLLQEDELDLELIRKAKVFHYGSISLITEPCKSAHIAAAKAAKDAGVILSYDPNLRLPLWP  240
SlFRK3    TLRKDGEREFMFYRNPSADMLLQEDELDLELIRKAKVFHYGSISLITEPCKSAHIAAAKAAKDAGVILSYDPNLRLPLWP  240
LeFRK3    TLRKDGEREFMFYRNPSADMLLQEDELDLELIRKAKVFHYGSISLITEPCKSAHIAAAKAAKDAGVILSYDPNLRLPLWP  237
St-FRK4A  TLKADGEREFMFFRNPSADMLLTEAELDKNLIQKARIFHYGSISLIAEPCRSAHLAAMETAKNAGCILSYDPNLRLPLWP  234
St-FRK4B  TLKADGEREFMFFRNPSADMLLTEAELDKNLIQKARIFHYGSISLIAEPCRSAHLAAMETAKNAGCILSYDPNLRLPLWP  224
LeFRK4    TLKSDGEREFMFFRNPSADMLLTEAELDKNLIQKARIFHYGSISLIAEPCRSAHLAAMETAKNAGCILSYDPNLRLPLWP  224
NtFRK4    TLRADGEREFMFFRNPSADMLLTEAELDKDLIQKARIFHYGSISLIAEPCRSAHLAAMEIAKKAGCILSYDPNLRLPLWP  233
          **..:*****:*.********* . **.. :*  * :********* ***::.*:.*:. ** .* :***********.
```

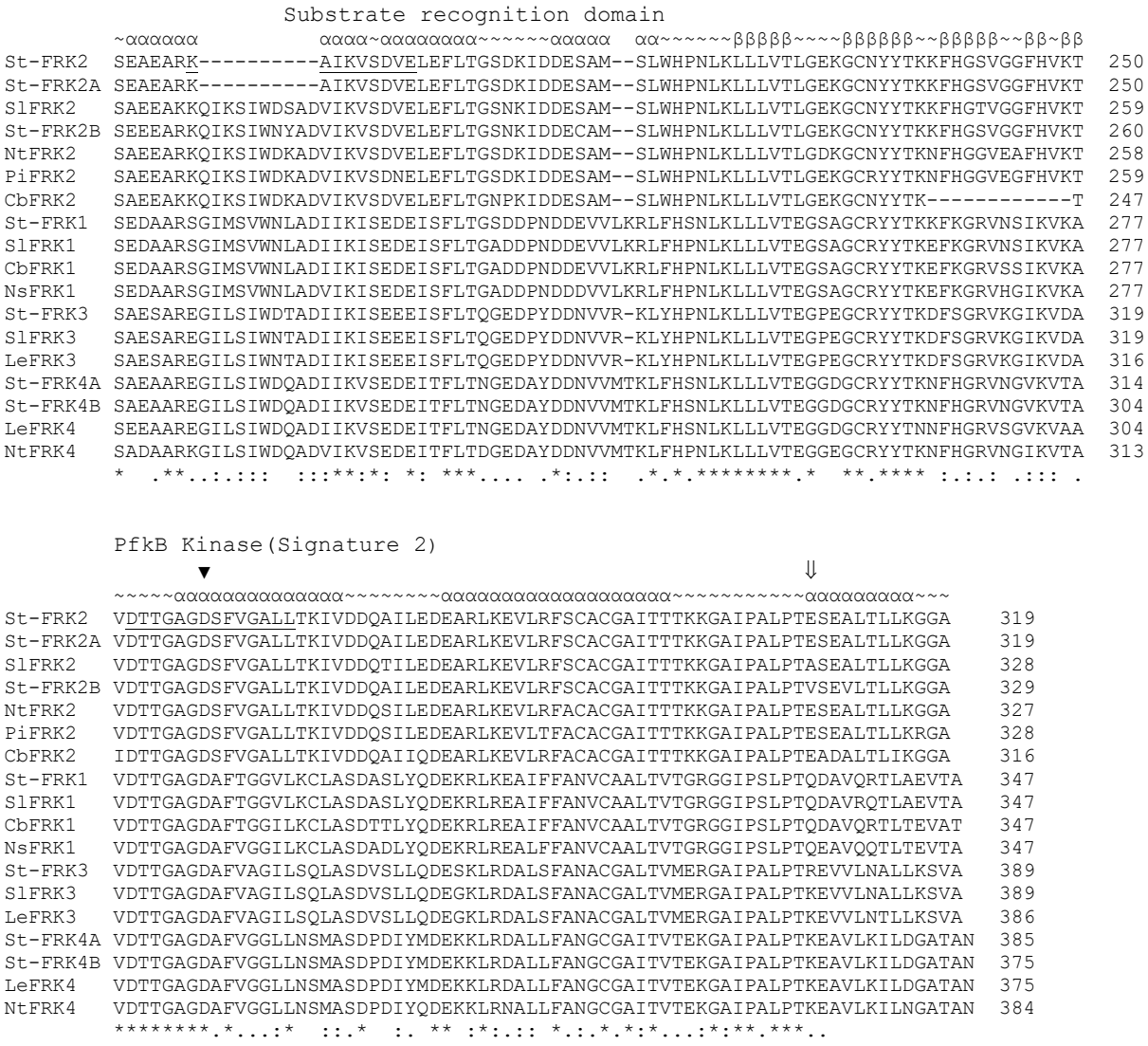

Fig. 4.13 Comparison of the predicted 18 full-length FRK sequences corresponding to the four major active isoforms from the *Solanaceae* family members namely potato, tomato, tobacco, petunia and capsicum. FRK2 isoform includes St-FRK2 (QIS79145), St-FRK2A (CAA78283), SlFRK2 (AAB57734), St-FRK2B (Sotub06g027780), NtFRK2 (NP_001312967), PiFRK2 (AAQ09999), CbFRK2 (PHT46403); FRK1 isoform includes St-FRK1 (Sotub03g007180), SlFRK1 (AAB57733), CbFRK1 (PHT53066), NsFRK1 (XP_009778351); FRK3 isoform includes St-FRK3 (AFX67038), SlFRK3 (NP_001234396) LeFRK3 (AAR24912); FRK4 isoform includes St-FRK4A (PGSC0003DMP400018156), St-FRK4B (Sotub10g016360), LeFRK4 (AAM44084), NtFRK4 (AIE16179). Multiple sequence alignment was done based on *MultAlin* software along with some minor manual adjustments. Dashes indicate gaps that arise during alignment. Asterisks '*' indicate the conserved/nearly conserved amino acids; ':' refers to the almost conserved or conservative substitutions; '.' refers to conserved amino acids in at least two FRK forms. The downward arrow '⇓' indicates the entire PfkB kinase region. The crucial regulatory/binding motifs are underlined in St-FRK2, and the ATP binding motif within PfkB Kinase (Signature 1) is over lined by '=', '▼' denotes the crucial amino acids involved in fructose-binding. 'α', 'β' and '∼' denote the propensity of the individual amino acids of St-FRK2 towards alpha helix, beta-sheet and random coil formation, respectively. The predicted N-terminal chloroplast transit peptides in potato FRK forms are grey highlighted.

most of the members are comparable in terms of size, but considerable sequence divergence could be noticed; moreover, St-FRK2, St-FRK2A and CbFRK2 were found shorter by 10 to 12-aa peptide segments. St-FRK2 and St-FRK2B appeared to be two distinct FRK2 variants in potato. The crucial motifs in the PfkB region of St-FRK2 included PfkB Kinase Signature 1 containing ATP binding motif (GGAPANVAIAVTRLGGKSAFVGKLG), PfkB Kinase Signature 2 (DTTGAGDSFVGALL), substrate recognition domains (LLSYDPNL and KAIKVSDVE) along with seven crucial amino acid residues important for Fru binding namely Glu18, Asp22, Ala45, Asn48, Val110, Arg177, and Asp258. The region spanning the substrate recognition domains appeared to be larger by a 10-aa segment in most of the FRK members except St-FRK2 and St-FRK2A. All the motifs and crucial amino acids are mostly conserved between the FRK members. Apart from the N-terminal and C-terminal regions, considerable sequence divergence as noticed in the flanking regions of the crucial motifs/amino acid residues could influence the secondary structures like α-helices/β-sheets and overall folding patterns of the FRKs.

The PfkB kinase region of an active FRK is known to consist of two major domains: the large domain contains a cluster of α-helices wherein a β-sheet is embedded; whereas the smaller domain also referred to as lid domain is another β-sheet attached to the aforesaid larger domain through a hinge made of short loops (Carberra et al. 2010). Sequential binding of carbohydrate and ATP to PfkB proteins triggers the closure of the lid domain. The enzymes attain an open state only at the end of catalysis which facilitates release of the products. Moreover, the hydrophobic β-sheet of the lid domain is involved in the formation of active dimers of the PfkB proteins. For most of the PfkB family members, ATP acts as a phosphate donor; but the same in excess could also trigger substrate inhibition possibly through binding to the allosteric site and consequently the formation of inactive tetramers. The regulatory role of ATP is yet unclear (Campos et al.1984; Riggs et al. 2017). Two signature motifs i.e., a di-Gly (GG) motif and a G/AXGD motif are found to be common in the PfkB proteins. The importance of each motif was assessed through mutational and structural analyses. The GG motif confers flexibility between the lid and the large domain, whereas the G/AXGD motif is directly involved in catalysis. In the *L. donovani* pfkB member ADK, a non-conservative substitution like the second glycine to aspartate in the GG motif led to drastic reduction of both enzyme activity and substrate binding affinity (Datta et al. 2005). The aspartate in the G/AXGD motif plays a

crucial role during catalytic conversion of Fru to Fru-6-P. FRK activity was drastically reduced by changing this Asp residue to Asn (Sigrell et al. 1998; Carbera et al. 2010).

All the PfkB kinase-specific important catalytic/binding motifs with the associated crucial amino acids were mostly conserved in all the FRK forms, and the flanking regions of these motifs showed considerable divergence. The N- and C-terminal regions were found to vary significantly between the isoforms. Both conservative and nonconservative substitutions were noticed at number of places. The variations were due to the cumulative point mutations, deletions/insertions which could have impact on their secondary structures, folding patterns, evolutionary relatedness and importantly their catalytic activities. All these aspects remain to be elucidated through corroborative experimental research.

Phylogenetic analysis: A total of 54 amino acid sequences comprising 45 from the different *Solanaceae* family members and 9 from *A. thaliana*, corresponding mostly to the different FRK isoforms along with some FLNs were used in making a phylogenetic tree to examine the sequence relatedness between them (Fig. 4.14). Sequence and phylogenetic analyses clearly indicated that *S. tuberosum* cv. KC-1 (QIS79145) i.e., St-FRK2 was a distinct FRK2 form. Two more KC-1 specific cDNA clones encoding a 256-aa FRK2 form and a 266-aa FLN form designated *S. tuberosum* cv. KC-1 (QIV66775) and *S. tuberosum* cv. KC-1 (QIV66777), respectively were included in the phylogenetic analysis. The branching patterns of some *A. thaliana* FRK forms clearly indicated significant sequence divergence with the corresponding *Solanaceae* family members.

Characterization of FRKs from the potato genome: A genome wide analysis of *FRK* gene family in potato *(Solanum tuberosum* L.) was performed on the data available in the complete potato genome sequence (Potato Genome Sequencing Consortium 2011), and ensemble plant. Seven FRK with their respective genes IDs were retrieved from the spudDB. It was revealed that four *FRK* genes code four different FRK isoforms (FRK1-4), whereas others encode FLN isoforms (Table 4.5). All the *FRKs* and *FLNs* encode different mRNAs due to alternate splicing except PGSC0003DMG400026916 which encodes single mRNA (FRK2) resulting into four polypeptides of variable amino acids ranging from 329 to 256. Hence, making *FRK2* an important and interesting domain to be studied. The respective positions of the FRKs on the different chromosomes is shown in Fig. 4.15. It was observed that the highest number of *FRK* genes (FRK2, PGSC0003DMG400026916 and FLN, PGSC0003DMG400020361) are located

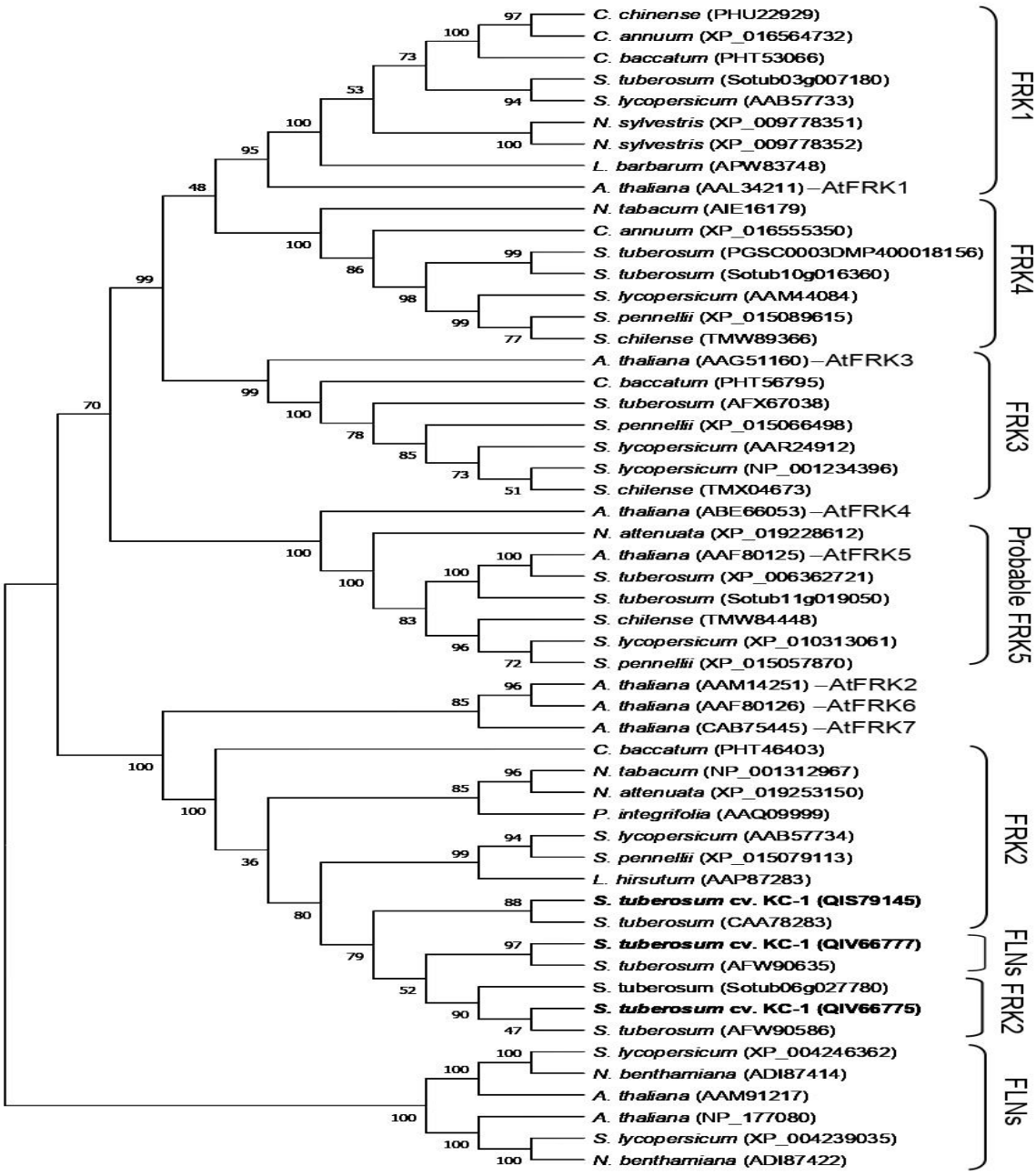

Fig. 4.14 A total of 54 amino acid sequences comprising 45 from the different *Solanaceae* family members and 9 from *A. thaliana*, corresponding mostly to the different FRK isoforms along with some FLNs were used in making a phylogenetic tree to examine the sequence relatedness between them. Sequence and phylogenetic analyses clearly indicated that *S. tuberosum* cv. KC-1 (QIS79145) i.e., St-FRK2 was a distinct FRK2 form. Two more KC-1 specific cDNA clones encoding a 256-aa FRK2 form and a 266-aa FLN form designated *S. tuberosum* cv. KC-1 (QIV66775) and *S. tuberosum* cv. KC-1 (QIV66777), respectively were included in the phylogenetic analysis. The branching patterns of some *A. thaliana* FRK forms clearly indicated significant sequence divergence with the corresponding *Solanaceae* family members.

Table 4.5 Features of the *FRK* genes in potato retrieved from genomic databases (Spud DB and Ensemble Plants)

PSGC Gene ID	PSGC Transcript ID	Uniprot I.D.	FRK Isoform	No. of Base pairs	No. of amino Acids	MW (kDa)	Chromoso-mal localization	Theor itical pI	Stability index	Aliphatic index	GRAVY analysis
PGSC0003DMG400024246	PGSC0003DMT400062304	M1C8V2	FRK1	1863	347	37.37	3	5.2	26.76	94.24	- 0.016
	PGSC0003DMT400062303	M1C8V3		922	262	28.90	3	4.75	34.48	99.12	0.079
	PGSC0003DMT400062305	M1C8V1		2581	309	33.43	3	5.15	27.76	96.96	0.004
	PGSC0003DMT400062306	MIC8V4		917	85	8.92	3	9.10	7.21	87.29	0.031
PGSC0003DMG400026916	PGSC0003DMT400069198	Q2PYY9	FRR2	1292	329	35.43	6	5.47	29.53	95.53	0.030
		P37829	FRK2		319	33.76	6	5.41	20.75	97.62	0.133
		K7VKD3	FLN		266	28.74	6	5.89	25.81	96.47	0.069
		K7WJT8	FRK2		256	27.88	6	5.79	26.19	99.16	0.020
PGSC0003DMG400020361	PGSC0003DMT400052461	M1BTG0	FLN	1845	388	44.74	9	5.74	49.91	74.33	-0.483
		D9IWP2			479	54.81	9	6.91	52.74	66.33	-0.606
PGSC0003DMG400027017	PGSC0003DMT400069497	M1CKJ7	FLN	2204	150	17.09	6	6.27	50.44	79.93	-0.315
	PGSC0003DMT400069498	Q3HVM6	FLN	1374	233	25.91	6	4.91	48.85	79.18	-0.395
PGSC0003DMG40002831 1	PGSC0003DMT400072749	M1CQW1	FLN	2459	650	72.94	5	5.81	55.08	71.80	-0.639
	PGSC0003DMT400072750	M1CQW0	FLN	1950	649	72.56	5	5.73	53.14	75.650	-0.004
PGSC0003DMG400030653	PGSC0003DMT400078779	K7WU45	FRK3	1768	389	41.78	2	5.37	36.19	93.86	-0.004
	PGSC0003DMT400078780	M1D0Q1	FRK3	1764	313	33.72	2	4.92	31.93	98.88	0.010
PGSC0003DMG4000010277	PGSC0003DMT400026604	M1ANF2	FRK4	1146	381	40.85	10	5.77	27.10	89.15	-0.001
	PGSC0003DMT400026605	M1ANF3	FRK4	1393	385	41.35	10	6.61	29.00	86.73	-0.068

on the chromosome number 6, while PGSC0003DMG400030653 on Ch2, PGSC0003DMG 400024246 on Ch3, PGSC0003DMG400028311 on Ch5, and PGSC0003DMG4000010277 on Ch10; no FRK gene was present in the rest of the chromosomes. The longest protein consisted of 650 amino acids (Uniprot ID: M1CQW1), the shortest protein consisted 85 amino acids (Uniprot ID: MIC8V4). The molecular weight also spanned in high range from 8.92 to 72.94 KDa. The instability index (II) is an estimator of protein stability in test-tube. This technique

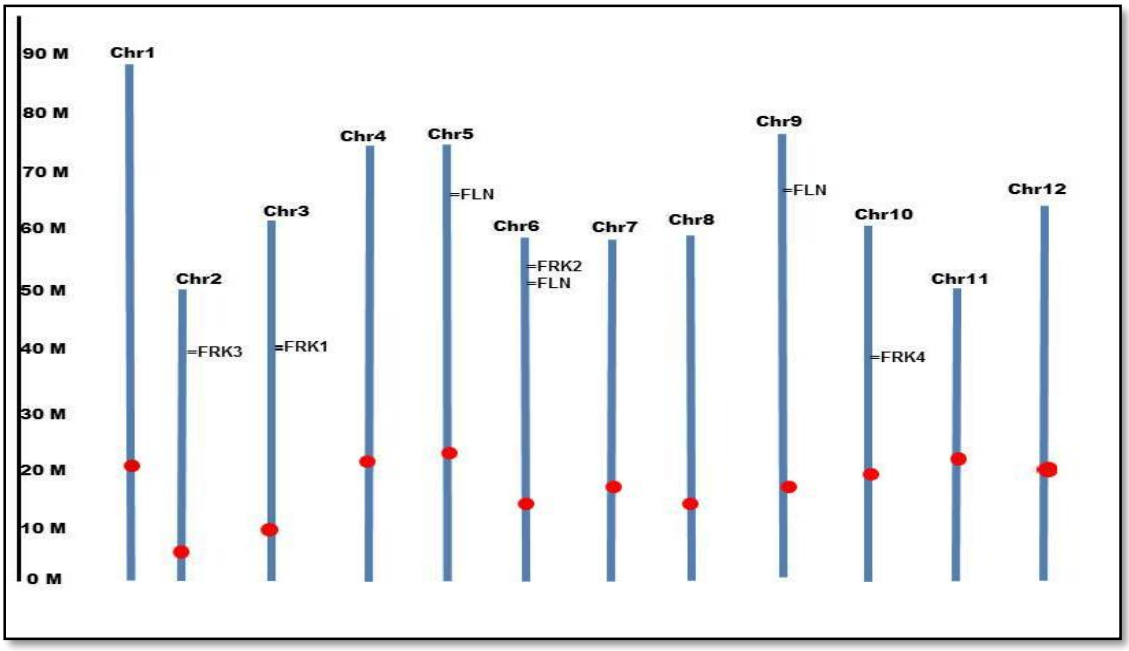

Fig. 4.15 A schematic presentation of chromosomal localization of the various potato fructokinase isoform genes retrieved from Potato Genome Sequencing Consortium (PGSC) database. The chromosomes are shown in blue, while the centromeres are shown in red. FRK1 is present on chromosome 3 at 41.2 Mb, FRK2 on chromosome 6 at 58.2 Mb, FRK3 on chromosome 2 at 71.62 Mb while FRK-like on chromosome 5 and 6 at 58.2 and 65.1 Mb, respectively.

assigns a weight value of instability that can be used to determine an instability index. Proteins with instability index values less than 40 are predicted as stable and values above 40 indicate instability of proteins. The II of FRK proteins ranged from 7.21 to 55.37 in the present study. Aliphatic index, which is an indicator for increase in thermostability of globular proteins, was found to be high in all proteins ranging from 71.80 to 97.87, indicating that FRKs are stable at wide ranges of temperature. The GRAVY value of FRK proteins ranged from −0.004 to 0.124 indicating their nature spans from hydrophilic to hydrophobic. Surprisingly, some of FRKs are translated by the mRNAs of the same gene, vary in amino acid number but representing the

same isoform, and proteins encoded by the same mRNA were also found to vary in their biochemical attribute which may be due to post translational modification thus making the allelic concept clearer.

Three-Dimensional (3-D) structure of FRKs: Structural information of a protein is a prerequisite in understanding its biological function. The energy minimized 3D structures of one *E. coli* FRK, one catalytically inactive potato FLN and five potentially active potato FRKs were predicted based on the reliable *ab initio* modelling approach using I-TASSER, a hierarchical protein structure modelling approach which effectively combined both threading and *ab initio* prediction methods. The quality of the threading alignment was assessed on the basis of Z-score i.e., the energy score in standard deviation units relative to statistical mean of alignments. Z-score values were found to be greater than 1 suggesting the reliable/confident alignments. The predicted 3D structures were visualized in the form of ribbons by PyMol (https://www.pymol.org) (Fig. 4.16 a–g). The large catalytic domain of the PfkB proteins except FLN contains a GAGD motif involved in catalysis; whereas the smaller peripheral β-sheet acts as the lid domain. The other motif i.e., an N-terminal GG pair is also crucial as it acts as a hinge between these two domains. shown in Fig. 4. 16 a–g. Earlier it was proposed that the close proximity of the N- and C- terminal regions could influence the bending and sliding patterns of the FRK proteins which in turn brought the catalytic GG and GAGD domains closer to each other for their activities (Riggs et al. 2017; Stein and Granot 2018). The predicted FRK 3D structures were consistent with the underlying mechanism of enzyme catalysis. Despite some common folding patterns in the PfkB regions, each 3D structure appeared to be considerably distinct with regard to the arrangements and relative positions of the α-helices, β-sheets, N-terminal, C-terminal and chloroplast-specific transit peptide regions. These structural attributes could influence the catalytic efficiency of the individual FRK forms.

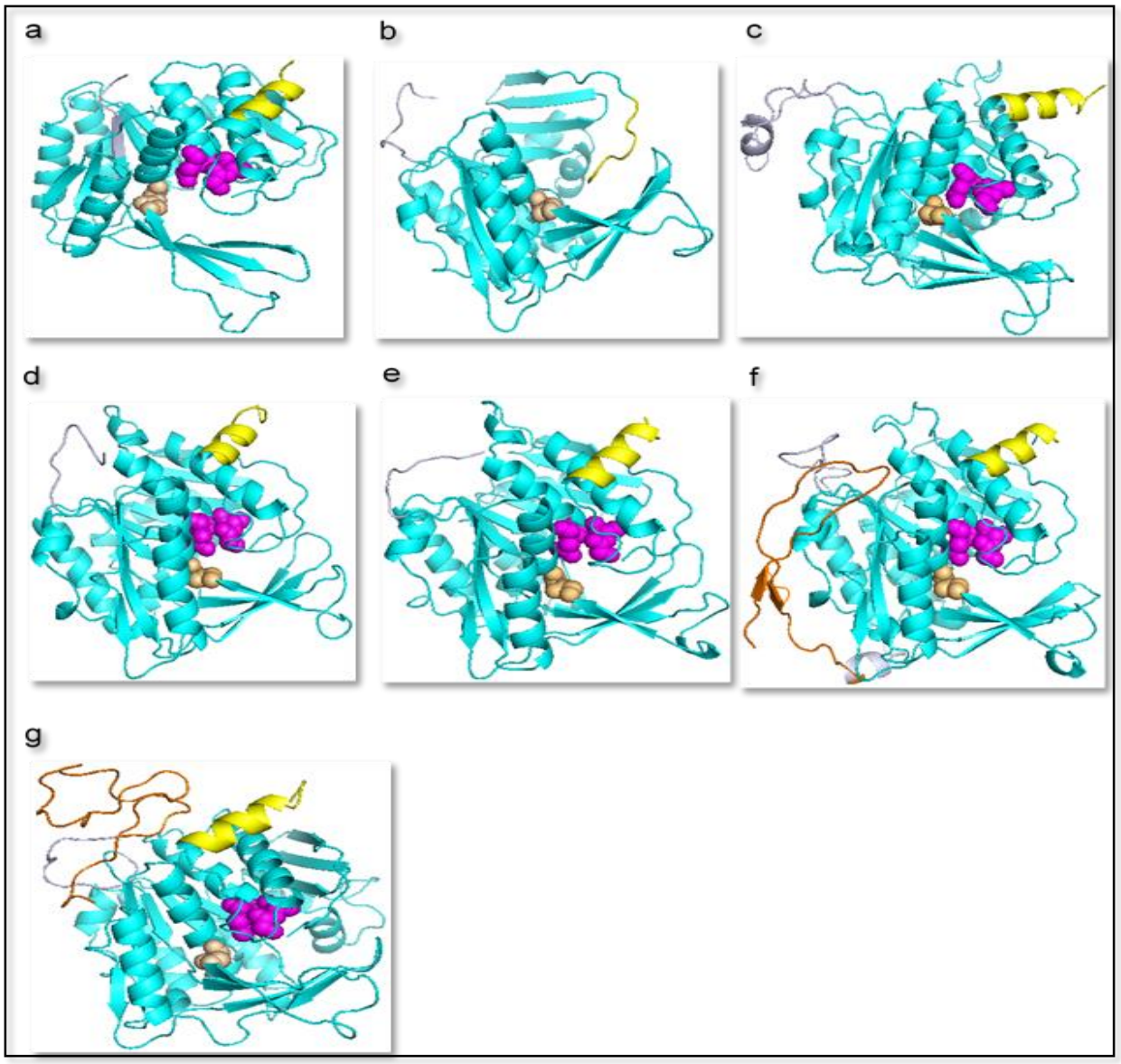

Fig. 4.16 Illustrated representation and catalytic domains of the predicted three-dimensional structure models of the FRKs. **a** 309-aa *E. coli* FRK (NP_416237); **b** 266-aa potato FLN; **c** 347-aa St-FRK1; **d** 319-aa St-FRK2; **e** 329-aa St-FRK2B; **f** 389-aa St-FRK3; **g** 375-aa St-FRK4B. The PfkB regions are depicted in cyan, outside of PfkB the N-terminal regions are in grey and the C-terminal regions are in yellow, chloroplast transit peptides in yellowish-orange, the catalytic GG and GAGD domains are in brown and magenta colours, respectively. The images were generated using the PyMol program (Schrödinger, Inc., New York, NY, USA).

4.2.3 Sequence Analyses of Calcium–dependent Protein Kinase (CDPK)

Multiple sequence alignment, Regulatory/Binding Motifs and other sequence features: Among the multiple CDPK isoforms present in the potato genome, only three i.e., *CDPK*1–3 are known to be involved in tuberization. Keeping this in view, the multiple sequence alignment was done by using protein sequences corresponding to these isoforms as shown in Fig. 4.17. The various catalytic domains present in the CDPKs play important role in the regulation of various physiological processes associated with biotic and abiotic stresses. The distinguishing features, functions and the relative location of the crucial domains such as cyclic AMP (cAMP)-dependent phosphorylation (regulates glycogen, sugar and lipid metabolism in cell), Tyrosine kinase phosphorylation (phosphorylation of the acidic proteins), the bipartite nuclear localization signal (membrane targeting and signal transduction in plants in responses to environmental stress), protein kinases ATP binding region are highlighted in Fig. 4.17.

Characterization of CDPKs from the potato genome: In plant genomes expansion of the gene families is believed to have occurred by different mechanisms such as genome-wide, tandem and dispersed duplications. A genome wide analysis of the *CDPK* gene family was performed in the complete potato genome sequence (Potato Genome Sequencing Consortium 2011 as reported earlier in database) (Fantino et al. 2017; Gromadka et al. 2018). Tables 4.6 and 4.7 provide a more comprehensive information on the *CDPK* gene family in potato which would help for further in-depth studies. The potato genome encodes 23 CDPKs and appears to exhibit high plasticity, as gene loss or duplication events and other structural mutations are found with high frequency. The *CDPK* genes were found to be localized on 11 chromosomes out of 12; on chromosome 9 no *CDPK* gene was found whereas the highest number (six) of *CDPK* genes are found on chromosome number 10 (Fig. 4.18). On some chromosomes the *CDPK* genes form clusters–a clue of gene duplication which suggests the gradual expansion of this gene family. Out of 23, 21 CDPKs are acidic, two are slightly basic and 14 of them contain myristoylation sites (Xu et al. 2015). All CDPKs contain four EF-hands; but like rice, maize, *A. thaliana* and potato have CDPK-like kinases that possess less than four or no EF-hands (Mittal et al. 2017). The gene lengths of different *CDPK*s ranging from 4.01 to 14.5 kb were found to contain 6 to 11 introns. The CDPK proteins consisted of 501–638 amino acids having molecular weights

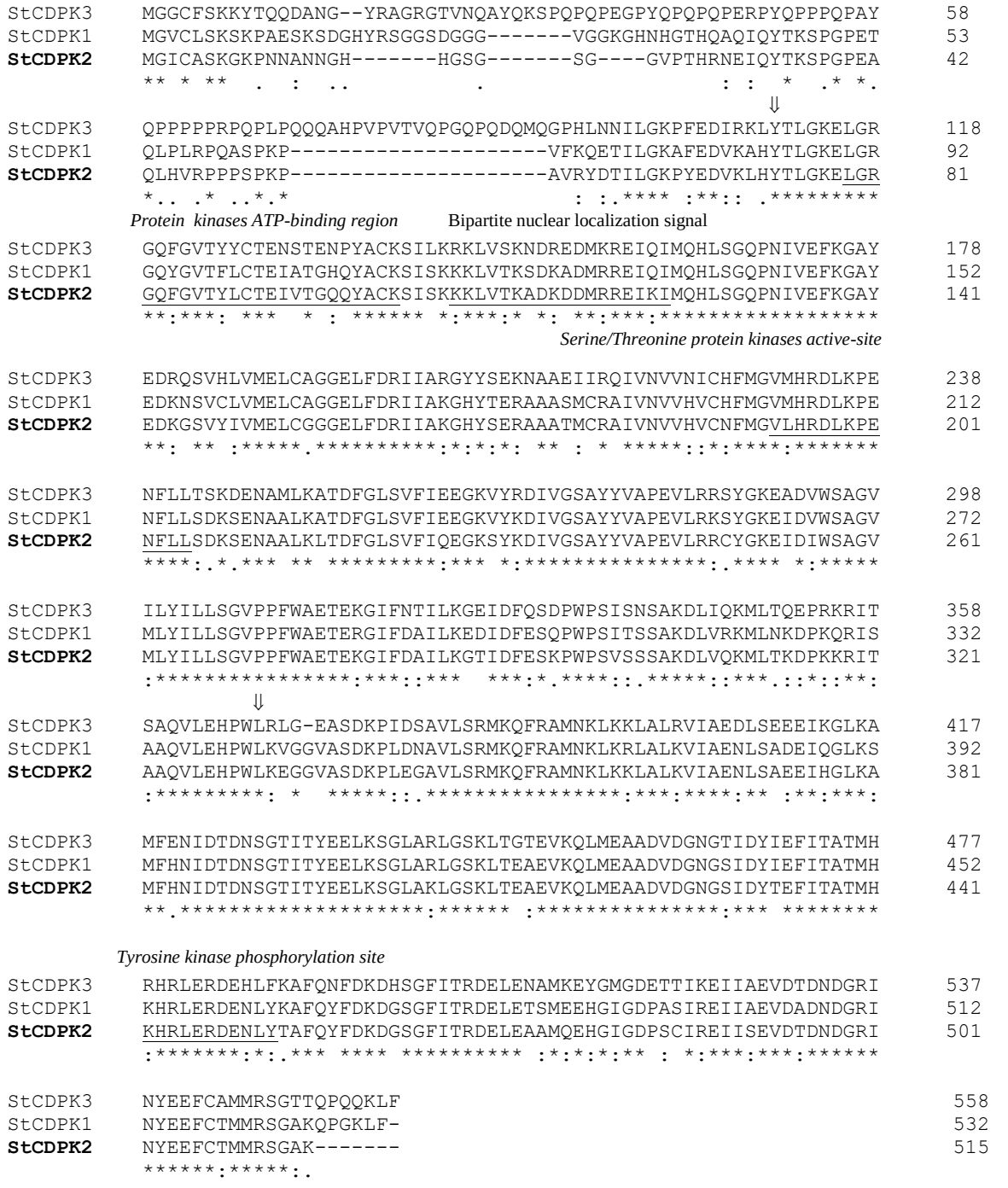

Fig. 4.17 Comparison between the sequences of three potato CDPKs: StCDPK1 (NP_001275322.1), StCDPK2 (QIS79146), StCDPK3 (AAQ08324.2) involved in tuberization. Multiple sequence alignment was done based on *MultAlin* software along with some minor manual adjustments. Dashes indicate gaps that arise during alignment. Asterisks '*' indicate the conserved/nearly conserved amino acids; ':' refers to the almost conserved or conservative substitutions; '.' refers to conserved amino acids in at least two CDPK forms. The downward arrow '⇓' indicates the entire protein kinase region. The crucial regulatory/binding motifs are underlined in StCDPK2, and the '▼' denotes the crucial active site.

Table 4.6 Characterization of 23 CDPK proteins in potato

Name	PGSC Transcript ID	PGSC Protein ID	GenBank no. (NCBI)	ORF (bp)	Aminoacid length (aa)	Molecular	Gene Length	No. of introns	Chromosome	Myristolation site	Theoretical pI
StCPK1 (former StCDPK1)	PGSC0003DMT400071663	PGSC0003DMP400048479	XM_006365894	1530	509	56.6	7.14	6	12	+	6.07
StCP K2 (former StCDPK2)	PGSC0003DMT400057484	PGSC0003DMP400038684	XM_006346152	1566	521	57.9	5.80	7	7	+	6.75
StCPK3 (former StCDPK3)	Not found	Not found	JF308510 NM_001288527	1665	554	63.0	11.02	7	10	+	5.81
StCPK4 (former StCDPK4)	PGSC0003DMT400043320	PGSC0003DMP400029382	XM_006365245	1704	567	63.4	4.31	6	10	–	5.56
StCPK5 (former StCDPK5)	Not found	Not found	AB279738 NM_001287861	1608	535	60.0	14.5	7	8	–	5.65
StCPK6	PGSC0003DMT400060262	PGSC0003DMP400040554	XM_006345687	1512	503	56.4	**5.80**	6	5	–	5.54
StCPK7	PGSC0003DMT400002592	PGSC0003DMP400001885	XM_006350871	1737	578	64.8	6.36	6	5	+	5.35
StCPK8	PGSC0003DMT400027809	PGSC0003DMP400018934	XM_006366477	1602	533	60.0	6.90	7	1	+	5.58
StCPK9	PGSC0003DMT400054983	PGSC0003DMP400036980	XM_006348373	1797	598	67.6	**3.90**	6	1	–	5.79
StCPK10	PGSC0003DMT400021055	PGSC0003DMP400014336	XM_006351162	1575	524	59.4	4.49	7	10	+	5.77
StCPK11	PGSC0003DMT400067082	PGSC0003DMP400045247	XM_006353564	1506	501	56.4	**4.34**	6	6	–	5.17
StCPK12	PGSC0003DMT400072554	PGSC0003DMP400049071	XM_006339117	1824	607	68.3	**5.26**	6	10	–	7.89
StCPK13	PGSC0003DMT400018575	PGSC0003DMP400012783	XM_006364680	1635	544	60.4	4.68	6	10	+	5.44
StCPK14	PGSC0003DMT400025581	PGSC0003DMP400017429	XM_006342017	1623	540	61.0	5.62	7	4	+	5.31

StCPK15	PGSC0003DMT400002331	PGSC0003DMP400001687	XM_006351851	1518	505	57.0	**4.47**	6	11	−	5.71
StCPK16	PGSC0003DMT400058126	PGSC0003DMP400039123	XM_006343307	1707	568	64.2	7.82	11	3	+	5.42
StCPK17	PGSC0003DMT400024436	PGSC0003DMP400016709	XM_006356324	1575	524	59.0	5.96	7	11	+	5.02
StCPK18	PGSC0003DMT400011824	PGSC0003DMP400008217	XM_006349734	1608	535	60.0	4.29	8	12	+	5.49
StCPK19	PGSC0003DMT400014939	PGSC0003DMP400010340	XM_006352199	1554	517	57.8	4.93	7	8	+	5.69
StCPK20	PGSC0003DMT400054991	PGSC0003DMP400036988	XM_006348361	1749	582	64.6	5.01	7	1	+	5.97
StCPK21	PGSC0003DMT400072292	PGSC0003DMP400048877	XM_006339122	1917	638	70.2	**4.56**	7	10	−	6.43
StCPK22	PGSC0003DMT400009177	PGSC0003DMP400006361	XM_006340676	1695	564	63.6	6.05	11	2	+	7.60
StCPK23	PGSC0003DMT400069175	PGSC0003DMP400046709	XM_006347224	1611	536	61.1	4.87	8	6	+	6.44

Table 4.7 *In silico* characterization of 23 CDPK proteins

Name	PGSC Transcript ID	Aliphatic index	Protein Instability Index	GRAVY	Protein Type	Protein kinase ATP Binding signature Start-end	Protein Domain Start-end	Tryosine kinase phosphorylating kinase domain Start-end	Serine/threonine-protein kinase-like domain Start-end	NTV
StCPK1 (former StCDPK1)	PGSC0003DMT400071663	81.28	37.42	-0.338	Acidic	67-90	61-319	432-440	181-193	MGVCLS
StCPK2 (former StCDPK2)	PGSC0003DMT400057484	80.31	29.40	-0.391	Acidic	79-102	73-331	444-452	193-205	MGIACS
StCPK3 (former StCDPK3)	Not found	72.36	44.86	-0.661	Acidic	116-143	110-368	110-196	230-242	MGGCFS
StCPK4 (former StCDPK4)	PGSC0003DMT400043320	79.47	40.3	-0.374	Acidic	100-123	94-352	159-167	214-226	MGNTCR
StCPK5 (former StCDPK5)	Not found	82.95	41.84	-0.352	Acidic	78-105	72-330	137-145	192-204	MGNACR
StCPK6	PGSC0003DMT400060262	90.52	44.02	-0.280	Acidic	41-74	35-293	100-108	155-167	MGNTCV
StCPK7	PGSC0003DMT400002592	77.44	42.82	-0.447	acidic	120-147	111-372	--------	234-246	MGNTCV
StCPK8	PGSC0003DMT400027809	81.39	37.82	-0.494	acidic	64-87	58-316	----------	178-190	MGNNCV
StCPK9	PGSC0003DMT400054983	82.68	44.41	-0.411	acidic	141-168	135-393	23-30	255-267	MGNCNS
StCPK10	PGSC0003DMT400021055	81.45	36.01	-0.527	acidic	59-82	53-311	---------	173-185	MGNCCS
StCPK11	PGSC0003DMT400067082	85.45	39.53	-0.368	acidic	38-61	32-290	--------	152-164	MGNCCV
StCPK12	PGSC0003DMT400072554	81.91	36.32	-0.451	acidic	150-177	144-402	--------	264-276	MGLCFT
StCPK13	PGSC0003DMT400018575	82.57	41.60	-0.411	acidic	101-128	95-353	466-474	215-227	MGGCCSS
StCPK14	PGSC0003DMT400025581	78.35	48.36	-0.439	acidic	98-121	92-350	463-471	212-224	MGNTCS
StCPK15	PGSC0003DMT400002331	83.23	37.76	-0.368	acidic	42-65	36-294	------	156-168	MGNTCI
StCPK16	PGSC0003DMT400058126	76.36	42.14	-0.630	basic	117-140	111-371	97-103	233-245	MGNNCV

StCPK17	PGSC0003DMT400024436	79.47	40.04	-0.504	acidic	73-100	67-325	438-446	187-199	MDSSDS
StCPK18	PGSC0003DMT400011824	78.60	42.35	-0.473	acidic	84-111	78-336	449-457	198-210	MEIPKSE
StCPK19	PGSC0003DMT400014939	78.84	41.08	-0.417	acidic	72-95	66-324	437-455	186-198	MAQVVA
StCPK20	PGSC0003DMT400054991	83.02	41.99	-0.408	acidic	139-166	133-391	504-512	253-265	MGTCMS
StCPK21	PGSC0003DMT400072292	86.77	45.60	-0.265	acidic	138-165	132-391	504-512	252-264	MGNCNA
StCPK22	PGSC0003DMT400009177	79.66	39.67	-0.550	basic	108-131	102-362	48-55	224-236	MGNCCA
StCPK23	PGSC0003DMT400069175	82.15	30.71	-0.380	acidic	68-95	60-320	298-306	182-194	MGNCCV

56.2 to 70.1 kDa. Their instability indexes ranged from 29.40 to 48.36; out of 23 CDPK proteins only 9 were stable proteins and the remaining 14 were unstable. Aliphatic indexes were found to be relatively higher in all the CDPK proteins, indicating that CDPK domains were stable at wide ranges of temperature. All these proteins showed negative GRAVY scores suggesting that they were soluble or hydrophilic (Kyte and Doolittle, 1982). In the CDPKs, nearly conserved 24-aa protein kinase ATP binding signature (LGRGQFGVTYY CTENSTENP YACK) was present towards the N-terminal region. A 13-aa (VMHRDLKP ENFLL) serine/threonine protein kinase-like domain containing Asp in the active site (Asp197

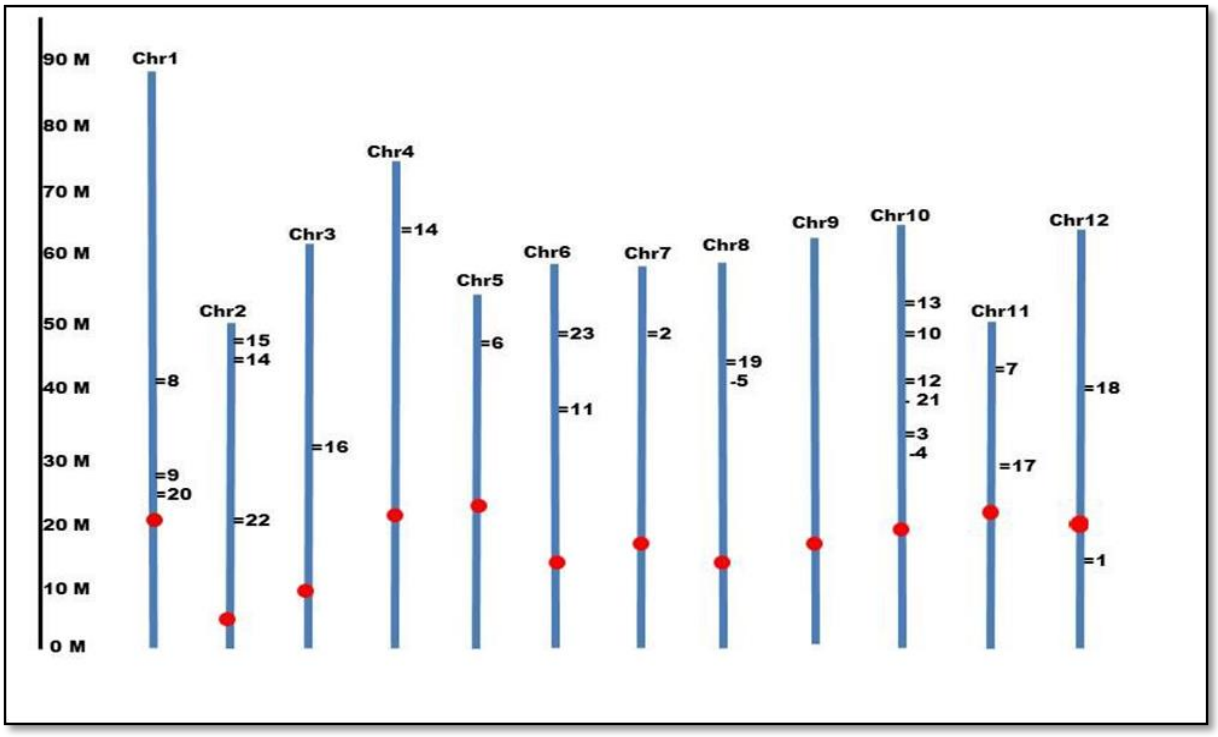

Fig. 4.18 Chromosomal localization of the calcium-dependent protein kinases genes (*StCDPKs*) in potato; retrieved from the Potato Genome Database (Potato Genome Sequencing Consortium 2011), and labelled as presented in the Table 4.6. Chromosomes are shown in blue and centromeres are marked by red.

in the case of StCDPK2) helps in positioning the ligand-binding domain into the extracellular space is found in the middle of protein shown earlier in Fig. 4.17. The CDPK proteins were acidic in nature. A total of 23 full-length CDPK amino acid sequences from potato were used in making a phylogenetic tree showing sequence relatedness between them (Fig. 4.19).

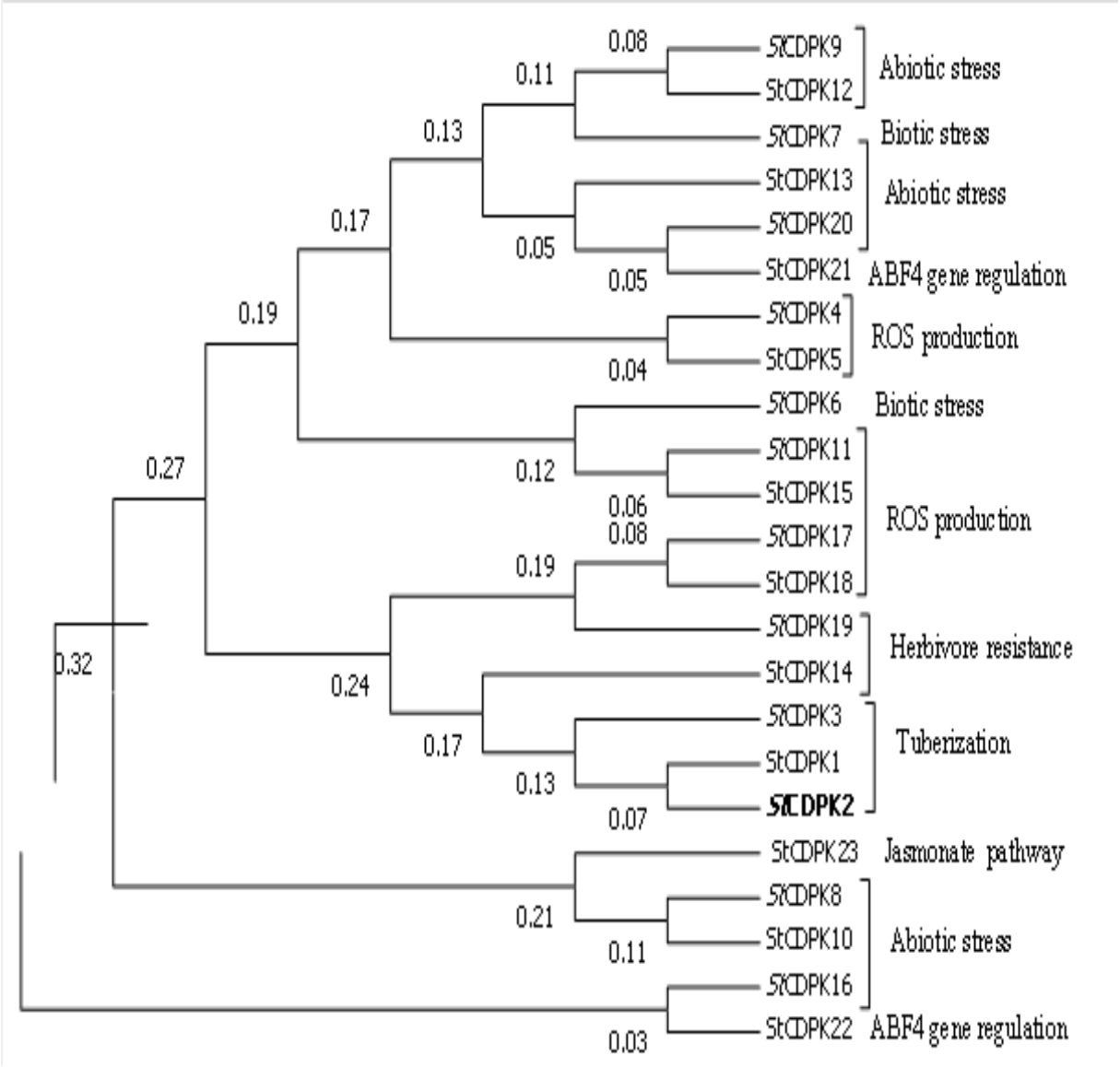

Fig. 4.19 The phylogenetic tree generated by the MEGA X software (Kumar et al. 2018) using the Neighbor-Joining method. The percentage of replicate trees in which the associated taxa clustered together in the bootstrap test (1000 replicates) are shown next to the branches. The evolutionary distances computed by the Poisson correction method are in the units of the number of amino acid substitutions per site. All ambiguous positions were removed for each sequence pair (pairwise deletion option). The evolutionary analyses involved 23 amino acid sequences of the potato CDPKs as available in the published reports and/or databases (the plant species and the GenBank Accession Numbers are indicated at each branch). The 515-aa StCDPK2 (QIS79146) specific to the culivar KC-1 of this study occupied a distinct position in the phylogenetic tree (shown in bold cases). Probable functions of the different CDPKs are also indicated.

Plant CDPKs were divided into four groups based on their biochemical properties, and roles in various physiological processes at different stages of development (Liu et al. 2016). In order to know the probable roles, the biochemical properties and expression patterns of a number of CDPKs were studied in different plants (Fantino et al. 2017; Gromadka et al. 2018, Grossi et al. 2021). The probable roles of the CDPK proteins were also investigated in the model plant *A. thaliana* (Asano et al. 2012; Mittal et al. 2017; Wen et al. 2020). In potato, StCDPK1, 2, 3, 9, 10, 12 ,13 and 20 belong to Group II, and undergo myrisotylation required for membrane targeting and signal transduction pathways in response to environmental stresses. StCDPK1, 2 and 3 were expressed during tuberization and known to activate GA2 oxidase. Increase in auxin concentration led to ABA-signalling pathways associated with stolon development, tuber formation and development and responses to hyperosmotic stress which were similar to the roles of AtCDPK9, 19, 33, 23, 15 and 21 (Gargantini et al. 2009; Grandellis et al. 2012; Liese and Romeis 2013; Gromadka et al. 2018; Bi et al. 2021). StCDPK9, 10, 12 and 13 play crucial role in salt, cold and drought stress like AtCDPK6, 26, 34 and 17 (Gutermuth et al. 2013). StCDPK4, 5, 6, 7, 8, 11, 14, 15, 16, 17, 18 and 19 belong to Group I. StCDPK4 and 5 regulate ROS production similar to AtCDPK5, 6 and 26 (Kobayashi et al. 2007; Liese and Romeis 2013; Gromadka et al. 2018). StCDPK6 and 7 are known to be crucial in formation of salicylic acid under biotic stress; thus, play a key role in pathogen resistance through convergent MAMP signaling as exhibited by AtCDPK1 and 5 (Asano et al. 2012). While other StCDPK members of this group are involved in herbivore resistance by blocking jasmonate and confer the drought tolerance, production of osmolyte proline and lowering lipid peroxidation probably through decrease in ROS production as observed in the cases of AtCDPK5, 6, 20, 11 and 25. StCDPK21 and 22 belong to Group III and involved in ABF4 gene regulation, salt tolerance and stomatal opening. Only StCDPK23 belongs to Group IV and involved in jasmonate pathway. The differential expression of the individual CDPKs could be correlated with their participation in specific signal transduction pathways in different plant organs. StCDPK1 was found to be expressed in sprouting tubers and tuberizing stolons. Expression of StCDPK3 was noticed in stolons, roots and leaves. StCDPK2 expression was noticed in all plant tissues and also during the developmental processes such as sprouting, tuberization and light-mediated signaling (Giammaria et al. 2011; Grossi et al. 2021); its elevated level was observed in the actively growing young leaves and tubers.

Model structure, active site prediction and validation: In order to predict biological function of any protein, it is essential to know its structure first. The powerful techniques like X-ray

crystallography and NMR are employed for determining the 3-D structures. These techniques require protein crystals; due to such constraints, structures of only a few membrane proteins have been determined (Schultz et al. 2000; SchuÈttelkopf and Van Aalten 2004; Roy et al. 2010; Kelley et al. 2015). Alternatively, to acquire the structural information in a timely manner, 3-D protein structures were developed by means of *ab-initio* modeling technique and found to be useful for drug development (Berendsen et al. 1995; Chou and Shen 2009). So, the model generated by I-TASSER (through the combination of threading and *ab initio* prediction) was taken for the study. I-TASSER, a meta server implements different threading programmes and its quality is assessed on the basis of Z-score (the energy score in standard deviation units relative to statistical mean of alignments). For confident alignment Z-score should be greater than 1. The best model with minimized energy (Fig. 4.20 A–C) was used to show the specific calcium signature domain and were visualized in the form of ribbons by PyMol (https://www.pymol.org). Transmembrane topology adopted by the proteins was predicted by Phyre2 tool (Fig. 4.20 D–F) which clearly showed that each CDPK protein had a distinct N-terminal extracellular region, approx. 15-aa helical transmembrane segment and the remaining C-terminal cytoplasmic region. Such topological arrangements of the CDPKs explains why they are effectively associated with Ca^{2+} signaling pathways.

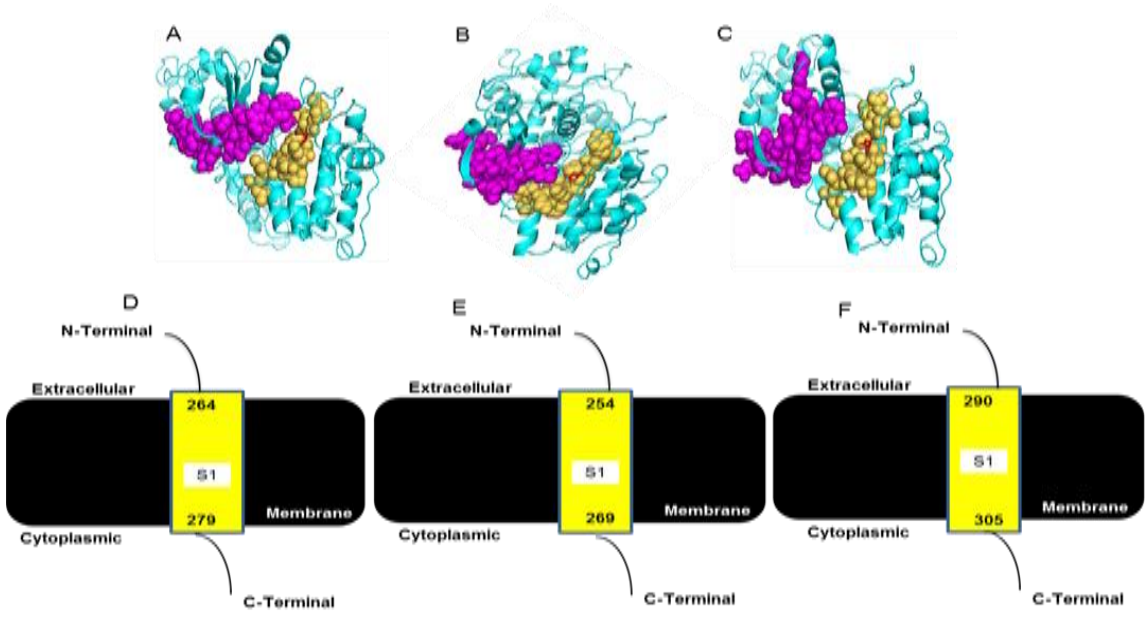

Fig. 4.20 (A–C) Illustrated representation and catalytic domains of the predicted three-dimensional structure models of the StCDPKs from potato. A 532-aa StCDPK1 (NP_001275322.1); B 515-aa StCDPK2 (QIS79146); C 558-aa StCDPK3 (AAQ08324.2). The entire protein regions are depicted in cyan, the catalytic protein kinase ATP-binding region and serine/threonine protein kinase domains are shown in magenta and brown colours, respectively as ribbon structures. The active sites are shown as stick and ball structures in red colour. The images were generated using the PyMol program (Schrödinger, Inc., New York, NY, USA). (D–F) Illustrated **Contd..**

representation of transmembrane helical segments by Phyre2; D StCDPK1, E StCDPK2, F StCDPK3. The extracellular and cytoplasmic sides of the plasma membrane are labelled; the beginning and end of each transmembrane segment are indicated by the positions of the amino acid residues.

The backbone ratification of the established model was corroborated by using Ramachandran plot through PROCHECK (https://www.ebi.ac.uk/thornton-srv/software/PROCHECK). The distribution of phi and psi angles for the amino acid residues was denoted by Ramachandran plot. The built model was proven to be highly plausible; as only approx. 1% residues were found to be in the disallowed region of the plot (Fig. 4.21). More than 98% amino acid residues were in the most favorable allowed regions-validating the predicted 3-D structures.

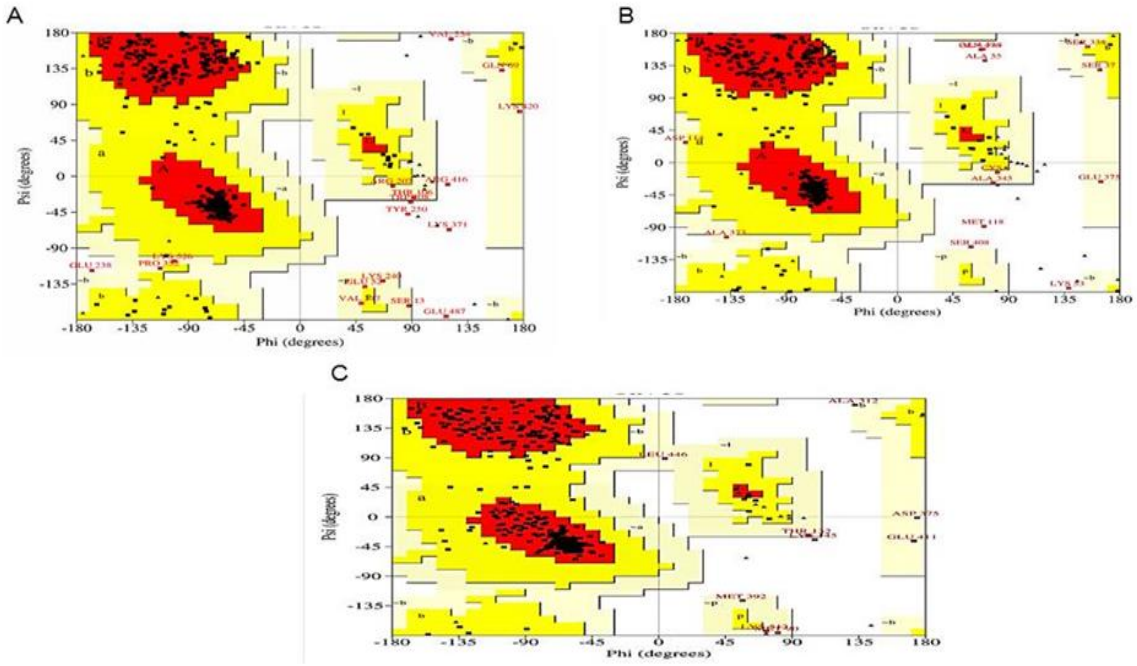

Fig. 4.21 (A-C) Ramachandran plot of the StCDPK models: A StCDPK1, B StCDPK2, C StCDPK3. The most favoured regions are coloured red; additional allowed, generously allowed and disallowed regions are indicated as yellow, light yellow and white fields, respectively.

4.2.4 Sequence Analyses of Catalases (CATs)

Multiple sequence alignment, protein motifs and phylogenetic analysis: Using the MultAlin software, multiple sequence alignment was done using a total of five CAT sequences corresponding to the three major active forms (*CAT1–3*) from the potato (Fig. 4.22). The purpose was to closely inspect the sequence similarities and divergences, nature and location of the amino acid substitutions, deletions/insertions within and between the different CAT isoforms in potato. Different members of the individual CAT isoforms became visibly distinct

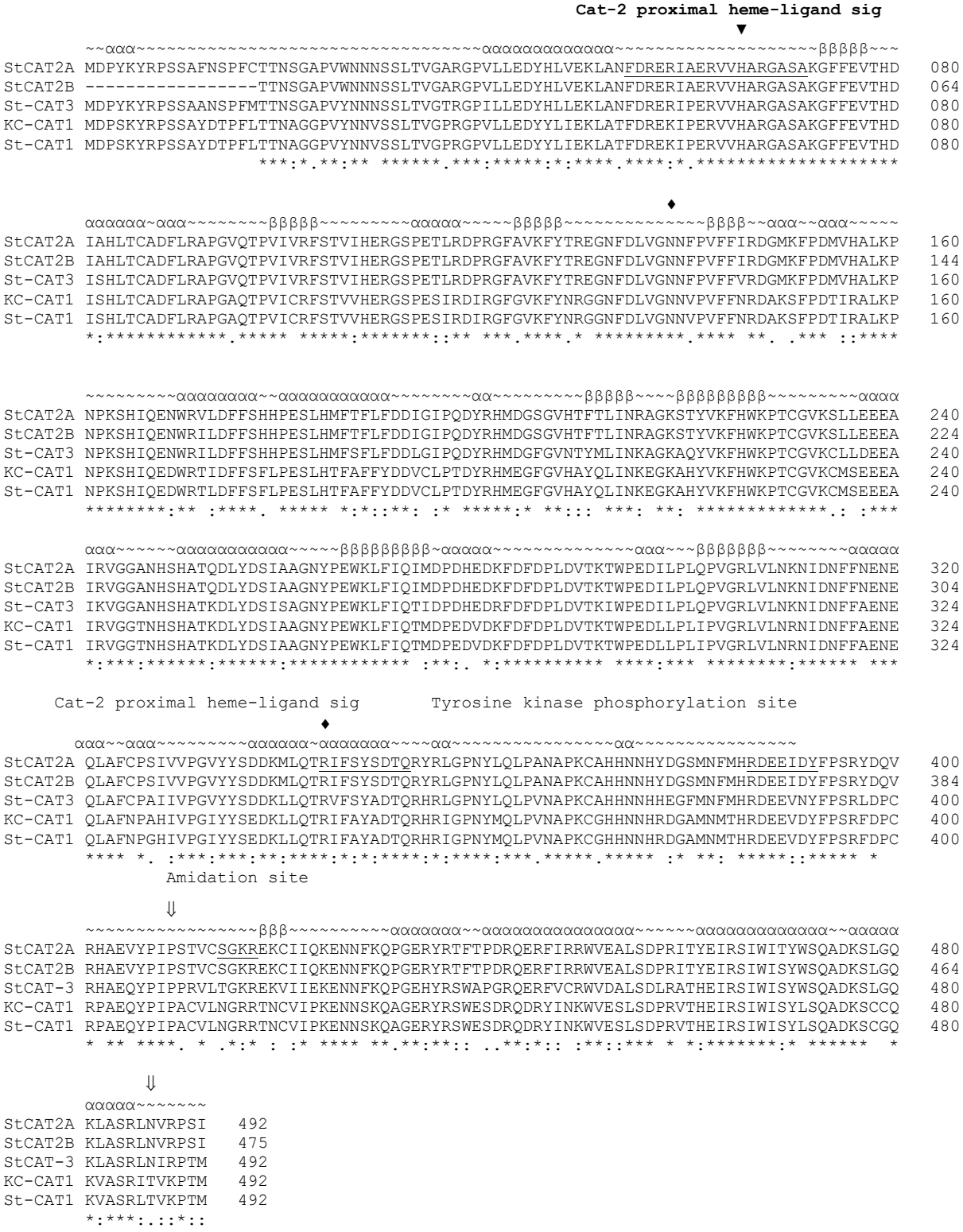

Fig. 4.22 Comparison of the predicted 5 full-length CAT sequences corresponding to the three major active isoform groups from the potato. *CAT* groupI includes KC-CAT1 (QWW18612), St-CAT1 (P49284); *CAT* groupII includes StCAT2A (M0ZMN7), StCAT2B (Q6T2D5); *CAT* groupIII includes StCAT3 (M1ALT0).

Contd..

Multiple sequence alignment was done based on *MultAlin* software along with some minor manual adjustments. Dashes indicate gaps that arise during alignment. Asterisks '*' indicate the conserved amino acids; ':' refers to the almost conserved or conservative substitutions; '.' refers to conserved amino acids in at least two CAT isoforms. The downward arrow '⇓' indicates the Catalase-related immune-responsive region (from 409–487aa) ,'▼' denotes the active site (His 65) and '♦' the crucial amino acids (Asp 138, Tyr 348) for enzyme activity . The crucial regulatory/binding motifs are underlined. 'α', 'β' and '~' denote the propensity of the individual amino acids of KC-CAT1 towards alpha helix, beta-sheet and random coil formation, respectively.

because of their nearly common C-terminal regions. All the motifs were conserved with variations in crucial amino acids between the CAT isoforms. Apart from the N-terminal regions, considerable sequence similarity was noticed in the flanking regions of the crucial motifs/amino acid residues.

The CAT protein are known to contain two main regulatory motifs namely; Catalase proximal heme-ligand signatures, responsible for the enzyme activity and Catalase-related immune-responsive domain for triggering the enzyme activity and controlling the nuclear trafficking in the cell (Table 4.8). Further , the catalase proximal heme-ligand signature is of two types i.e., type 1 present at N- terminus containing an active site (His 65) and type 2 present near the C-terminus. In the 3-D structure, it was observed that these two signatures occupy a position in close proximity thus effecting the enzyme activity. Another important motif Amidation site which is present towards C-terminus plays a key role post translational and targeting the signal receptor, thus aiding in protein functioning. The various catalytic domains present in the CAT proteins, that are crucial for enzyme activity and characterisation namely; catalase heme-ligand proximal signatures, tyrosine kinase phosphorylation site, amidation site were predicted with their location and function as shown in Table 4.8, Fig. 4.22 Phylogenetic analysis of the 13 CATs; 5 from potato, 3 from tomato and 5 from *Arabidopsis* indicated that the *CAT* gene family is clearly divided into three major *CAT* groups (Fig. 4.23).

CAT gene family in potato: Recently, benefiting from the whole genome sequencing of model plants, multiple genes encoding CAT isozymes have been identified from various plant species using the comparative genome approach Previously, genome-wide studies have demonstrated that CAT is encoded by a small gene family which has been studied extensively in different plant species (Sharma and Ahmad 2014) including three in tobacco (Willekens et al. 1994,97); two in barley (Skadsen et al. 1995), three maize (Polidoros and Scandalios 1999), three in *Arabidopsis* (Du et al. 2008), three in tomato (Drory and Woodson 1992), three in chilli (Lee and An 2005), four genes in rice (Alam and Ghosh 2018), two genes in sugarcane (Sun et al. 2018) and two genes in cucumber (Hu et al. 2016), three in amaranthus

Table 4.8 Catalytic domains and their predicted functions in Catalase (KC-CAT1)

Catalytic domain		Position	Function
CATALASE_1 proximal heme-ligand signature	Catalase	344-352	consist of glycine rich sequence followed by a conserved lysine and a serine or threonine,help in the binding of ATP and GTP and enzyme activity
CATALASE_2 proximal heme-ligand signature	Catalase	54-70	consist of glycine rich sequence followed by a conserved lysine and a serine or threonine, help in the binding of ATP and GTP and enzyme activity
Tyrosine kinase phosphorylation site		386-392	catalyzes the transfer of glycosyl groups to a nucleophilic acceptor with either retention or inversion of configuration at the anomeric centre
Catalase-related immune-responsive		409-487	helps in transfer of protein from nucleus to cytoplasm and other cell organelles, thus accurate cellular localization plays a crucial role in the effective nuclear trafficking
Amidation site		414-417	C-terminal alpha-amidation is the most important PTM for various important biological activities like signal transfer and receptor recognition

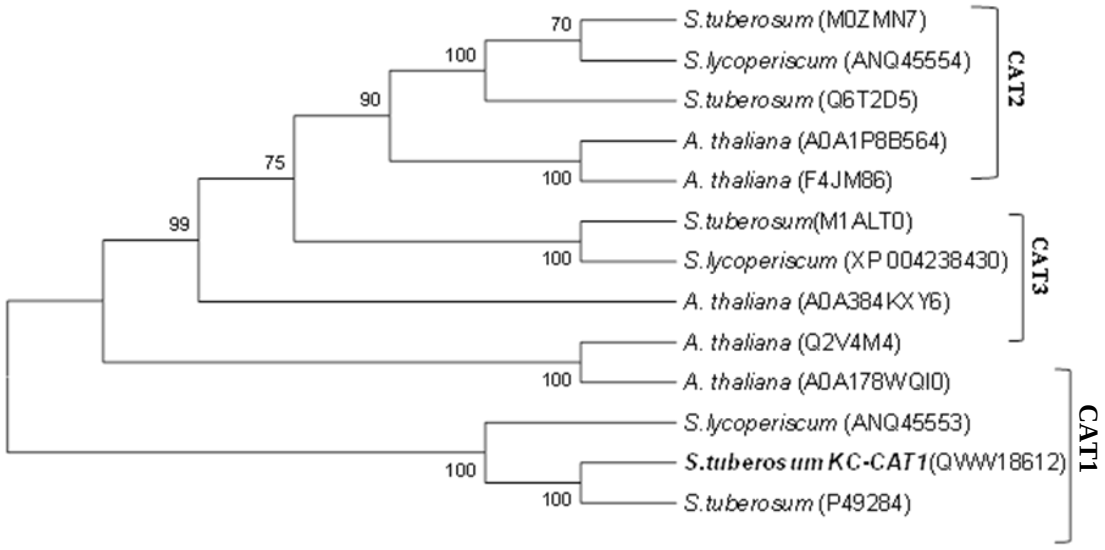

Fig. 4.23 The phylogenetic tree was generated by the MEGA X software using the Neighbor-Joining method with the bootstrap test (1000 replicates) shown next to the branches and computing the evolutionary distances computed by the Poisson correction method. The analyses involved 13 CATprotein sequences from the potato,tomato and *A. thaliana* as available in the published reports and/or databases (the plant species and the GenBank Acc Nos are indicated at each branch). The 492-aa KC-CAT (QWW18612) corresponding to the culivar KC-1 of this study occupied distinct positions in the phylogenetic tree (shown in bold cases). The three CAT groups are also indicated.

(Ni and Trelease 1991). But, now in some plants like cotton and *Brassica napus* seven and fourteen CAT genes were identified (Wang et al. 2019; Raza et al. 2021).

By screening the *S. tuberosum* whole genome and transcriptome database (Spud DB and *Ensembl Plants*), four *CAT* genes annotated as *CAT1* (PGSC0003DMG400029408), *CAT2* (PGSC0003DMG400001570), *CAT3* (PGSC0003DMG400009906) and *CAT-like* (PGSC0003 DMG400021382) were identified (Table 4.9). It was observed that all these genes encode a single mRNA each. Also, only CAT2 was found to encode two proteins of length 492 and 475 aa, while CAT1 and CAT3 encoded a protein of 492 aa. The molecular weight for CAT1-3 spanned in a narrow range of 54-57 kDa. The instability index of CAT proteins ranged from 36.25 to 40.29, which classified the proteins as relatively stable. Aliphatic index of CAT proteins ranged from 68.35 to 73.52 indicating the proteins to be less thermostable. The GRAVY value of CAT proteins ranged from - 0.52 to - 0.57 indicating their nature spans from hydrophilic to hydrophobic. Further, CAT1, CAT2 and CAT3 were found to be encoded by genes on chromosome 12, 2 and 4 respectively (Fig.4.24). Surprisingly, even though the three CAT isoforms are encoded by individual genes with different chromosomal localization, but the proteins encoded by these isoforms consists of the same number (492 aa) of amino acids and have many similar biological parameters. This might be due to their expression at different time intervals and in different organs, though further studies are needed for confirmation.

3-D model structure, active site prediction and validation: In order to annotate biological function of any protein it is essential to know its structure first. So, the model generated by I-TASSER (through the combination of threading and *ab initio* prediction) was taken for the study. I-TASSER, a meta server implements different threading programmes and its quality is asssed on the basis of Z-score (the energy score in standard deviation units relative to statistical mean of alignments). For confident alignment Z-score should be greater than 1. The model with minimized energy was used to show Catalase proximal heme-ligand signatures. The active site and the crucial features and domains as reported earlier were studied and the 3-D structure visualized in the form of ribbons by PyMol shown in Fig. 4.25A (Hu et al. 2016). The generated 3-D structure was further validated using the Structural Analysis and Verification Server (http://nihserver.mbi.ucla.edu/SAVES) (Fig.4.25 B). From the predicted structure, could be hypothesised that the two crucial proximal catalase haeme signature motifs lie close

Table 4.9 Features of the *CAT* genes from potato genome database

Gene Symbol	PSGC Gene ID	PSGC Transcript ID	Uniprot ID	Base pair	Amino acid	MW (kDa)	Chr position	pI	Instability index	Aliphatic index	Gravy
CAT1	PGSC0003DMG400029408	PGSC0003DMT400075611	P49284	1736	492	56.31	12	6.56	40.29	68.35	- 0.57
CAT2	PGSC0003DMG400001570	PGSC0003DMT40003986	M0ZMN7	1841	492	56.93	2	6.73	37.73	70.53	- 0.54
CAT2	PGSC0003DMG400001570	PGSC0003DMT40003986	Q6T2D5	1841	475	54.94	2	6.59	36.25	73.05	- 0.53
CAT3	PGSC0003DMG400009906	PGSC0003DMT400025653	M1ALT0	1987	492	56.81	4	6.93	38.17	73.52	- 0.52
CAT-like	PGSC0003DMG400021382	PGSC0003DMT400055104	M1BXD1	6969	2322	19.9	1	6.66	40..85	93.90	- 0.03

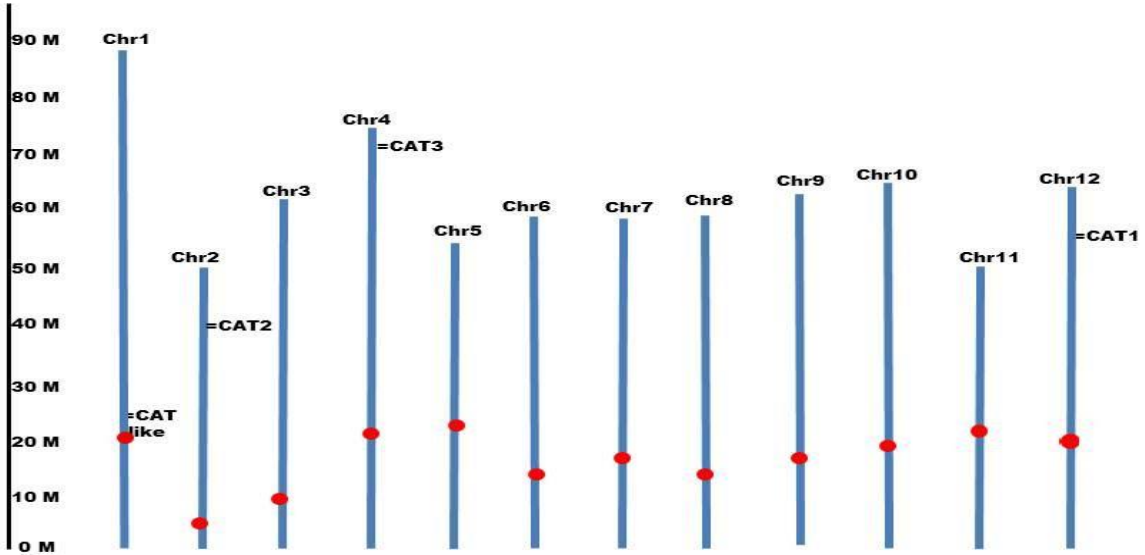

Fig. 4. 24 A schematic presentation of chromosomal localization of the various potato catalase isoform genes retrieved from Potato Genome Sequencing Consortium (PGSC) database. The chromosomes are shown in blue, while the centromeres are shown in red. *CAT1* is present on chromosome 12 at 57.45 Mb, *CAT2* on chromosome 2 at 38.56 Mb, *CAT3* on chromosome 4 at 71.62 Mb while CAT-like on chromosome 1 at 24.5 Mb.

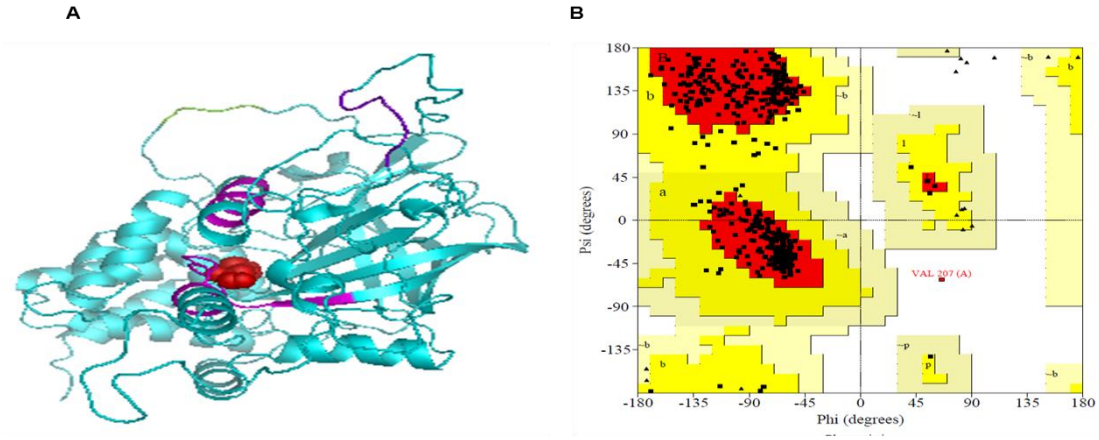

Fig. 4.25 A Illustrated representation and catalytic domains of the predicted three-dimensional structure model of the KC-CAT. The CAT protein is depicted cyan, Catalase proximal heme ligands in magenta, Catalase-related immune-responsive in green, Amidation site in deep blue colour as a ribbons respectively. The active site is shown in red sphere. The images were generated using the PyMol program (Schrödinger, Inc., New York, NY, USA), **B** Ramachandran plot of the KC-CAT model. The most favored regions are colored red, additional allowed, generously allowed and disallowed regions are indicated as yellow, light yellow and white fields, respectively.

to each other in their 3-D conformation with the active site (His65) in between them. This bending pattern might be responsible for triggering the enzyme activity (Reid et al.1981). Thus, proving this ab-initio approach of predicting 3-D structures to be significantly reliable.

According to Objective 2, close inspection of the amino acid sequences helped to know sequence identities and divergence between the multiple forms of SuSy, FRK, CDPK and CAT mostly from the *Solanaceae* family members. Moreover, sequence analyses unfolded a number salient features not reported earlier. Importantly, it is a comprehensive report with regard to the individual gene families and their categories corresponding to the above enzymes in potato as revealed by genome-wide characterization and further supported by chromosomal localization studies. Phylogenetic analyses could provide clues to predict evolutionary aspects of the genes in potato. Prediction of secondary/3-D structures could reveal the folding patterns, stability and catalytic aspects of the enzymes.

4.3 *Objective 3:* To study the expression patterns of the individual forms of the above enzymes in different potato tissues including the various stages of tuber development

The purpose of this objective was to have an insight into the expression patterns of the individual enzymes namely SuSy, FRK, CDPK and CAT in different potato organs including various stages of tuber development. In order to achieve, both experimental and *in silico* approaches were adopted to study the expression patterns. mRNA expression patterns of the corresponding genes were demonstrated by semi-quantitative RT-PCR using total RNA from different potato organs; further substantiated by the expression values specific to different organs retrieved from EMBL-EBI Expression Atlas, a database enriched by wide array of RNA-Seq and Microarray studies. Enzyme assays were carried out at various stages of tuber development. Based on the String database, protein-protein interactions were also predicted.

4.3.1. Expression Patterns of Sucrose Synthase (SuSy/SUS)

SuSy mRNA expression patterns: In this study, the *SUS* gene expression pattern was examined in some potato organs namely tuberizing stolon, growing tuber, leaf, stem, and flower. By semi-quantitative RT-PCR, ~0.98 kb DNA was amplified using total RNA from tuberizing stolon and tuber (Fig. 4.26). The size matched with the KC-SuSy i.e., St-SUS4 (a member of SUS group I) specific transcripts towards the 5′-end. The transcript levels appeared to be comparable for tuberizing stolon and tuber; in contrast, the transcripts were not detected in the cases of leaf, stem and flower. The levels of actin transcripts were found to be nearly uniform in all the potato organs. Also, the heatmap generated by the Expression Atlas (Fig 4.27), clearly reflected that *SUSI* genes (PGSC0003DMG400002895 also known as *SuSy*/*SUS4*, PGSC0003DMG400013546 and PGSC0003DMG400013547) are highly expressed in the sink tissues, while the other two i.e., *SUSII* (PGSC0003DMG4000006672) and *SUSIII* (PGSC0003DMG400031046 and PGSC0003DMG400016730) are constitutively expressed in various organs**.** As SuSy 4 isoform belonging to SUSI was found to be expressed tenfold more in tubers in comparison to other photosynthetically active tissues and was consistent with the results of RT-PCR approach of the study as it could detect KC-SuSy specific transcripts only in tuberizing stolons and tubers. Hence, KC-SuSy, a SuSy4 form seems to play a key role in

maintaining carbon flux towards tuber formation as it gets a signal through apolplastic unloading for the tuber formation and sink strength (Zrenner et al. 1995, Viola et al. 2001, Baroja-Fernández et al. 2009).

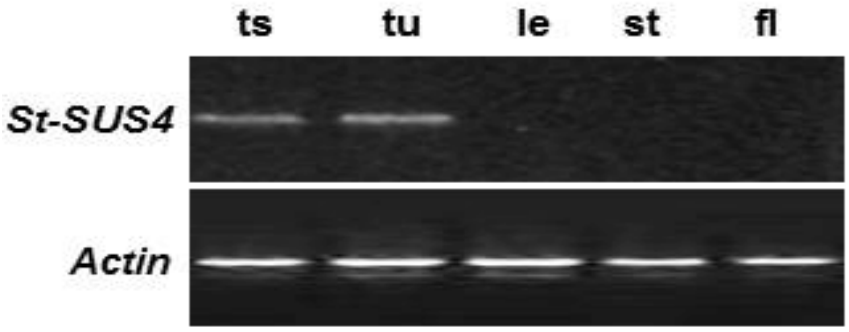

Fig. 4.26 Semi-quantitative RT-PCR for *SuSy 4 g*ene expression analysis using total RNA from different potato organs (cultivar KC-1) and the primers SSF1-0025 and SSR1-0986. ts tuberizing stolon, tu tuber, le leaf, st stem, fl flower. The size of the *SuSy 4*-specific amplified product was ~0.98 kb in ts, and tu. Actin-specific primers were used as an internal control (the size of the amplified product ~0.65 kb in each organ).

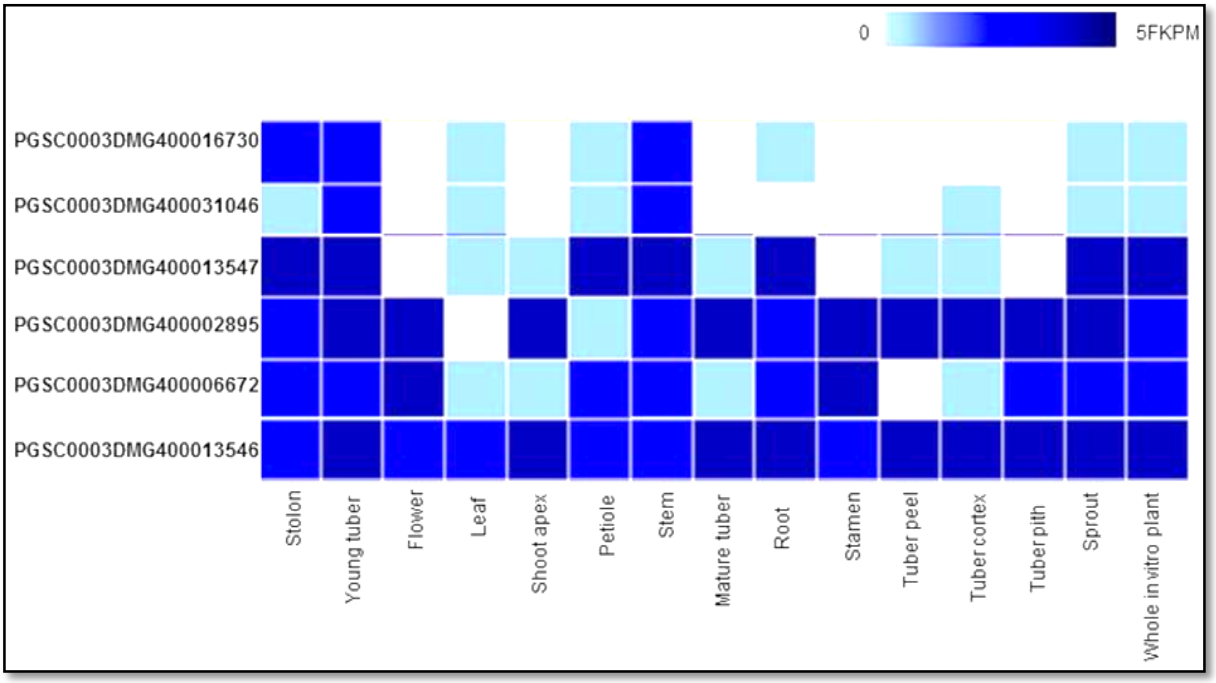

Fig. 4.27 Tissue expression patterns of *SUS* genes in potato. The expression values were retrieved from large scale RNA-seq data in Expression Atlas. FPKM: Fragments per kilobase of exon model per million reads mapped.

SuSy activities at various stages of tuber development: To know the involvement of SuSys in maintaining carbon flux towards starch formation at the sink organ, SuSy activities were measured in the successive stages of tuberization i.e, from hooked stolon tip (S1) to mature tuber (S8) as shown in Fig. 4. 28 and Table 4.10.

Fig. 4.28 Morphology of various stages of tuberization in potato under field condition (cultivar KC-1). 8 stages of tuberization are shown: S1 hooked apical stolon tip, S8 mature tuber, S2−S7 stages are indicated in Table 4.10.

Table 4.10 Morphological features and SuSy activity profiles during different stages of tuberization in potato (cultivar KC-1) under field condition (the experimental data are presented as mean ± SD of n=3 extracts.)

Stages of tuberization	Morphological features		SuSy activity (nmol/min/g FW)
	Diameter (cm)	Fresh weight (g)	
S1 (hooked apical stolon tip)	0.06 ± 0.01	0.01 ± 0.00	21.45 ± 1.27
S2 (initiation of tuber formation)	0.31 ± 0.02	0.07 ± 0.01	72.13± 7.45
S3 (initial tuber)	0.89 ± 0.07	0.52 ± 0.03	168.39± 11.58
S4 (developing tuber)	1.68 ± 0.25	2.57 ± 0.33	269.91± 9.29
S5 (developing tuber)	2.31 ± 0.11	6.99 ± 0.79	561.55± 11.23
S6 (developing tuber)	3.23 ± 0.49	18.33 ± 1.42	769.44 ± 19.61
S7 (developing tuber)	5.11 ± 0.16	38.11 ± 2.57	623.79± 11.57
S8 (mature tuber)	7.43 ± 0.57	55.79 ± 4.35	511.87± 13.51

During tuber development, since the initiation of tuber formation after the swelling of the stolon tip, the activity of SuSy was found to increase exponentially, making it an indicator of sink strength. After reaching towards maturity, the activity declined, which could be due to the

feedback inhibition by fructose (Schaffer and Petreikov, 1997; Kanayama et al. 1998, German et al., 2003). As also in studies done by D'aoust et al. (1999) on tomato plant it was hypothesized that the greater sink strength caused by the over expression of SUS gene triggers the growth of plant. Similarly, in other plants like Arabidopsis, cotton fibre and seed, rice, pea, tobacco, wheat and tomato high activity of SuSy was reported in reproductive tissues highlighting the role of SuSy in determining the sink strength and in the breakdown of sucrose (Ruan et al. 2007, Ruan and Chourey, 1998). D'aoust et al. (1999) demonstrated that the overexpression of *SUS* gene could trigger the growth of the tomato plants due to an increase of sink strength. Similarly, in other plants like *Arabidopsis*, cotton fiber and seed, rice, pea, tobacco, wheat and tomato high activity of SuSy was reported in reproductive tissues indicating the role of SuSy in Suc cleavage and determining the sink strength (Ruan and Chourey, 1998; Ruan et al. 2007). Depending upon the cellular localization in plants, SuSy plays various roles However, the mechanism by which SuSy proteins bind to cellular targets and the structural aspects that control their catalytic functions still remain to be elucidated at a molecular level (Stein and Granot, 2019).

Protein-protein interactions: The STRING database was used to study the interaction of SuSy protein with other proteins in the cell and to predict their role in the plant metabolism (Fig. 4.29). The analysis was done by the basic setting of the image using full STRING basic network involving the data from the multiple sources namely Textmining, Experiments, Databases, Co-expression, Co-occurrence, Gene Fusion and Neighbourhood. In this approach, high stringency level was adopted to understand the protein-protein interactions and functions of the selected enzyme/protein in a more significant way. The biological, molecular and cellular enrichments and probable roles were deduced from the database. SuSy was found to be involved primarily in response to starch biosynthetic and sucrose metabolism along with the photoperiodism, flowering, amino acid metabolism, and cellular carbohydrate metabolic processs. It was found to be linked with a number of enzymes namely; Glucose-1-phosphate adenylyltransferase (PGSC0003DMT400097320), AGPS2 (PGSC 0003DMT400041215), AGPS3 (PGSC0003DMT400023304, PGSC0003DMT400079823), Beta-fructofuranosidase (PGSC0003DMT400023091), InvGE (PGSC0003DMT400023090), InvGF (PGSC0003DMT 400072606) Sucrose-phosphatase (PGSC0003DMT400072296, SPP2), UTP-glucose-1-phos-

phate uridylyltransferase (PGSC0003DMT400034699,UDPG), (Granule-bound starch synthase 1 (PGSC0003DMT400031568, WAXY).

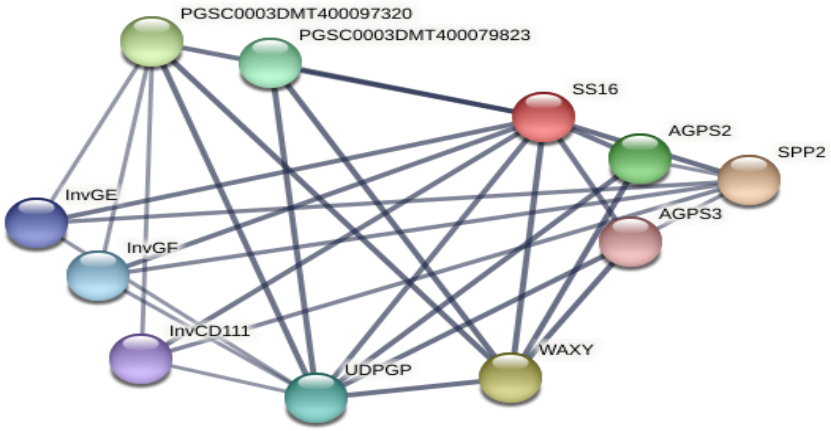

Fig. 4.29 Protein relationship network of potato *SUS I* (PGSC0003DMG400002895, SS16) derived from the STRING database

All these enzymes associated with the metabolic functioning of *SUS* I gene are mainly involved in the starch, glycogen, glucose and sucrose related pathways, hence aiding the *SUS* in allocating carbon towards the sink issues. Thus, from the analysis of the protein interactions of *SUS* it could be deduced that SuSys are the key players in allocating carbon towards the sink formation and could possibly be involved in double break mechanism in coherence with sucrose synthase (Stein and Granot 2019). The *SUS* gene was also found to be involved in the flowering, stress metabolism, nucleotide synthesis and photoperiodism, which might be co related with its localization in different cell organelles as reported earlier. As SuSys have also been reported to participate in plant resistance to various environmental stresses like in hypoxia and dehydration in Arabidopsis (Martin et al. 1993; Dejardin et al. 1999; Baud et al. 2004), wheat (Marana et al. 1990), maize (Zeng et al. 1998) and rice (Hirose et al. 2008) , carrot (Sturm et al. 1999), pigeon pea (Kumutha et al. 2008) potato (Biemelt et al. 1999) weed (Harada et al. 2004, 2005), low temperature and drought stress in barley and rubber plant (Xiao et al. 2014), glycolytic demand in tobacco (Kleines et al. 1999). Also, the role of SuSy in starch, cellulose and callose synthesis have been reported in many plants like cotton tobacco and popular (Ruan and Chourey,1998; Wei et al. 2015, Coleman et al. 2009). Depending upon the localization of SuSy, it plays various roles (Stein and Granot, 2019). However, the mechanism by which SuSy binds to cellular targets, the structural aspects which controls the SuSy partitioning, and impact of it on catalytic function are unknown at a molecular level.

4.3.2 *Expression Patterns of Fructokinases (FRKs)*

FRK mRNA expression patterns: The *FRK2* gene expression patterns were examined in some potato organs namely tuberizing stolon, growing tuber, leaf, stem, and flower. By semi-quantitative RT-PCR, ~0.6 kb cDNA was only amplified using total RNA from tuberizing stolon, tuber and leaf (Fig. 4.30). The size matched with the *St-FRK2* transcripts towards the 5′-end. The transcript levels of both tuberizing stolon and tuber appeared to be comparable and higher as compared with leaf; interestingly, the transcripts were not detected in the cases of stem and flower. The actin expression level was found to be uniform in all these potato organs. Semi-quantitative RT-PCR suggested that *FRK2* gene could predominantly express in tuberizing stolon, growing tubers and considerably in leaves. Possibly, FRK2 isoform plays a key role during tuberization. The expression patterns of the individual *FRK* genes remain to be elucidated.

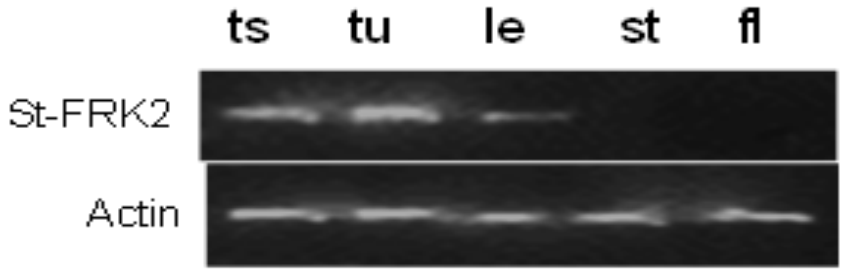

Fig. 4.30 Semi-quantitative RT-PCR for *FRK2* gene expression analysis using total RNA from different potato organs (cultivar KC-1) and the primers F1-FK0001 and R1-FK0606. ts tuberizing stolon, tu tuber, le leaf, st stem, fl flower. The size of the *FRK2*-specific amplified product was ~0.6 kb in ts, tu, and le. Actin-specific primers were used as an internal control (the size of the amplified product ~0.65 kb in each organ).

The *FRK2A and FLN* gene expression patterns were also examined experimentally, in some potato organs namely tuberizing stolon, growing tuber, leaf, stem, and flower. By semi-quantitative RT-PCR, ~0.4 kb *StFRK2A* cDNA was amplified using total RNA from all the above organs whereas *StFLN* was only amplified from leaf and stem total RNA (Fig. 4.31). The size matched with the *StFRK* and *StFLN* transcripts towards the 5'-end. The actin expression level was found to be uniform in all these potato organs.

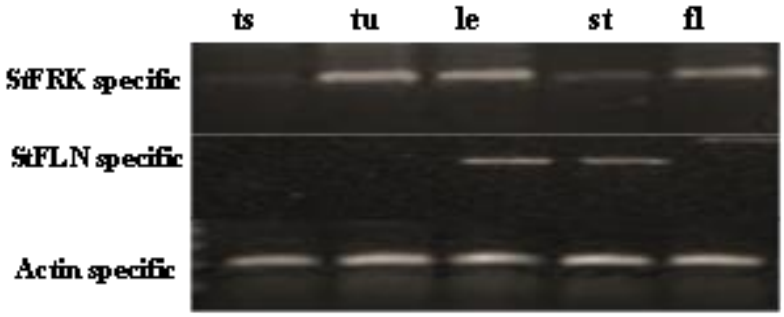

Fig. 4.31 Semi-quantitative RT-PCR for *FRK2A and FLN* gene expression analysis using total RNA from different potato organs (cultivar KC-1) and the primers F1-FK0001 and R1-FK0343 a FLF1-0001 and FLR2-500 respectively ts tuberizing stolon, tu tuber, le leaf, st stem, fl flower. The size of the *FRK2A*-specific amplified product was ~0.34 kb in ts, tu, le, st and fl and *FLN*- specific was ~0.5kb in case of le only. Actin-specific primers were used as an internal control (the size of the amplified product ~0.65 kb in each organ).

From the results of semi-quantitative RT-PCR and analyses from the literature survey, it was deduced that smaller FRK form (St-CFK23) was present in all the organs suggesting its role in stress metabolism and the FLN (St-CFL27) was present only in leaves, suggesting its possible role in cholororplast development and the FRK2 isoform (St-CFK21) was present in leaf and tubers suggesting its role in sink metabolism. These findings were in concordance with the earlier reports on these isoforms in potato (Smith et al. 1993; Gangadhar et al. 2014).

To study the expression pattern bioinformatically, the heat map was generated from the curated data in the various experiments of expression atlas (Fig. 4.32). It clearly reflected that *FRK1* (PGSC0003DMG400024246), *FRK3*(PGSC0003DMG400030653*)* and FLN (PGSC0003 DMG400020361, PGSC0003DMG400027017) isoforms has constitutive moderate to high expression, *FRK2* isoform (PGSC0003DMG400026916) was highly expressed in the sink organ (young and mature tubers), while *FRK4* (PGSC0003DMG400010277) was found to be expressed in reproductive organs.

FRK activities at various stages of tuber development: Facile biochemical techniques were employed in determining the total extractable FRK activities at different stages of tuber development i.e., hooked stolon tip (S1) to mature tuber (S8) as shown in Fig. 4.28 (Table 4.11) to know the involvement of FRKs in maintaining carbon flux towards starch formation at the sink organ. Transition from hooked apical stolon tip to initiation of tuber formation i.e., S1 to S2 was associated with a significant increase of FRK activity and kept on increasing abruptly in the actively growing tubers (S2–S5 stages) followed by gradual decrease till

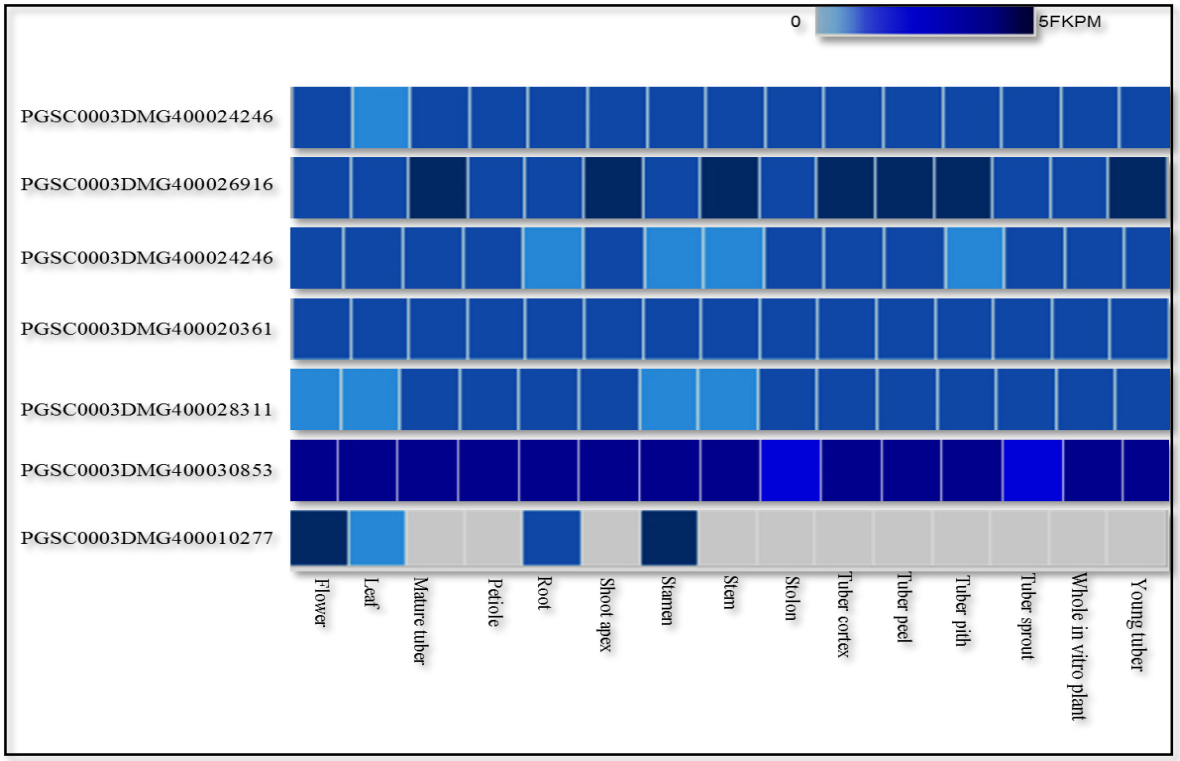

Fig. 4. 32 Tissue expression patterns of *FRK* genes in potato. The expression values were retrieved from large scale RNA-seq data in Expression Atlas. FPKM: Fragments per kilobase of exon model per million reads mapped.

Table 4.11 Morphological features and FRK activity profiles during different stages of tuberization in potato (cultivar KC-1) under field condition (the experimental data are presented as mean ± SD of n=3 extracts.)

Stages of tuberization	Morphological features		FRK activity (nmol/min/g FW)
	Diameter (cm)	Fresh weight (g)	
S1 (hooked apical stolon tip)	0.06 ± 0.01	0.01 ± 0.00	31.45 ± 1.27
S2 (initiation of tuber formation)	0.31 ± 0.02	0.07 ± 0.01	157.79 ± 7.45
S3 (initial tuber)	0.89 ± 0.06	0.49 ± 0.03	458.40 ± 11.87
S4 (developing tuber)	1.62 ± 0.23	2.34 ± 0.35	1011.58 ± 21.77
S5 (developing tuber)	2.31 ± 0.11	7.39 ± 0.66	1322.23 ± 27.23
S6 (developing tuber)	3.13 ± 0.55	17.76 ± 1.23	947.20 ± 17.33
S7 (developing tuber)	4.23 ± 0.29	35.91 ± 2.55	442.33 ± 13.35
S8 (mature tuber)	6.27 ± 0.83	53.83 ± 4.35	363.43 ± 9.51

Maturation. Taylor et al. (1995) also noticed similar FRK activity profile in potato. FRK-mediated fructose metabolism and shifting of carbon flux to storage starch are crucial during the early stages of tuber development. Moreover, FRK helps in enhancing the SuSy-catalysed sucrolytic pathway by reducing the feedback inhibition by Fru. Apart from catalytic roles, FRKs are also involved in sugar sensing and signalling.

Protein-protein interactions: The STRING database was used to study the interactions of FRK protein with other proteins in the cell and to predict their role in the plant metabolism (Fig. 4.33). The basic process of analysis remained same as mentioned earlier. The biological, molecular and cellular enrichments and probable roles were deduced from the database. FRK was found to be involved in response to various sugar metabolism particularly sucrose metabolism with its expression mainly in vacuoles.

.

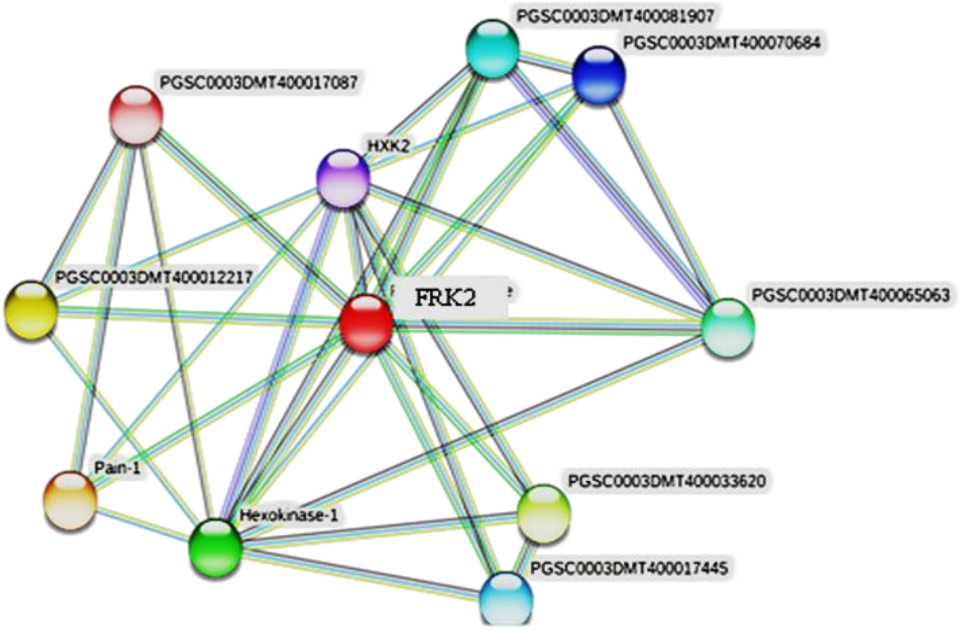

Fig. 4.33 Protein relationship network of potato FRK2 (PGSC0003DMG400026916) derived from the STRING database

It was found to be linked with a number of enzymes namely sucrose synthase (PGSC0003 DMT400017087), xylose isomerase (PGSC0003DMT400070684), vacuolar invertase (PGSC 0003DMT400035987), hexokinase (PGSC0003DMT400000795).

All these enzymes are associated with sugar signaling and maintain the homeostasis in the cell. Thus, from the analysis of the protein interactions of FRK it could be deduced that FRKs are the key players in allocating carbon towards the sink formation and could possibly be involved in double break mechanism in coherence with sucrose synthase (Stein and Granot 2019).

4.3.3 *Expression Patterns of Calcium-dependent Protein Kinase (CDPKs)*

CDPK mRNA expression patterns: CDPK2 gene expression pattern was examined in some potato organs namely tuberizing stolon, growing tuber, leaf, stem, and flower. By semi-quantitative RT-PCR, a DNA product of ~0.9 kb was only amplified using total RNA from tuberizing stolon, tuber, leaf and stem (Fig. 4.34). The size matched with *CDPK2-A* transcripts towards the 5′-end. The transcript level appeared to be comparabibly high in tuberizing stolon, tuber in comparison to leaf and stem (where it was low); interestingly, the transcript was not detected in the case of flower. The actin expression level was found to be nearly uniform in the potato organs.

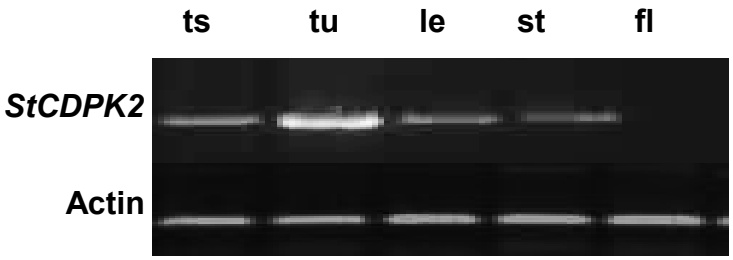

Fig. 4.34 Semi-quantitative RT-PCR for *StCDPK2* expression analysis using total RNA from different potato (cultivar KC-1) organs and the primers SC2F1-0001 and SC2R1-0920. ts tuberizing stolon, tu tuber, le leaf, st stem, fl flower. The size of the amplified product was ~ 0.9 kb in ts, tu, le and st. Actin-specific primers were used as an internal control (size of the amplified product ~ 0.65 kb in each organ).

To study the expression patterns of the CDPKs using bioinformatics tools, heatmap was generated from the curated RNAseq-derived data from Expression Atlas (Fig. 4.35). *StCDPK1*, *2* and *3* genes are found to be highly expressed in the tubers indicating their potential role in tuberization, whereas *StCDPK4, 5, 6, 9, 10, 11, 16* and *19* genes are constitutive ones as they are expressed in all organs potraying their role in plant immunity. StCDPK7 protein was found to be associated with tuber, more specifically in tuber peel and sprout. *StCDPK12, 17, 20* and

23 genes are specific to flower and stem, predominantly in stamen indicating their involvement in floral development. *StCDPK14* gene is highly expressed in stem and root. All these data clearly suggest that *CDPK* genes vary with regard to spatio-temporal expression patterns indicating functional specializations of the individual CDPK forms.

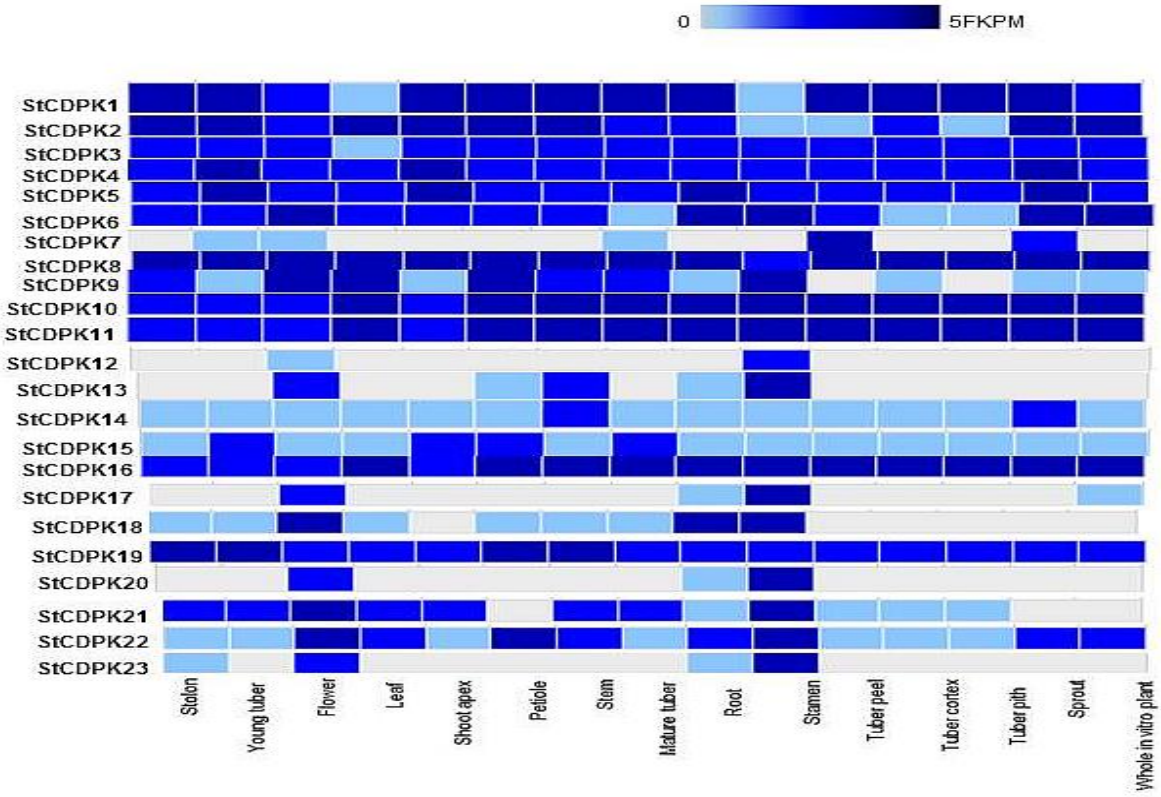

Fig. 4.35 Tissue expression patterns of *CDPK* genes in potato. The expression values were retrieved from large scale RNA-seq data in Expression Atlas. FPKM: Fragments per kilobase of exon model per million reads mapped.

Protein-protein interactions: The STRING database was used to study the interaction of CDPK2 protein with other proteins in the cell and to predict their role in the plant metabolism (Fig. 4.36). As analysed in the cases of other genes, the biological, molecular and cellular enrichments and probable roles of CDPK2 protein were deduced from the database. CDPK2 was found to be associated with only respiratory brust (RBOH) at higher confidence, so lower confidence level at 4.00 was selected to know the interactions of CDPK2 with other proteins. It was observed that CDPK2 interacts with Respiratory burst oxidase homolog protein (PGSC0003DMT400032088, RBOHA; PGSC0003DMT400063688, RBOHB; PGSC0003

DMT400036734, RBOHC), Cyclic nucleotide-gated ion channel 1 (PGSC0003DMT 400046350), Tellurite resistance protein tehA (PGSC0003DMT400021864, PGSC0003 DMT400074359, PGSC0003DMT400009999, PGSC0003DMT400051388), wrky transcription factor 32 (PGSC0003DMT400029069), Calcium/calmodulin-dependent protein kinase kinase (PGSC0003DMT400074993).

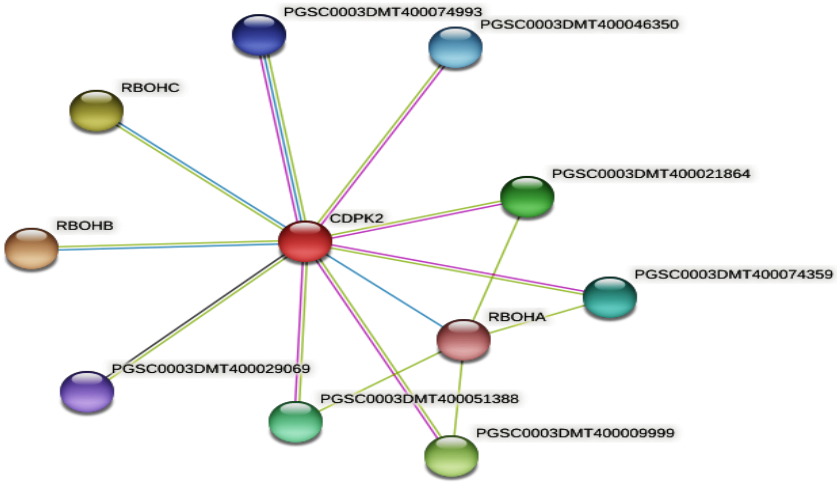

Fig. 4. 36 Protein relationship network of potato CDPK2 derived from the STRING database

CDPK2 plays a crucial role in maintaining the cellular ion homeostasis (by regulating the calcium ion flux), responses to water and abiotic stress and chemical stimulus as evident from gene ontology enrichment. Where as at molecular level it plays a role in calcium ion binding, oxidoreductase and peroxidase activity, voltage gated ion and anion channel activity.

4.3.4 Expression Patterns of Catalase (CAT)

CAT mRNA expression patterns: CAT1 gene expression pattern was examined in some potato organs namely tuberizing stolon, growing tuber, leaf, stem, and flower. By semi-quantitative RT-PCR, a DNA product of ~0.4 kb was only amplified using total RNA from tuberizing stolon, tuber (relatively high), leaf and stem (relatively low), interestingly, the transcript was not detected in the case of flower (Fig. 4.37). The size matched with *CAT1* transcripts towards the 5′-end. The actin expression level was found to be nearly uniform in the potato organs.

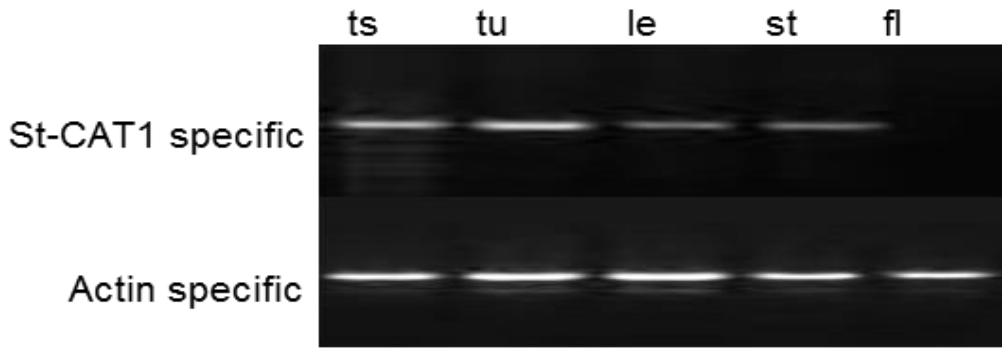

Fig. 4.37 Semi-quantitative RT-PCR for *CAT1 g*ene expression analysis using total RNA from different potato organs (cultivar KC-1) and the primers F1-CT0001 and CT- R10403. ts tuberizing stolon, tu tuber, le leaf, st stem, fl flower. The size of the *CAT1*-specific amplified product was ~0.4 kb in ts, tu, le and st. Actin-specific primers were used as an internal control (the size of the amplified product ~0.65 kb in each organ).

The expression studies available in the expression atlas indicated that *CAT1* (PGSC0003DMG 400029408) is specifically expressed more in sink organs, viz. tubers and mature leaves, exhibiting fragments per kilobase of exon model per million reads mapped (FPKM) as 5FPKM and 4.5FPKM respectively (Fig. 4. 38). The expression reduced by almost 50% in other potato organs such as flower, petiole, stem and shoot. *CAT2* (PGSC0003DMG400001570) exhibited a specifically high expression in stamen and leaves (~4FPKM) as compared to other organs. *CAT3* (PGSC0003DMG400009906) displayed abundant expression in tuber sprout, flower and breaking of dormancy. These results conclusively indicate that *CAT1* is tuber-specific and caters to potato tuberization. Also, from the RT-PCR studies the *CAT* transcripts were detected high in tuberizing stolons and tubers as compared to leaves and stems. Thus it could be concluded that, this isoform plays a vital role in controlling the ROS production by decomposing hydrogen peroxide during the tuberization (Agrawal et al. 2008; Gill and Tuteja 2010; Mittler 2017).

CAT activities at various stages of tuber development: To know the involvement of CATs in maintaining balance between generation and breakdown of reactive oxygen species (ROS) in developing tubers the CAT activity was measured in the successive stages of tuberization i.e, from hooked stolon tip (S1) to mature tuber (S8) shown earlier in Fig. 4.28. The results clearly showed that the CAT activity significantly increased during the early stages of tuber

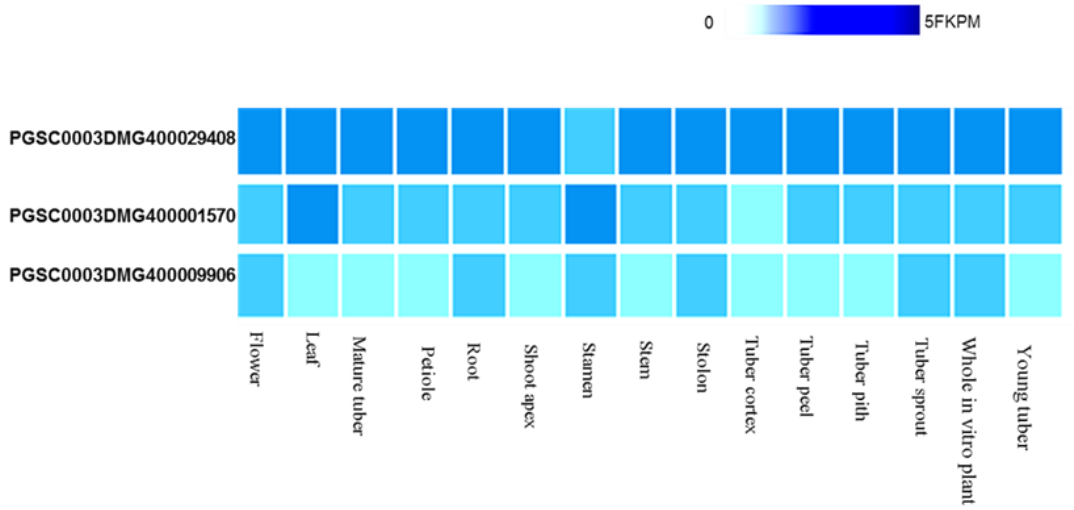

Fig. 4.38 Tissue expression pattern of *CAT* genes in potato. The expression values were retrieved from large scale RNA-seq with Expression Atlas. FPKM: Fragments per kilobase of exon model per million reads mapped.

development (S1–S3) shown in Table 4.12. The activity peaked in the actively growing tubers mainly at S3 stage. Such trend more or less continued till the attainment of nearly maturation stages (S4–S7); while the activity considerably declined at maturation (S8). This decline may be attributed to the low stress level during maturation period. During the tuber growth, the activity of KC-CAT1 was found to increase exponentially from the initiation of tuber, marking CAT1 as a key player in mitigating the harmful effects of ROS. With progression towards maturity, the CAT activity was observed to decline, which may be attributed to the low H_2O_2 levels. Thorough studies on the individual components of the antioxidant machinery can help in understanding such metabolic aspects in a more compreshensive manner.

Table 4.12 Morphological features and CAT activity profiles during different stages of tuberization in potato under field conditions. The experimental data is presented as mean ± SD of n=3 extracts.

Stages of tuberization	**Morphological features**		**CAT activity (μmol H_2O_2/min per mg protein)**
	Diameter (cm)	Fresh weight (g)	
S1 (hooked apical stolon tip)	0.06 ± 0.01	0.01 ± 0.00	321.45 ± 11.27
S2 (initiation of tuber formation)	0.31 ± 0.02	0.07 ± 0.01	472.13 ± 17.45
S3 (initial tuber)	0.89 ± 0.07	0.52 ± 0.03	1300.39 ± 26.67
S4 (developing tuber)	1.68 ± 0.25	2.57 ± 0.33	1003.91 ± 9.29
S5 (developing tuber)	2.31 ± 0.11	6.99 ± 0.79	808.55 ± 21.23
S6 (developing tuber)	3.23 ± 0.49	18.33 ± 1.42	899.23 ± 29.41
S7 (developing tuber)	5.11 ± 0.16	38.11 ± 2.57	951.79 ± 31.57
S8 (mature tuber)	7.43 ± 0.57	55.79 ± 4.35	611.87 ± 17.51

Protein-protein interactions: Every protein functions by interacting with the other proteins in the cell leading to the change in metabolic process. The results from STRING database indicate that KC-CAT1 has binding partners, some of which are enzymes that produce hydrogen peroxide (Fig. 4.39).

.

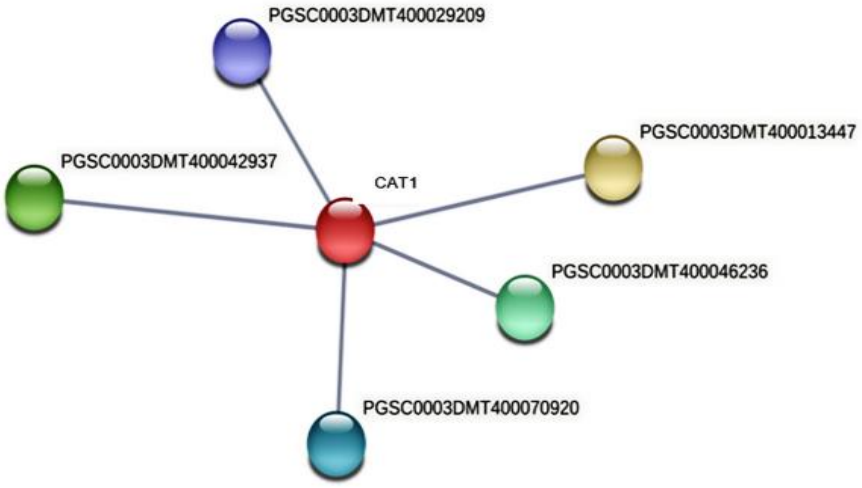

Fig. 4.39 Protein relationship network of potato CAT1 derived from the STRING database. Here, the various Potato Genome Sequencing Consortium (PGSC) IDs correspond to these enzymes: PGSC0003DMT400013447, PGSC0003DMT400046236 and PGSC0003DMT400070920 to chloroplastic SOD, PGSC0003DMT400042937 to mitochondrial SOD and PGSC0003DMT400029209 to peroxisome biogenesis protein.

Thus, it makes sense that they bind directly to catalase, as the latter can turn their product into water, thus completing the detoxification process. (For example, SOD converts the superoxide radical, a highly harmful ROS into hydrogen peroxide, so it begins the detoxification process, and by binding to catalase, the process is completed). The above has to do with the fact that KC-CAT1 has a region (1-67 aa) which is, on one hand, solvent-exposed, and on the other hand, contains a large hydrophobic patch. Boguszewska et al. (2020) also studied the protein interactions of stress related genes in potato in two cultivars. This study may provide new insight to know the possible interactions of underlying mechanisms involved in tuber development and could facilitate the targeted alteration of genes responsible to combat the stress and enhance tuber production. As evident in the profile of Expression Atlas CAT1 isoform is expressed specifically high in sink organs (tubers) as compared to other organs. Also, the expression of the ROS catabolizing enzymes such as SOD, APX and CAT was significantly increased during transition from stolons to tubers clearly indicative of active

cellular defence during growth and development. In other words, the developing tubers are inherently associated with active antioxidative machinery to combat stresses (Agrawal et al. 2008). Various stresses as mentioned earlier adversely affect growth, development, productivity even may lead to huge crop loss (Lawlor 2002). Enhanced activities of some antioxidant enzymes including some CAT isozymes were reported in potato under salt stress (Rahnama and Ebrahimzadeh 2005). Boguszewska et al. (2010) carried out experiments with some potato cultivars sensitive to soil drought and other stresses.

According to Objective 3, the spatio-temporal expression patterns of the genes encoding SuSy, FRK, CDPK and CAT were shown in different potato organs including various stages of tuberization i.e., initiation to maturation. In the initial stages of tuberization, SuSy and FRK activitities were markedly increased followed by a decline towards maturity clearly indicating the crucial role of both the enzymes in determining sink strength which supported the idea of double break mechanism i.e., SuSy-mediated production of Fru was subject to feedback inhibition. The CDPK2 mRNA level was found to be higher in developing tubers suggesting its importance in minimizing the adverse effects of oxidative burst during tuberization. CAT activities were significantly higher at the early stages of tuberization clearly indicating the role of enzymatic antioxidants in scavenging the harmful ROS like H_2O_2. Protein-protein interaction studies could predict some mutual regulatory aspects of metabolism.

In conclusion, tuberization is a complex process in potato life cycle involving a number of enzymes/proteins, transcription factors and multiple signaling pathways. In this study, the genetic resources of an Indian potato cultivar were explored for isolation of the cDNAs encoding the distinct isoforms of SuSy, FRK, CDPK and CAT. Since these enzymes are crucial in the developmentally-regulated tuberization process in potato. Isolation and characterization of the members of the individual gene families, corresponding deduced protein sequences, multiple sequence alignments, identifying the crucial motifs/domains, predicting the secondary/3-D structures and their expression were the major focus areas of this study as some aspects/features were not reported earlier in potato system. Expression patterns/enzyme assays showed significantly higher expression levels of *Susy4*, *FRK2*, *CDPK2* and *CAT1* genes in the developing tubers which indicated that in concert with Suc, Fru and starch metabolism, Ca^{2+} signaling and ROS metabolism are also crucial in the process of tuberization. The datasets would be quite useful in improving not only the potato crops but the other members of the *Solanaceae* family as well. Keeping in view, this thesis work is quite relevant and useful.

4.4 Concluding remarks and future prospects

Potato is a non-cereal food crop; its commercial importance is rapidly increasing globally mainly because of nutritional aspects. In other words, it is promising to fight hunger and malnutrition in many countries. Therefore, a thorough understanding of tuber growth and development has become a very attractive area of research in recent decades. It becomes necessary to increase productivity of this tuber crop. Like other crops, potato plants are highly prone to both abiotic and biotic stresses and show low photoassimalitation capacity (Powell et al. 2012). Therefore, new approaches are to be adopted to face such challenges by developing stress tolerant crops.

In potato lifecycle, the process of developmentally-regulated tuberization involves multiple proteins/enzymes associated with carbohydrate, starch, storage protein and stress metabolism. Higher sink strength of developing tubers depends on some crucial factors like sugar signalling and effective stress management regulated by the nature of spatio-temporal expression patterns of different genes. In plants, various factors like genetic makeup (G), environment (E) and importantly, the interactions between them (G x E) have profound influence on growth, development, fitness, performance, adaptation, and other physiological aspects. A particular species with different genotypes respond differently by exposure to the same environmental factors (El-Soda et al. 2014). A particular gene could vary in its express pattern in different cultivars of potato depending on genotype. Tuberization is a complex process which requires expression of multiple genes and the complex interplay of the gene products. Studying the structure, function, characterization and expression patterns of different forms of the crucial genes would be helpful to understand tuberization. Moreover, it would help to develop potato cultivars with desirable genotype by modern biotechnological approaches and hence contribute to increasing crop productivity under both normal and stressful conditions.

In the area of potato molecular genetics, there are some issues that require further attention e.g., organization of the genes in the individual potato chromosomes, size of the gene families and their groupings, structural aspects and the transcriptional control of the individual members of a gene family, biochemical attributes of various protein forms including their catalytic aspects and their functional specializations. In-depth understanding of protein–protein interactions such as formation of protein complexes are also crucial as they could influence the overall metabolic activities during various stages of tuber development.

This thesis work deals with some of the enzymes/proteins involved in tuberization namely Sucrose synthase (SuSy), Fructokinase (FRK), Calcium-dependent protein kinase (CDPK) and Catalase (CAT). The isoforms of these enzymes are involved in tuberization and their coordinated activities determine the sink strength of a storage organ like potato tuber. The cDNAs encoding the above enzymes were isolated and characterized for the first time from a commercially important processing Indian cultivar, Kufri Chipsona-1 (KC-1). During the process of tuber induction, the apoplastic phloem unloading of sucrose (Suc) is predominantly replaced by symplastic phloem unloading. Therefore, SuSy-mediated sucrolytic pathway becomes predominant as compared to invertase-mediated Suc breakdown in the apical region of swollen tip. It is very likely, this process is responsible for up regulation of several genes involved in sucrose metabolism such as FRK. As evident from the experiments, *SUS4* belonging to group I, is highly expressed during tuberization in comparison to other *SUS* forms. In this context, cloning and characterization of a *SUS4* member from potato cultivar KC-1 along with *in silico* studies of its crucial glycosyl transferase site, CoDY helix domains, 3-D structure, and its expression patterns in various organs and stages of tuber development are important aspects of the study, particularly in the area of Suc metabolism in developing tubers. The importance of allocating carbon sources towards the sink tuber is well known. However, we know little about various forms of FRKs involved in tuberization. Here, a cDNA encoding a distinct 319-aa FRK2 isoform i.e., St-FRK2 is reported from the cultivar KC-1 along with two more cDNA clones encoding 256-aa FRK2A and 266-aa FLN variants involved in stress metabolism and plant development. The predicted 3-D structures could distinguish between the different FRK forms in potato suggesting they could vary with regard to catalytic aspects. The expression pattern of the FRK2 isoform clearly suggests its involvement in determining sink strength of tuber. In addition, adequate information/analyses are provided describing the FRK gene family, chromosomal maps and the expression of the individual members. *In silico* analyses also helped to generate some new datasets which could be used in genetic manipulations.

Along with starch-sucrose metabolism in the growing tuber, there is concomitant influx of Ca^{2+} ions into the cytoplasm paving towards activation of calcium signals (specifically CDPKs) to trigger the cascade of activation/deactivation of proteins/enzymes/transcription factors/growth regulators associated with tuberization (Bi et al. 2021). Keeping in view, a cDNA encoding a

distinct CDPK2 form was cloned and characterized from the cultivar KC-1 involved in tuberization. *In silico* analyses helped to generate some datasets which were not reported earlier. The influx of calcium ions is usually accompanied with generation of ROS inside the cytoplasm causing a stressful situation. Catalase (CAT) plays a crucial role during the process of tuberization as it actively dismutates harmful hydrogen peroxide to water. The biochemical, molecular and *in silico* studies on CAT remain important aspects of this thesis work. Here, we report cloning and characterization of a cDNA encoding distinct CAT1 form involved in tuberization. Also an insight into the gene family, the crucial domains/catalytic sites and their probable functions are predicted.

In conclusion, this thesis work mainly focussed on the enzymes involved in sucrose/starch metabolism, calcium signalling and ROS metabolism closely associated with tuberization. This is a comprehensive report with regard to an Indian potato cultivar. All the data/findings of the study would help in gaining molecular insights into the complex interplay of metabolic and signalling pathways that facilitate the tuberization process under normal and stressful field conditions. Thorough sequence analyses of different genes and their products as done in this study would be useful in several biotechnological approaches such as diploid breeding, gene editing or marker assisted breeding technologies for development of designer potato crops.

6. References

Abbasi F, Onodera H, Toki S, Tanaka H, Komatsu S (2004) OsCDPK13, a calcium dependent protein kinase gene from rice, is induced by cold and gibberellin in rice leaf sheath. Plant Mol Biol 55: 541–552.

Abdullah M, Cao Y, Cheng X, Meng D, Chen Y, Shakoor A, Gao J, Cai Y (2018) The sucrose synthase gene family in Chinese pear (*Pyrus bretschneideri* Rehd.): structure, expression, and evolution. Molecules 23:1–16

Acevedo A, Scandalios JG (1990). Expression of the catalase and superoxide dismutase genes in mature pollen in maize. Theor Appl Genet *80*(5) :705–711

Acevedo A, Williamson J, Scandalios, JG (1991) Photoregulation of the Cat2 and Cat3 catalase genes in pigmented and pigment-deficient maize: the circadian regulation of Cat3 is superimposed on its quasi-constitutive expression in maize leaves. Genetics 127:601–607

Aebi H (1984) Catalase *in vitro*, Methods Enzymol 105:121–126

Agrawal L, Chakraborty S, Jaiswal DK, Gupta S, Datta A, Chakraborty N (2008) Comparative proteomics of tuber induction, development and maturation reveal the complexity of tuberization process in potato (*Solanum tuberosum* L.). J Proteome Res 7:3803–3817

Ahmed B, Alam M, Hasan F, Emdad EM, Islam S, Rahman N (2020) Jute CDPK genes and their role in stress tolerance and fiber development: A genome-wide bioinformatic investigation of *Corchorus capsularis* and *C. olitorius*. Plant Gene 24:100252

Akira S, Uematsu S, Takeuchi O (2006) Pathogen recognition and innate immunity. Cell 124: 783–801.

Aksenova NP, Konstantinova TN, Golyanovskaya SA, Sergeeva LI, Romanov GA (2012) Hormonal Regulation of Tuber Formation in Potato Plants. Russ J Plant Physl 59:451–466

Alam NB, Ghosh A (2018) Comprehensive analysis and transcript profiling of Arabidopsis thaliana and *Oryza sativa* catalase gene family suggests their specific roles in development and stress responses. Plant Physiol Biochem 123:54–64

Amor Y, Haigler CH, Johnson S, Wainscott M, Delmer DP (1995) A membrane-associated form of sucrose synthase and its potential role in synthesis of cellulose and callose in plants. Proc Natl Acad Sci USA 92: 9353–9357 doi: 10.1073/pnas.92.20.9353

An X, Chen Z, Wang J, Ye M, Ji L, Wang J, Liao W, Ma H (2014) Identification and characterization of the *Populus* sucrose synthase gene family. Gene 539:58–67

Appeldoorn NJG, De Bruijn SM, Koot-Gronsveld EAM, Visser RGF, Vreugdenhil D, Van Der Plas LHW (1999) Developmental changes in enzymes involved in the conversion of hexose phosphate and its subsequent metabolites during early tuberization of potato. Plant Cell Environ 22:1085–1096

Arsova B, Hoja U, Wimmelbacher M, Greiner E, Ustun S, Melzer M et al (2010) Plastidial thioredoxin z interacts with two fructokinase-like proteins in a thiol-dependent manner: evidence for an essential role in chloroplast development in Arabidopsis and Nicotiana benthamiana. Plant Cell 22:1498–1515. doi: 10.1105/tpc.109.071001

Asano T, Hayashi N, Kikuchi S, Ohsugi R (2012) CDPK-mediated abiotic stress signaling. Plant Signal Behav 7:817–821

Avigad G (1982) Sucrose and other disaccharides. In: Loewus F A, Tanner W (eds), Encyclopedia of Plant Physiol, vol. 13A, Springer-Verlag, Heidelberg, pp 217–347

Bachem C, van der Hoeven R, Lucker J, Oomen R, Casarini E, Jacobsen E, Visser R (2000) Functional genomic analysis of potato tuber life-cycle. Potato Res 43: 297–312

Bae YS, Oh H, Rhee SG, Yoo YD (2011) Regulation of reactive oxygen species generation in cell signaling. Mol Cells 32(6):491−509. doi: 10.1007/s10059-011-0276-3

Bandopadhyay R, Haque I, Singh D, Mukhopadhyay K (2010) Levels and stability of expression of transgenes. In: Kole C et al. (eds) Transgenic Crop Plants, Springer-Verlag Berlin, Heidelberg

Banks JA, Nishiyama T, Hasebe M, Bowman JL, Gribskov M, Albert VA, Aono N, Aoyama T, Ambrose BA, Ashton NW (2011) The Selaginella genome identifies genetic changes associated with the evolution of vascular plants. Science 332: 960–963

Baroja-Fernandez E, Munoz FJ, Montero M, Etxeberria E, Sesma MT, Ovecka M, Bahaji A, Ezquer I, Li J, Prat S, Pozueta-Romero J (2009) Enhancing sucrose synthase activity in transgenic potato (*Solanum tuberosum* L.) tubers results in increased levels of starch, ADPglucose and UDPglucose and total yield. Plant Cell Physiol 50:1651–1662

Baroja-Fernandez E, Munoz FJ, Saikusa T, Rodriguez-Lopez M, Akazawa T, Pozueta-Romero J (2003) Sucrose synthase catalyzes the de novo production of ADPglucose linked to starch biosynthesis in heterotrophic tissues of plants. Plant Cell Physiol 44:500–509

Barratt PDH, Derbyshire P, Findlay K, Pike M, Wellner N, Lunn J et al (2009) Normal growth of *Arabidopsis* requires cytosolic invertase but not sucrose synthase. Proc Natl Acad Sci USA 106: 13124–13129 doi: 10.1073/ pnas.0900689106

Baud S, Vaultier MN, Rochat C (2004) Structure and expression profile of the sucrose synthase multigene family in *Arabidopsis*. J Exp Bot 55:397–409

Baysdorfer C, Kremer DF, Sicher RC (1989) Partial purification and characterization of fructokinase activity from barley leaves. J Plant Physiol 134:156–161 doi: 10.1016/S0176-1617(89)80049-5

Beaumont F, Jouve H-M, Gagnon J, Gaillard J, Pelmont J (1990) Purification and properties of a catalase from potato tubers (*Solanum tuberosum*). Plant Sci 72:19–26

Benetka W, Mehlmer N, Maurer-Stroh S, Sammer M, Koranda M, Neum€uller R, Betschinger J, Knoblich JA, Teige M, Eisenhaber F (2008) Experimental testing of predicted myristoylation targets involved in asymmetric cell division and calcium dependent signaling. Cell Cycle 7: 3709–3719

Berendsen HJ, van der Spoel D, van Drunen R (1995) GROMACS: a message passing parallel molecular dynamics implementation. Comput Phys Commun 91:43–56

Bevan M (1991) Gene activity during tuber formation in potato (*Solanum tuberosum*). In: Grierson D (ed) Developmental regulation of plant gene expression pp. 75–93

Bi Z, Wang Y, Li P, Sun C, Qin T, Bai J (2021) Evolution and expression analysis of CDPK genes under drought stress in two varieties of potato. Biotechnol Lett 43:511–521

Biemelt S, Hajirezaei MR, Melzer M, Albrecht G, Sonnewald U (1999) Sucrose synthase activity does not restrict glycolysis in roots of transgenic potato plants under hypoxic conditions. Planta 210:41–49

Bienert GP, Møller ALB, Kristiansen KA, Schulz A, Møller IM, Schjoerring JK, Jahn TP (2007) Specific aquaporins facilitate the diffusion of hydrogen peroxide across membranes. J Biol Chem 282:1183–1192

Bieniawska Z, Paul Barratt DH, Garlick AP, Thole V, Kruger NJ, Martin C et al (2007) Analysis of the sucrose synthase gene family in Arabidopsis. Plant J 49:810–828 doi: 10.1111/j.1365-313X.2006.03011.x

Bindschedler LV, Dewdney J, Blee KA, Stone JM, Asai T, Plotnikov J, Denoux C, Hayes T, Gerrish C, Davies DR (2006) Peroxidase dependent apoplastic oxidative burst in *Arabidopsis* required for pathogen resistance. Plant J 47:851–863

Birnboim HC, Doly J (1979) A rapid alkaline extraction procedure for screening recombinant plasmid DNA. Nuc Acids Res 7: 1513-1523

Boguszewska D, Grudkowska M, Zagdańska B (2010) Drought-responsive antioxidant enzymes in potato (*Solanum tuberosum* L.). Potato Res 53:373–382

Boguszewska-Mańkowska D, Gietler M, Nykiel M (2020) Comparative proteomic analysis of drought and high temperature response in roots of two potato cultivars. Plant Growth Regul 92:345–363

Boudsocq M, Droillard MJ, Regad L, Lauriere C (2012) Characterization of Arabidopsis calcium-dependent protein kinases: activated or not by calcium? Biochem J 447: 291–299

Boudsocq M, Sheen J (2013) CDPKs in immune and stress signalling. Trends Plant Sci 18:30–40

Bowler C, Slooten L, Vandenbranden S, Rycke RD, Botterman J, Sybesma C, Montagu MV, Inzé D (1991) Manganese superoxide dismutase can reduce cellular damage mediated by oxygen radicals in transgenic plants. EMBO J 10:1723–1732

Bredow M, Monaghan J, (2019) Regulation of plant immune signaling by calcium-dependent protein kinases. Mol Plant Microbe Interact 32:6–19

Buckeridge MS, Vergara CE, Carpita NC (1999) The mechanism of synthesis of a mixed-linkage (1– > 3), (1– > 4) beta-D-glucan in maize. Evidence for multiple sites of glucosyl transfer in the synthase complex. Plant Physiol 120:1105–1116

Bund'o M, Coca M. (2017) Calcium-dependent protein kinase OsCPK10 mediates both drought tolerance and blast disease resistance in rice plants. J Exp Bot erx145

Cabiscol E, Tamarit J, Ros J (2000) Oxidative stress in bacteria and protein damage by reactive oxygen species. Int Microbiol 3:3–8

Cabrera R, Babul J, Guixe V (2010) Ribokinase family evolution and the role of conserved residues at the active site of the PfkB subfamily representative, Pfk-2 from *Escherichia coli*. Arch Biochem Biophys 502:23–30

Cai G, Faleri C, Del Casino C, Emons AM, Cresti M (2011) Distribution of callose synthase, cellulose synthase, and sucrose synthase in tobacco pollen tube is controlled in dissimilar ways by actin filaments and microtubules. Plant Physiol 155:1169–1190 doi: 10.1104/pp.110.171371

Campos G, Guixe V, Babul J (1984) Kinetic mechanism of phosphofructokinase-2 from *Escherichia coli*. A mutant enzyme with a different mechanism. J Biol Chem 259:6147–6152

Carlson SJ, Chourey PS (1996) Evidence for plasma membrane-associated forms of sucrose synthase in maize. Mol Gen Genet 252:303–310 doi: 10.1007/ BF02173776

Cheatham TI, Miller JL, Fox T, Darden TA, Kollman TA (1995) Molecular dynamics simulations on solvated biomolecular systems: the particle mesh Ewald method leads to stable trajectories of DNA, RNA, and protein. J Am Chem Soc 117:4193–4194

Chelikani P, Fita I, Loewen PC (2004) Diversity of structures and properties among catalases. Cell Mol Life Sci 61: 192–208

Chen A, He S, Li F, Li Z, Ding M, Liu Q, Rong J (2012) Analyses of the sucrose synthase gene family in cotton: structure, phylogeny and expression patterns. BMC Plant Biol 12:85

Chen F, Fasoli M, Tornielli GB, Santo SD, Pezzotti M, Zhang L, Cai B, Cheng ZM (2013) The evolutionary history and diverse physiological roles of the grapevine calcium dependent protein kinase gene family. PLoS One 8:e80818

Chen HJ, Wu SD, Huang GJ, Shen C, Afiyanti M, Li WJ, Lin YH (2012) Expression of a cloned sweet potato catalase SPCAT1 alleviates ethephon-mediated leaf senescence and H_2O_2 elevation. J Plant Physiol 169:86–97

Chen Y, Zhang Q, Hu W, Zhang X, Wang L, Hua X (2017) Evolution and expression of the fructokinase gene family in *Saccharum*. BMC Genome 18:197

Cheng SH, Willmann MR, Chen HC, Sheen J (2002) Calcium signaling through protein kinases. The Arabidopsis calcium-dependent protein kinase gene family. Plant Physiol 129:469–485

Chengappa S, Loader N, Shields R (1998) The electronic plant gene register. Plant Physiol 118:1533–1536

Chia T, Thorneycroft D, Chapple A, Messerli G, Chen J, Zeeman SC, Smith SM, Smith AM (2004) A cytosolic glucosyl transferase is required for conversion of starch to sucrose in Arabidopsis leaves at night. Plant Journal 37: 853–863

Chopra S, Del-Favero J, Dolferus R, Jacobs M (1992) Sucrose synthase of *Arabidopsis*: genomic cloning and sequence characterization. Plant Mol Biol 18:131–134 doi: 10.1007/BF00018465

Chou KC, Shen HB (2009) Recent advances in developing web-servers for predicting protein attributes. Nat Sci 1:63

Choudhury FK, Rivero RM, Blumwald E, Mittler R (2017) Reactive oxygen species, abiotic stress and stress combination. Plant J 90:856–867

Chourey PS, Nelson OE (1976) The enzymatic deficiency conditioned by the shrunken-1 mutations of maize. Biochem Genet 14:1041–1055 doi: 10.1007/BF00485135

Claeyssen E and Rivoal J (2007) Isozymes of plant hexokinase: occurrence, properties and functions. Phytochemistry 68:709–731

Coleman HD, Ellis DD, Gilbert M, Mansfield SD (2006) Up-regulation of sucrose synthase and UDP-glucose pyrophosphorylase impacts plant growth and metabolism. Plant Biotechnol J 4:87–101

Coleman HD, Yan J, Mansfield SD (2009) Sucrose synthase affects carbon partitioning to increase cellulose production and altered cell wall ultrastructure. Proc Natl Acad Sci USA 106:13118–13123

Copeland L, Morell M (1985) Hexose kinases from the plant cytosolic fraction of soybean nodules. Plant Physiol 79:114–117

Corpet F (1988) Multiple sequence alignment with hierarchical clustering. Nucleic Acids Res 16:10881–10890

Counce PA, Gravois KA (2006) Sucrose synthase activity as a potential indicator of high rice grain yield. Crop Sci 46:1501–1507 doi: 10.2135/ cropsci2005.0240

Craig J, Barrat P, Tatge H, Dejardin A, Handle L, Gardner CD et al (1999) Mutations at the *rug4* locus alter the carbon and nitrogen metabolism of pea plants through an effect on sucrose synthase. Plant J 17:353–362. doi: 10.1046/j.1365-313X.1999.00382.x

Cumino A, Curatti L, Giarrocco L, Salerno GL (2002) Sucrose metabolism: Anabaena sucrose-phosphate synthase and sucrose-phosphate phosphatase define minimal functional domains shuffled during evolution. FEBS Lett 517:19–23

D'Aoust MA, Yelle S, Nguyen-Quoc B (1999) Antisense inhibition of tomato fruit sucrose synthase decreases fruit setting and the sucrose unloading capacity of young fruit. Plant Cell 11:2407–2418

Daloso DM, Williams TC, Antunes WC, Pinheiro DP, Muller C, Loureiro ME, Fernie AR (2016) Guard cell-specific upregulation of sucrose synthase 3 reveals that the role of sucrose in stomatal function is primarily energetic. New Phytol 209:1470–1483

Damari-Weissler H, Kandel-Kfir M, Gidoni D, Mett A, Belausov E, Granot, D (2006) Evidence for intracellular spatial separation of hexokinases and fructokinases in tomato plants. Planta 224:1495–1502 doi: 10.1007/ s00425-006-0387-9

Damari-Weissler H, Rachamilevitch S, Aloni R, German MA, Cohen S, Zwieniecki MA et al (2009) *LeFRK2* is required for phloem and xylem differentiation and the transport of both sugar and water. Planta 230:795–805 doi: 10.1007/s00425-009-0985-4

Dammann C, Ichida A, Hong B et al (2003) Subcellular targeting of nine calcium-dependent protein kinase isoforms from Arabidopsis. Plant Physiol 132:1840–1848. doi:10.1104/pp.103.020008.

Das K, Roychoudhury A (2014) Reactive oxygen species (ROS) and response of antioxidants as ROS-scavengers during environmental stress in plants. Front Environ Sci 2:53

Datta R, Das I, Sen B, Chakraborty A, Adak S, Mandal C, Datta AK (2005) Mutational analysis of the active-site residues crucial for catalytic activity of adenosine kinase from *Leishmania donovani*. Biochem J 387:591–600

Davies H, Louise V, Burrell M, Carrari F, Urbanczyk W, Leisse A, Hancock R, Taylor M, Viola R, Ross H, McRae D, Willmitzer L, Fernie A (2005) Modulation of Fructokinase Activity of Potato *(Solanum tuberosum).* Plant Cell Physiol 46:1103–1115

Deepika D, Poddar N, Kumar S, Singh A (2022) Molecular Characterization Reveals the Involvement of Calcium Dependent Protein Kinases in Abiotic Stress Signaling and Development in Chickpea

(*Cicer arietinum*). Front Plant Sci (Abiotic Stress Signaling in Plants: Functional Genomic Intervention, Volume II) doi.org/10.3389/fpls.2022.831265

DeFalco TA, Bender KW, Snedden WA (2010) Breaking the code: Ca^{2+} sensors in plant signalling. Biochem J 425:27–40

Dejardin A, Sokolov LN, Kleczkowski LA (1999) Sugar/osmoticum levels modulate differential abscisic acid-independent expression of two stress-responsive sucrose synthase genes in Arabidopsis. Biochem J 344:503–509

DeLano WL. *The PyMOL Molecular Graphics System.* San Carlos, CA: DeLano Scientific; 2002.

Demagante AL, Vander Zaag P (1988) The response of potato (*Solanum* spp.) to photoperiod and light intensity under high temperatures. Pot Res 31:73–83

Dennison C, Lovrien R (1997) Three phase partitioning: concentration and purification of proteins. Protein Expres Purif 11:149–161

Dinh QD, Finkers R, Westphal AH, van Dongen WMAM, Visser RGF, Trindade LM (2018) Exploring natural genetic variation in tomato sucrose synthases on the basis of increased kinetic properties. PLoS One 13:e0206636

Doehlert DC (1990) Fructokinases from developing maize kernels differ in their specificity for nucleoside triphosphates. Plant Physiol 93:353–355 doi: 10.1104/pp.93.1.353

Doolittle RF (1989) Redundancies in protein sequences. In: Fasman GD (ed) Prediction of protein structure and the principles of protein conformation. Plenum Press, New York, pp 599–623

Draffehn AM, Meller S, Li L, Gebhardt C (2010) Natural diversity of potato (*Solanum tuberosum*) invertases. BMC Plant Biol 10:271

Drory A, Woodson WR (1992) Molecular cloning and nucleotide sequence of a cDNA encoding catalase from tomato. Plant Physiol 100:1605

Du Y Y, Wang P C, Chen J, Song C P (2008).Comprehensive functional analysis of the catalase gene family in Arabidopsis thaliana. J Integr Plant Biol 50(10): 1318–1326.

Du YY, Wang PC, Chen J, Song CP (2008) Comprehensive functional analysis of the catalase gene family in *Arabidopsis thaliana*. J Integr Plant Biol 50:1318–1326

Duan Y, Yang L, Zhu H, Zhou J, Sun H, Gong H (2021) Structure and Expression Analysis of Sucrose Phosphate Synthase, Sucrose Synthase and Invertase Gene Families in *Solanum lycopersicum*. Int J Mol Sci 22:4698

Duman YA, Kaya E (2013) Three-phase partitioning as a rapid and easy method for the purification and recovery of catalase from sweet potato tubers (*Solanum tuberosum*). Appl Biochem Biotechnol 170:1119–1126

Duncan KA, Hardin SC, Huber SC (2006) The three maize sucrose synthase Isoforms differ in distribution, localization, and phosphorylation. Plant Cell Physiol 47:959-971

Dutt S, Manjul AS, Raigond P, Singh B, Siddappa S, Bhardwaj V, Kawar PG, Patil VU, Kardile HB (2017) Key players associated with tuberization in potato: potential candidates for genetic engineering. Crit Rev Biotechnol 37:942–957

El-Soda M, Malosetti M, Zwaan BJ, Koornneef M, Aarts MG (2014) Genotype× environment interaction QTL mapping in plants: lessons from *Arabidopsis*. Trends Plant Sci 19(6):390–398

Etxeberria E, Gonzalez P (2003) Evidence for a tonoplast-associated form of sucrose synthase and its potential involvement in sucrose mobilization from the vacuole. J Exp Bot 54:1407–1414

Fahnenstich H, Scarpeci TE, Valle EM, Flügge UI, Maurino VG (2008) Generation of hydrogen peroxide in chloroplasts of Arabidopsis overexpressing glycolate oxidase as an inducible system to study oxidative stress. Plant Physiol 148:719–729

Fang P, Long X, Fang Y, Chen H, Yu M (2021) A predominant isoform of fructokinase, HbFRK2, is involved in *Hevea brasiliensis* (para rubber tree) latex yield and regeneration. Plant Physiol Biochem 162:211–220

Fantino E, Segretin ME, Santin F (2017) Analysis of the potato calcium-dependent protein kinase family and characterization of StCDPK7, a member induced upon infection with *Phytophthora infestans*. Plant Cell Rep 36:1137–1157

Felsenstein J (1985) Confidence limits on phylogenies: An approach using the bootstrap. Evolution 39:783–791

Fernie A R, Willmitzer L, Trethewey Ri N (2002) Sucrose to starch: a transition in molecular plant physiology. Trends Plant Sci 7:35–41

Figueroa-Yáñez L, Cano-Sosa J, Castaño E, Arroyo-Herrera AL, Caamal-Velazquez JH, Sanchez-Teyer F, López-Gómez R, Santos-Briones CDL, Rodríguez-Zapata L (2012) Phylogenetic relationships and expression in response to low temperature of a catalase gene in banana (Musa acuminata cv. "Grand Nain") fruit. Plant Cell Tiss Organ Cul 109: 429–438

Fischer L, Lipavska H, Hausman J-F, Opatrny Z (2008) Morphological and molecular characterization of a spontaneously tuberizing potato mutant: an insight into the regulatory mechanisms of tuber induction. BMC Plant Biol 8: 117

Foyer CH, Noctor G (2005) Redox homeostasis and antioxidant signaling: a metabolic interface between stress perception and physiological responses. Plant Cell 17:1866–1875

Franceschini A, Szklarczyk D, Frankild S, Kuhn M, Simonovic M, Roth A, Lin J, Minguez P, Bork P, von Mering C, Jensen LJ (2013) STRING v9.1: protein-protein interaction networks, with increased coverage and integration. Nucleic Acids Res 41:D808-D815

Franz S, Ehlert B, Liese A, Kurth J, Cazale AC, Romeis T (2011) Calcium-dependent protein kinase CPK21 functions in abiotic stress response in Arabidopsis thaliana. Mol Plant 4: 83–96.

Frattini M, Morello L, Breviario D (1999) Rice calcium-dependent protein kinase isoforms OsCDPK2 and OsCDPK11 show different responses to light and different expression patterns during seed development. Plant Mol Biol 41:753–64

Freymark G, Diehl T, Miklis M, Romeis T, Panstruga R (2007) Antagonistic control of powdery mildew host cell entry by barley calcium-dependent protein kinases (CDPKs). Mol Plant-Microbe Interact 20: 1213–1221

Fu H, Du J, Park W (1991) “Cloning and sequencing of two differentially expressed sucrose synthase genes from potato,” in *Proceedings of the Third International Congress of Plant Molecular Biology*, Tucson, AZ

Fu H, Park WD (1995) Sink- and vascular-associated sucrose synthase functions are encoded by different gene classes in potato. Plant Cell 7:1369– 1385

Fuglevand G, Phillips W, Mozzanega P, Corley S, Chengappa S, Shields R (1998) Mapping of tomato genes associated with sugar metabolism. Rep tomato gen coop 48:22–23

Gangadhar BH, Yu WJ, Sajeesh K, Park SW (2014) A systematic exploration of high-temperature stress-responsive genes in potato using large-scale yeast functional screening. Mol Genet Genomics 289:185–201

Gangappa S N, Maurya J P, Yadav V, Chattopadhyay S (2013) The Regulation of the Z- and G-Box containing promoters by light signaling components, SPA1 and MYC2, in Arabidopsis. PLoS Biol 8:e62194

Gapper C, Dolan L (2006) Control of Plant Development by Reactive Oxygen Species. Plant Physiol 141:341–345

Gardener A, Davies H, Burch L (1992) Purification and properties of fructokinase from developing tubers of potato (*Solanum tuberosum* L.). Plant Physiol 100:178–183

Gargantini PR, Giammaria V, Grandellis C, Feingold SE, Maldonado S, Ulloa RM (2009) Genomic and functional characterization of StCDPK1. Plant Mol Biol 70:153–172

Gebhardt C, Valkonen JP (2001) Organization of genes controlling disease resistance in the potato genome. Ann Rev Phytopathol 39: 79–102

Genova AD, Goverse A, Massa AN (2011) Genome sequence and analysis of the tuber crop potato. In: The Potato Genome Consortium. Nature 475:189–195

German AM, Asher I, Petreikov M, Dai N, Schaffer AA, Granot D (2004) Cloning, expression and characterization of LeFRK3, the fourth tomato (*Lycopersicon esculentum* Mill.) gene encoding fructokinase. Plant Sci 166:285–291

German AM, Dai N, Chmelnitsky I, Sobolev I, SaltsY, Barg R, Schaffer AA, Granot D (2002) LeFRK4, a novel tomato (*Lycopersicon esculentum* Mill.) fructokinase specifically expressed in stamens. Plant Sci 163:607–613

German MA, Dai N, Matsevitz T, Hanael R, Petreikov M, Bernstein N, Ioffe M, Shahak Y, Schaffer AA, Granot D (2003) Suppression of fructokinase encoded by *LeFRK2* in tomato stem inhibits growth and causes wilting of young leaves. Plant J 34:837–846

Giammaria V, Grandellis C, Bachmann S, Gargantini PR, Feingold SE, Bryan G, Ulloa RM (2011) *St*CDPK2 expression and activity reveal a highly responsive potato calcium-dependent protein kinase involved in light signalling. Planta 233:593–609

Gilkerson J, Perez-Ruiz JM, Chory J, Callis J (2012) The plastid-localized pfkB-type carbohydrate kinases FRUCTOKINASE-LIKE 1 and 2 are essential for growth and development of *Arabidopsis thaliana*. BMC Plant Biol 12:102. doi: 10.1186/1471-2229-12-102

Gill SS, Tuteja N (2010) Reactive oxygen species and antioxidant machinery in abiotic stress tolerance in crop plants. Plant Physiol Biochem 48:909–930

Gilman M (1987) Phenol/SDS method for plant RNA preparation. In Current Protocols in Molecular Biology, Ausubel FM et al (eds), John Wiley and Sons, *New York*, pp 431–434

Gleadow R, Johnson A, Tausz M (2013) Crops for a future climate. Funct Plant Biol 40:iii–vi

Gonzali S, Pistelli L, De Bellis L, Alpi A (2001) Characterization of two *Arabidopsis thaliana* fructokinases. Plant Sci 160:1107–1114 doi: 10.1016/ S0168-9452(01)00350-8

Gordon AJ, Minchin FR, James CL, Komina O (1999) Sucrose synthase in legume nodules is essential for nitrogen fixation. Plant Physiol 120: 867–877 doi: 10.1104/pp.120.3.867

Goren S, Huber SC, Granot D (2011) Comparison of a novel tomato sucrose synthase, SlSUS4, with previously described SlSUS isoforms reveals distinct sequence features and differential expression patterns in association with stem maturation. Planta 233:1011–1023

Goren S, Lugassi N, Stein O, Yeselson Y, Schaffer AA, David-Schwartz R, Granot D (2017) Suppression of sucrose synthase affects auxin signaling and leaf morphology in tomato. PLoS One 12:e018233

Grandellis C, Giammaria V, Bialer M, Santin F, Lin T, Hannapel DJ, Ulloa RM (2012) The novel *Solanum tuberosum* calcium dependent protein kinase, StCDPK3, is expressed in actively organs. Planta 236:1831–1848l

Granot D, David-Schwartz R, Kelly G (2013) Hexose kinases and their role in sugar-sensing and plant development. Front Plant Sci 4:44

Granot D, Kelly G, Stein O, Schwartz R (2014) Substantial roles of hexokinase and fructokinase in the effects of sugars on plant physiology and development. J Expt Bot 65:809–819

Grant JJ, Yun BW, Loake GJ (2000) Oxidative burst and cognate redox signaling reported by luciferase imaging: identifi cation of a signal network that functions independently of ethylene, SA and Me-JA but is dependent on MAPK activity. Plant J 24: 569–582

Gromadka R, Cieśla J, Olsza K, Szczegielniak J, Muszyńska G, Polkowska-Kowalczyk L (2018) Genome-wide analysis and expression profiling of calcium-dependent protein kinases in potato (*Solanum tuberosum*). Plant Growth Regul 84:303–315

Grossi CEM, Santin F, Quintana SA, Fantino E, Ulloa RM (2021) Calcium-dependent protein kinase 2 plays a positive role in the salt stress response in potato. Plant Cell Rep 41:535–548

Guan L, Scandalios JG (1996) Molecular evolution of maize catalases and their relationship to other eukaryotic and prokaryotic catalases. J Mol Evol 42:570–579

Guerin J, Carbonero P (1997) The spatial distribution of sucrose synthase isozymes in barley. Plant Physiol 114:55–62

Gutermuth T, Lassig R, Portes MT, Maierhofer T, Romeis T, Borst JW, Hedrich R, Feijó JA, Konrad KR (2013) Pollen Tube Growth Regulation by Free Anions Depends on the Interaction between the Anion Channel SLAH3 and Calcium-Dependent Protein Kinases CPK2 and CPK20. Plant Cell 25:4525-4543

Hackenberg T, Juul T, Auzina A, Gwizdz S, Malolepszy A, Van Der Kelen K, Dam S, Bressendorff S, Lorentzen A, Roepstorff P, Lehmann Nielsen K, Jørgensen JE, Hofius D, Van Breusegem F, Petersen M, Andersen SU (2013) Catalase and no catalase activity1 promote autophagy-dependent cell death in Arabidopsis. Plant Cell25(11):4616–26

Halford NG, Curtis TY, Muttucumaru N, Postles J, Mottram DS (2011) Sugars in crop plants. Ann Appl Biol 158:1–25

Hammond-Kosack KE, Jones JDG (1996) Resistance gene-dependent plant defense responses. Plant Cell 8:1773–1791

Han Y, Gasic K, Sun F, Xu M, Korban SS (2007) A gene encoding starch branching enzyme I (SBEI) in apple (*Malus* x *domestica*, Rosaceae) and its phylogenetic relationship to *Sbe* genes from other angiosperms. Mol Phylogenet Evol 43:852–863

Handayani T, Gilani SA, Watanabe KN (2019) Climatic changes and potatoes: How can we cope with the abiotic stresses? Breed Sci 69: 545–563

Harada T, Satoh S, Yoshioka T, Ishizawa K (2004) Induction of sucrose synthase and its roles during anaerobic growth in pondweed turions. Plant Cell Physiol 45:S151–S151

Harada T, Satoh S, Yoshioka T, Ishizawa K (2005) Expression of sucrose synthase genes involved in enhanced elongation of pondweed (*Potamogetondistinctus*) turions under anoxia. Ann Bot 96:683–692

Hardin SC, Tang GQ, Scholz A, Holtgraewe D, Winter H, Huber SC (2003) Phosphorylation of sucrose synthase at serine 170: occurrence and possible role as a signal for proteolysis. Plant J 35:588–603

Harmon AC, Gribskov M, Gubrium E, Harper JF (2001) The CDPK superfamily of protein kinases. New Phytol 151:175–183

Harper JF, Breton G, Harmon AC (2004) Decoding Ca^{2+} signals through plant protein kinases. Annu Rev Plant Biol 55:263–288

Hazarika P and Rajam MV (2011) Biotic and abiotic stress tolerance in transgenic tomatoes by constitutive expression of S-adenosylmethionine decarboxylase gene. Physiol Mol Biol Plants 17: 115-128

Hetherington AM, Trewavas A (1982) Calcium-dependent protein kinase in pea shoot membranes. FEBS Lett 145:67–71

Hirose T, Scofield GN, Terao T (2008) An expression analysis profile for the entire sucrose synthase gene family in rice. Plant Sci 174:534–543

Ho LC (1988) Metabolism and compartmentation of imported sugars in sink organs in relation to sink strength. Annu Rev Plant Physiol Plant Mol Biol 39:355–378
doi: 10.1146/annurev.pp.39.060188.002035

Hoepfner SW, Botha FC (2004) Purification and characterization of fructokinase from the culm of sugarcane. Plant Sci 167:645–654

Holmes DS, Quigley M (1981) A rapid boiling method for the preparation of bacterial plasmids. Anal Biochem.114: 193–197

Hu L, Yang Y, Jiang L, Liu S (2016) The catalase gene family in cucumber: genome-wide identification and organization. Genet Mol Biol 39:408–415

Hu Z, Lv X, Xia X, Zhou J, Shi K, Yu J, Zhou Y (2016) Genomewide identification and expression analysis of calcium-dependent protein kinase in tomato. Front Plant Sci 7:469. https://doi. org/10.3389/fpls.2016.00469

Huang T, Luo X, Fan Z, Yang Y, Wan W (2020) Genome-wide Identification and Analysis of the Sucrose Synthase Gene Family in Cassava (*Manihot esculenta* Crantz). Gene 769:145191

Huang Y, Liao Q, Hu SL, Ca Y, Xu G, Long ZJ, Lu X (2018) Molecular cloning and expression analysis of seven sucrose synthase genes in bamboo (*Bambusa emeiensis*): investigation of possible roles in the regulation of cellulose biosynthesis and response to hormones. Biotechnol Equip 32:316–323

Huang YC, Hsiang EC, Yang CC, Wang AY (2016) New insight into the catalytic properties of rice sucrose synthase. Plant Mol Biol 90:127–135

Huber SC, Huber JL (1996) Role and regulation of sucrose-phosphate synthase in higher plant. Annu Rev Plant Physiol Plant Mol Biol 47: 431–444

Iida K, Fukami-Kobayashi K, Toyoda A, Sakaki Y, Kobayashi M, Seki M, Shinozaki K (2009) Analysis of multiple occurrences of alternative splicing events in Arabidopsis thaliana using novel sequenced full-length cDNAs. DNA Res 16:155–164

Ishida S, Yuasa T, Nakata M, Takahashi Y (2008) A tobacco calcium-dependent protein kinase, CDPK1, regulates the transcription factor repression of shoot growth in response to gibberellins. Plant Cell 20: 3273– 3288.

Ivashuta S, Liu J, Liu J, Lohar DP, Haridas S, Bucciarelli B, VandenBosch KA, Vance CP, Harrison MJ, Gantt JS (2005) RNA interference identifies a calcium-dependent protein kinase involved in *Medicago truncatula* root development. Plant Cell 17:2911–2921

Jackson SD (1999) Multiple signaling pathways control tuber induction in potato. Plant Physiol. 119: 1–8

Jammer A, Gasperl A, Luschin-Ebengreuth N, Heyneke E, Chu H, Cantero-Navarro E (2015) Simple and robust determination of the activity signature of key carbohydrate metabolism enzymes for physiological phenotyping in model and crop plants. J Exp Bot 66:5531–5542

Jena PK, Reddy ASN, Poovaiah BW (1989) Molecular cloning and sequencing of a cDNA for plant calmodulin: signal-induced changes in the expression of calmodulin. Proc Natl Acad Sci USA 86:3644–3648

Jennings SA, Koehler AK, Nicklin KJ, Deva C, Sait SM, Challinor AJ (2020) Global Potato Yields Increase Under Climate Change with Adaptation and CO2 Fertilisation. Front Sustain Food Syst 4:519324

Jiang H, Dian W, Liu F, Wu P (2003) Isolation and characterization of two fructokinase cDNA clones from rice. Phytochemistry 62:47–52. doi: 10.1016/S0031-9422(02)00428-4

Jones DT (1999) Protein secondary structure prediction based on position-specific scoring matrices. J Mol Biol 292:195–202

Kamiyoshihara Y, Iwata M, Fukaya T, Tatsuki M, Mori H (2010) Turnover of LeACS2, a wound inducible 1-aminocyclopropane-1-1-carboxylic acid synthase in tomato, is regulated by phosphorylation/dephosphorylation. Plant J 64: 140–150

Kanayama Y, Dai N, Granot D, Petreikov M, Schaffer A, Bennett AB (1997) Divergent fructokinase genes are differentially expressed in tomato. Plant Physiol 113:1379–1384

Kanayama Y, Granot D, Dai N, Petreikov M, Schaffer A, Powell A, Bennett AB (1998) Tomato fructokinases exhibit differential expression and substrate regulation. Plant Physiol 117:85–90

Kandukuri SS, Noor A, Ranjini SS, Vijayalakshmi MA (2012) Purification and characterization of catalase from sprouted black gram (*Vigna mungo*) seeds. J Chromatogr B 889–890:50–54

Kappachery S, Yu JW, Baniekal-Hiremath G, Park SW (2013) Rapid identification of potential drought tolerance genes from *Solanum tuberosum* by using a yeast functional screening method. C R Biol 336:530–545

Karni L, Aloni B (2002) Fructokinase and hexokinase from pollen grains of bell pepper (*Capsicum annuum* L.): possible role in pollen germination under conditions of high temperature and CO2 enrichment. Ann Bot 90:607–612 doi: 10.1093/aob/mcf234

Kaur G, Das N (2022) A predominant isoform of Sucrose Synthase (StSUS); involved in sink strength of potato (*Solanum tuberosum* L): molecular cloning, sequence analyses, 3-D structure, catalytic site and expression studies, S Afr J Bot 149: 446–457

Kaur G, Das N (2022) Molecular cloning, expression and in silico analyses of calcium-dependent protein kinase 2 (CDPK2) in potato (*Solanum tuberosum L.*). S Afr J Bot 148: 634–642

Kaur G, Sharma S, Das N (2020) Comparison of catalase activity in different organs of the potato (*Solanum tuberosum* L.) cultivars grown under field condition and purification by three-phase partitioning . Acta Physiol Plant 42:10

Kawakami S, Mizuno M, Tsuchida H (2000) Comparison of antioxidant enzyme activities between *Solanum tuberosum* L. cultivars Danshaku and Kitaakari during low-temperature storage. J Agric Food Chem 48:2117−2121

Keller F, Frehner M, Wiemken A (1988) Sucrose synthase, a cytosolic enzyme in protoplasts of Jerusalem artichoke tubers (*Helianthus tuberosus* L.). Plant Physiol 88:239–241

Kelley LA, Mezulis S, Yates CM, Wass MN , Sternberg MJ (2015) The Phyre2 web portal for protein modeling, prediction, and analysis. Nat Protoc 10:845–858

Kim MS, HS Kim, YS Kim, KH Baek, HW Oh, KW Hahn, RN Bae, IJ Lee, H Joung, J.H. Jeon (2007b) Superoxide anion regulates plant growth and tuber development of potato. Plant Cell Rep. 26: 1717–1725

Kirkman H, Gaetani G. (2007) Mammalian catalase: A venerable enzyme with new mysteries. Trends Biochem Sci 32: 44–50

Kiss É, Szamos J, Tamás B, Borbás R (1998) Interfacial behavior of proteins in three-phase partitioning using salt-containing water/*tert*-butanol systems. Colloids Surf A: Physicochem Eng Asp 142:295–302

Kleines M, Elster RC, Rodrigo MJ, Blervacq AS, Salamini F, Bartels D (1999) Isolation and expression analysis of two stress-responsive sucrose-synthase genes from the resurrection plant *Craterostigma plantagineum* (Hochst.). Planta 209:13–24

Kloosterman B, Vorst O, Hall RD, Visser RGF, Bachem CW (2005) Tuber on a chip: differential gene expression during potato tuber development. Plant Biotech J 3:505–519 Koch

Klotz MG, Loewen PC (2003) The molecular evolution of catalatic hydroperoxidases: evidence for multiple lateral transfer of genes between prokaryota and from bacteria into eukaryota. Mol Biol Evol 20:1098–1112

Kobayashi M, Ohura I, Kawakita K, Yokota N, Fujiwara M, Shimamoto K, Doke N, Yoshioka H (2007) Calcium-dependent protein kinases regulate the production of reactive oxygen species by potato NADPH oxidase. Plant Cell 19:1065–1080

Kobayashi M, Yoshioka M, Asai S, Nomura H, Kuchimura K, Mori H, Doke N, Yoshioka H (2012) StCDPK5 confers resistance to late blight pathogen but increases susceptibility to early blight pathogen in potato via reactive oxygen species burst. New Phytol 196: 223–237

Koch K (2004) Sucrose metabolism: regulatory mechanisms and pivotal roles in sugar sensing and plant development. Curr Opin Plant Biol 7: 235-246

Koch KE (1996) Carbohydrate-modulated Gene expression in plants. Annu Rev Plant Physiol Plant Mol Biol 47:509–540

Koenig D, Jiménez-Gómez JM, Kimura S, Fulop D, Chitwood DH, Headland LR et al (2013) Comparative transcriptomics reveals patterns of selection in domesticated and wild tomato. Proc Natl Acad Sci USA110:E2655–E2662 doi: 10.1073/pnas.1309606110

Kolomiets MV, Hannapel DJ, Chen H, Tymeson M, Gladon RJ (2001) Lipoxygenase is involved in the control of potato tuber development. Plant Cell 13:613–626

Kong X, Lv W, Jiang S, Zhang D, Cai G, Pan J, Li D (2013) Genomewide identification and expression analysis of calcium-dependent protein kinase in maize. BMC Genom 14:433. https://doi. org/10.1186/1471-2164-14-433

Konishi T, Ohmiya Y, Hayashi T (2004) Evidence that sucrose loaded into the phloem of a poplar leaf is used directly by sucrose synthase associated with various beta-glucan synthases in the stem. Plant Physiol 134:1146–1152

Kumar D (1998) Kufri Chipsona-1: A potato variety for processing Indian Potato J. Association 25: 113-118

Kumar S, Stecher G, Li M, Knyaz C, Tamura K (2018) MEGA X: molecular evolutionary genetics analysis across computing platforms. Mol Biol Evol 35:1547–1549

Kumar V, Luthra SK, Bhardwaj V, Singh BP (2014) Indian Potato Varieties and their Salient Features. CPRI Technical Bulletin No. 78 (revised), ICAR-Central Potato Research Institute, Shimla, Himachal Pradesh, India

Kumari V, Das N (2013) Vacuolar invertases in potato (*Solanum tuberosum* L.): molecular cloning, characterization, sequence comparison, and analysis of gene expression in the cultivars. Acta Physiol Plant 35:2055–2068

Kumutha D, Sairam RK, Ezhilmathi K, Chinnusamy V, Meena RC (2008) Effect of waterlogging on carbohydrate metabolism in pigeon pea (*Cajanus cajan* L.): upregulation of sucrose synthase and alcohol dehydrogenase. Plant Sci 175:706–716

Kyte J, Doolittle R (1982) A simple method for displaying the hydropathic character of a protein. J Mol Biol 157:105–132

Laemmli UK (1970) Cleavage of structural proteins during the assembly of the head of bacteriophage T4. Nature 227:680–685

Lao J, Oikawa A, Bromley JR, McInerney P, Suttangkakul A, Smith-Moritz AM, Plahar H, Chiu TY, Gonzalez Fernandez-Nino SM, Ebert B, Yang F, Christiansen KM, Hansen SF, Stonebloom S, Adams PD, Ronald PC, Hillson NJ, Hadi MZ, Vega-Sanchez ME, Loque D, Scheller HV, Heazlewood JL (2014) The plant glycosyltransferase clone collection for functional genomics. Plant J 79:517–529

Laskowski, Roman & Swindells, Mark. (2011). LigPlot+: Multiple Ligand–Protein Interaction Diagrams for Drug Discovery. Journal of chemical information and modeling. 51. 2778-86. 10.1021/ci200227u.

Lawlor DW (2002) Limitation to photosynthesis in water-stressed leaves: stomata vs. metabolism and the role of ATP. Ann Bot 89:871–885

Lee SH, An CS (2005) Differential expression of three catalase genes in hot pepper (*Capsicum annuum* L.). Mol Cells 20:247–255

Lee SS, Yoon GM, Rho EJ, Moon E, Pai HS (2006) Functional characterization of NtCDPK1 in tobacco. Mol Cells 28:141–146

Lemoine R, Camera SL, Atanassova R, Dédaldéchamp F, Allario T, Pourtau N, Bonnemain J-L, Laloi M, Coutos-Thévenot P, Maurousset L, Faucher M, Girousse C, Lemonnier P, Parrilla J, Durand M (2013) Source-to-sink transport of sugar and regulation by environmental factors. Front Plant Sci 4:272

Li J, Liu JT, Wang GQ, Cha JY, Li GN, Chen S, Li Z, Guo JH, Zhang CG, Yang YQ (2015) A chaperone function of no catalase activity1 is required to maintain catalase activity and for multiple stress responses in *Arabidopsis*. Plant Cell 27(3):908–25

Li L, Strahwald J, Hofferbert HR, Lubeck J, Tacke E, Junghans H, Wunder J, Gebhardt C (2005) DNA variation at the invertase locus invGE/GF is associated with tuber quality traits in populations of potato breeding clones. Genetics 170: 813–821

Li Y, Fei X, Dai H, Li J, Zhu W, Deng X, (2019) Genome-wide identification of calcium-dependent protein kinases in Chlamydomonas reinhardtii and functional analyses in nitrogen deficiency-induced oil accumulation. Front Plant Sci 10: 1147

Li YS, Chen LC, Mu JY, Zuo JR (2013) Lesion simulating disease1 interacts with catalases to regulate hypersensitive cell death in *Arabidopsis*. Plant Physiol 163(2):1059–70

Liese A, Romeis T (2013) Biochemical regulation of in vivo function of plant calcium-dependent protein kinases (CDPK). Biochim Biophys Acta 1833:1582–1589

Liu F, Song R, Zhang X, Shahnazari A, Andersen MN, Plauborg F, Jacobsen S-E, Jensen C R (2008) Measurement and modelling of ABA signalling in potato (*Solanum tuberosum* L.) during partial root-zone drying. Environ Exp Bot 63:385-391

Liu H, Che Z, Zeng X, Zhou X, Sitoe HM, Wang H, Yu D (2016) Genome-wide analysis of calcium-dependent protein kinases and their expression patterns in response to herbivore and wounding stresses in soybean. Funct Integr Geno 16:481–93

Liu W, Li W, He Q, Daud MK, Chen J, Zhu S (2014) Genome-wide survey and expression analysis of calcium dependent protein kinase in Gossypium raimondii. PLoS One. 9: e98189

Lopez-Huertas E, Charlton WL, Johnson B, Graham IA, Baker A (2000) Stress induces peroxisome biogenesis genes. EMBO J 19:6770–6777

Lowry OH, Rosebrough NJ, Farr AL, Randall RJ (1951) Protein measurement with the folin phenol reagent. J Biol Chem 193:265–275

Ludwig AA, Saitoh H, Felix G, Freymark G, Miersch O, Wasternack C, Boller T, Jones JDG, Romeis T (2005) Ethylene-mediated cross-talk between calcium dependent protein kinase and MAPK signaling controls stress responses in plants. Proc Natl Acad Sci USA 102: 10736–10741

Mandel M, Higa A (1970) Calcium-dependent bacteriophage DNA infection. J Mol Biol 53: 159– 162

Marana C, Garcia-Olmedo F, Carbonero P (1990) Differential expression of two types of sucrose synthase-encoding genes in wheat in response to anaerobiosis, cold shock and light. Gene 88:167–172

Martin T, Frommer WB, Salanoubat M, Willmitzer L (1993) Expression of an *Arabidopsis* sucrose synthase gene indicates a role in metabolization of sucrose both during phloem loading and in sink organs. Plant J 4:367–377

Matschi S, Hake K, Herde M, Hause B, Romeis T (2015) The calcium-dependent protein kinase CPK28 regulates development by inducing growth phase-specific, spatially restricted alterations in jasmonic acid levels independent of defense responses in Arabidopsis. Plant Cell 27: 591–606

Matschi S, Werner S, Schulze WX, Legen J, Hilger HH, Romeis T (2013) Function of calcium dependent protein kinase CPK28 of Arabidopsis thaliana in plant stem elongation and vascular development. Plant J 73: 883 – 896

McCarty DR, Shaw JR, Hannah LC (1986) The cloning, genetic mapping, and expression of the constitutive sucrose synthase locus of maize. Proc Natl Acad Sci USA 83:9099–9103

McClung CR (1997) Regulation of catalases in Arabidopsis. Free Radic Biol Med 23(3):489–96

Mehlmer N, Wurzinger B, Stael S, Hofmann Rodrigues D, Csaszar E, Pfister B, Bayer R, Teige M (2010) The Ca^{2+} dependent protein kinase CPK3 is required for MAPK independent salt stress acclimation in Arabidopsis. Plant J 63: 484–498

Menéndez CM, Ritter E, Schäfer-Pregl R, Walkemeier B, Kalde A, Salamini F, Gebhardt C (2002) Cold sweetening in diploid potato: mapping quantitative trait loci and candidate genes. Genetics 162:1423–1434

Mhamdi A, Queval G, Chaouch S, Vanderauwera S, Breusegem FV, Noctor G (2010) Catalase function in plants: a focus on *Arabidopsis* mutants as stress-mimic models. J Expt Bot 61:4197–4220

Mittler R (2002) Oxidative stress, antioxidants and stress tolerance. Trends Plant Sci 7:405–410

Mittler R (2017) ROS Are Good. Trends Plant Sci 22:11−19

Miyagawa Y, Tamoi M, Shigeoka S (2000) Evaluation of the defense system in chloroplasts to photooxidative stress caused by paraquat using transgenic tobacco plants expressing catalase from *Escherichia coli*. Plant Cell Physiol 41:311–320

Morell M, Copeland L (1985) Sucrose synthase of soybean nodules. Plant Physiol 78:149–154

Morrell S, Rees TA (1986) Sugar metabolism in developing tubers of *Solanum tuberosum*. Phytochemistry 25:1579–1585
doi: 10.1016/S0031- 9422(00)81212-1

Morris GM, Goodsell DS, Halliday RS, Huey R, Hart WE, Belew RK, Olson AJ (1998) Automated docking using a Lamarckian genetic algorithm and empirical binding free energy function. J Comput Chem 19:1639–1662

Moshchenskaya J, Galibina NA, Novitskaya LL, Nikerova KK (2019) The Role of Sucrose Synthase in Sink Organs of Woody Plants. Russ J Plant Physiol 66 (1):10–21

Myers C, Romanowsky SM, Barron YD, Garg S, Azuse CL, Curran A, Davis RM, Hatton J, Harmon AC, Harper JF (2009) Calcium-dependent protein kinases regulate polarized tip growth in pollen tubes. Plant J 59:528–539

Niewiadomska E, Polzien L, Desel C, Rozpadek P, Miszalski Z, Krupinska K (2009) Spatial patterns of senescence and development-dependent distribution of reactive oxygen species in tobacco (Nicotiana tabacum) leaves. J Plant Physiol 166:1057–1068

Niu Y, Li G, Jian Y, Duan S, Liu J, Xu J, Jin L (2022).Genes related to circadian rhythm are involved in regulating tuberization time in potato. Hortic Plant J 8: 369–380

Nolte KD, Koch KE (1993) Companion-cell specific localization of sucrose synthase in zones of phloem loading and unloading. Plant Physiol 101:899–905
doi: 10.1104/pp.101.3.899

Nookaraju A, Pandey SK , Upadhyaya CP, Heung JJ , Kim H S , Chun S C , Kim DH , Park S W (2012) Role of Ca^{2+}-mediated signaling in potato tuberization: An overview Bot Stud 53: 177–189

Odanaka S, Bennett AB, Kanayama Y (2002) Distinct physiological roles of fructokinase isozymes revealed by gene-specific suppression of frk1 and frk2 expression in tomato. Plant Physiol 129:1119–1126

Pagni M, Loannidis V, Cerutti L, Zahn-Zabal M, Jongeneel CV , Falquet L (2004) MyHits: a new interactive resource for protein annotation and domain identification, *Nucleic Acids Res* 32: W332–W335

Patra N, Hariharan S, Gain, Maiti M K, Das A, Banerjee J (2021) TypiCal but DeliCate Ca^{++}re: Dissecting the Essence of Calcium Signaling Network as a Robust Response Coordinator of Versatile Abiotic and Biotic Stimuli in Plants. Front Plant Sci 12 doi 10.3389/fpls.2021.75224

Pego JV, Smeekens SC (2000) Plant fructokinases: a sweet family get-together. Trends Plant Sci 5:531–536

Persia D, Cai G, Del Casino C, Faleri C, Willemse MT, Cresti M (2008) Sucrose synthase is associated with the cell wall of tobacco pollen tubes. Plant Physiol 147:1603–1618 doi: 10.1104/pp.108.115956

Petreikov M, Dai N, Granot D, Schaffer AA (2001) Characterization of native and yeast-expressed tomato fruit fructokinase enzymes. Phytochemistry 58:841–847

Poli Y, Nallamothu V, Balakrishnan D, Ramesh P, Desiraju S, Mangrauthia SK, Voleti SR, Neelamraju S (2018) Increased Catalase Activity and Maintenance of Photosystem II Distinguishes High-Yield Mutants from Low-Yield Mutants of Rice var. Nagina22 Under Low-Phosphorus Stress. Front Plant Sci 9:1543

Polidoros AN, Scandalios JG (1999) Role of hydrogen peroxide and different classes of antioxidants in the regulation of catalase and glutathione S-transferase gene expression in maize (*Zea mays* L.). Physiol Plant 106:112–120

Poovaiah BW, Du L, Wang H, Yang T (2013) Recent advances in calcium/calmodulin mediated signaling with an emphasis on plant-microbe interactions. Plant Physiol 163: 531–542

Potato Genome Sequencing Consortium (2011) Genome sequence and analysis of the tuber crop potato. Nature 475:189–197

Powell N, Ji X, Ravash R, Edlington J, Dolferus R (2012) Yield stability for cereals in a changing climate. Funct Plant Biol 39:539–552

Prat S, Frommer WB, Hofgen R, Keil M, Kossmann J (1990) Gene expression during tuber development in potato plants. FEBS Lett 268:334–338

Purev M, Kim YJ, Kim MK, Pulla RK, Yang DC (2010) Isolation of a novel catalase (Cat1) gene from Panax ginseng and analysis of the response of this gene to various stresses. Plant Physiol Biochem 48(6):451–460

Qin QP, Cui YY, Zhang LL, Lin FF, Lai QX (2014) Isolation and induced expression of a fructokinase gene from loquat. Russ J Plant Physiol 61:289–297

Queval G, Issakidis-Bourguet E, Hoeberichts FA, Vandorpe M, Gakiere B, Vanacker H (2007). Conditional oxidative stress responses in the *Arabidopsis* photorespiratory mutant *cat2* demonstrate that redox state is a key modulator of daylength-dependent gene expression, and define photoperiod as a crucial factor in the regulation of H_2O_2-induced cell death. Plant J 52:640–657

Rahnama H, Ebrahimzadeh H (2005) The effect of NaCl on antioxidant enzyme activities in potato seedlings. Biol Plantarum 49:93–97

Raices M, Chico JM, Te´llez-In˜o´n MT, Ulloa RM (2001) Molecular characterization of StCDPK1, a calcium-dependent protein kinase from Solanum tuberosum that is induced at the onset of tuber development. Plant Mol Biol 46:591–601

Raíces M, Gargantini PR, Chinchilla D, Crespi M, Téllez-Iñón MT, Ulloa RM (2003) Regulation of CDPK isoforms during tuber development. Plant Mol Biol 52:1011–1024

Ray S, Agarwal P, Arora R, Kapoor S, Tyagi AK (2007) Expression analysis of calcium-dependent protein kinase gene family during reproductive development and abiotic stress conditions in rice (Oryza sativa L. ssp. indica). Mol Genet Genom 278:493–505

Raza A, Su W, Gao A, Mehmood SS, Hussain MA, Nie W, Lv Y, Zou X, Zhang X (2021) Catalase (CAT) Gene Family in Rapeseed (*Brassica napus* L.): Genome-Wide Analysis, Identification, and Expression Pattern in Response to Multiple Hormones and Abiotic Stress Conditions. Int J Mol Sci 22 (8):4281

Regelsberger G, Jakopitsch C, Furtmüller PG, Rueker F, Switala J, Loewen PC, Obinger C (2001) The role of distal tryptophan in the bifunctional activity of catalase-peroxidases. Biochem Soc Trans 29:99–105

Regelsberger G, Jakopitsch C, Plasser L, Schwaiger H, Furtmüller PG, Peschek GA, Zámocky M, Obinger C (2002) Occurrence and biochemistry of hydroperoxidase in oxygenic phototrophic prokaryotes (cyanobacteria). Plant Physiol Biochem 40: 479– 490

Regmi, KC, Zhang S, Gaxiola RA (2016) Apoplasmic loading in the rice phloem supported by the presence of sucrose synthase and plasma membrane-localized proton pyrophosphatase. Ann Bot 117:257–268 doi: 10.1093/aob/ mcv174

Reid TJ, Murthy MR, Sicignano A, Tanaka N, Musick WD, Rossmann MG (1981) Structure and heme environment of beef liver catalase at 2.5 A resolution. Proc Natl Acad Sci USA 78(8):4767–4771

Rensink WA, Iobst S, Hart A, Stegalkina S, Liu J, Buell CR (2005) Gene expression profiling of potato responses to cold, heat, and salt stress. Funct Integr Genomics 5: 201–207

Renz A, Stitt M (1993) Substrate specificity and product inhibition of different forms of fructokinases and hexokinases in developing potato tubers. Planta 190:166–175

Riggs JW, Cavales PC, Chapiro SM, Callis J (2017) Identification and biochemical characterization of the fructokinase gene family in *Arabidopsis thaliana*. BMC Plant Biol 17:83

Rojas-Beltran JA, Dejaeghere F, Abd Alla Kotb M, Du Jardin P (2000) Expression and activity of antioxidant enzymes during potato tuber dormancy. Potato Res 43:383–393

Romeis T, Ludwig AA, Martin R, Jones JD (2001) Calcium-dependent protein kinases play an essential role in a plant defence response. EMBO J 20:5556–5567

Romero AP, Alarcón A, Valbuena RI, Galeano CH (2017) Physiological assessment of water stress in potato using spectral information. Front Plant Sci 8:1608

Ronning CM, Stegalkina S S, Ascenzi R A et al. (2003) Comparative analyses of potato expressed sequence tag libraries. Plant Physiol 131: 419–429

Roy A, Kucukural A, Zhang Y (2010) I-TASSER: a unified platform for automated protein structure and function prediction. Nat Prot 5:725

Ruan YL (2007) Rapid cell expansion and cellulose synthesis regulated by plasmodesmata and sugar: insights from the single-celled cotton fibre. Funct Plant Biol 34:1–10

Ruan YL (2014) Sucrose metabolism: gateway to diverse carbon use and sugar signaling. Annu Rev Plant Biol 65:33–67

Ruan YL, Chourey PS (1998) A fiberless seed mutation in cotton is associated with lack of fiber cell initiation in ovule epidermis and alterations in sucrose synthase expression and carbon partitioning in developing seeds. Plant Physiol 118:399–406

Saijo Y, Hata S, Kyozuka J, Shimamoto K, Izui K (2000) Overexpression of a single Ca^{2+} dependent protein kinase confers both cold and salt/drought tolerance on rice plants. Plant J 23: 319–327.

Saitou N, Nei M (1987) The neighbor-joining method: A new method for reconstructing phylogenetic trees. Mol Biol Evol 4:406–425

Salanoubat M, Belliard G (1989) The steady-state level of potato sucrose synthase mRNA is dependent on wounding, anaerobiosis and sucrose concentration. Gene 84:181–185

Salanoubat M, Belliard G (1987) Molecular cloning and sequencing of sucrose synthase cDNA from potato (*Solanum tuberosum* L.): Preliminary charactertzation of sucrose synthase mRNA distribution. Gene 60:47–56

Salerno GL, Curatti L (2003) Origin of sucrose metabolism in higher plants: when, how and why? Trends Plant Sci 8:63–69

Sambrook J, Fritsch EF, Maniatis T (1989) Molecular cloning: a laboratory manual. Cold Spring Harbor Laboratory Press, New York

Sanders D, Pelloux J, Brownlee C, Harper JF (2002) Calcium at the crossroads of signaling. Plant Cell 14:S401–S417

Santos I, H Pires, Almeida JM, Fidalgo F, Confraria A, Duarte M, Borlido J, Salema R (2006) Phylogenetic Relationship of Potato CAT1 and CAT2 Genes, Their Differential Expression in Non-photosynthetic Organs and During Leaf Development, and Their Association with Different Cellular Processes. Funct Plant Biol 33(7): 639–651

Sarkar D (2008) The signal transduction pathways controlling in planta tuberization in potato: an emerging synthesis. Plant Cell Rep 27:1–8

Sarkar D, Sharma S (2010) Oxidative Burst-mediated ROS Signaling Pathways Regulating Tuberization in Potato. Chapter ROS Signals Regulating Potato Tuberization pp 80-100 DOI: 10.1201/9781439854082-6

Sarker, Umakanta & Oba, Shinya. (2018). Catalase, superoxide dismutase and ascorbate-glutathione cycle enzymes confer drought tolerance of Amaranthus tricolor. Scientific Reports. 8. 10.1038/s41598-018-34944-0.

Sato S, Tabata S, Hirakawa H, Asamizu E, Shirasawa K, Isobe S (2012) The tomato genome sequence provides insights into fleshy fruit evolution. Nature 485:635–641

Scandalios JG, Guan L, Polidoros AN (1997) Catalases in Plants: Gene Structure, Properties, Regulation, and Expression, in: J.G. Scandalios (Ed.), Oxidative Stress and the Molecular Biology of Antioxidant Defenses. Cold Spring Harbor Liboratory Press, pp 343–406

Schaffer AA, Petreikov M (1997a) Inhibition of fructokinase and sucrose synthase by cytosolic levels of fructose in young tomato fruit undergoing transient starch synthesis. Physiol Plant 101: 800–806 doi: 10.1111/j.1399-3054.1997.tb01066.x

Schaffer AA, Petreikov M (1997b) Sucrose-to-starch metabolism in tomato fruit undergoing transient starch accumulation. Plant Physiol 113:739–746

Schägger H, Jagow Gv (1991) Blue native electrophoresis for isolation of membrane protein complexes in enzymatically active form. Anal Biochem 199:223–231

Schmolzer K, Gutmann A, Diricks M, Desmet T, Nidetzky B (2016) Sucrose synthase: a unique glycosyltransferase for biocatalytic glycosylation process development. Biotechnol Adv 34:88–111

SchuÈttelkopf AW, Van Aalten DM (2004) PRODRG: a tool for high-throughput crystallography of protein-ligand complexes. Acta Crystallogr D 60:1355–1363

Schultz J, Copley RR, Doerks T, Ponting CP, Bork P (2000) SMART: a web-based tool for the study of genetically mobile domains. Nucleic Acids Res 28:231–234

Schulz P, Herde, Romeis T (2013) Calcium-dependent protein kinases: hubs in plant stress signaling and development. Plant Physiol. 163: 523–530

Sharma I, Ahmad P Editor(s): Parvaiz Ahmad Catalase: A Versatile Antioxidant in Plants Oxidative Damage to Plants, Academic Press, 2014, pages 131−148

Shaw JR, Ferl RJ, Baier J, St Clair D, Carson C, Mccarty DR, Hannah LC (1994) Structural features of the maize sus1 gene and protein. Plant Physiol 106:1659–1665

Sheen J, Zhou L, Jang JC (1999) Sugars as signaling molecules. Curr Opin Plant Biol 2:410–418

Shi Y, Wang MB, Powell KS, Vandamme E, Hilder VA, Gatehouse AMR et al (1994) Use of the rice sucrose synthase-1 promoter to direct phloem-specific expression of beta-glucuronidase and snowdrop lectin genes in transgenic tobacco plants. J Exp Bot 45:623–631
doi: 10.1093/jxb/45. 5.623

Shikanai T, Takeda T, Yamauchi H, Sano S, Tomizawa KI, Yokota A, Shigeoka S (1998) Inhibition of ascorbate peroxidase under oxidative stress in tobacco having bacterial catalase in chloroplasts. FEBS Lett 428:47–51

Sigrell JA, Cameron AD, Jones TA, Mowbray SL (1998) Structure of Escherichia coli ribokinase in complex with ribose and dinucleotide determined to 1.8 A resolution: insights into a new family of kinase structures. Structure 6:183–193

Sigrist CJA, de Castro E, Cerutti L, Cuche BA, Hulo N, Bridge A, Bougueleret L, Xenarios I (2013) New and continuing developments at PROSITE. Nucleic Acids Res 41:D344–D347

Singh D, Ambroise A, Haicour R, Sihachakr D, Rajam MV (2014) Increased resistance to fungal wilts in transgenic eggplant expressing alfalfa glucanase gene. Physiol Mol Biol Plants 20:143–150

Skadsen RW, Schulze-Lefert P, Herbst JM (1995) Molecular cloning, characterization and expression analysis of two catalase isozyme genes in barley. Plant Mol Biol 29:1005–1014

Smirnoff N, Arnaud D (2019) Hydrogen peroxide metabolism and functions in plants. New Phytol 221:1197–1214

Smith AM, Zeeman SC, Smith SM (2005) Starch degradation. Annu Rev Plant Biol 56:73–98

Smith S, Taylor M, Burch L, Davies H (1993) Primary Structure and Characterization of a cDNA Clone of Fructokinase from Potato (*Solanum tuberosum* cv record). Plant Physiol 102:1043

Spooner DM, Hijmans RJ (2001) Potato systematics and germplasm collecting, 1989–2000. Am J Pot Res 78: 237–268

Spooner DM, McLean K, Ramsay G, Waugh R, Bryal GJ (2005) A single domestication for potato based on multilocus amplified fragment length polymorphism genotyping. Proc Natl Acad Sci 102: 14694-14699

Spooner DM, Nunez J, Trujillo G, Mdel R H., Guzman F, Ghislain M. (2007) Extensive simple sequence repeat genotyping of potato landraces supports a major reevaluation of their gene pool structure and classification. Proc Natl Acad Sci U S A 104: 19398–19403

Spychalla JP, Desborough SL (1990) Superoxide dismutase, catalase, and α-tocopherol content of stored potato tubers. Plant Physiol 94:1214–1218

Stein O, Damari-Weissler H, Secchi F, Rachamilevitch S, German MA, Yeselson Y (2016) The tomato plastidic fructokinase SlFRK3 plays a role in xylem development. New Phytol 209:1484–1495

Stein O, Granot D (2018) Plant Fructokinases: evolutionary, developmental, and metabolic aspects in sink tissues. Front Plant Sci 9:339

Stein O, Granot D (2019) An Overview of Sucrose Synthases in Plants. Front Plant Sci. 10. 10.3389/fpls.2019.00095.

Stitt M, Huber SC, Kerr PS (1987) Control of photosynthetic sucrose formation. In MD Hatch, NK Boardman, eds, The Biochemistry of Plants. Academic Press, New York, pp 327–409

Sturm A, Lienhard S, Schatt S, Hardegger M (1999) Tissue-specific expression of two genes for sucrose synthase in carrot (*Daucuscarota* L.). Plant Mol Biol 39:349–360

Su Y, Guo J, Ling H, Chen S, Wang S, Xu L, Allan A C, Que, Y (2014). Isolation of a novel peroxisomal catalase gene from sugarcane, which is responsive to biotic and abiotic stresses. PloS one, 9(1), e84426.

Su Y, Guo J, Ling H, Chen S, Wang S, Xu L, Allan AC, Que Y (2014) Isolation of a novel peroxisomal catalase gene from sugarcane, which is responsive to biotic and abiotic stresses. PloS one 9:e84426

Subbaiah CC, Palaniappan A, Duncan K, Rhoads DM, Huber SC, Sachs MM (2006) Mitochondrial localization and putative signaling function of sucrose synthase in maize. J Biol Chem 281:15625–15635

Sun JD, Loboda T, Sung SJS, Black CC (1992) Sucrose synthase in wild tomato, *Lycopersicon chmielewskii*, and tomato fruit sink strength. Plant Physiol 98:1163–1169 doi: 10.1104/pp.98.3.1163

Sun T, Liu F, Wang W, Wang L, Wang Z, Li J, Que Y, Xu L, Su Y (2018) The Role of Sugarcane Catalase Gene *ScCAT2* in the Defense Response to Pathogen Challenge and Adversity Stress Int J Mol Sci 19:2686

Sung SJS, Xu DP, Black CC (1989) Identification of actively filling sucrose sinks. Plant Physiol 89:1117–1121 doi: 10.1104/pp.89.4.1117

Swain S, Roy S, Shah J, Van Wees S, Pieterse CM, Nandi AK (2011). Arabidopsis thaliana cdd1 mutant uncouples the constitutive activation of salicylic acid signalling from growth defects. Mol Plant Pathol 12:855-865

Sytykiewicz H, Czerniewicz P, Leszczyñski B (2008) Molecular characteristics of sucrose synthase isolated from bird cherry leaves. Herba Pol 54:41–49

Szklarczyk D, Gable AL, Nastou KC, Lyon D, Kirsch R, Pyysalo S, Doncheva NT, Legeay M, Fang T, Bork P, Jensen LJ, von Mering C (2021) The STRING database in 2021: customizable protein-protein networks, and functional characterization of user-uploaded gene/measurement sets. Nucleic Acids Res 49:D605–D612

Takahashi H, Chen Z, Du H, Liu Y, Klessig DF (1997) Development of necrosis and activation of disease resistance in transgenic tobacco plants with severely reduced catalase levels. Plant J 11:993–1005

Takehara K, Murata K, Yamaguchi T, Yamaguchi K, Chaya G, Kido S et al (2018) Thermo-responsive allele of sucrose synthase 3 (Sus3) provides high- temperature tolerance during the ripening stage in rice (*Oryza sativa* L.). *Breed Sci* 68:336–342 doi: 10.1270/jsbbs.18007

Tamura K, Peterson D, Peterson N, Stecher G, Nei M, Kumar S (2011) MEGA5: Molecular Evolutionary Genetics Analysis using Maximum Likelihood, Evolutionary Distance, and Maximum Parsimony Methods. Mol Biol Evol 28:2731–2739

Taneja D, Das N (2014) Molecular cloning, sequence analyses, and expression studies of sucrose-phosphate synthase in the potato (*Solanum tuberosum* L.) cultivars. Acta Physiol Plant 36:2253–2269

Taylor MA (2018) Routes to genetic gain in potato. Nature Plants 4: 631–632

Taylor MA, Ross HA, Gardner A and Davies HV (1995) Characterization of a cDNA encoding fructokinase from potato (*Solanum tuberosum* L.). J Plant Physiol 145:253–256

Tetlow IJ (2018) Starch Biosynthesis in Crop Plants. Editorial for Agronomy Special Edition. Agronomy 8: 1–4

Thomas B (2006) Light signals and flowering. J Exp Bot 57: 3387–3393

Tong XL, Wang ZY, Ma BQ, Zhang CX, Zhu LC, Ma FW, Li M (2018) Structure and expression analysis of the sucrose synthase gene family in apple. Integrat Agric 17:847–856

Turner JF, Harrison DD, Copeland L (1977) Fructokinase (fraction IV) of pea seeds. Plant Physiol 60:666–669

van de Wal MHBJ, Jacobsen E, Visser RGF (2001) Multiple allelism as a control mechanism in metabolic pathways: GBSSI allelic composition affects the activity of granule-bound starch synthase I and starch composition in potato. Mol Genet Genomics 265:1011–1021

Verma D, Upadhayay SK, Singh K (2022) Characterization of *APX* and *APX-R* gene family in *Brassica juncea* and *B. rapa* for tolerance against abiotic stresses. Plant Cell Rep 41: 571 –592

Verma E, Sharma B, Singal HR, Munjal R (2018) Purification of sucrose synthase from thermotolerant wheat grains and its characterization. J Environ Biol 39:459–466
doi: 10.22438/jeb/39/4/MRN-503

Verma S S, Yajima WR, Rahman MH, Shah S, Liu J-J, Ekramoddoullah A, Kav NNV (2012) A cysteine-rich antimicrobial peptide from Pinus monticola (PmAMP1) confers multiple disease resistance in canola (*Brassica napus*). Plant Mol Biol 79: 61-74

Veronica N, Subrahmanyam D, Kiran TV, Yugandhar P, Bhadana VP, Padma V, Jayasree G, Voleti SR (2017) Influence of low phosphorus concentration on leaf photosynthetic characteristics and antioxidant response of rice genotypes. Photosynthetica 55:285–293

Verslues PE, Agarwal M, Katiyar-Agarwal S, Zhu J, Zhu JK (2006) Methods and concepts in quantifying resistance to drought, salt and freezing, abiotic stresses that affect plant water status. Plant J 45: 523–39

Viola R, Roberts AG, Haupt S, Gazzani S, Hancock RD, Marmiroli N, Machray GC, Oparka KJ (2001) Tuberization in potato involves a switch from apoplastic to symplastic phloem unloading. Plant Cell 13:385–398

Visser RGF, Bachem CWB, de Boer JM (2009) Sequencing the potato genome: outline and first results to come from the elucidation of the sequence of the world's third most important food crop. Am J Pot Res 86:417–429

Vivek PJ, Tuteja N, Soniya EV (2013) CDPK1 from ginger promotes salinity and drought stress tolerance without yield penalty by improving growth and photosynthesis in Nicotiana tabacum. PLoS One. 8: e76392.

Vogel C, Silva GM, Marcotte EM (2011) Protein expression regulation under oxidative stress. Mol. Cell Proteomics 10 (12)

Vuosku J, Sutela S, Kestila J, Jokela A, Sarjala T, Haggman H (2015) Expression of catalase and retinoblastoma-related protein genes associates with cell death processes in Scots pine zygotic embryogenesis. BMC Plant Biol 15

Wang AY, Yu WP, Juang RH, Huang JW, Sung HY, Su JC (1992) Presence of three rice sucrose synthase genes as revealed by cloning and sequencing of cDNA. Plant Mol Biol 18:1191–1194

Wang F, Smith AG, Brenner ML (1993) Isolation and sequencing of tomato fruit sucrose synthase cDNA. Plant Physiol 103:1463–1464.

Wang JP, Xu YP, Munyampundu JP, Liu TY, Cai XZ (2015) Calcium-dependent protein kinase (CDPK) and CDPK-related kinase (CRK) gene families in tomato: genome-wide identification and functional analyses in disease resistance. Mol Genet Genomics 84:303–315

Wang W, Cheng Y, Chen D, Liu D, Hu M, Dong J, Zhang X, Song L, Shen F (2019) The catalase gene family in cotton: Genome-wide characterization and bioinformatics analysis. Cells 8:86

Wang Z, Wei P, Wu M, Xu Y, Li F, Luo Z, Zhang J, Chen A, Xie X, Cao P, Lin F, Yang J (2015) Analysis of the sucrose synthase gene family in tobacco: structure, phylogeny, and expression patterns. Planta 242:153–166

Wei S, Hu W, Deng X, Zhang Y, Liu X, Zhao X, Luo Q, Jin Z, Li Y, Zhou S (2014) A rice calcium-dependent protein kinase OsCPK9 positively regulates drought stress tolerance and spikelet fertility. BMC Plant Biol 14: 133.

Wei Z, Qu Z, Zhang L, Zhao S, Bi Z, Ji X, Wang X, Wei H (2015) Overexpression of poplar xylem sucrose synthase in tobacco leads to a thickened cell wall and increased height. PLoS One 10:e0120669. doi: 10.1371/journal.pone.0120669

Wen F, Ye F, Xiao Z (2020) Genome-wide survey and expression analysis of calcium-dependent protein kinase (CDPK) in grass Brachypodium distachyon. BMC Genom 21:1–17

Werr W, Frommer WB, Maas C, Starlinger P (1985) Structure of the sucrose synthase gene on chromosome 9 of *Zea mays* L. EMBO J 4:1373–1380

Willekens H, Chamnongpol S, Davey M, Schraudner M, Langebartels C, Montagu MV, Inzé D, Camp WV (1997) Catalase is a sink for H_2O_2 and is indispensable for stress defence in C-3 plants. EMBO J 16:4806–4816

Willekens H, Langebartels C, Tire C, Montagu MV, Inzé D, Camp WV (1994) Differential expression of catalase genes in *Nicotiana plumbaginifolia* (L.). Proc Natl Acad Sci USA 91:10450−10454

Winter H, Huber JL, Huber SC (1997) Membrane association of sucrose synthase: changes during the graviresponse and possible control by protein phosphorylation. FEBS Lett 420:151–155

Winter H, Huber JL, Huber SC (1998) Identification of sucrose synthase as an actin-binding protein. FEBS Lett 430:205–208

Winter H, Huber SC (2000) Regulation of sucrose metabolism in higher plants: localization and regulation of activity of key enzymes. Crit Rev Biochem Mol Biol 35:253–289

Witte CP, Keinath N, Dubiella U et al (2010) Tobacco calcium dependent protein kinases are differentially phosphorylated in vivo as part of a kinase cascade that regulates stress response. J Biol Chem 285:9740–9748

Wu G, Shah DM (1995) Isolation and Characterization of a potato catalase cDNA. Plant Physiol 108:1748

Wu P, Wang W, Duan W, Li Y, Hou X (2017) Comprehensive analysis of the CDPK-SnRK superfamily genes in Chinese cabbage and its evolutionary implications in plants. Front Plant Sci 8: 162.

Xiao X, Tang C, Fang Y, Yang M, Zhou B, Qi J, Zhang Y (2014) Structure and expression profile of the sucrose synthase gene family in the rubber tree: indicative of roles in stress response and sucrose utilization in the laticifers. FEBS J 281:291–305

Xing T, Wang XJ, Malik K, Miki BL (2001) Ectopic expression of an Arabidopsis calmodulin-like domain protein kinase-enhanced NADPH oxidase activity and oxidative burst in tomato protoplasts. Mol Plant-Microbe Interact 14: 1261–1264

Xu J, Tian YS, Peng, RH, Xiong AS, Zhu B, Jin XF, Gao F, Fu XY, Hou XL, Yao QH (2010) AtCPK6, a functionally redundant and positive regulator involved in salt/drought stress tolerance in Arabidopsis. Planta 231: 1251–1260.

Xu W, Zhao Y, Chen S, Xie J, Zhang D (2020) Evolution and functional divergence of the fructokinase gene family in populus. Front Plant Sci 11:484

Xu X, Liu M, Lu L, He M, Qu W, Xu Q, Qi X, Chen X (2015) Genome-wide analysis and expression of the calcium-dependent protein kinase gene family in cucumber. Mol Genet Genomics 290:1403–1414

Xu X, Vreugdenhil D, van Lammeren AAM (1998) Cell division and cell enlargement during potato tuber formation. J Exp Bot 49: 573–582

Xu X, Yang Y, Liu C, Sun Y, Zhang T, Hou M, Huang S, Yuan H (2019) The evolutionary history of the sucrose synthase gene family in higher plants. BMC Plant Biol 19:5661

Yan JK, Wang YY, Qiu WY, Ma H, Wang ZB, Wu JY (2017) Three-phase partitioning as an elegant and versatile platform applied to nonchromatographic bioseparation processes. Crit Rev Food Sci Nutri 58:2416–2431

Yang NS, Russell D (1990) Maize sucrose synthase-1 promoter directs phloem cell-specific expression of GUS gene in transgenic tobacco plants. Proc Natl Acad Sci USA 87: 4144–4148 doi: 10.1073/pnas.87.11.4144

Yang TB, Poovaiah BW (2002) Hydrogen peroxide homeostasis: Activation of plant catalase by calcium/calmodulin. Proceedings of the National Academy of Sciences of the United States of America. 99: 4097–102. 10.1073/pnas.052564899.

Yanisch-Perron C, Viera J, Messing J (1985) Improved M13 phage cloning vectors and host strains: nucleotide sequences of the M13mp8 and pUC19 vectors. Gene 33: 103–119

Yao Y, Geng MT, Wu XH, Sun C, Wang YL, Chen X, Shang L, Lu XH, Li Z, Li RM, Fu SP, Duan RJ, Liu J, Hu XW, Guo JC (2017) Identification, expression, and functional analysis of the fructokinase gene family in cassava. Int J Mol Sci 18:2398

Yarnes SC, Sengupta-Gopalan C (2009) Sucrose synthase levels do not limit or regulate carbon transfer in the arbuscular mycorrhizal symbiosis. J Plant Interact 4:113–117 doi: 10.1080/17429140902898429

Yu WP, Wang AY, Juang RH, Sung HY, Su JC (1992) Isolation and sequences of rice sucrose synthase cDNA and genomic DNA. Plant Mol Biol 18:139–142

Zamocky M, Furtmüller PG, Obinger C (2008) Evolution of catalases from bacteria to humans. Antioxid Redox Signal 10:1527–1548

Zámocký M, Gasselhuber B, Furtmüller PG, Obinger C (2012) Molecular evolution of hydrogen peroxide degrading enzymes. Arch Biochem Biophys 525:131–144

Zeeman SC, Kossmann J, Smith AM (2010) Starch: Its Metabolism, Evolution, and Biotechnological Modification in Plants. Annu Rev Plant Biol 61:209–234

Zeng Y, Wu Y, Avigne WT, Koch KE (1998) Differential regulation of sugar-sensitive sucrose synthases by hypoxia and anoxia indicate complementary transcriptional and posttranscriptional responses. Plant Physiol 116:1573–1583

Zhang J, Arro J, Chen Y, Ming R (2013) Haplotype analysis of sucrose synthase gene family in three *Saccharum* species. BMC Genomics 14:314

Zhang K, Han Y-T, Zhao F-L et al (2015) Genome-wide identification and expression analysis of the CDPK gene family in grape, Vitis spp. BMC Plant Biol 15:164. doi:10.1186/s12870-015-0552-z

Zhang S, Nichols SE, Dong JG (2003) Cloning and characterization of two fructokinases from maize. Plant Sci 165:1051–1058

Zhang Y (2008) I-TASSER server for protein 3D structure prediction. BMC Bioinform 23: 9–40

Zhao C, Hua LN, Liu XF, Li YZ, Shen YY, Guo JX (2017) Sucrose synthase FaSS1 plays an important role in the regulation of strawberry fruit ripening. Plant Growth Regul 81:175–181.doi: 10.1007/s10725-016-0189-4

Zhao LN, Shen LK, Zhang WZ, Zhang W, Wang Y, Wu WH (2013) Ca^{2+}dependent protein kinase11 and 24 modulate the activity of the inward rectifying K^+ channels in Arabidopsis pollen tubes. Plant Cell 25: 649–661.

Zheng Y, Anderson S, Zhang Y, Garavito RM (2011) The structure of sucrose synthase-1 from Arabidopsis thaliana and its functional implications. J Biol Chem 286:36108–36118

Zhong H, McClung C (1996) The circadian clock gates expression of two Arabidopsis catalase genes to distinct and opposite circadian phases. Mol Gen Genet 251 :196– 203

Zhu X, Wang M, Li X, Jiu S, Wang C, Fang J (2017) Genome-wide analysis of the sucrose synthase gene family in grape (*Vitis vinifera*): structure, evolution, and expression profiles. Genes 8:E111

Zimmermann P, Heinlein C, Orendi G, Zentgraf U (2006) Senescence-specific regulation of catalases in *Arabidopsis thaliana* (L.) Heynh. Plant Cell Environ 29:1049–1060

Zou JJ, Li XD, Ratnasekera D, Wang C, Liu WX, Song LF, Zhang WZ, Wu WH. (2015) *Arabidopsis* calcium-dependent protein kinase8 and catalase3 function in abscisic acid-mediated signaling and H_2O_2 homeostasis in stomatal guard cells under drought stress. Plant Cell 27(5):1445–60

Zrenner R, Salanoubat M, Willmitzer L, Sonnewald U (1995) Evidence of the crucial role of sucrose synthase for sink strength using transgenic potato plants (*Solanum tuberosum* L.). Plant J 7:97–10

Zuckerkandl E, Pauling L (1965) Evolutionary Divergence and Convergence in Proteins. In: Bryson V, Vogel HJ (eds) Evolving Genes and Proteins. Academic Press, pp 97−166

Zuo R, Hu R, Chai G, Xu M, Qi G, Kong Y, Zhou G (2013) Genome-wide identification, classification, and expression analysis of CDPK and its closely related gene families in poplar (*Populus trichocarpa*). Mol Biol Rep 40:2645–2662

.

7. Publications

- Kaur G, Sharma S, Das N (2020) Comparison of catalase activity in different organs of the potato (*Solanum tuberosum* L.) cultivars grown under field condition, and purification by three-phase partitioning. Acta Physiologiae Plantarum 42:10, Page 1–11 (Journal Impact Factor: **2.736**)
- Kaur G, Das N (2022) Molecular cloning, expression and in silico analyses of calcium-dependent protein kinase 2 (CDPK2) in potato (*Solanum tuberosum L.*). South African Journal of Botany 148): 634–642 (Journal Impact Factor: **3.111**)
- Kaur G, Das N (2022) An isoform of sucrose synthase involved in sink strength of potato (*Solanum tuberosum* L): Molecular cloning, sequence analyses, 3-D structure, crucial motifs and expression. South African Journal of Botany 149: 446–457 (Journal Impact Factor: **3.111)**

Abstracts Published in Conference Proceedings:

- Kaur G, Kaur Y, Das N (2022) Three phase partitioning (TPP): An easy and cost–effective methods for purification of enzymes. ISER International Conference Webinar on July 25, 2022
- Kaur G, Kaur Y, Das N (2022) Polyphenols from potato (*Solanum tuberosum* L.) tubers: During growth and storage and their anticancerous effects on animal cell lines. 3rd European Food Chemistry Congress Webinar on May 25-26, 2022.
- Kaur G, Das N (2018) *In silico* approaches for structure and function analysis of calcium-dependent protein kinases (CDPKs) in potato (*Solanum tuberosum* L.). 12th International Conference on Agriculture and Horticulture July 09-10, 2018 Sydney, Australia, Agrotechnol 2018, Volume 7 DOI: 10.4172/2168-9881-C1-030
- Kaur G, Das N (2018) In silico approaches for structure and function analysis of sucrose synthase (SuSy) isoforms in potato (*Solanum tuberosum* L.) at the International Conference Industrial Applications in Engineering, Information Technology, Basic and Applied Sciences held during July 14-15, 2018 in Melbourne, Australia
- Kaur G, Kumar R, Das N (2018) Soyabean waste okara: A promising feedstock for biodegradable plastics. 5th World congress on green chemistry and green engineering, J Environ Anal Chem 2018, Volume 5. DOI: 10.4172/2380-2391-C1-003
- Kaur G, Das N (2017) Studies on catalase activity in different Indian potato cultivars (*Solanum tuberosum* L.). 15th Asia-Pacific Biotechnology Congress, J Bioprocess Biotech. DOI: 10.4172/2155-9821-C1-013
- Kaur G, Das N (2015) Calcium Dependent Protein Kinases Isoforms in potato (*Solanum tuberosum* L.) at International conference on INDO-UK Workshop on Sustainable Polymer Applications (IUWSPA 2015) at Thapar University Patiala.

.

South African Journal of Botany 149 (2022) 446–457

Contents lists available at ScienceDirect

South African Journal of Botany

journal homepage: www.elsevier.com/locate/sajb

An isoform of sucrose synthase involved in sink strength of potato (*Solanum tuberosum* L): Molecular cloning, sequence analyses, 3-D structure, crucial motifs and expression

Gurpreet Kaur*, Niranjan Das

Department of Biotechnology, Thapar Institute of Engineering & Technology, Patiala, Punjab 147004, India

ARTICLE INFO

Article History:
Received 9 November 2021
Revised 19 May 2022
Accepted 17 June 2022
Available online xxx

Edited by Dr S.C. Pendota

Keywords:
Potato (*Solanum tuberosum* L.)
Sucrose synthase (SuSy)
cDNA cloning
Sequence analyses
Three-dimensional (3-D) structure
Enzyme assay

ABSTRACT

Sucrose synthase (SuSy, EC 2.4.1.13) refers to a glycosyltranferase (GT) that plays a crucial role in sugar metabolism mainly in the sink tissues of plants. Using uridine diphosphate (UDP) or adenosine diphosphate (ADP), SuSy catalyzes the reversible cleavage of sucrose into fructose, and UDP-glucose (UDP-Glc) or ADP-glucose (ADP-Glc), respectively. In plants, SuSy is encoded by relatively small gene families. It exists in multiple forms distributed differentially in the plant tissues suggesting their functional specializations. SuSy activity is regulated by a hierarchy of mechanisms including transcriptional control. Here, we report isolation and characterization of a 2,668-bp cDNA encoding a distinct full-length SuSy4 form, corresponding to *SUS I* group gene family, from a commercially important Indian potato (*Solanum tuberosum* L.) cultivar, Kufri Chipsona-1 by RT-PCR using tuber total RNA. The predicted protein consisted of 805 amino acids (designated KC-SuSy). All of the available potato SuSy proteins could be categorized into 3 groups i.e., *SUS* I–III as reported earlier in other plants. Phylogenetic analysis was carried out using the SuSy sequences from the potato, tomato and *Arabidopsis*. Multiple sequence alignments revealed segment-wise identity and divergence between the SuSy forms. Using KC-SuSy sequence, secondary structures, crucial domains/motifs and amino acids, and a three-dimensional (3-D) structure were predicted. KC-SuSy was found to be predominantly expressed in tuber. The early stages of tuber development were associated with high levels of SuSy activity. This report would be particularly useful for further studies on the SuSy proteins in potato and other *Solanaceae* family members.
© 2022 SAAB. Published by Elsevier B.V. All rights reserved.

1. Introduction

In plants, sucrose (Suc) refers to the primary product of photosynthetic tissues. This nonreducing sugar is transported from the source tissues to the non-photosynthetic tissues i.e., sink tissues through the phloem. The transported Suc is crucial in regard to providing energy, many metabolic pathways, synthesis of different organic molecules for growth and development, and also for sugar signalling. Moreover, it acts as a storage reserve, compatible solute under stresses, and regulates the expression of sugar-responsive genes (Huber and Huber 1996; Ruan 2014; Stein and Granot 2019). Sucrose-biosynthesis-related proteins (SBRPs) usually include sucrose-phosphate synthase (SPS; EC 2.4.1.14), sucrose synthase (SuSy; EC 2.4.1.13) and sucrose-phosphate phosphatase (SPP; EC 3.1.3.24). Briefly, SPS catalyzes the synthesis of sucrose-6-phosphate (Suc-6-P) by transferring the hexosyl group from uridine diphosphate glucose (UDP-Glc) to fructose-6-phosphate (Fru-6-P), followed by its hydrolysis to produce sucrose by the enzyme SPP. In the sink tissues, Suc can be hydrolyzed into Glc and Fru by the cell-wall invertase (cwINV) and vacuolar/cytosolic invertases; whereas, with the help of uridine diphosphate (UDP) the enzyme SuSy reversibly and efficiently hydrolyzes Suc into UDP-Glc and Fru (Salerno and Curatti, 2003; Ruan, 2014).

SuSy, a glycosyltransferase (GT), is found in plants and has recently been reported in bacteria. In cereal endosperm and potato tuber, SuSy is regarded as the predominant sucrose cleavage enzyme, and provides substrates for starch synthesis (Winter and Huber, 2000). It meets the increased glycolytic demand under anaerobic condition and cold stress, and provides UDP-Glc for cell wall biosynthesis; also plays a crucial role by providing substrate for respiration by supplying energy during loading and unloading in phloem (Fu and Park, 1995; Sheen et al., 1999; Coleman et al., 2006). SuSy proteins are typically homotetrameric, and the monomer is around 90 kDa

Abbreviations: SUS/SuSy, Sucrose synthase; KC-1, Kufri Chipsona-1; CPRI, Central Potato Research Institute; RNA, ribonucleic acid; cDNA, complementary deoxyribonucleic acid; RT-PCR, reverse transcription polymerase chain reaction; NCBI, National Center for Biotechnology Information; ORF, open reading frame; ExPASy, Expert Protein Analysis System; pI, isoelectric point; SIB, Swiss Institute of Bioinformatics; MSA, multiple sequence alignment; MEGA, molecular evolutionary genetic analysis; I-TASSER, iterative threading assembly refinement; SAVES, Structural Analysis and Verification Server; MW, molecular weight; AI, aliphatic index; 3-D, three-dimensional; Ch, chromosome

* Corresponding author.
E-mail address: Gsainibt@gmail.com (G. Kaur).

https://doi.org/10.1016/j.sajb.2022.06.032
0254-6299/© 2022 SAAB. Published by Elsevier B.V. All rights reserved.

consisting of 800 amino acids. The monomers may vary between 53 to 110 kDa in different plants. SuSy could act as a heterotetramer as reported in some plant species namely maize, barley, rice and bird cherry. The activity of SuSy was known to be regulated by pH. It showed Suc-synthesis activity at pH 7.5–9.5; whereas for Suc degradation, the optimal pH values were between 5.5–7.5. SuSy requires UDP for the cleavage of Suc. However, ADP can also be utilized at a lower affinity for the same reaction (Guerin and Carbonero, 1997; Duncan et al., 2006; Sytykiewicz et al., 2008; Schmölzer et al., 2016). Earlier, the SuSy proteins were considered to be only cytosolic, but the recent studies showed that they are also localized in various organelles such as vacuoles, plastid, mitochondria, golgi apparatus, cytoskeleton and tonoplasts to play different roles such as carbon allocation to plastid for starch synthesis, regulation of the solutes between the cytosol and mitochondria, and cytoskeleton functioning (Morell and Copeland, 1985; Keller et al., 1988; Etxeberria and Gonzalez, 2003; Winter et al., 1998; Subbaiah et al., 2006; Buckeridge et al., 1999; Konishi et al., 2004). The two major domains of a SuSy monomer are ~250-amino acid N-terminal domain for cellular targeting, and ~500-amino acid C-terminal GT-B domain having the enzyme's glycosyl transferase activity (Zheng et al., 2011).

Werr et al. (1985) first cloned and sequenced a *SUS* i.e., *Shrunken* (*Sh*) gene from maize. Since then, many *SUS* genes have been cloned and characterized from different plants such as maize, *Arabidopsis*, rice, potato (*Solanum tuberosum* L.) and tomato. Because of the advances in genome sequencing, assembly and annotations, the *SUS* gene families were studied in a comprehensive manner in plants (McCarty et al., 1986; Shaw et al.,1994; Martin et al., 1993; Wang et al., 1992; Yu et al., 1992; Salanoubat and Belliard,1987; Fu et al., 1991; Fu and Park, 1995; Goren et al., 2011; Huang et al., 2016; Dinh et al., 2018; Stein and Granot, 2019; Xu et al., 2019; Huang et al., 2021; Duan et al., 2021). Usually, this enzyme is encoded by small gene families between four to seven *SUS* genes, and divided into three different clades in both monocots and dicots. However, more number of *SUS* genes were also reported in some plant species (Avigad, 1982; Stein and Granot, 2019). The number of *SUS* genes could vary between different plants: two in *Amborella trichopoda*, five in grape and sugarcane, six in *Arabidopsis*, rice, tomato, rubber tree and peach, and seven in cotton, bamboo and tobacco; while in apple, tobacco, poplar and Chinese pear, 11, 14, 15 and 30 *SUS* genes were identified, respectively (Zhang et al., 2013; Zhu et al., 2017; Baud et al., 2004; Hirose et al., 2008; Goren et al., 2017; Wang et al., 2015; Chen et al., 2012; Huang et al., 2018; Tong et al., 2018; Wang et al., 2015; An et al., 2014; Abdullah et al., 2018).

Salanoubat and Belliard (1987) first isolated and characterized a SuSy cDNA clone from potato and showed relatively higher levels of its transcripts in developing tubers as compared to other organs. It was demonstrated that SuSy activity was regulated by wounding and anaerobiosis (Salanoubat and Belliard, 1989). Two classes of sucrose synthase genes, *Sus3* and *Sus4*, were isolated and characterized from a potato cultivar (FL1607), and found to be differentially expressed (Fu and Park, 1995). Zrenner et al. (1995) demonstrated that SuSy was responsible for the sucrose cleavage in tuber (a sink organ), rather than invertases. They established the crucial role of SuSy regarding to carbon partitioning and determining the sink strength in potato. Later, two more SuSy isoforms were also characterized from potato (Baroja-Fernandez et al., 2003; Daloso et al., 2016). Most of the potato cultivars are autotetraploid (2*n*= 4*x*=48) and highly heterozygous. High levels of DNA polymorphisms in the potato genome are well known. Cumulative mutations contribute to multiple allelism and natural allelic variations in potato (Draffehn et al., 2010). It is likely that multiple SuSy forms corresponding to each class of *SUS* gene family could exist in potato depending on the cultivar genotype. The individual *SUS* genes could show differential expression patterns in both photosynthetic and non-photosynthetic tissues in potato, and influence their growth and development. Unlike tobacco and tomato, there is no comprehensive report available in the literature with regard to molecular cloning of different *SUS* genes and their expression patterns at various stages of tuber development in potato, particularly in the Indian potato cultivars. Close inspection of the sequences, prediction of the crucial motifs and 3-D structures, are equally important in order to establish the structure-function relationships in the individual SuSy proteins.

Here, we report isolation and characterization of a cDNA encoding SuSy4 from a potato cultivar Kufri Chipsona-1 (KC-1). The Spud DB Potato Genomics Resource, NCBI GenBank and other databases were also explored to find more SuSy proteins in potato. Along with sequence comparison and phylogenetic analysis using these proteins, the crucial domains, motifs, active sites and three-dimensional (3-D) structure were also predicted in the SuSy4 form under study. *SUS*-specific expression patterns were examined in the potato organs including developing tubers based on the semi-quantitative RT-PCR, and RNA-seq data available in the potato genome database. SuSy activities were measured in the different stages of tuber development. This is a comprehensive report regarding the SuSy isoforms particularly in potato which would be useful for further in-depth molecular and biochemical studies, and *in silico* approaches.

2. Materials and methods

2.1. Plant materials, growing conditions, and reagents

An Indian potato cultivar Kufri Chipsona-1 (KC-1), procured from Central Potato Research Institute (CPRI), Shimla, India was used in this study. It is a high-yielding and commercially important processing variety suitable to different agro-climatic zones of the Indian subcontinent. It was routinely micropropagated in the laboratory under controlled conditions (25–27 °C, ~70% relative humidity under 16 h photoperiod with a light intensity of 40–42 μmol m^{-2} s^{-1} spectral flux photon of photo-synthetically active i.e., 460–700 nm radiations) on MS-basal medium with 2.5% sucrose at 4–5 wk intervals. The micropropagated potato plantlets were acclimatized and then cultivated in the field for 15–16 wks (mid of November to early of March). Different potato organs namely tuberizing stolons, developing tubers at different stages along with young leaf, stem, and flower were harvested, frozen in liquid nitrogen and stored at −80 °C for further molecular and biochemical studies. Chemicals and enzymes were procured from Sigma-Aldrich Pvt. Ltd, Genei, SRL and HiMedia Laboratories, India.

2.2. RNA extraction, RT-PCR, and SuSy cDNA cloning

Total RNA was isolated from the growing tuber, tuberizing stolon, leaf, stem, and flower from the potato cultivar KC-1 by SDS-Phenol method as reported earlier (Gilman, 1987). Quality of the total RNA preparations was checked by determining the A_{260}/A_{280} ratio spectrophotometrically followed by regular and formaldehyde agarose gel electrophoresis along with RT-PCR using different potato gene-specific primers. The following oligonucleotide primers were used based on the potato cDNA sequence encoding a SuSy4 form (M18745, Salanoubat and Belliard, 1987): the forward primer SSF1-0025, 5′–TCTCAAAGTTGAACTTTGTC–3′ (corresponding to the bases 25–44); and the two reverse primers namely SSR1-0986, 5′–ACAACCTGGCCACCGGTGTC–3′ (complementary to the bases 967–986), and SSR3-2693, 5′–ATCTCTTATTCATACCAACAG–3′ (complementary to the bases 2673–2693). For the internal control, constitutively expressed potato actin gene (XM_006348930)-specific forward (F1-AC0591, 5′–CCACATGCTATCCTTCGTCTC–3′) and reverse (R1-AC1149, 5′–TCCACATCTGTTGGAAGGTAC–3′) primers were used.

Reverse transcription (RT) was carried out using the RevertAid™ H Minus First Strand cDNA Synthesis Kit with M-MuLV reverse

transcriptase (Fermentas Life Sciences). Approx. 2.0 μg of purified total tuber RNA as template and oligo $(dT)_{18}$ primer were used in the reverse transcription reaction. In order to isolate the full-length cDNA, PCR was carried out using the RT product, the SuSy cDNA-specific primers SSF1-0025 and SSR3-2693, and 1.0 unit of high fidelity XT-5 PCR System (Genei). After initial denaturation at 94 °C for 1 min 30 s, the thermal cycling parameters during PCR were denaturation at 94 °C for 1 min, annealing at 55 °C for 2 min; polymerization at 72 °C for 3 min for 30 cycles followed by final extension at 72 °C for 5 min. The amplified RT-PCR product was treated with Klenow enzyme, purified, and cloned into the *Sma*I site of the pUC19 vector according to the protocol as described by Sambrook et. al., (1989). *E. coli*DH5α was used as a host for molecular cloning. The cDNA was sequenced in both directions by Bioserve Biotechnologies, India.

2.3. Sequence analyses and phylogenetic tree

The nucleotide and amino acid sequences corresponding to the SuSy cDNA of this study along with other SuSy isoforms in potato retrieved from the available databases (Spud DB; (http://solanaceae.plantbiology.msu.edu and *EnsemblPlants*; https://plants.ensembl.org/index.html) were analyzed by National Center for Biotechnology Information (NCBI; http://www.ncbi.nlm.nih.gov/) by the BLAST and ORF-finder tools. The molecular weight, isoelectric point (p*I*), and amino acid composition of the predicted proteins were determined by the ProtParam tools of Expert Protein Analysis System (ExPASy) of Proteins and Proteomes server of the Swiss Institute of Bioinformatics (SIB; https://www.expasy.org/). The secondary structures like α-helix, β-strand, and coil were examined by the PSIPRED secondary structure prediction method of Jones (1999) (http://bioinf.cs.ucl.ac.uk/psipred/). The relationships between the protein sequences and motifs were investigated by MyHits tool of ExPASy (https://myhits.sib.swiss/cgi-bin/motif_scan). For multiple sequence alignment, the MultAlin software (http://www.multalin.toulouse.inra.fr/multalin/; Corpet, 1988) was used. For construction of phylogenetic tree, the Clustal Omega multiple sequence alignment program, an EMBL-EBI sequence analysis tool (https://www.ebi.ac.uk/Tools/msa/clustalo/) was used followed by evolutionary analyzes by the Neighbor-Joining method with bootstrap test (1000 replicates) and Poisson correction method of MEGA X software (Kumar et al., 2018). This analysis involved a total of 28 amino acid sequences including 17from potato and six from tomato and five from *Arabidopsis* (Iida et al., 2009; Lao et al., 2014; Fuglevand et al., 1998; Wang et al., 1993).

2.4. 3-D structure prediction and validation of the model

The 3D model was constructed using a bioinformatics method i.e., I-TASSER (Iterative Threading Assembly Refinement; https://zhanglab.ccmb.med. umich.edu/I-TASSER/) (Zhang, 2008). The model was validated using the Structural Analysis and Verification Server (http://nihserver.mbi.ucla.edu/SAVES/; Cheatham et al., 1995). The predicted structures were visualized in the form of ribbons by PyMol software (https://www.pymol.org). The transmembrane helices were also predicted using Phyre2 tools of a protein fold recognition server to know the transmembrane topology of the protein (http://www.sbg.bio.ic.ac.uk/phyre2/; Kelley et al., 2015).

2.5. SuSy expression patterns in potato

The expression patterns of the *SUS* genes in potato were examined by the bioinformatics datasets and experimental approaches. The expression values in different organs were accessed in the large scale RNA-Seq and microarray studies, protein expression datasets in Expression Atlas maintained by the European Bioinformatics Institute (https://www.ebi.ac.uk/gxa/home), and the potato genomic resource Spud DB (http://solanaceae.plantbiology.msu.edu/). The average signal intensity values of a gene were obtained from a high diversity of experiments covering different organs, developmental stages, and treatments.

The expression patterns at transcription level were also studied by a semi-quantitative RT-PCR approach to identify the SuSy expression patterns in several potato organs namely tuberizing stolon, tuber, leaf, stem and flower. Reverse transcription was carried out in a reaction volume of 20 μL using 2.0 μg of total RNA from each organ, oligo $(dT)_{18}$ primer and the cDNA Synthesis Kit from Fermentas Life Sciences. 3.0 μL of each RT product was used as template in PCR of 50 μL reaction volume using the SuSy cDNA specific forward and reverse primers, SSF2-0076 and SSR1-0986, respectively and 1.0 unit of Taq DNA polymerase (Genei). During PCR, the thermal cycling parameters remained the same as mentioned earlier, except for polymerisation for 1min. For the internal control, the actin gene-specific forward (F1-AC0591) and reverse (R1-AC1149) primers were used to amplify a ~0.65 kb fragment using the same RT products as the template. All the RT-PCR products were resolved using 0.9% agarose gel electrophoresis. The relative expression levels between the potato organs were examined by the quantification tool of the gel documentation system (Bio-Rad, USA).

2.6. Assay of SuSy activity

Protein extraction and SuSy assay were carried out according to the protocols reported earlier (Jammer et al., 2015). Briefly, ~500 mg of the freshly-harvested maturing potato tubers at different stages of growth were homogenized in liquid nitrogen with 0.1% Polyvinylpolypyrrolidone (PVPP). All the extraction steps were performed on ice and/or in a cold room at 4 °C. The ground plant materials were extracted with 1.0 mL of extraction buffer (40 mM Tris-HCl pH 7.6, 3.0 mM $MgCl_2$, 1.0 mM EDTA, 0.1 mM PMSF, 1 mM benza- midine, 14 mM β-mercaptoethanol, 24 μM $NADP^+$). The homogenate was centrifuged at 4 °C and 20,000 g for 35 min until a solid pellet was obtained. The suspended particles in the supernatant i.e., crude extract were removed by filtration, and dialysed overnight against 20 mM potassium phosphate buffer (pH 7.4) at 4 °C. This step was required to remove highly abundant substrates of SuSy and a few other enzymes as well. The protein contents in the crude extracts were determined according to the Lowry method (Lowry, 1951), using BSA as a standard. All of the extracts were frozen in liquid nitrogen and stored at −20 °C in aliquots until further use. The SuSy activity was determined in two reactions: in presence of 1.0 mM UDP to determine a total of Susy and cytosolic invertase activities, and without UDP for the background cytosolic invertase activity only. The SuSy activity was calculated by subtracting background invertase activity from the total activities. For both reactions, the composition of the common assay buffer was 1.0 mM EDTA, 2.0 mM $MgCl_2$, 5.0 mM DTT, 250 mM sucrose, 1.3 mM ATP, 0.5 mM NAD^+, 0.672 U of HXK, 0.56 U of PGI, and 0.32 U of G6PDH in 50 mM HEPES/NaOH at pH 7.0. Suc was omitted in the controls. The progress of the reaction was monitored by an increase in absorbance at 340 nm due to conversion of NAD^+ to NADH. The total extractable enzyme activities were measured and expressed in nmol/min/g FW.

2.7. Statistical analysis

Each of the SuSy assays in different tuber extracts and other biochemical experiments were carried out in triplicate and the data were presented as the Mean ± SD of $n = 3$ independent experiments. Standard deviation and mean values were calculated using SPSS software of IBM.

3. Results

3.1. Cloning of cDNA and sequence analyses

A cDNA clone, designated St-CSS01, specific to the potato cv. KC-1 was obtained through PCR (Fig. 1). The nucleotide sequence was

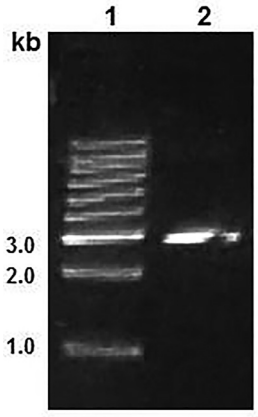

Fig. 1. RT-PCR amplification of SuSy cDNA. *Lane 1* 1 kb DNA ladder; *Lane 2* RT-PCR product (~2.7 kb) using total RNA from the growing potato tuber of the cultivar KC-1 and the SuSy cDNA-specific primers, SSF1-0025 and SSR3-2693.

analyzed by the NCBI BLAST tool and found to encode a distinct form of SuSy4. The sequence information was submitted to the GenBank database (MT731684). The 2,668-bp St-CSS01 consisted of 51-bp 5′-UTR, 2418-bp ORF (bases 52– 2469), and 199-bp 3′-UTR. The G+C contents of the 5′-UTR, coding region, and 3′-UTR were found to be 48, 43 and 34%, respectively. As revealed by NCBI BLAST search, it showed 99% sequence identity with a full-length SuSy cDNA from the potato cv. Sirtema (M18745). The coding region of St-CSS01 showed significant sequence identities with other *SUS* cDNAs (XM_006345182.2, NM_001288357.1, XM_015204139.2, NM_001247726.2, L19762.1, KF977579.1, NM_001313910.1, EU908020.1, DQ834312.1, AM087674.1) encoding different SuSy forms in the *Solanceae* and other plants.

The predicted protein, designated KC-SuSy shown in Fig. 2 (QWW18611), consisted of 805 amino acids. Based on the ProtParam tool, the calculated molecular weight (MW) of KC-SuSy was found to be 92.4 kDa with a predicted isoelectric point (p*I*) of 8.63. Out of its total 805 amino acids, 94 were strongly basic (+) (Lys, Arg), 114 were strongly acidic (−) (Asp, Glu), 298 were hydrophobic (Ala, Ile, Leu, Phe, Trp, Val), and 168 were polar (Asn, Cys, Gln, Ser, Thr, Tyr). The instability index of KC-SuSy was computed as 34.69, which classified the protein as stable. The amino acid composition data revealed that some of the amino acids such as Gln (4.2%), Ser (4.6%), Glu (9.4%) and Leu (11.1%) occurred more frequently as compared to their average occurrence; whereas, the amino acids, namely Cys (0.9%), Ser(4.6%), Asn (3.7%) occurred less frequently (Doolittle, 1989). Sequence and phylogenetic analyses clearly indicated that KC-1 specific SuSy of the study was a distinct member of SuSy4 isoform, belonging to group I with specific signature sequences of this enzyme, preserved in all the SuSy isoforms of the *Solanaceae* family (Fig. 2).

3.2. Sequence alignment, regulatory/binding motifs, distinct sequence features and phylogenetic tree

Six potato SuSy sequences representing three different groups were used for alignment to identify the sequence relatedness and divergence. The crucial domains/motifs involved in the catalysis and regulation under various biotic and abiotic stresses include ATP/GTP-binding site motif A (P-loop), bipartite nuclear localization signal, CodY helix-turn-helix domain, glycosyl transferase domain and cAMP- and cGMP-dependent protein kinase phosphorylation sites; their relative locations and functions are presented in Table 1 and Fig. 2. Phylogenetic analysis of the SuSy proteins from potato, tomato and *Arabidopsis* indicated that the *SUS* gene family was clearly divided into three major groups (Fig. 3).

3.3. Potato SUS gene family

By screening the potato whole genome and transcriptome databases, Spud DB, and *EnsemblPlants* (https://plants.ensembl.org/index.html), six *SUS* genes encoding sucrose synthase designated *SuS*, *SUS4* and *SuSy2* were retrieved, and categorised into three *SUS* groups (I–III) on the basis of phylogenetic analysis as reported earlier (Table 2, Fig. 3). Some of the *SUS* genes except PGSC0003DMG400031046 and PGSC0003DMG 400013547 (which encode only a single transcript) were found to encode multiple transcripts: e.g., PGSC0003DMG400002895, PGSC0003DMG400031046, PGSC0003DMG400016730 encode two transcripts each, PGSC0003DMG400013546 encodes four while PGSC0003DMG4000006672 encodes five transcripts. The number of exons varied from 1 to 15, and the ORF size in these transcripts ranged from 372 to 3537 base pairs. The predicted proteins encoded by the transcripts consisted of 55–840 amino acids (6.13–95.57 kDa). The smaller transcripts are variants of the SuSy proteins, which might be involved in other physiological processes that still remain an enigma. The instability index of the functional SuSy proteins ranged from 30.22 to 41.87, which classified them as relatively stable proteins. The aliphatic index of the SuSy proteins ranged from 77.76 to 102.91 and indicated that they are thermostable. The GRAVY values of these proteins ranged from −0.428 to 0.324 indicating their segment-wise hydrophilic and hydrophobic characteristics. The p*I* values ranged from 4.78 to 6.95 and indicated their slightly acidic nature. The *SUS* genes were localised on five chromosomes: briefly, PGSC0003DMG400002895 at 30.85 Mb on Ch12, PGSC0003DMG400031046 on Ch3 at 44.88 Mb, PGSC0003DMG4000006672 on Ch9 at 61.46 Mb, PGSC0003DMG400016730 on Ch2 at 36.93 Mb and PGSC0003DMG400013546 at 40.64 Mb, PGSC0003DMG400013547 at 40.61 on Ch7 (Fig. 4). The biological characteristics of the published SuSy isoforms available in the NCBI database were also studied (Table 3). Although the number of amino acids were the same in some isoforms, they could differ in other biochemical parameters such as theoretical p*I* and molecular weight. Like tomato and *Arabidopsis* and other plants, the *SuS* genes could be divided into three groups in potato (Duan et. al., 2021).

3.4. Modeling, active site prediction and validation

It is essential to know the structural aspects of a protein to annotate its biological function. A model of KC-SuSy was generated by I-TASSER (through the combination of threading and *ab initio* prediction). I-TASSER, a meta server implements different threading programmes and its quality is assessed on the basis of Z-score (the energy score in standard deviation units relative to statistical mean of alignments) and for the confident alignment Z-score should be greater than 1. The model with minimized energy shows the specific glycosyl transfer signature domain. The active site, the crucial features and domains as reported earlier were studied; the 3-D structure was visualized in the form of ribbons by PyMol (https://www.pymol.org) as shown in Fig. 5 (Zheng et al., 2011; Huang et al., 2016). Moreover, the Normalized B-factor which represents the secondary structure as predicted by I-TASSER is shown in Fig. 6. The modeled structure was validated using the Structural Analysis and Verification Server (http://nihserver.mbi.ucla.edu/SAVES) (Fig. 7). The transmembrane helices were predicted using Phyre2, a protein fold recognition tool (sbg.bio.ic.ac.uk) shown in Fig. 8.

3.5. Expression patterns in potato organs, sugar content and SuSy activities during tuber development

The heatmap generated by the Expression Atlas (Fig. 9), clearly reflected that *SUSI* genes are highly expressed in the sink tissues, while the other two i.e., *SUSII* and *SUSIII* are constitutively expressed in various organs**.** In this study, the *SUS* gene expression pattern was

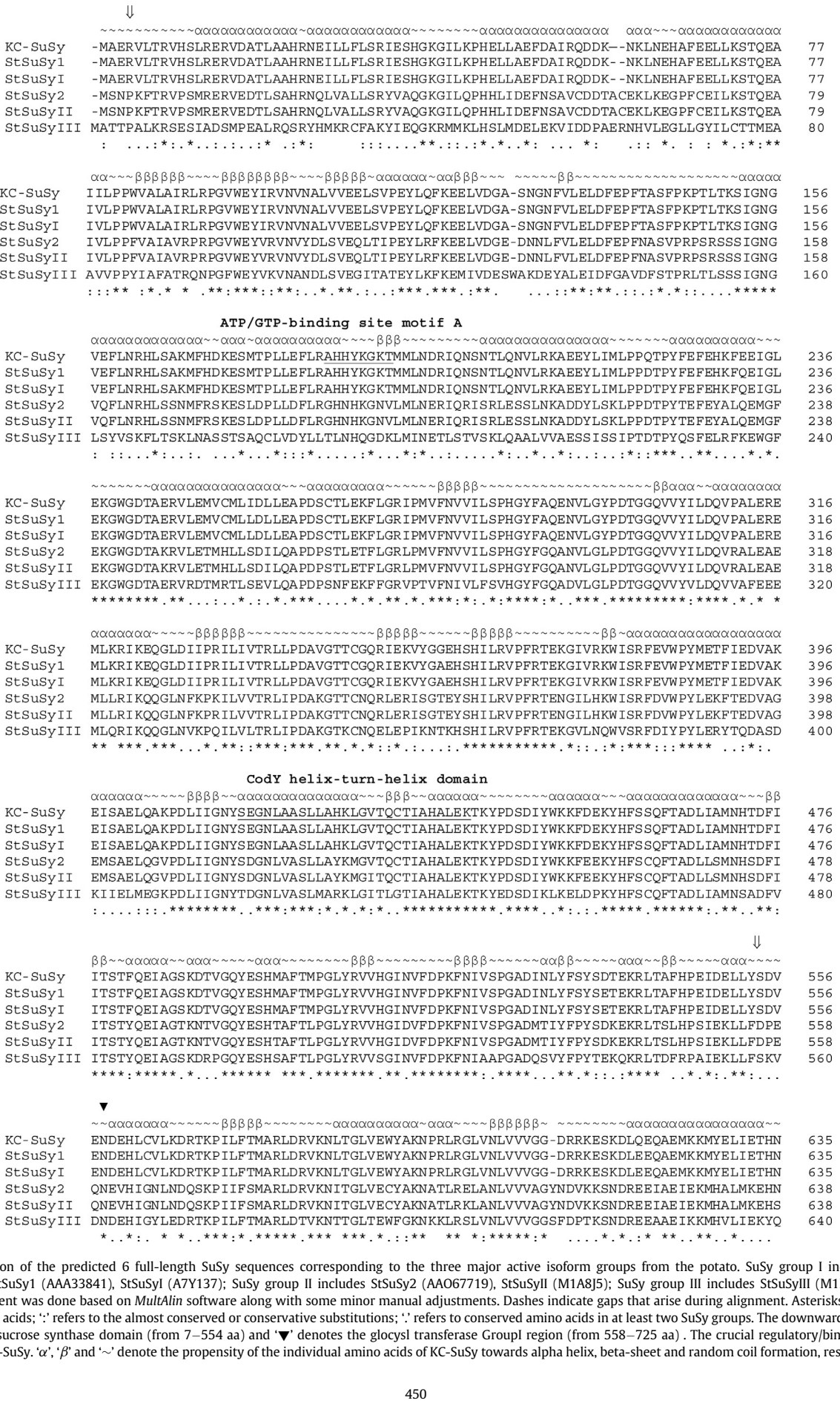

Fig. 2. Comparison of the predicted 6 full-length SuSy sequences corresponding to the three major active isoform groups from the potato. SuSy group I includes KC-SuSy (QWW18611), StSuSy1 (AAA33841), StSuSyI (A7Y137); SuSy group II includes StSuSy2 (AAO67719), StSuSyII (M1A8J5); SuSy group III includes StSuSyIII (M1BE45). Multiple sequence alignment was done based on *MultAlin* software along with some minor manual adjustments. Dashes indicate gaps that arise during alignment. Asterisks '*' indicate the conserved amino acids; ':' refers to the almost conserved or conservative substitutions; '.' refers to conserved amino acids in at least two SuSy groups. The downward arrow '⇓' indicates the entire sucrose synthase domain (from 7–554 aa) and '▼' denotes the glocysl transferase GroupI region (from 558–725 aa) . The crucial regulatory/binding motifs are underlined in KC-SuSy. '*α*', '*β*' and '~' denote the propensity of the individual amino acids of KC-SuSy towards alpha helix, beta-sheet and random coil formation, respectively.

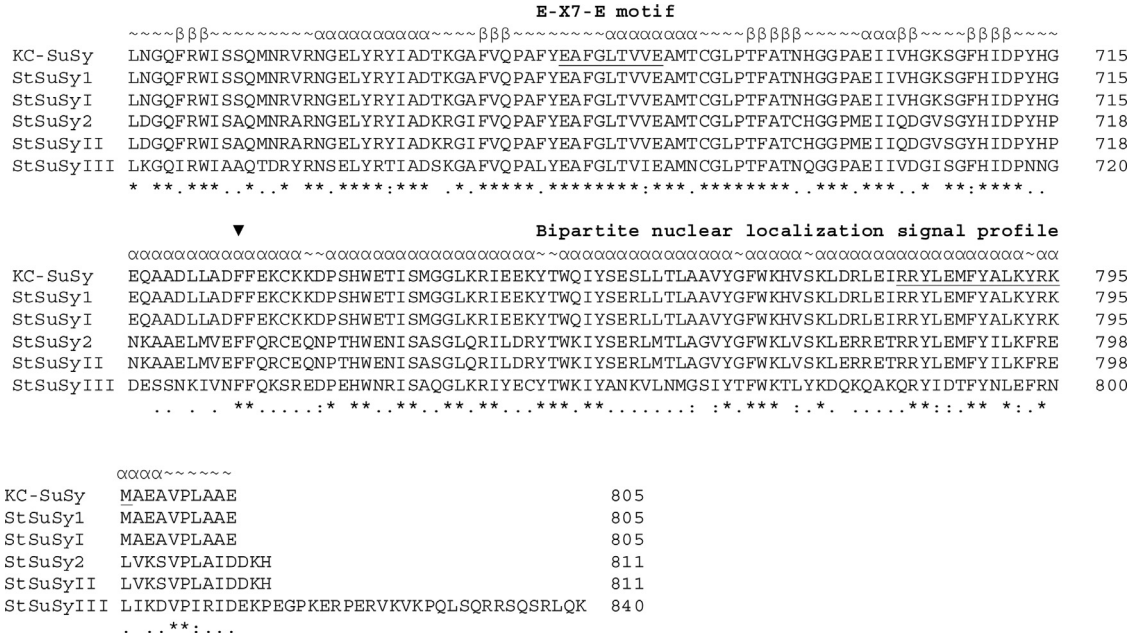

Fig. 2. Continued.

Table 1
Catalytic domains / motifs and their predicted functions in potato SuSy.

Catalytic domain	Position	Function
ATP/GTP-binding site motif A (P-loop)	184–191	consist of glycine rich sequence followed by a conserved lysine and a serine or threonine to help the binding of ATP and GTP for enzyme activity
Glycosyl transferase Group I	558–725	catalyzes the transfer of glycosyl groups to a nucleophilic acceptor with either retention or inversion of configuration at the anomeric centre
Bipartite nuclear localization signal profile	782–796	aids transfer of protein from nucleus to cytoplasm and other cell organelles, for the appropriate protein functioning
CodY helix-turn-helix domain	414–440	A DNA-binding motif (recognition helix) binds to the major groove of DNA
cAMP- and cGMP-dependent protein kinase phosphorylation site	539–542, 612–615	phosphorylates proteins with exposed motif of arginine-arginine-X-serine to gain biological activity

examined in some potato organs namely tuberizing stolon, growing tuber, leaf, stem, and flower. By semi-quantitative RT-PCR, ~0.98 kb DNA was amplified using total RNA from tuberizing stolon and tuber (Fig. 10). The size matched with the KC-SuSy specific transcripts towards the 5′-end. The transcript levels appeared to be comparable for tuberizing stolon and tuber; in contrast, the transcripts were not detected in the cases of leaf, stem and flower. The levels of actin transcripts were found to be nearly uniform in all the potato organs.

SuSy plays a key role in maintaining carbon flux towards starch formation in the sink tissues. In view of this, the SuSy activities were measured in the successive stages of tuberization i.e., from hooked stolon tip (S1) to mature tuber (S8) shown in Fig. 11 (Table 4). The data in Table 4 clearly showed that there was a significant increase of SuSy activity during the early stages of tuber development (S1–S5); reached a maximum level at the mid-maturation stage (S6), and gradually declined until maturation (S7–S8) probably due to inhibition by its own substrates such as Fru.

4. Discussion

Tuberization in the potato is a complex developmental process associated with distinct changes at various morphological, cellular, molecular and biochemical levels. Synthesis of storage starch and accumulation of proteins occur significantly during tuber formation. Suc is the major source of carbon for starch synthesis in the tuber. A switch from apoplastic to symplastic sucrose unloading during tuber induction is coincident with a biochemical change from an invertase-mediated Suc cleavage to a SuSy-mediated Suc cleavage pathway in the subapical region of the stolon tip. SuSy undergoes feedback inhibition by free Fru. With regard to carbon allocation in the potato tuber, SuSy is crucial as it acts as a key player in maintaining the carbon flux toward starch formation (Viola et al., 2001; Sarkar, 2008). Apart from the storage tissues, the *SUS* genes are also expressed in different plant organs such as leaves, vascular tissues, stems, flowers, fruits, cotyledons and developing seeds (Stein and Granot, 2019). Plant SuSys were extensively studied at biochemical and molecular levels. A number of cDNA/genomic clones encoding different SuSy isoforms, their expression patterns along with structure-function and phylogenetic relationships, and catalytic activities were reported in different plant species including *Arabidopsis*, rice and some commercially important *Solanaceae* family members namely tomato and tobacco (Stein and Granot, 2019). Potato is the world's most important and promising non-grain food crop in terms of production and global food security (Genova et al., 2011). Unlike tomato and tobacco, the SuSy isoforms are yet to be comprehensively studied in potato in terms of their expression patterns and structure-function relationships. This present study is relevant and useful due to the potato's importance in global food supply.

In the present study, the KC-1 specific cDNA clone, St-CSS01 which encodes a distinct SuSy4 form and is predominantly expressed

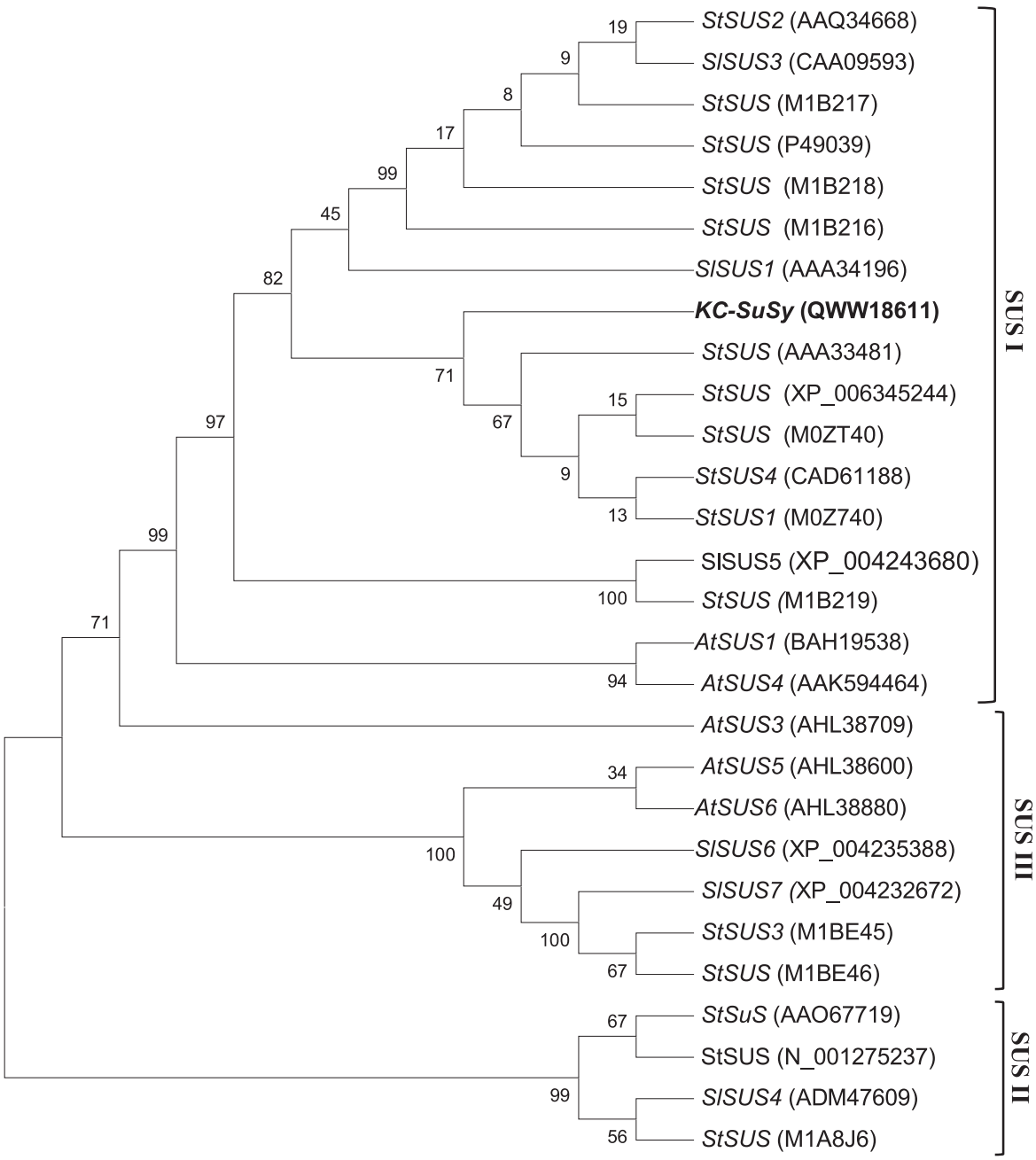

Fig. 3. The phylogenetic tree was generated by the MEGA X software using the Neighbor-Joining method with the bootstrap test (1000 replicates) shown next to the branches and computing the evolutionary distances computed by the Poisson correction method . The analyzes involved 28 SuSy protein sequences; 17 from the potato (*StSUS*), 6 from tomato (*SlSUS*) and 5 from *A. thaliana (AtSUS)* as available in the published reports and/or databases (the plant species and the GenBank/ Uniprot accession numbers are indicated at each branch). The 805-aa KC-1 specific SuSy (QWW18611) corresponding to the culivar KC-1 of this study occupied distinct positions in the phylogenetic tree (shown in bold cases). The three *SUS* groups are also indicated.

in developing tubers suggesting its role in Suc metabolism was cloned and characterized. It belongs to *SUS I* group gene family having conserved function in cellular sucrose metabolism and allocation (Xu et al., 2019). Various protein parameters such as approx. molecular weight, theoretical p*I*, amino acid composition and their average occurrence and stability were predicted. Apart from the cDNA cloning studies, five more potato SuSy sequences were retrieved from the databases and thoroughly analyzed. The available potato SuSy proteins could now be categorized into three potentially active isoforms consistent with the earlier reports. Multiple sequence alignments helped to identify the sequence relatedness and divergence within and between the members of the major SuSy isoforms in potato.

Typically, a SuSy protein is known to contain two major regulatory domains namely a ~250-aa N-terminal domain responsible for cellular targeting that includes the cellular targeting domain (CTD) and an early nodulin 40 (ENOD40) peptide-binding domain (EPBD), and almost double the C-terminal GT-B domain of 500 amino acids playing a role in the glycosyl transferase activity. The active sites in the GT-B domains are found to be conserved, both within and among the three SuSy subgroups, hence they are subject to more evolutionary constraints than the “regulatory” domains which are responsible for the cellular localization of the *SUS* genes (Zheng et al., 2011; Xu et al., 2019). Two important serine phosphorlyation sites occurring at the segment 11–15 and at position 170 are found to be responsible for membrane association, and regulation of protein

Table 2
Features of *SUS* genes in potato extracted from genomic databases (Spud DB and Ensembl Plants).

Gene Group	PGSC Gene ID	Ch local	PGSC Transcript ID	Uniprot ID	Base pairs	Exons	Amino acids	Mol. Wt.	pI	Instability Index	Aliphatic Index	Gravy
SUSI	PGSC0003DMG400002895	12	PGSC0003DMT400007505	A7Y137	2821	13	805	92.47	5.87	33.36	92.42	-0.246
			PGSC0003DMT400007506	M0ZT40	2746	13	805	92.47	5.87	33.96	92.42	-0.246
SUSIII	PGSC0003DMG400031046	3	PGSC0003DMT400079728	M1D2C2	1017	1	176	19.91	5.79	39.78	77.76	-0.428
SUSII	PGSC0003DMG4000006672	9	PGSC0003DMT400017087	M1A8J5	2915	15	811	92.79	6.01	40.32	89.42	-0.288
			PGSC0003DMT400017088	M1A8J6	3537	11	436	49.87	6.44	41.87	97.18	-0.191
			PGSC0003DMT400017093	M1A8J8	1290	1	55	6.13	4.78	31.84	102.91	0.324
			PGSC0003DMT400017094	M1A8J9	952	1	93	10.83	6.39	40.15	86.99	-0.146
			PGSC0003DMT400017092	M1A8J7	372	1	80	8.63	6.01	38.40	93.75	0.154
SUSIII	PGSC0003DMG400016730	2	PGSC0003DMT400043117	M1BE45	2697	14	840	95.57	6.95	35.21	84.27	-0.392
			PGSC0003DMT400043118	M1BE46	1785	10	566	63.85	5.48	30.22	87.60	-0.256
SUSI	PGSC0003DMG400013546	7	PGSC0003DMT400035262	M1B217	2922	12	808	92.95	6.07	34.97	93.38	-0.225
			PGSC0003DMT400035261	M1B216	2828	14	805	92.60	6.03	34.61	93.85	-0.240
			PGSC0003DMT400035260	P49039	2809	14	805	92.57	5.98	34.28	93.85	-0.240
			PGSC0003DMT400035263	M1B218	2534	10	641	73.88	6.17	35.21	90.03	-0.237
SUSI	PGSC0003DMG400013547	7	PGSC0003DMT400035264	M1B219	2698	11	803	91.43	5.83	37.35	88.51	-0.287

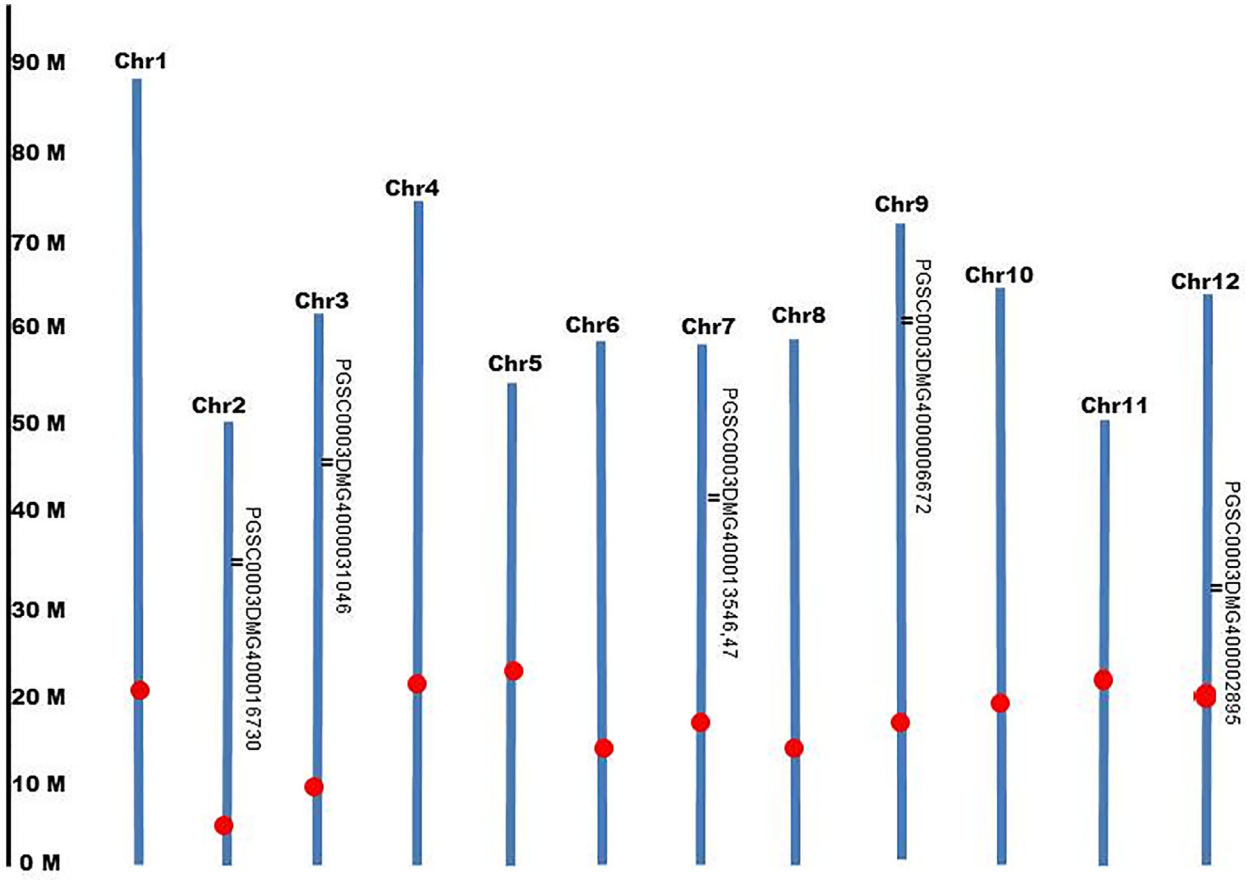

Fig. 4. A schematic presentation of chromosomal localization of the potato *SUS* genes retrieved from Potato Genome Sequencing Consortium (PGSC) and *Ensembl Plants* database. The chromosomes are shown in blue, while the centromeres are shown in red. (For interpretation of the references to color in this figure legend, the reader is referred to the web version of this article.).

Table 3
Biological information of the potato SuSys extracted from the NCBI database.

Gene Name	Accession No. (Nucleotide)	Accession No. (Protein)	ORF (bp)	Coding Region	Protein (aa)	Mol. Wt. (kDa)	pI
Sucrose synthase (SS16)	XM_006345182	XP_006345244	2813	156.. 2573	805	92.47	5.87
Sucrose synthase	M18745	AAA33841	2711	76.. 2493	805	92.41	5.83
Sucrose synthase 2	AY205084	AAO34668	2701	122.. 2539	805	92.61	5.98
Sucrose synthase 4	AJ537575	CAD61188	2429	6.. 2423	805	92.44	5.91
Sucrose synthase 2	AY205302	AAO67719	2679	22.. 2457	811	92.77	5.99
Sucrose synthase 3	NM_001288308	NP_001275237	2679	22.. 2457	811	92.77	5.99

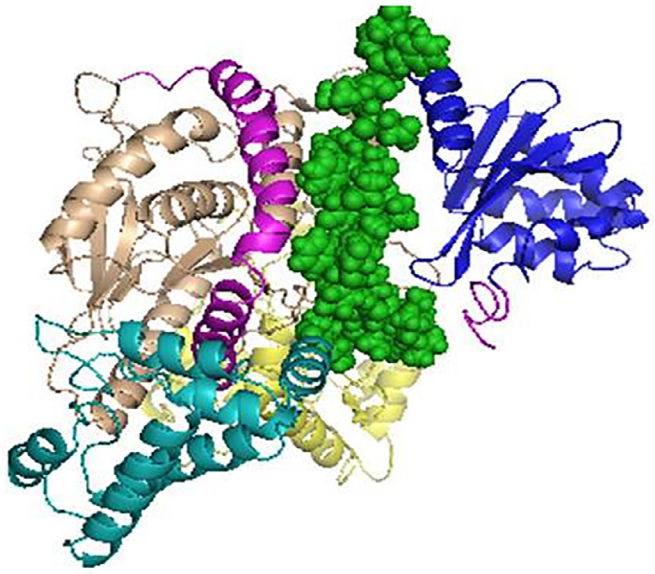

Fig. 5. Illustrated representation and catalytic domains of the predicted three-dimensional structure model of the KC-1 specific SuSy. The CTD domain is depicted in blue, EPBD domain in cyan, the GTB-N domain in wheat, GTB-C domain in yellow and the extra N and C terminal regions in magenta color in the form of cartoon. The other important linker region between CTD and EPBD domain is shown as sphere in green color. The images were generated using the PyMol program (Schrödinger, Inc., New York, NY, USA). (For interpretation of the references to color in this figure legend, the reader is referred to the web version of this article.).

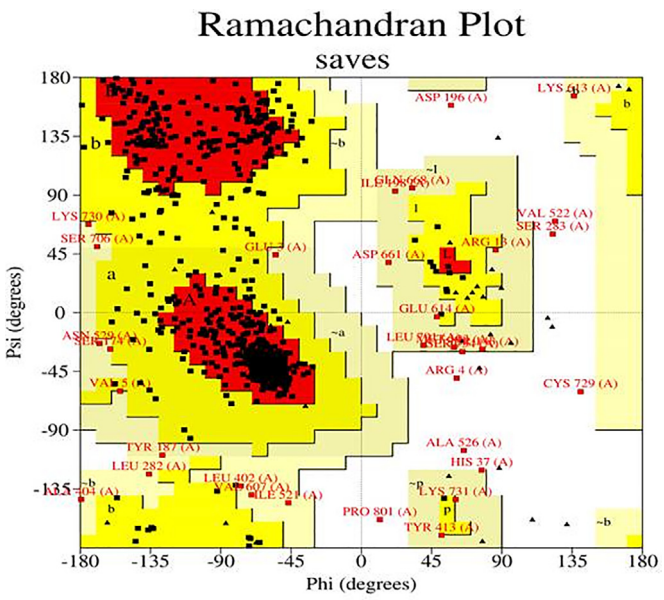

Fig. 7. Ramachandran plot of the KC- SuSy model. The most favored regions are colored red, additional allowed, generously allowed and disallowed regions are indicated as yellow, light yellow and white fields, respectively (For interpretation of the references to color in this figure legend, the reader is referred to the web version of this article.).

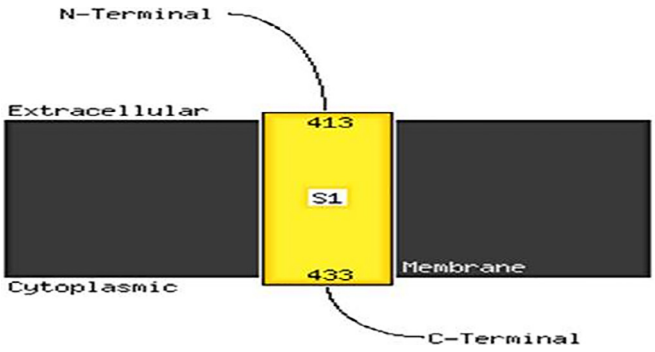

Fig. 8. Illustrated representation of transmembrane helix prediction of KC- SuSy by Phyre2. The extracellular and cytoplasmic sides of the membrane are labeled and the beginning and of each transmembrane helix illustrated with a number indicating the residue index.

degradation (Hardin et al., 2003). Another most important conserved motif is E-X_7-E found in the region from F671 to E700 of GT4 proteins. The first E residue in the E-X_7-E motif is invariant, while the second one could be substituted by Gln or Tyr. These two Glu (E) residues are known to play crucial role in the enzyme catalysis as studied by mutational and structural analysis (Huang et al., 2016). Several other domains like ATP/GTP-binding site motif A (P-loop) contains a glycine rich sequence followed by lysine residues that help in ATP binding. Bipartite nuclear localization signal profile helps in targeting the protein localization, and CodY helix-turn-helix domain aids in protein functioning.

Recently, because of whole genome sequencing, a number of genes encoding SuSy isoforms have been identified from different plant species using the comparative genomics approach (Stein and Granot, 2019; Xu et al., 2019). Close inspection of the databases revealed the presence of six *SUS* genes in the potato genome belonging to three groups viz. *SUS I*, SUS *II, SUS III* shown in Fig. 3). The SuSy proteins significantly vary in terms of size, suggesting their roles in diverse biological processes such as sugar sensing and stress response (Stein and Granot, 2019). The presence of multiple transcripts may be due to existence of the allelic variants of the gene-a common feature

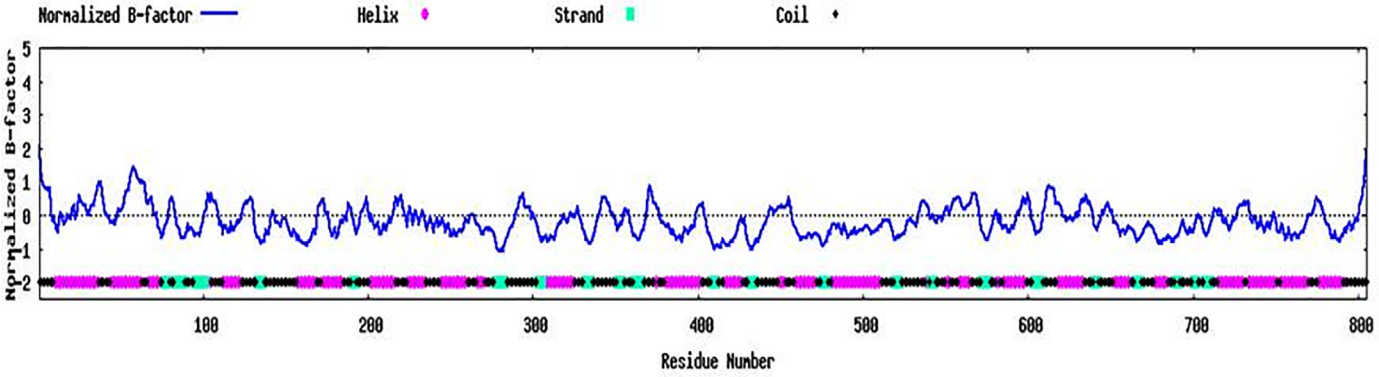

Fig. 6. Normalized Bfactor and 2D structure prediction of the KC- SuSy (blue: alpha helix, red: extended strand, green: beta turn, yellow: random coil) by I-TASSER. (For interpretation of the references to color in this figure legend, the reader is referred to the web version of this article.).

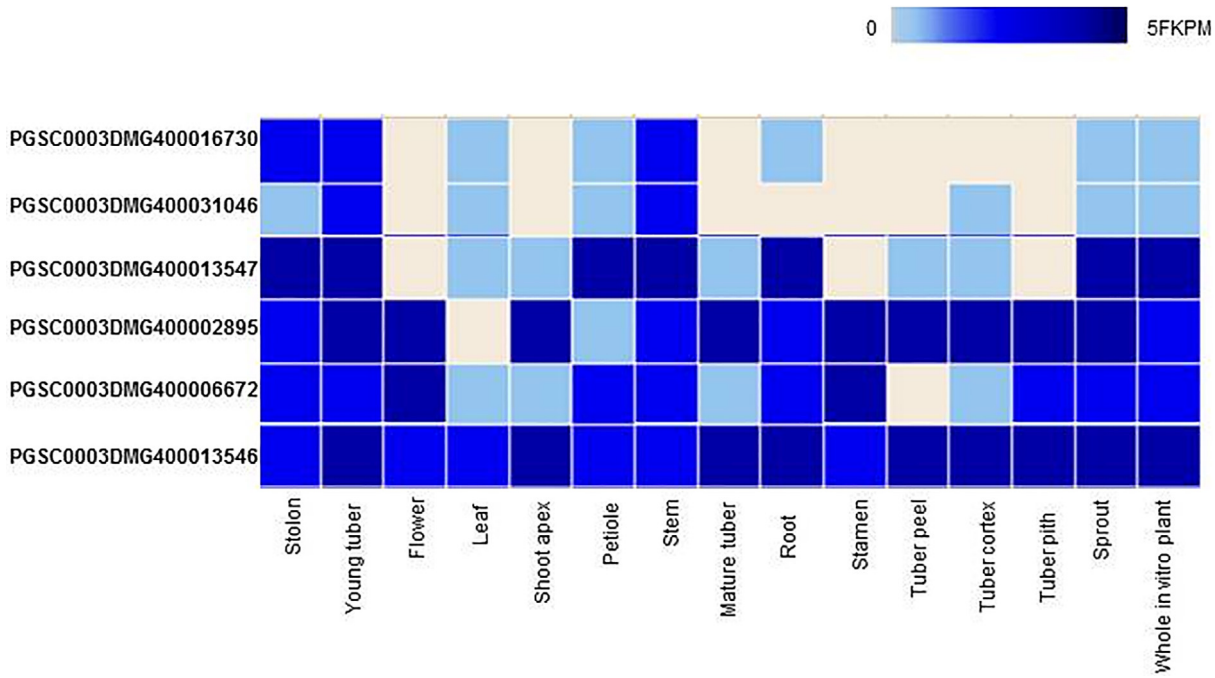

Fig. 9. Tissue expression pattern of *SUS* genes in potato. The expression values were retrieved from large scale RNA–seq with Expression Atlas. FPKM: Fragments per kilobase of exon model per million reads mapped

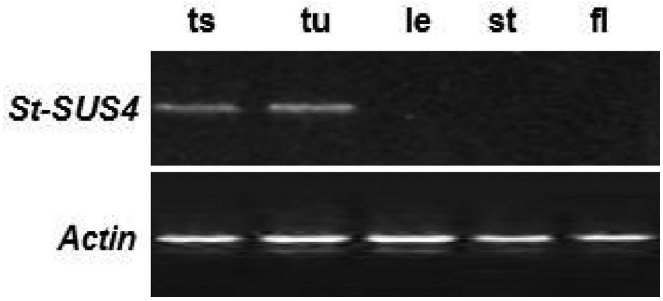

Fig. 10. Semi-quantitative RT-PCR for *SuSy 4* (KC-Specific) gene expression analysis using total RNA from different potato organs (cultivar KC-1) and the primers SSF1-0025 and SSR1-0986. ts tuberizing stolon, tu tuber, le leaf, st stem, fl flower. The size of the *SuSy 4* -specific amplified product was ~0.98 kb in ts, and tu,. Actin-specific primers were used as an internal control (the size of the amplified product ~0.65 kb in each organ).

Fig. 11. Morphology of various stages of tuberization in potato under field condition (cultivar KC-1). 8 stages of tuberization are shown: S1 hooked apical stolon tip, S8 mature tuber, S2–S7 stages are indicated in Table 4.

of the polyploid potato plants. The number of exons was also found to vary between the *SUS* group members. In the case of transcripts encoded by the PGSC0003DMG400002895, the exon number was the same but there was a difference in the number of base pairs (Table 2). Some differences in the exon-intron structure were reported in some plants. As reported in the NCBI database, some SuSy isoforms consisted of the same number of amino acids but showed variations in other parameters (Table 3). These isoforms could be allelic variants of the individual *SUS* genes. As mentioned earlier, the size of the *SUS* gene family significantly varies between the plant species ranging from two to thirty, suggesting gene duplication events might have led to the expansion of this gene family (Abdullah et al., 2018; Stein and Granot, 2019; Xu et al., 2019).

According to the expression profile data of Expression Atlas, SuSy 4 isoform is expressed tenfold more in tubers in comparison to other photosynthetically active tissues. This was consistent with the RT-PCR approach of the study as it could detect KC-SuSy specific transcripts only in tuberizing stolons and tubers. KC-SuSy, a SuSy4 form seems to play a key role in maintaining carbon flux towards tuber

Table 4
Morphological features and SuSy activity profiles during different stages of tuberization in potato (cultivar KC-1) under field condition (the experimental data are presented as mean ± SD of $n = 3$ extracts.).

Stages of tuberization	Morphological features		SuSy activity (nmol/min/g FW)
	Diameter (cm)	Fresh weight (g)	
S1 (hooked apical stolon tip)	0.06 ± 0.01	0.01 ± 0.00	21.45 ± 1.27
S2 (initiation of tuber formation)	0.31 ± 0.02	0.07 ± 0.01	72.13 ± 7.45
S3 (initial tuber)	0.89 ± 0.07	0.52 ± 0.03	168.39 ± 11.58
S4 (developing tuber)	1.68 ± 0.25	2.57 ± 0.33	269.91 ± 9.29
S5 (developing tuber)	2.31 ± 0.11	6.99 ± 0.79	561.55 ± 11.23
S6 (developing tuber)	3.23 ± 0.49	18.33 ± 1.42	769.44 ± 19.61
S7 (developing tuber)	5.11 ± 0.16	38.11 ± 2.57	623.79 ± 11.57
S8 (mature tuber)	7.43 ± 0.57	55.79 ± 4.35	511.87 ± 13.51

formation as it gets a signal through apolplastic unloading for the tuber formation and sink strength (Zrenner et al.,1995; Viola et al., 2001; Baroja-Fernández et al., 2009). The phylogenetic analysis revealed that *SUS I* group gene family evolved independently from the monocot and dicot subfamilies (Xu et al., 2019).

During tuber development, since the initiation of tuber formation after the swelling of the stolon tip, the activity of SuSy was found to increase exponentially, making it an indicator of sink strength. After reaching towards maturity, the activity declined, which could be due to the feedback inhibition by fructose (Schaffer and Petreikov, 1997; German et al., 2003). D'aoust et al. (1999) demonstrated that the overexpression of *SUS* gene could trigger the growth of the tomato plants due to an increase of sink strength. Similarly, in other plants like *Arabidopsis*, cotton fiber and seed, rice, pea, tobacco, wheat and tomato high activity of SuSy was reported in reproductive tissues indicating the role of SuSy in Suc cleavage and determining the sink strength (Ruan and Chourey, 1998; Ruan et al., 2007). Depending upon the cellular localization in plants, SuSy plays various roles. However, the mechanism by which SuSy proteins bind to cellular targets and the structural aspects that control their catalytic functions still remain to be elucidated at a molecular level (Stein and Granot, 2019).

5. Conclusion

In plants, SuSy activity is known to play key roles in sugar metabolism, particularly in the sink tissues. Potato is a major food crop known for the high sink capacity of its tubers. Many laboratories now adopt various marker-assisted breeding and genetic modification techniques for improving the desirable traits in potato such as high yield, processing qualities, tolerance to varying agro-climatic conditions, value-added nutrients, disease resistance, and prolonged postharvest storage. Such efforts require the identification and thorough characterization of the genes and their allelic variants involved in the desired traits. Therefore, in-depth understanding of the SuSy proteins could help in developing designer crops through genetic manipulations.

Ethical approval

This article does not contain any studies with human participants or animals performed by any of the authors.

Declaration of Competing Interest

All the authors do not have any possible conflicts of interest. Neither the entire paper nor any part of its content has been published or has been accepted elsewhere. It is not being submitted to any other journal. All the authors agree with the contents of this manuscript and hope the manuscript could be considered for publication in South African Journal of Botany, Elsevier.

Acknowledgments

Not applicable.

References

Abdullah, M., Cao, Y., Cheng, X., Meng, D., Chen, Y., Shakoor, A., Gao, J., Cai, Y., 2018. The sucrose synthase gene family in Chinese pear (Pyrus bretschneideri Rehd.): structure, expression, and evolution. Molecules 23, 1–16.

An, X., Chen, Z., Wang, J., Ye, M., Ji, L., Wang, J., Liao, W., Ma, H., 2014. Identification and characterization of the *Populus* sucrose synthase gene family. Gene 539, 58–67.

Avigad, G., Loewus, F.A., Tanner, W., 1982. Sucrose and other disaccharides. Encyclopedia of Plant Physiol, 13A. Springer-Verlag, Heidelberg, pp. 217–347.

Baroja-Fernandez, E., Munoz, F.J., Montero, M., Etxeberria, E., Sesma, M.T., Ovecka, M., Bahaji, A., Ezquer, I., Li, J., Prat, S., Pozueta-Romero, J., 2009. Enhancing sucrose synthase activity in transgenic potato (*Solanum tuberosum* L.) tubers results in increased levels of starch, ADPglucose and UDPglucose and total yield. Plant Cell Physiol. 50, 1651–1662.

Baroja-Fernandez, E., Munoz, F.J., Saikusa, T., Rodriguez-Lopez, M., Akazawa, T., Pozueta-Romero, J., 2003. Sucrose synthase catalyzes the de novo production of ADPglucose linked to starch biosynthesis in heterotrophic tissues of plants. Plant Cell Physiol. 44 (5), 500–509.

Baud, S., Vaultier, M.N., Rochat, C., 2004. Structure and expression profile of the sucrose synthase multigene family in *Arabidopsis*. J. Exp. Bot. 55, 397–409.

Buckeridge, M.S., Vergara, C.E., Carpita, N.C., 1999. The mechanism of synthesis of a mixed-linkage (1− >3), (1− >4)beta-D-glucan in maize. Evidence for multiple sites of glucosyl transfer in the synthase complex. Plant Physiol. 120, 1105–1116.

Cheatham, T.I., Miller, J.L., Fox, T., Darden, T.A., Kollman, T.A., 1995. Molecular dynamics simulations on solvated biomolecular systems: the particle mesh Ewald method leads to stable trajectories of DNA, RNA, and protein. J. Am. Chem. Soc. 117, 4193–4194.

Chen, A., He, S., Li, F., Li, Z., Ding, M., Liu, Q., Rong, J., 2012. Analyses of the sucrose synthase gene family in cotton: structure, phylogeny and expression patterns. BMC Plant Biol. 12, 85.

Coleman, H.D., Ellis, D.D., Gilbert, M., Mansfield, S.D., 2006. Up-regulation of sucrose synthase and UDP-glucose pyrophosphorylase impacts plant growth and metabolism. Plant Biotechnol. J. 4, 87–101.

Corpet, F., 1988. Multiple sequence alignment with hierarchical clustering. Nucleic Acids Res. 16, 10881–10890.

D'Aoust, M.A., Yelle, S., Nguyen-Quoc, B., 1999. Antisense inhibition of tomato fruit sucrose synthase decreases fruit setting and the sucrose unloading capacity of young fruit. Plant Cell 11, 2407–2418.

Daloso, D.M., Williams, T.C., Antunes, W.C., Pinheiro, D.P, Muller, C., Loureiro, M.E, Fernie, A.R., 2016. Guard cell-specific upregulation of sucrose synthase 3 reveals that the role of sucrose in stomatal function is primarily energetic. New Phytol. 209 (4), 1470–1483.

Dinh, Q.D., Finkers, R., Westphal, A.H., van Dongen, W.M.A.M., Visser, R.G.F., Trindade, L.M., 2018. Exploring natural genetic variation in tomato sucrose synthases on the basis of increased kinetic properties. PLoS One 13 (10), e0206636. https://doi.org/10.1371/journal.pone.0206636 PMID: 30372500; PMCID: PMC6205638.

Doolittle, R.F., Fasman, G.D., 1989. Redundancies in protein sequences. Prediction of Protein Structure and the Principles of Protein Conformation. Plenum Press, New York, pp. 599–623.

Draffehn, A.M., Meller, S., Li, L., Gebhardt, C., 2010. Natural diversity of potato (*Solanum tuberosum*) invertases. BMC. Plant Biol. 10, 271.

Duan, Y., Yang, L., Zhu, H., Zhou, J., Sun, H., Gong, H., 2021. Structure and expression analysis of sucrose phosphate synthase, sucrose synthase and invertase gene families in *Solanum lycopersicum*. Int. J. Mol. Sci. 22 (9), 4698. https://doi.org/10.3390/ijms22094698 PMID: 33946733; PMCID: PMC8124378.

Duncan, K.A., Hardin, S.C., Huber, S.C., 2006. The three maize sucrose synthase Isoforms differ in distribution, localization, and phosphorylation. Plant Cell Physiol. 47, 959–971.

Etxeberria, E., Gonzalez, P., 2003. Evidence for a tonoplast-associated form of sucrose synthase and its potential involvement in sucrose mobilization from the vacuole. J. Exp. Bot. 54, 1407–1414.

Fu, H., Du, J., Park, W., 1991. Cloning and sequencing of two differentially expressed sucrose synthase genes from potato. In: Proceedings of the 3rd International Congress of Plant Molecular Biology, Tucson, AZ.

Fu, H., Park, W.D., 1995. Sink- and vascular-associated sucrose synthase functions are encoded by different gene classes in potato. Plant Cell 7, 1369–1385. https://doi.org/10.1105/tpc.7.9.1369.

Fuglevand, G., Phillips, W., Mozzanega, P., Corley, S., Chengappa, S., Shields, R., 1998. Mapping of tomato genes associated with sugar metabolism. Tomato Genet. Co-op Rep. 48, 22–23.

Genova, A.D., Goverse, A., Massa, A.N., 2011. Genome sequence and analysis of the tuber crop potato. Nature 475, 189–195.

German, M.A., Dai, N., Matsevitz, T., Hanael, R., Petreikov, M., Bernstein, N., Ioffe, M., Shahak, Y., Schaffer, A.A., Granot, D., 2003. Suppression of fructokinase encoded by *LeFRK2* in tomato stem inhibits growth and causes wilting of young leaves. Plant J. 34, 837–846.

Gilman, M., 1987. Phenol/SDS method for plant RNA preparation. In: Ausubel, F.M. et al., (eds) Current Protocols in Molecular Biology. John Wiley and Sons, New York, pp. 431–434.

Goren, S., Huber, S.C., Granot, D., 2011. Comparison of a novel tomato sucrose synthase, SlSUS4, with previously described SlSUS isoforms reveals distinct sequence features and differential expression patterns in association with stem maturation. Planta 233, 1011–1023.

Goren, S., Lugassi, N., Stein, O., Yeselson, Y., Schaffer, A.A., David-Schwartz, R., Granot, D., 2017. Suppression of sucrose synthase affects auxin signaling and leaf morphology in tomato. PLoS One 12, e0182334.

Guerin, J., Carbonero, P., 1997. The spatial distribution of sucrose synthase isozymes in barley. Plant Physiol. 114, 55–62.

Hardin, S.C., Tang, G.Q., Scholz, A., Holtgraewe, D., Winter, H., Huber, S.C., 2003. Phosphorylation of sucrose synthase at serine 170: occurrence and possible role as a signal for proteolysis. Plant J. 35, 588–603.

Hirose, T., Scofield, G.N., Terao, T., 2008. An expression analysis profile for the entire sucrose synthase gene family in rice. Plant Sci. 174, 534–543.

Huang, Y.C., Hsiang, E.C., Yang, C.C., Wang, A.Y., 2016. New insight into the catalytic properties of rice sucrose synthase. Plant Mol. Biol. 90, 127–135. https://doi.org/10.1007/s11103-015-0401-3.

Huang, Y., Liao, Q., Hu, S.L., Cao, Y., Xu, G., Long, Z.J., Lu, X., 2018. Molecular cloning and expression analysis of seven sucrose synthase genes in bamboo (*Bambusa emeiensis*): investigation of possible roles in the regulation of cellulose biosynthesis and response to hormones. Biotechnol. Equip. 32, 316–323.
Huang, T., Luo, X., Fan, Z., Yang, Y., Wan, W., 2021. Genome-wide identification and analysis of the sucrose synthase gene family in Cassava (Manihot esculenta Crantz). Gene (769), 145191.
Huber, SC, Huber, JL, 1996. Role and regulation of sucrose-phosphate synthase in higher plant. Annu Rev Plant Physiol Plant Mol Biol 47, 431–444.
Iida, K., Fukami-Kobayashi, K., Toyoda, A., Sakaki, Y., Kobayashi, M., Seki, M., Shinozaki, K., 2009. Analysis of multiple occurrences of alternative splicing events in Arabidopsis thaliana using novel sequenced full-length cDNAs. DNA Res. 16 (3), 155–164.
Jammer, A., Gasperl, A., Luschin-Ebengreuth, N., Heyneke, E., Chu, H., Cantero-Navarro, E., 2015. Simple and robust determination of the activity signature of key carbohydrate metabolism enzymes for physiological phenotyping in model and crop plants. J. Exp. Bot. 66, 5531–5542.
Jones, D.T., 1999. Protein secondary structure prediction based on position-specific scoring matrices. J. Mol. Biol 292, 195–202.
Keller, F., Frehner, M., Wiemken, A., 1988. Sucrose synthase, a cytosolic enzyme in protoplasts of Jerusalem artichoke tubers (*Helianthus tuberosus* L.). Plant Physiol. 88, 239–241.
Kelley, L.A., Mezulis, S., Yates, C.M., Wass, M.N., Sternberg, M.J., 2015. The Phyre2 web portal for protein modeling, prediction, and analysis. Nat. Protoc. 10, 845–858.
Konishi, T., Ohmiya, Y., Hayashi, T., 2004. Evidence that sucrose loaded into the phloem of a poplar leaf is used directly by sucrose synthase associated with various beta-glucan synthases in the stem. Plant Physiol. 134, 1146–1152.
Kumar, S., Stecher, G., Li, M., Knyaz, C., Tamura, K., 2018. MEGA X: molecular evolutionary genetics analysis across computing platforms. Mol. Biol. Evol. 35, 1547–1549.
Lao, J., Oikawa, A., Bromley, J.R., McInerney, P., Suttangkakul, A., Smith-Moritz, A.M., Plahar, H., Chiu, T.Y., Gonzalez Fernandez-Nino, S.M., Ebert, B., Yang, F., Christiansen, K.M., Hansen, S.F., Stonebloom, S., Adams, P.D., Ronald, P.C., Hillson, N.J., Hadi, M.Z., Vega-Sanchez, M.E., Loque, D., Scheller, H.V., Heazlewood, J.L, 2014. The plant glycosyltransferase clone collection for functional genomics. Plant J. 79 (3), 517–529.
Lowry, O.H., Rosebrough, N.J., Farr, A.L., Randall, R.J., 1951. Protein measurement with the folin phenol reagent. J. Biol. Chem. 193, 265–275.
Martin, T., Frommer, W.B., Salanoubat, M., Willmitzer, L., 1993. Expression of an *Arabidopsis* sucrose synthase gene indicates a role in metabolization of sucrose both during phloem loading and in sink organs. Plant J. 4, 367–377.
McCarty, D.R., Shaw, J.R., Hannah, L.C., 1986. The cloning, genetic mapping, and expression of the constitutive sucrose synthase locus of maize. Proc. Natl. Acad. Sci. U. S. A. 83, 9099–9103.
Morell, M., Copeland, L., 1985. Sucrose synthase of soybean nodules. Plant Physiol. 78, 149–154.
Ruan, YL., 2014. Sucrose metabolism: gateway to diverse carbon use and sugar signaling. Annu. Rev. Plant Biol. 65, 33–67.
Ruan, Y.L., 2007. Rapid cell expansion and cellulose synthesis regulated by plasmodesmata and sugar: insights from the single-celled cotton fibre. Funct. Plant Biol. 34, 1–10.
Ruan, Y.L., Chourey, P.S., 1998. A fiberless seed mutation in cotton is associated with lack of fiber cell initiation in ovule epidermis and alterations in sucrose synthase expression and carbon partitioning in developing seeds. Plant Physiol. 118, 399–406.
Salanoubat, M., Belliard, G., 1987. Molecular cloning and sequencing of sucrose synthase cDNA from potato (*Solanum tuberosum* L.): preliminary charactertzation of sucrose synthase mRNA distribution. Gene 60 (1), 47–56.
Salanoubat, M., Belliard, G., 1989. The steady-state level of potato sucrose synthase mRNA is dependent on wounding, anaerobiosis and sucrose concentration. Gene 84, 181–185.
Salerno, G.L., Curatti, L., 2003. Origin of sucrose metabolism in higher plants: when, how and why? Trends Plant Sci. 8, 63–69.
Sambrook, J., Fritsch, E.F., Maniatis, T., 1989. Molecular Cloning: A Laboratory Manual. Cold Spring Harbor Laboratory Press, New York.
Sarkar, D., 2008. The signal transduction pathways controlling in planta tuberization in potato: an emerging synthesis. Plant Cell Rep. 27, 1–8.
Schaffer, A.A., Petreikov, M., 1997. Inhibition of fructokinase and sucrose synthase by cytosolic levels of fructose in young tomato fruit undergoing transient starch synthesis. Physiol. Plant. 101, 800–806. https://doi.org/10.1111/j.1399-3054.1997.tb01066.x.
Schmolzer, K., Gutmann, A., Diricks, M., Desmet, T., Nidetzky, B., 2016. Sucrose synthase: a unique glycosyltransferase for biocatalytic glycosylation process development. Biotechnol. Adv. 34, 88–111.
Shaw, J.R., Ferl, R.J., Baier, J., St Clair, D., Carson, C., Mccarty, D.R., Hannah, L.C., 1994. Structural features of the maize sus1 gene and protein. Plant Physiol. 106, 1659–1665.
Sheen, J., Zhou, L., Jang, J.C., 1999. Sugars as signaling molecules. Curr. Opin.Plant Biol. 2, 410–418.
Stein, O., Granot, D., 2019. An overview of sucrose synthases in plants. Front. Plant Sci. 10. https://doi.org/10.3389/fpls.2019.00095.
Subbaiah, C.C., Palaniappan, A., Duncan, K., Rhoads, D.M., Huber, S.C., Sachs, M.M., 2006. Mitochondrial localization and putative signaling function of sucrose synthase in maize. J. Biol. Chem. 281, 15625–15635.
Sytykiewicz, H., Czerniewicz, P., Leszczyński, B., 2008. Molecular characteristics of sucrose synthase isolated from bird cherry leaves. Herba Pol. 54, 41–49.
Tong, X.L., Wang, Z.Y., Ma, B.Q., Zhang, C.X., Zhu, L.C., Ma, F.W., Li, M., 2018. Structure and expression analysis of the sucrose synthase gene family in apple. Integrat. Agric. 17, 847–856.
Viola, R., Roberts, A.G., Haupt, S., Gazzani, S., Hancock, R.D., Marmiroli, N., Machray, G.C., Oparka, K.J., 2001. Tuberization in potato involves a switch from apoplastic to symplastic phloem unloading. Plant Cell 13, 385–398.
Wang, A.Y., Yu, W.P., Juang, R.H., Huang, J.W., Sung, H.Y., Su, J.C., 1992. Presence of three rice sucrose synthase genes as revealed by cloning and sequencing of cDNA. Plant Mol. Biol. 18, 1191–1194.
Wang, Z., Wei, P., Wu, M., Xu, Y., Li, F., Luo, Z., Zhang, J., Chen, A., Xie, X., Cao, P., Lin, F., Yang, J., 2015. Analysis of the sucrose synthase gene family in tobacco: structure, phylogeny, and expression patterns. Planta 242, 153–166.
Wang, F., Smith, A.G., Brenner, M.L., 1993. Isolation and sequencing of tomato fruit sucrose synthase cDNA. Plant Physiol. 103 (4), 1463–1464.
Werr, W., Frommer, W.B., Maas, C., Starlinger, P., 1985. Structure of the sucrose synthase gene on chromosome 9 of *Zea mays* L. EMBO J. 4, 1373–1380.
Winter, H, Huber, SC, 2000. Regulation of sucrose metabolism in higher plants: localization and regulation of activity of key enzymes. Crit Rev Biochem Mol Biol 35, 253–289.
Winter, H., Huber, J.L., Huber, S.C., 1998. Identification of sucrose synthase as an actin-binding protein. FEBS Lett. 430, 205–208. https://doi.org/10.1016/S0014-5793(98)00659-0.
Xu, X., Yang, Y., Liu, C., Sun, Y., Zhang, T., Hou, M., Huang, S., Yuan, H., 2019. The evolutionary history of the sucrose synthase gene family in higher plants. BMC Plant Biol. 19 (1), 5661.
Yu, W.P., Wang, A.Y., Juang, R.H., Sung, H.Y., Su, J.C., 1992. Isolation and sequences of rice sucrose synthase cDNA and genomic DNA. Plant Mol. Biol. 18, 139–142.
Zhang, J., Arro, J., Chen, Y., Ming, R., 2013. Haplotype analysis of sucrose synthase gene family in three *Saccharum* species. BMC Genom. 14, 314.
Zhang, Y., 2008. I-TASSER server for protein 3D structure prediction. BMC Bioinform. 23, 9–40.
Zheng, Y., Anderson, S., Zhang, Y., Garavito, R.M., 2011. The structure of sucrose synthase-1 from Arabidopsis thaliana and its functional implications. J. Biol. Chem. 286, 36108–36118.
Zhu, X., Wang, M., Li, X., Jiu, S., Wang, C., Fang, J., 2017. Genome-wide analysis of the sucrose synthase gene family in grape (*Vitis vinifera*): structure, evolution, and expression profiles. Genes 8, E111.
Zrenner, R., Salanoubat, M., Willmitzer, L., Sonnewald, U., 1995. Evidence of the crucial role of sucrose synthase for sink strength using transgenic potato plants (*Solanum tuberosum* L.). Plant J. 7, 97–107. https://doi.org/10.1046/j.1365-313X.1995.07010097.x.

South African Journal of Botany 148 (2022) 634–642

Contents lists available at ScienceDirect

South African Journal of Botany

journal homepage: www.elsevier.com/locate/sajb

Molecular cloning, expression and *in silico* analyses of calcium-dependent protein kinase 2 (CDPK2) in potato (*Solanum tuberosum* L.)

Gurpreet Kaur*, Niranjan Das

Department of Biotechnology, Thapar Institute of Engineering & Technology, Patiala, Punjab 147004, India

ARTICLE INFO

Article History:
Received 14 November 2021
Revised 11 March 2022
Accepted 12 April 2022
Available online 23 April 2022

Edited by: Dr M. Naeem

Keywords:
Potato (*Solanum tuberosum* L.)
Calcium-dependent protein kinases (CDPKs)
Molecular cloning
Sequence analyses
Expression
3-D protein structures

ABSTRACT

In plants, calcium-dependent protein kinases (CDPKs) play crucial role in the regulation of growth and development in response to various stresses. They act as sensor-transducers in decoding the calcium (Ca^{2+}) ions associated with multiple signal transduction pathways. The plant CDPK isoforms are encoded by the nuclear multigene families. Some CDPK isoforms were reported earlier in potato; but their three-dimensional (3-D) structures were not predicted. Based on the RT-PCR approach using tuber total RNA, a 1560-bp cDNA clone encoding 515-aa CDPK2 isoform (designated StCDPK2) was isolated and characterized from the potato cultivar Kufri Chipsona-1(KC-1). A thorough sequence analysis revealed both sequence identities and crucial motifs in the potato CDPKs. Semi-quantitative RT-PCR approach was adopted to show the expression patterns of *StCDPK2* in different potato organs grown under field condition. The three-dimensional (3-D) structures of potato CDPK1–3 were predicted by a composite approach using *ab initio* modeling, and further validated and assessed by Ramachandran plot analyses. In addition, a number of the CDPK isoforms were retrieved from the potato genome sequence database; their probable biochemical properties and functional aspects were predicted based on both bioinformatics tools and published reports.

© 2022 SAAB. Published by Elsevier B.V. All rights reserved.

1. Introduction

In plants, calcium ion (Ca^{2+}) plays pivotal role in various processes such as growth, development and stress responses. Transient increase in cyotosolic Ca^{2+} concentrations triggers the signaling pathways that lead to the cellular changes like stomatal movements, increased water retention, and responses to the biotic stress such as pathogen attack (DeFalco et al., 2010; Tong et al., 2021). Plant Ca^{2+}signatures are understood by some calcium sensors such as calmodulins (CaMs), calmodulin-like proteins (CaMLs), calcineurin B-like proteins (CBLs) and Ca^{2+}-dependent protein kinases (CDPKs) (Sanders et al., 2002; Zhao et al., 2021). Upon binding with Ca^{2+} ions these proteins undergo conformational changes, thus activating many downstream proteins. Among all these sensors, CDPKs are unique as they act Ca^{2} $^{+}$ion responders (Atif et al., 2019; Sharma et al., 2021). Hetherington and Trewavas (1982) first reported the CDPK activities in peas followed by other plant species. Their structural analogs could be found in protists and alveolates; whereas, no CDPKs were found in fungi, insects and mammals (Sanders et al., 2002). CDPKs (M_r: 40 to 90 kDa) are encoded by the multigene family in plants. They possess five distinct domains: N-terminal variable domain, kinase domain, auto-inhibitory domain, regulatory domain i.e., calmodulin-like domain (CaM-LD), and a C-terminal domain of variable length. CDPK transmits the signal by phosphroylating the substrate i.e., target protein at the N-terminus via catalytic kinase. Activation of CDPKs occurs by the phosphorylation of serine/threonine residues in the conserved protein kinase domain. Calcium influx into the cell leads to a conformational change in CDPK due to interactions between the CAM-like domain and the auto-inhibitory domain, and finally kinase domain is activated (Harmon et al., 2001; Singh et al., 2017; Tong et al., 2021).

The CDPK multigene family consists of at least 12 subfamilies which are derived from a common ancestor for both monocot and eudicots. CDPKs occur in both soluble and membrane bound forms, and found in multiple locations such as cyotosol, nucleus, ER, peroxisomes, mitochondria (Harper et al., 2004). The occurrence of gene duplication and subsequent divergence of CDPKs with distinct functions have been revealed by the genome wide analysis of *Arabidopsis* containing 34 genes for CDPKs. Genome sequencing and expressed sequence tag (EST) data indicated the presence of multigene families

Abbreviations: Ca^{2+}, Calcium ion; CaMs, Calmodulins; CaMLs, calmodulin-like proteins; CBLs, calcineurin b-like proteins; CDPKs, Ca^{2+}-dependent protein kinases; CaM-LD, calmodulin-like domain; KC-I, Kufri Chipsona-1; CPRI, central potato research institute; RNA, ribonucleic acid; cDNA, complementary deoxyribonucleic acid; RT-PCR, reverse transcription polymerase chain reaction; NCBI, national center for biotechnology information; ORF, open reading frame; ExPASy, expert protein analysis system; Pi, isoelectric point; SIB, swiss institute of bioinformatics; MSA, multiple sequence alignments; MEGA, molecular evolutionary genetic analysis; I-TASSER, iterative threading assembly refinement; SAVES, structural analysis and verification server

* Corresponding author.
E-mail address: gsainibt@gmail.com (G. Kaur).

https://doi.org/10.1016/j.sajb.2022.04.018
0254-6299/© 2022 SAAB. Published by Elsevier B.V. All rights reserved.

of CDPKs in other plants that included rice, *Arabidopsis*, tomato, maize, potato, soyabean, fox tail millet, Fragaria and *Medicago truncatula* (Cheng et al., 2002; Chen et al., 2013; Zuo et al., 2013; Yu et al., 2018; Wang et al., 2019; Crizel et al., 2020; Zhao et al., 2021). CDPKs were found to be associated with the activity of phytohormones such as GA_3. Also, they are recognized as key players participating in the translation of pathogen signal-induced changes in the Ca^{2+} concentration into plant defense reactions that included the synthesis of free radicals, changes and alterations of gene expression, phytohormone synthesis, cell signaling, cell death, plant immune signaling, nitrogen-deficiency induced oil accumulation and protein-protein interaction networks (Frattini et al., 1999; Romeis et al., 2001; Sanders et al., 2002; Boudsocq and Sheen, 2013; Bredow and Monaghan, 2019; Li et al., 2019; Ahmed et al., 2020; Marques et al., 2022). CDPK proteins play major biological and functional roles viz., root development (Ivashuta et al., 2005), pollen tube elongation (Myers et al., 2009), cell differentiation, programmed cell death (Lee et al., 2006), hormone signaling (Liese and Romeis, 2013), and fiber development (Ahmed et al., 2020). The role of CDPKs is also well-recognized in the complex tuberization process in potato (Raices et al., 2003). CDPK activities with different substrate and cellular specificity are known to play important role in potato life cycle. For example, StCDPK3 is expressed predominantly during early initiation of stolon elongation, while StCDPK1 is expressed during apical swelling in the stolon tip, StCDPK2 is expressed during tuberization and in leaves (Raices et al., 2003). Also, StCDPK2 was found to play a crucial role in light sensing and stress metabolism (Grossi et al., 2022). Moreover, StCDPK4 and StCDPK5 were identified as modulators of early defense reactions in response to the challenges from *Phytophthora infestans* in potato (Kobayashi et al., 2007). Apart from these forms, other CDPK isoforms were known to be crucial for stress metabolism (Bi et al., 2021).

Potato (*Solanum tuberosum* L.) is a major non-grain food crop and grown all over the world. It ranks third, and comes only after wheat and rice (http://faostat.fao.org/). Potato belongs to the family *Solanaceae* which consists of more than 3000 members. Most of the potato cultivars are autotetraploid (2*n*=4*x*=48), and highly heterozygous. High level of DNA polymorphism in the potato (*Solanum tuberosum* L.*)* genome is well known. Because of cumulative mutations, multiple allelism and natural allelic variations are common in potato (Draffehn et al., 2010). It is likely that each class of gene family could have multiple members in potato. Various morphological, biochemical and molecular processes are involved in potato tuberization (Viola et al., 2001; Sarkar, 2008). Keeping in view of the importance of Ca^{2+}signaling, this study focused on the different forms of CDPKs involved in potato tuberization. We isolated a CDPK isoform, StCDPK2, from potato tuber, and characterized it by molecular, biochemical and *in silico* approaches. In addition, a number of other CDPK isoforms in the potato genome were also studied.

2. Materials and methods

2.1. Plant materials and growth conditions

In this study, we used a high-yielding and commercially important Indian potato cultivar namely Kufri Chipsona-1 (KC-1), procured from Central Potato Research Institute (CPRI), Shimla, India. It is routinely micropropagated in our laboratory under controlled conditions (16 h light/8 h dark, light intensity approximately 40–42 μmol m^{-2} s^{-1}, 25–27°C, 70% relative humidity) on MS-basal medium with 2.5% sucrose. The micropropagated potato plantlets were acclimatized and then cultivated in the field for 16 wks (mid-November to mid-March). The tubers, leaves and other organs were harvested and frozen in liquid nitrogen for further molecular and biochemical studies.

2.2. RNA extraction, RT-PCR, and CDPK cDNA cloning

Total RNA was isolated from the leaves and freshly harvested tubers from the potato cultivar Kufri Chipsona-1 by SDS-Phenol method as reported earlier by Gilman (1987). RNA quality was checked by determining A_{260}/A_{280} ratio spectrophotometrically, and the values were around 2.0. The quality of total RNA preparations was further checked by regular and formaldehyde agarose gel electrophoresis along with reverse transcription polymerase chain reaction (RT-PCR) using different potato gene-specific primers. The following oligonucleotide primers were used based on the potato calcium-dependent protein kinase 2 (CDPK2) sequence (AF418563, Raices et al., 2003): the forward primer SC2F1-0001, 5′-ATGGGTATTTGTGCTAGTA-3′ (corresponding to the bases 1–19); and the reverse primer SC2R2-1560, 5′-GACCTTGCCTGGTTATTTGG-3′ (complementary to the bases 1541–1560).

Reverse transcription (RT) was carried out using the RevertAid™ H Minus First Strand cDNA Synthesis Kit with M-MuLV reverse transcriptase (Fermentas Life Sciences). Approx. 2.0 μg of purified total RNA from the growing tubers of KC-1 and oligo $(dT)_{18}$ primer were used in reverse transcription reaction. In order to isolate the full-length cDNA, PCR was carried out using the RT product, the *CDPK* cDNA-specific primers namely SC2F1-0001 and SC2R2-1560, and 1.0 unit of *Taq* DNA polymerase (Genei). After initial denaturation at 94 ° C for 1 min 30 s, the thermal cycling parameters during PCR were: denaturation at 94 °C for 1 min, annealing at 55 °C for 2 min, and polymerization at 72 °C for 2 min for 30 cycles followed by final extension at 72 °C for 5 min. The amplified RT-PCR product was treated with Klenow enzyme, purified, and cloned into the *Sma*I site of pUC19 vector according to the protocol as described by Sambrook et al. (1989). *E. coli* DH5α was used as a host for molecular cloning. The cloned cDNA was sequenced in both directions by Bioserve Biotechnologies, India.

2.3. Semi-quantitative RT-PCR

Semi-quantitative RT-PCR was carried out to know the *CDPK2* expression patterns in several potato organs namely tuberizing stolon (ts), tuber (tu), leaf (le), stem (st) and flower (fl). Reverse transcription was carried out in a reaction volume of 20 μL using 2.0 μg of total RNA from each organ, oligo $(dT)_{18}$ primer and cDNA Synthesis Kit from Fermentas Life Sciences. 3.0 μL of each RT product was used as template in PCR (50 μL reaction volume) using the *CDPK2*-specific forward primer SC2F1-0001, and the reverse primer SC2R1-0920, 5′-AGGTCCTTGGCACTACTTGA-3′ (complementary to the bases 901–920), and 1.0 unit of *Taq* DNA polymerase (Bangalore Genei). During PCR, the thermal cycling parameters were kept same as mentioned earlier except polymerization at 72 °C for 2 min. For internal control, constitutively expressed potato actin gene (XM_006348930)-specific forward primer F1-AC0591, 5′-CCACATGCTATCCTTCGTCTC-3′ (corresponding to the bases 591–612); and the reverse primer R1-AC1149, 5′-TCCACATCTGTTGGAAGGTAC-3′ (complementary to the bases 1128 to 1149) were used. The *CDPK* and actin-specific RT-PCR products were resolved in 0.9% agarose gel electrophoresis. The relative expression levels between the potato organs were assessed by the quantification tool of the gel documentation system (Bio-Rad, USA).

2.4. Sequence analyses, retrieval and phylogenetic tree

The nucleotide sequence of the *CDPK* cDNA was analysed by NCBI (http://www.ncbi.nlm.nih.gov/) Blast tools. The amino acid sequence was predicted by the open reading frame (ORF) finder available at the NCBI. For calculating the theoretical molecular weight, isoelectric point (pI), and amino acid composition of the predicted protein, the ProtParam tool of Expert Protein Analysis System (ExPASy)

proteomics server of the Swiss Institute of Bioinformatics (SIB; URL: http://expasy.org/tools/) was used.To investigate the relationships between the protein sequences and motifs, MyHits tool of ExPASy (https://myhits.sib.swiss/cgi-bin/motif_scan) was used. For multiple sequence alignment, the *MultAlin* software (http://www.multalin.toulouse.inra.fr/multalin/; Corpet, 1988) was used.

All the available CDPK protein sequences of potato were retrieved from the Spud DB (Potato Genomics Resource) in fasta format. The different biochemical parameters of the proteins such as molecular weight, theoretical pI, aliphatic index, GRAVY and instability indexes were calculated using ProtParam tool of ExPASy Proteins & Proteomes server of the Swiss Institute of Bioinformatics (SIB, http://www.expasy.org/). Protein domains were predicted by PROSITE scan (Sigrist et al., 2013), and myristoylation sites by NMT−The MYR Predictor script (http://mendel.imp.ac.at/myristate/SUPLpredictor.htm). Further chromosomal location, gene length, number of exons were predicted using the annotation tool of Spud DB Potato Genomics Resource (http://solanceae.plantbiology.msu.edu).

Phylogenetic analysis of the 23 CDPKs was performed to study their evolutionary relationship. Multiple sequence alignments (MSA) followed by neighbor joining method with bootstrap 1000 were done to understand the nodes using Molecular Evolutionary Genetic Analysis (MEGA X) software (Kumar et al., 2018).

2.5. 3-D structure prediction of protein

The amino acid sequences of the CDPK proteins (StCDPK1−3) were retrieved in fasta format. It was observed that no single template with lower e-value and acceptable identity was able to satisfy the 100% query coverage. Therefore, the initial 3D model was constructed using I-TASSER (Iterative Threading Assembly Refinement), a complete, comprehensive and hierarchical approach for prediction of structure and function of proteins. It uses the restraints from templates identified by multiple threading program to build a full length model using a replica exchange Monte-Carlo simulation. Most reliable model was selected using Discrete Optimized Protein Energy (DOPE). The estimated global accuracy of the model was indicated by the C-score and estimated TM-score. Normal Z-score >1 was considered for the better alignment. The residue with high negative value of predicted Normalised B-factor was taken as it is considered to be more stable (Zhang, 2008).

2.6. Correction and validation of the model

Stable state of any system is defined as the minimum energy state of its atoms; in order to remove the inner constraints of the atoms leading to distorted geometry energy minimization becomes essential. Hence, energy minimization was performed on the best models of the CDPKs by refining the local side chain and protein packing using the tools provided by NOMAD-Ref web server (http://lorentz.dynstr.pasteur.fr). After correction, models were validated using the Structural Analysis and Verification Server (http://nihserver.mbi.Ucla.edu/SAVES/; Cheatham et al., 1995). The predicted structures were visualized in the form of ribbons by PyMol (https://www.pymol.org). The transmembrane helices were predicted using Phyre2 tools of a protein fold recognition server (http://www.sbg.bio.ic.ac.uk/phyre2/).

3. Results

3.1. Cloning of cDNA and sequence analyses

The nucleotide sequence of the cDNA clone (1560 bp, designated *CDPK2-A*) specific to Kufri Chipsona-1 was analyzed by NCBI BLAST tool, and found to be a distinct form of *CDPK2* gene family; the sequence information was submitted to the GenBank database (MN420514; protein_id QIS79146). The 1560-bp *CDPK2-A* lacking 5′-UTR consisted of 1548-bp ORF, and 12-bp 3′-UTR; the G+C content of the coding region and 3′-UTR were found to be 41.4% and 66.7%, respectively. Nucleotide BLAST search revealed that *CDPK2-A* shared 99% sequence identity with AF418563, a full-length *CDPK2* cDNA clone from the potato cultivar spunta (Raices et al., 2003). The coding region of *CDPK2-A* also showed significant sequence identities with some other plant cDNAs having the following Accession Numbers: NM_001288442.1, XM_006346152.2, XM_015226573.1, NM_001247653.2, BT013334.1, AF363784.1, LC156099.1, AF115406.3, JN662020.1, XM_016701298.1, XM_016631157.1 belonging to different forms of CDPK and CDPK-like proteins in the *Solanaceae* family.

The predicted protein, designated StCDPK2, consisted of 515 amino acids (Fig. 1). Based on the ProtParam tool, the calculated molecular weight (MW) of StCDPK2 was found to be 57.14 kDa with a predicted isoelectric point (p*I*) of 6.59. Out of total 515 amino acids, 67 were strongly basic (+) (Lys, Arg), 70 were strongly acidic (−) (Asp, Glu), 163 were hydrophobic (Ala, Ile, Leu, Phe, Trp, Val), and 118 were polar (Asn, Cys, Gln, Ser, Thr, Tyr). The instability index of StCDPK2 was computed as 28.35, which classified the protein as stable. The amino acid composition data revealed that some of the amino acids such as Gly (8.7%), Lys (8.9%), Glu (7.8%), and Ile (6.4%) occurred more frequently as compared to their average occurrence; whereas, the amino acids, namely Thr (4.9%), Gln (2.7%), Arg (4.1%), Phe (2.7%), and Trp (0.8%), occurred less frequently (Doolittle, 1989).

3.2. Sequence alignment, regulatory/binding motifs and distinguishing sequence features

Among the multiple CDPK isoforms present in the potato genome, only three i.e., *CDPK*1−3 are known to be involved in tuberization. The various catalytic domains present in the CDPKs play important role in the regulation of various physiological processes associated with biotic and abiotic stresses. The distinguishing features, functions and the relative location of the crucial domains such as cyclic AMP (cAMP)-dependent phosphorylation (regulates glycogen, sugar and lipid metabolism in cell), Tyrosine kinase phosphorylation (phosphorylation of the acidic proteins), the bipartite nuclear localization signal (membrane targeting and signal transduction in plants in responses to environmental stress), protein kinases ATP binding region are highlighted in Fig. 1.

3.3. Characterization of CDPKs from the potato genome

In plant genomes, expansion of the gene families is believed to have occurred by different mechanisms such as genome-wide, tandem and dispersed duplications. A genome wide analysis of the *CDPK* gene family was performed in the complete potato genome sequence (Potato Genome Sequencing Consortium 2011 as reported earlier in database) (Fantino et al., 2017; Gromadka et al., 2018). Supplementary Tables 1 and 2 provide a more comprehensive information on the *CDPK* gene family in potato which would help for further in-depth studies. The potato genome encodes 23 CDPKs and appears to exhibit high plasticity, as gene loss or duplication events and other structural mutations are found with high frequency. The *CDPK* genes were found to be localized on 11 chromosomes out of 12; on chromosome 9 no *CDPK* gene was found whereas the highest number (six) of *CDPK* genes are found on chromosome number 10 (Fig. 2). On some chromosomes the *CDPK* genes form clusters a clue of gene duplication which suggests the gradual expansion of this gene family. A total of 23 full-length CDPK amino acid sequences from potato were used in making a phylogenetic tree showing sequence relatedness between them (Fig. 3).

Fig. 1. Comparison between the sequences of three potato CDPKs: StCDPK1 (NP_001275322.1), StCDPK2 (QIS79146), StCDPK3 (AAQ08324.2) involved in tuberization. Multiple sequence alignment was done based on *MultAlin* software along with some minor manual adjustments. Dashes indicate gaps that arise during alignment. Asterisks '*' indicate the conserved/nearly conserved amino acids; ':' refers to the almost conserved or conservative substitutions; '.' refers to conserved amino acids in at least two CDPK forms. The downward arrow '⇓' indicates the entire protein kinase region. The crucial regulatory/binding motifs are underlined in StCDPK2, and the '▼' denotes the crucial active site.

3.4. *Expression patterns of* CDPK2 *in potato organs*

The *CDPK2* gene expression pattern was examined in some potato organs namely tuberizing stolon, growing tuber, leaf, stem, and flower. By semi-quantitative RT-PCR, a DNA product of ~0.9 kb was only amplified using total RNA from tuberizing stolon, tuber, leaf and stem (Fig. 4). The size matched with *CDPK2-A* transcripts towards the 5′-end. The transcript level appeared to be comparable in tuberizing stolon, tuber, leaf and stem; interestingly, the transcript was not detected in the case of flower. The actin expression level was found to be nearly uniform in the potato organs.

3.5. *Modeling and structure validation*

In order to predict biological function of any protein, it is essential to know its structure first. So, the model generated by I-TASSER (through the combination of threading and *ab initio* prediction) was taken for the study. I-TASSER, a meta server implements different threading programmes and its quality is assessed on the basis of Z-score (the energy score in standard deviation units relative to statistical mean of alignments). For confident alignment Z-score should be greater than 1. The best model with minimized energy (Fig. 5A–C) was used to show the specific calcium signature domain and were

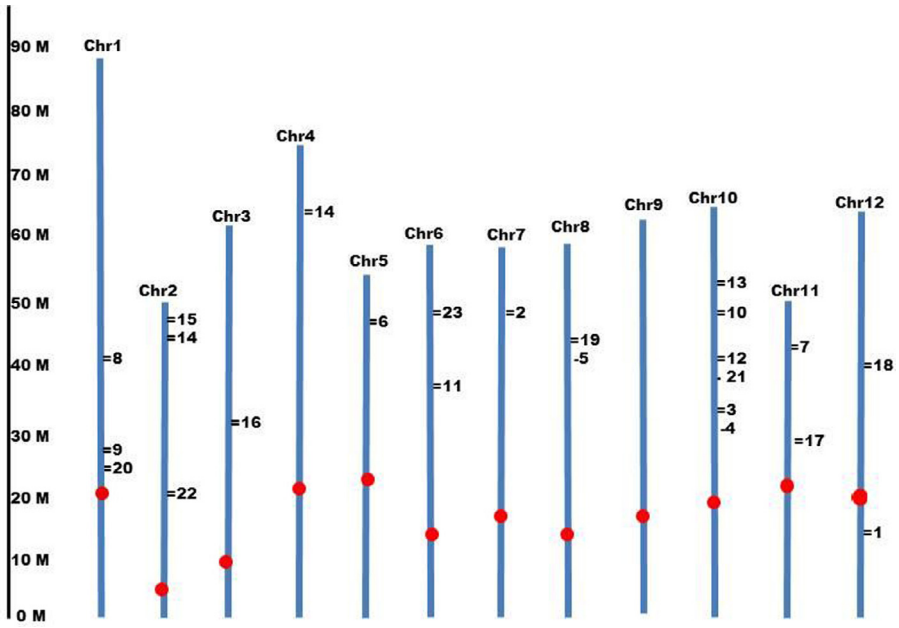

Fig. 2. Chromosomal localization of the calcium-dependent protein kinases genes (*StCDPKs*) in potato; retrieved from the Potato Genome Database (Potato Genome Sequencing Consortium 2011), and labelled as presented in the Supplementary Table1. Chromosomes are shown in blue and centromeres are marked by red.

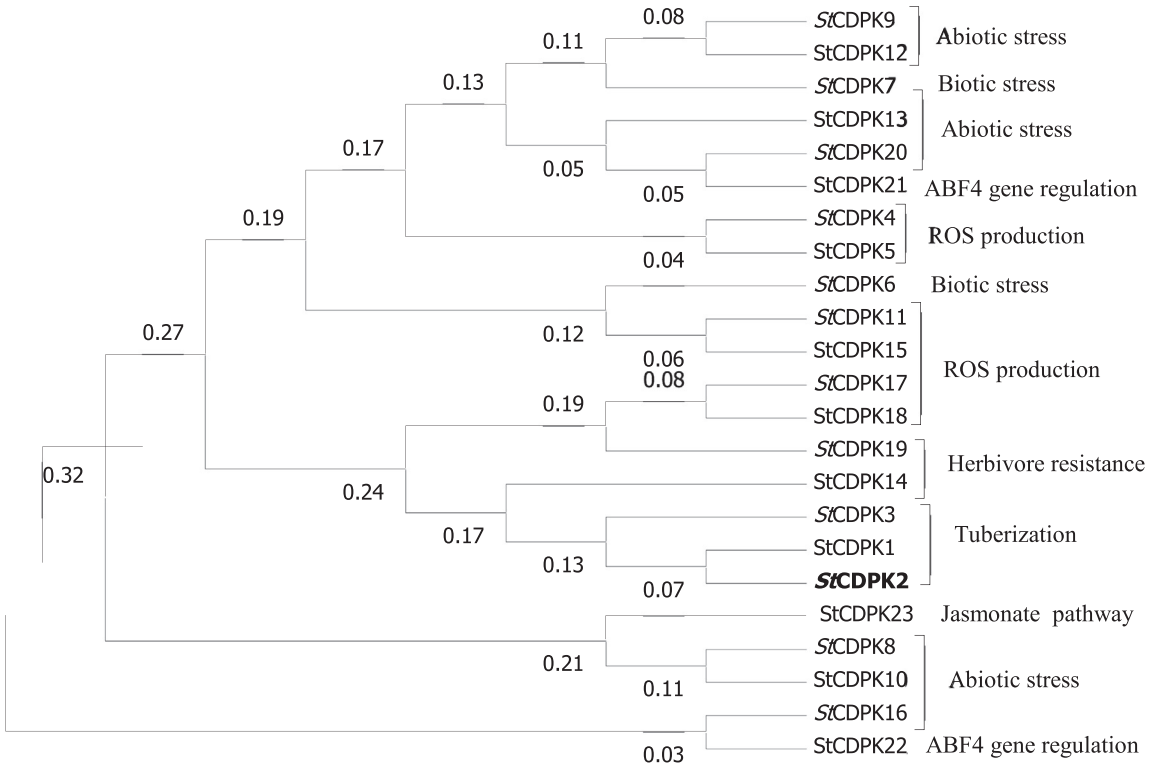

Fig. 3. The phylogenetic tree generated by the MEGA X software (Kumar et al., 2018) using the Neighbor-Joining method. The percentage of replicate trees in which the associated taxa clustered together in the bootstrap test (1000 replicates) are shown next to the branches. The evolutionary distances computed by the Poisson correction method are in the units of the number of amino acid substitutions per site. All ambiguous positions were removed for each sequence pair (pairwise deletion option). The evolutionary analyses involved 23 amino acid sequences of the potato CDPKs as available in the published reports and/or databases (Labelled according to the names as in Supplementary table S1) The 515-aa StCDPK2 (QJS79146) specific to the culivar KC-1 of this study occupied a distinct position in the phylogenetic tree (shown in bold cases). Probable functions of the different CDPKs are also indicated.

visualized in the form of ribbons by PyMol (https://www.pymol.org). Transmembrane topology adopted by the proteins was predicted by Phyre2 tool (Fig. 5D–F). The backbone ratification of the established model was corroborated by using Ramachandran plot through PROCHECK (https://www.ebi.ac.uk/thornton-srv/software/PROCHECK). The distribution of phi and psi angles for the amino acid residues was

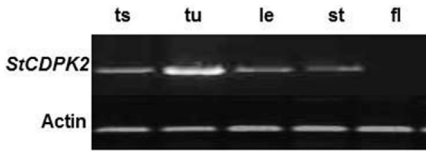

Fig. 4. Semi-quantitative RT-PCR for *StCDPK2* expression analysis using total RNA from different potato (cultivar KC-1) organs and the primers SC2F1-0001 and SC2R1-0920. ts tuberizing stolon, tu tuber, le leaf, st stem, fl flower. The size of the amplified product was ~ 0.9 kb in ts, tu, le and st. Actin-specific primers were used as an internal control (size of the amplified product ~ 0.65 kb in each organ).

denoted by Ramachandran plot. The built model was proven to be highly plausible; as only approx. 1% residues were found to be in the disallowed region of the plot (Fig. 6).

4. Discussion

Potato is one of the major non-grain food crop grown all over the world. It is a promising crop due to its high nutritional value. It ranks third, and comes only after wheat and rice. Currently, the major objectives of global potato and other crop breeding programs are to understand the various signaling pathways associated with the process of growth, development, tuberization, stress responses, and importantly crop yield. Efforts are being made in producing the resistant varieties towards various challenging biotic and abiotic stresses such as attacks by the pathogenic viruses and microbes, drought, frost and heat for improving crop yield, nutritional values and storage stability (Singh et al., 2014; Atif et al., 2019).

Calcium-dependent protein kinases (CDPKs), one of the largest groups of calcium sensors in plants, bind to calcium ions directly and modulate their activities. The calcium-activated kinases regulate diverse developmental processes and defense responses in plants. Considerable progress has been made on molecular and biochemical studies on CDPKs during last more than two decades. Research reports and database search revealed that multiple CDPK forms are present in the *Solanaceae* family members namely tobacco and tomato (Witte et al., 2010; Wang et al., 2015). Out of 23, 21 CDPKs are acidic, two are slightly basic and 14 of them contain myristoylation sites (Xu et al., 2015). All CDPKs contain four EF-hands; but rice, maize, *A. thaliana* and potato have CDPK -like kinases that possess less than four or no EF-hands (Mittal et al., 2017).

The gene lengths of different *CDPK*s ranging from 4.01 to 14.5 kb were found to contain 6 to 11 introns. The CDPK proteins consisted of 501–638 amino acids having molecular weights 56.2 to 70.1 kDa. Their instability indexes ranged from 29.40 to 48.36; out of 23 CDPK proteins only 9 were stable proteins and the remaining 14 were unstable (Supplementary Table S1). Aliphatic indexes were found to be relatively higher in all the CDPK proteins (Supplementary Table S2), indicating that CDPK domains were stable at wide ranges of temperature. All these proteins showed negative GRAVY scores suggesting that they were soluble or hydrophilic (Kyte and Doolittle, 1982). In the CDPKs, nearly conserved 24-aa protein kinase ATP binding signature (LGRGQFGVTYYCTENSTENPYACK) was present towards the N-terminal region. A 13-aa (VMHRDLKPENFLL) serine/threonine protein kinase-like domain containing Asp-in the active site (Asp197 in the case of StCDPK2) helps in positioning the ligand-binding domain into the extracellular space is found in the middle of protein (Fig. 1). The CDPK proteins were found to be acidic in nature.

Plant CDPKs were divided into four groups based on their biochemical properties, and roles in various physiological processes at different stages of development (Liu et al., 2016). In order to know the probable roles, the biochemical properties and expression patterns of a number of CDPKs were studied in different plants

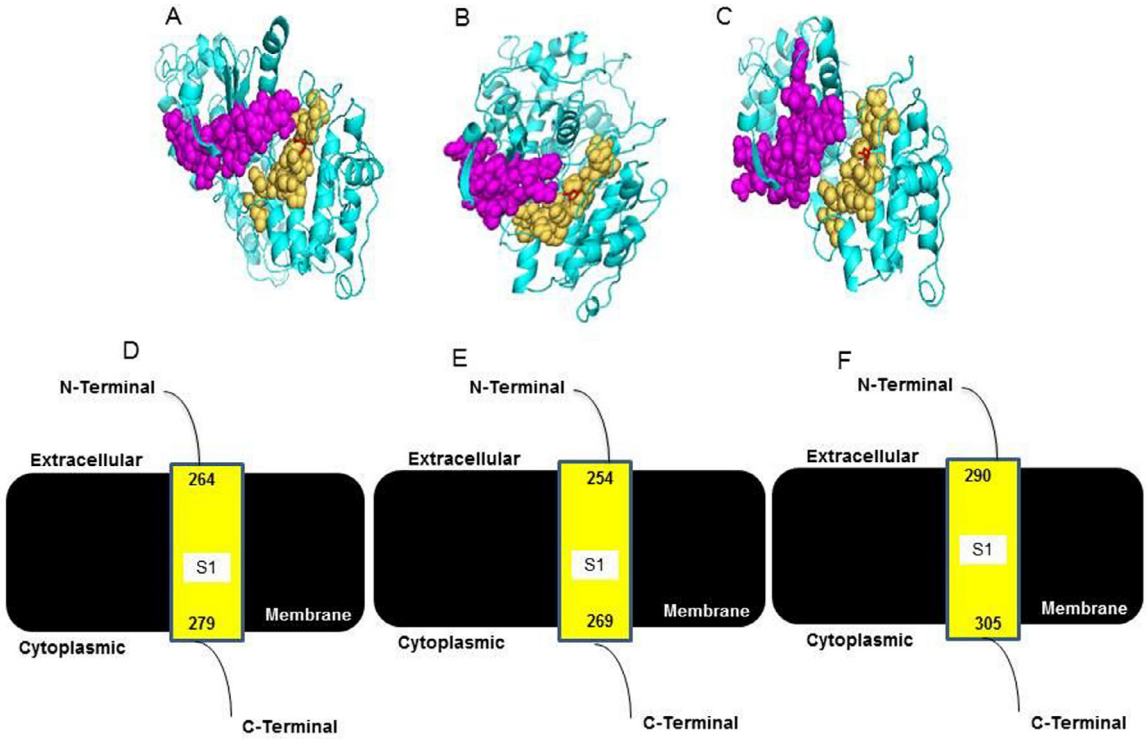

Fig. 5. (A–C) Illustrated representation and catalytic domains of the predicted three-dimensional structure models of the StCDPKs from potato. A 532-aa StCDPK1 (NP_001275322.1); B 515-aa StCDPK2 (QIS79146); C 558-aa StCDPK3 (AAQ08324.2). The entire protein regions are depicted in cyan, the catalytic protein kinase ATP-binding region and serine/threonine protein kinase domains are shown in magenta and brown colours, respectively as ribbon structures. The active sites are shown as stick and ball structures in red color. The images were generated using the PyMol program (Schrödinger, Inc., New York, NY, USA). (D–F) Illustrated representation of transmembrane helical segments by Phyre2; D StCDPK1, E StCDPK2, F StCDPK3. The extracellular and cytoplasmic sides of the plasma membrane are labelled; the beginning and end of each transmembrane segment are indicated by the positions of the amino acid residues.

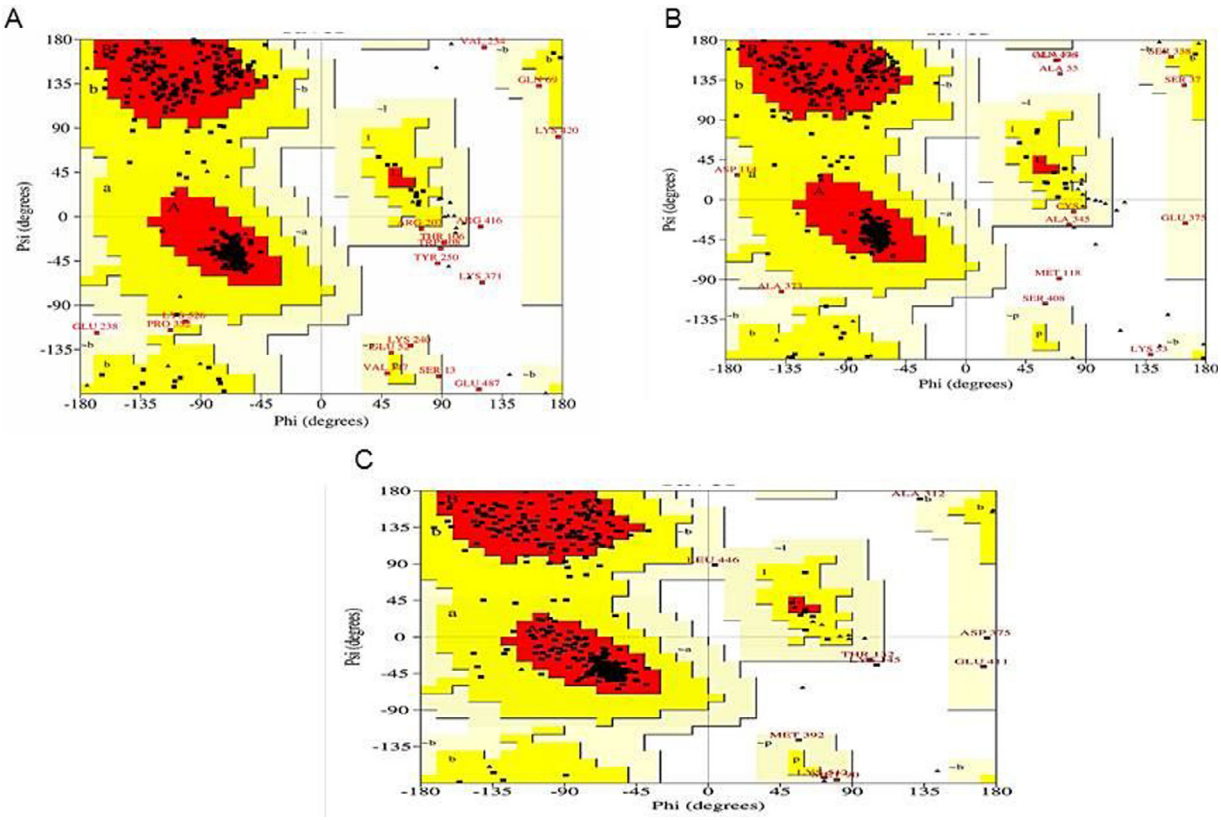

Fig. 6. (A– C) Ramachandran plot of the StCDPK models: A StCDPK1, B StCDPK2, C StCDPK3. The most favoured regions are coloured red; additional allowed, generously allowed and disallowed regions are indicated as yellow, light yellow and white fields, respectively.

(Fantino et al., 2017; Gromadka et al., 2018; Grossi et al., 2022). The probable roles of the CDPK proteins were also investigated in the model plant *A. thaliana* (Asano et al., 2012; Mittal et al., 2017; Wen et al., 2020). In potato, StCDPK1, 2, 3, 9, 10, 12, 13 and 20 belong to Group II, and undergo myrisotylation required for membrane targeting and signal transduction pathways in response to environmental stresses. StCDPK1, 2 and 3 were expressed during tuberization and known to activate GA2 oxidase. Increase in auxin concentration led to ABA-signaling pathways associated with stolon development, tuber formation and development and responses to hyperosmotic stress which were similar to the roles of AtCDPK9, 19, 33, 23, 15 and 21 (Gargantini et al., 2009; Grandellis et al., 2012; Liese and Romeis, 2013; Gromadka et al., 2018; Bi et al., 2021). StCDPK9, 10, 12 and 13 play crucial role in salt, cold and drought stress like AtCDPK6, 26, 34 and 17 (Gutermuth et al., 2013). StCDPK4, 5, 6, 7, 8, 11, 14, 15, 16, 17, 18 and 19 belong to Group I. StCDPK4 and 5 regulate ROS production similar to AtCDPK5, 6 and 26 (Kobayashi et al., 2007; Liese and Romeis, 2013; Gromadka et al., 2018). StCDPK6 and 7 are known to be crucial in formation of salicylic acid under biotic stress; thus, play a key role in pathogen resistance through convergent MAMP signaling as exhibited by AtCDPK1 and 5 (Asano et al., 2012). While other StCDPK members of this group are involved in herbivore resistance by blocking jasmonate and confer the drought tolerance, production of osmolyte proline and lowering lipid peroxidation probably through decrease in ROS production as observed in the cases of AtCDPK5, 6, 20, 11 and 25. StCDPK21 and 22 belong to Group III and involved in ABF4 gene regulation, salt tolerance and stomatal opening. Only StCDPK23 belongs to Group IV and involved in jasmonate pathway. The differential expression of the individual CDPKs could be correlated with their participation in specific signal transduction pathways in different plant organs. StCDPK1 was found to be expressed in sprouting tubers and tuberizing stolons. Expression of StCDPK3 was noticed in stolons, roots and leaves. StCDPK2 expression was noticed in all plant tissues and also during the developmental processes such as sprouting, tuberization and light-mediated signaling (Giammaria et al., 2011; Grossi et al., 2022); its elevated level was observed in the actively growing young leaves and tubers.

This study focused mainly on the three CDPKs (i.e., StCDPK1, 2 and 3) as each of them was expressed during the complex tuberization process in potato. Along with sequence identities, the important motifs of these forms are shown in Fig. 1. Prediction of the protein 3-D structures is also an important aspect of this report. The powerful techniques like X-ray crystallography and NMR are employed for determining the 3-D structures. These techniques require protein crystals; due to such constraints, structures of only a few membrane proteins have been determined (Schultz et al., 2000; SchuÈttelkopf and Van Aalten, 2004; Roy et al., 2010; Kelley et al., 2015). Alternatively, to acquire the structural information in a timely manner, 3-D protein structures were developed by means of *ab-initio* modeling technique and found to be useful for drug development (Berendsen et al., 1995; Chou and Shen, 2009). Here, the 3-D structures of StCDPK(1–3) were predicted using the composite molecular modeling web-server I-TASSER which relies on the threading techniques, and their energy levels were minimized by NOMAD-Ref. These structures were evaluated through Ramachandran plot analyses. More than 98% amino acid residues were in the most favorable allowed regions-validating the predicted 3-D structures. However, molecular optimization of these structures through molecular dynamics simulation got terminated prematurely as the protein structures contained a number of missing atom coordinates and were associated with poor quality parameters.

In conclusion, tuberization is a complex developmental process in potato life cycle. It still remains an enigma as multiple signaling pathways are believed to influence this process. Various signaling molecules, number of transcription factors and different enzymes are

involved in this complex morpho-physiological process. Isolation and characterization of cDNA/genomic clones corresponding to the multiple forms of the signal receptors/transducers, transcription/protein factors and enzymes involved in the different stages of tuber development remain the focus areas of potato research. Sequence analyses at protein level and predicting 3-D structures could help in understanding the structure-function relationships. Keeping in view, the findings on the potato CDPKs as presented in this report are relevant and would be useful in crop improvement.

Human and animal rights statement

This study did not involve human participants and/or animals.

Declaration of competing interest

All the authors do not have any possible conflicts of interest. Neither the entire paper nor any part of its content has been published or has been accepted elsewhere. It is not being submitted to any other journal. All the authors agree with the contents of this manuscript and hope the manuscript could be considered for publication in South African Journal of Botany. The authors declare no conflict of interest.

CRediT authorship contribution statement

Gurpreet Kaur: Visualization, Investigation, Formal analysis, Validation, Writing – original draft. **Niranjan Das:** Formal analysis, Writing – review & editing, Project administration.

Acknowledgments

We gracefully thank UGC, Government of India, for providing UGC:MAN Fellowship to G. Kaur.

Supplementary materials

Supplementary material associated with this article can be found in the online version at doi:10.1016/j.sajb.2022.04.018.

References

Ahmed, B., Alam, M., Hasan, F., Emdad, E.M., Islam, S., Rahman, N., 2020. Jute CDPK genes and their role in stress tolerance and fiber development: a genome-wide bioinformatic investigation of *Corchorus capsularis* and *C. olitorius*. Plant Gene 24, 100252.

Asano, T., Hayashi, N., Kikuchi, S., Ohsugi, R., 2012. CDPK-mediated abiotic stress signaling. Plant Sig. Behav. 7, 817–821. https://doi.org/10.4161/psb.20351.

Atif, R.M., Shahid, L., Waqas, M., Ali, B., Rashid, M.A.R., Azeem, F., Nawaz, M.A., Wani, S.H., Chung, G., 2019. Insights on Calcium-Dependent Protein Kinases (CPKs) signaling for abiotic stress tolerance in plants. Int. J. Mol. Sci. 20, 5298.

Berendsen, H.J., van der Spoel, D., van Drunen, R., 1995. GROMACS: a message passing parallel molecular dynamics implementation. Comput. Phys. Commun. 91, 43–56.

Bi, Z., Wang, Y., Li, P., Sun, C., Qin, T., Bai, 2021. Evolution and expression analysis of CDPK genes under drought stress in two varieties of potato. Biotechnol. Lett. 43 (2), 511–521.

Boudsocq, M., Sheen, J., 2013. CDPKs in immune and stress signalling. Trends Plant Sci. 18, 30–40.

Bredow, M., Monaghan, J., 2019. Regulation of plant immune signaling by calcium-dependent protein kinases. Mol. Plant Microbe Interact 32, 6–19.

Cheatham, T.I., Miller, J.L., Fox, T., Darden, T.A., Kollman, T.A., 1995. Molecular dynamics simulations on solvated biomolecular systems: the particle mesh Ewald method leads to stable trajectories of DNA, RNA, and protein. J. Am. Chem. Soc. 117, 4193–4194.

Chen, F., Fasoli, M., Tornielli, G.B., Santo, S.D., Pezzotti, M., Zhang, L., Cai, B., Cheng, Z.M., 2013. The evolutionary history and diverse physiological roles of the grapevine calcium dependent protein kinase gene family. PLoS One 8, e80818. https://doi.org/10.1371/journal.pone.0080818.

Cheng, S.H., Willmann, M.R., Chen, H.C., Sheen, J., 2002. Calcium signaling through protein kinases. The arabidopsis calcium-dependent protein kinase gene family. Plant Physiol. 129, 469–485.

Chou, K.C., Shen, H.B., 2009. Recent advances in developing web-servers for predicting protein attributes. Nat. Sci. 1, 63.

Corpet, F., 1988. Multiple sequence alignment with hierarchical clustering. Nucl. Acids Res. 16, 10881–10890.

Crizel, R.L., Perin, E.C., Vighi, I.L., Woloski, R., Seixas, A., da Silva Pinto, L., Rombaldi, C.V., Galli, V., 2020. Genome-wide identification, and characterization of the CDPK gene family reveal their involvement in abiotic stress response in Fragaria x ananassa. Sci. Rep. 10, 1–17.

DeFalco, T.A., Bender, K.W., Snedden, W.A., 2010. Breaking the code: Ca^{2+} sensors in plant signalling. Biochem. J. 425, 27–40.

Doolittle, R., 1989. Redundancies in protein sequences. In: Fasman, G.D. (Ed.), Prediction of Protein Structure and the Principles of Protein Conformation. Plenum Press, New York, pp. 599–623.

Draffehn, A.M., Meller, S., Li, L., Gebhardt, C., 2010. Natural diversity of potato (*Solanum tuberosum*) invertases. BMC. Plant Biol. 10, 271.

Fantino, E., Segretin, M.E., Santin, F., 2017. Analysis of the potato calcium-dependent protein kinase family and characterization of StCDPK7, a member induced upon infection with Phytophthora infestans. Plant Cell Rep. 36, 1137–1157.

Frattini, M., Morello, L., Breviario, D., 1999. Rice calcium-dependent protein kinase isoforms OsCDPK2 and OsCDPK11 show different responses to light and different expression patterns during seed development. Plant Mol. Biol. 41 (6), 753–764.

Gargantini, P.R., Giammaria, V., Grandellis, C., Feingold, S.E., Maldonado, S., Ulloa, R.M., 2009. Genomic and functional characterization of StCDPK1. Plant Mol. Biol. 70, 153–172.

Giammaria, V., Grandellis, C., Bachmann, S., Gargantini, P.R., Feingold, S.E., Bryan, G., Ulloa, R.M., 2011. *St*CDPK2 expression and activity reveal a highly responsive potato calcium-dependent protein kinase involved in light signalling. Planta 233, 593–609.

Gilman, M., 1987. Phenol/SDS method for plant RNA preparation. In: Ausubel, F.M. (Ed.), Current Protocols in Molecular Biology. John Wiley and Sons, New York, pp. 431–434. et al. (eds).

Grandellis, C., Giammaria, V., Bialer, M., Santin, F., Lin, T., Hannapel, D.J., Ulloa, R.M., 2012. The novel *Solanum tuberosum* calcium dependent protein kinase, StCDPK3, is expressed in actively organs. Planta 236, 1831–1848l.

Gromadka, R., Cieśla, J., Olsza, K., Szczegielniak, J., Muszyńska, G., Polkowska-Kowalczyk, L., 2018. Genome-wide analysis and expression profiling of calcium-dependent protein kinases in potato (*Solanum tuberosum*). Plant Growth Regul. 84, 303–315.

Grossi, C.E.M., Santin, F., Quintana, S.A., Fantino, E., Ulloa, R.M., 2022. Calciumdependent protein kinase 2 plays a positive role in the salt stress response in potato. Plant Cell Rep. 41 (3), 535–548. https://doi.org/10.1007/s00299-021-02676-7 PMID: 33651205.

Gutermuth, T., Lassig, R., Portes, M.T., Maierhofer, T., Romeis, T., Borst, J.W., Hedrich, R., Feijó, J.A., Konrad, K.R., 2013. Pollen tube growth regulation by free anions depends on the interaction between the anion channel SLAH3 and calcium-dependent protein kinases CPK2 and CPK20. Plant Cell 25, 4525–4543.

Harmon, A.C., Gribskov, M., Gubrium, E., Harper, J.F., 2001. The CDPK superfamily of protein kinases. New Phytol. 151, 175–183.

Harper, J.F., Breton, G., Harmon, A.C., 2004. Decoding Ca^{2+} signals through plant protein kinases. Annu. Rev. Plant Biol. 55, 263–288.

Hetherington, A.M., Trewavas, A., 1982. Calcium-dependent protein kinase in pea shoot membranes. FEBS Lett. 145, 67–71.

Ivashuta, S., Liu, J., Lohar, D.P., Haridas, S., Bucciarelli, B., VandenBosch, K.A., Vance, C.P., Harrison, M.J., Gantt, J.S., 2005. RNA interference identifies a calcium-dependent protein kinase involved in *Medicago truncatula* root development. Plant Cell 17, 2911–2921.

Kelley, L.A., Mezulis, S., Yates, C.M., Wass, M.N., Sternberg, M.J., 2015. The Phyre2 web portal for protein modeling, prediction, and analysis. Nat. Protoc. 10, 845–858.

Kobayashi, M., Ohura, I., Kawakita, K., Yokota, N., Fujiwara, M., Shimamoto, K., Doke, N., Yoshioka, H., 2007. Calcium-dependent protein kinases regulate the production of reactive oxygen species by potato NADPH oxidase. Plant Cell 19, 1065–1080.

Kumar, S., Stecher, G., Li, M., Knyaz, C., Tamura, K., 2018. MEGA X: molecular evolutionary genetics analysis across computing platforms. Mol. Biol. Evol. 35, 1547–1549.

Kyte, J., Doolittle, R., 1982. A simple method for displaying the hydropathic character of a protein. J. Mol. Biol. 157, 105–132.

Lee, S.S., Yoon, G.M., Rho, E.J., Moon, E., Pai, H.S., 2006. Functional characterization of NtCDPK1 in tobacco. Mol. Cells 28, 141–146.

Li, Y., Fei, X., Dai, H., Li, J., Zhu, W., Deng, X., 2019. Genome-wide identification of calcium-dependent protein kinases in Chlamydomonas reinhardtii and functional analyses in nitrogen deficiency-induced oil accumulation. Front. Plant Sci. 10, 1147. https://doi.org/10.3389/2Ffpls.2019.01147.

Liese, A., Romeis, T., 2013. Biochemical regulation of *in vivo* function of plant calcium-dependent protein kinases (CDPK). Biochim. Biophys. Acta 1833 (7), 1582–1589.

Liu, H., Che, Z., Zeng, X., Zhou, X., Sitoe, H.M., Wang, H., Yu, D., 2016. Genome-wide analysis of calcium-dependent protein kinases and their expression patterns in response to herbivore and wounding stresses in soybean. Funct. Integr. Genom. 16 (5), 481–493.

Marques, J., Matiolli, C.C., Abreu, I.A., 2022. Visualization of a curated *Oryza sativa* L. CDPKs Protein-Protein Interaction Network (CDPK-OsPPIN). MicroPubl Biol. 10, 17912 /micropub.biology.000513. doi: 10.17912/micropub.biology.000513. PMID: 35098050; PMCID: PMC8792674.

Mittal, S., Mallikarjuna, M.G., Rao, A.R., Jain, P.A., Dash, P.K., Thirunavukkarasu, N., 2017. Comparative analysis of CDPK family in maize, arabidopsis, rice, and sorghum revealed potential targets for drought tolerance improvement. Front. Chem. 5, 115.

Myers, C., Romanowsky, S.M., Barron, Y.D., Garg, S., Azuse, C.L., Curran, A., Davis, R.M., Hatton, J., Harmon, A.C., Harper, J.F., 2009. Calcium-dependent protein kinases regulate polarized tip growth in pollen tubes. Plant J. 59, 528–539.

Raíces, M., Gargantini, P.R., Chinchilla, D., Crespi, M., Téllez-Iñón, M.T., Ulloa, R.M., 2003. Regulation of CDPK isoforms during tuber development. Plant Mol. Biol. 52, 1011–1024.
Romeis, T., Ludwig, A.A., Martin, R., Jones, J.D., 2001. Calcium-dependent protein kinases play an essential role in a plant defence response. EMBO J. 20, 5556–5567.
Roy, A., Kucukural, A., Zhang, Y., 2010. I-TASSER: a unified platform for automated protein structure and function prediction. Nat. Prot. 5, 725.
Sambrook, J., Fritsch, E.F., Maniatis, T., 1989. Molecular Cloning: A Laboratory Manual. Cold Spring Harbor Laboratory Press, New York.
Sanders, D., Pelloux, J., Brownlee, C., Harper, J.F., 2002. Calcium at the crossroads of signaling. Plant Cell 14, S401–S417.
Schuèttelkopf, A.W., Aalten, D.M.F.V., 2004. PRODRG: a tool for high-throughput crystallography of protein-ligand complexes. Acta Crystallo. Sect. D Bio. Crystallo. 60, 1355–1363.
Schultz, J., Copley, R.R., Doerks, T., Ponting, C.P., Bork, P., 2000. SMART: a web-based tool for the study of genetically mobile domains. Nucl. Acids Res. 28, 231–234.
Sharma, M., Choudhury, H., Roy, R., Michaels, A.S., Ojo, K.K., Bansal, A., 2021. CDPKs: the critical decoders of calcium signal at various stages of malaria parasite development. Comput. Struct. Biotechnol. J. 19, 5092–5107.
Sigrist, C.J.A., de Castro, E., Cerutti, L., Cuche, B.A., Hulo, N., Bridge, A., Bougueleret, L., Xenarios, I., 2013. New and continuing developments at PROSITE. Nucl. Acids Res. 41, D344–D347.
Singh, A., Sagar, S., Biswas, D.K., 2017. Calcium dependent protein kinase, a versatile player in plant stress management and development. CRC Crit. Rev. Plant Sci. 36, 336–352.
Singh, D., Ambroise, A., Haicour, R., Sihachakr, D., Rajam, M.V., 2014. Increased resistance to fungal wilts in transgenic eggplant expressing alfalfa glucanase gene. Physiol. Mol. Biol. Plants 20 (2), 143–150.
Tong, T., Li, Q., Jiang, W., Chen, G., Xue, D., Deng, F., Zeng, F., Chen, Z.H., 2021. Molecular evolution of calcium signaling and transport in plant adaptation to abiotic stress. Int. J. Mol. Sci. 22, 12308.
Viola, R., Roberts, A.G., Haupt, S., Gazzani, S., Hancock, R.D., Marmiroli, N., Machray, G.C., Oparka, K.J., 2001. Tuberization in potato involves a switch from apoplastic to symplastic phloem unloading. Plant Cell 13, 385–398.
Wang, D., Liu, Y.X., Yu, Q., Zhao, S.P., Zhao, J.Y., Ru, J.N., Cao, X.Y., Fang, Z.W., Chen, J., Zhou, Y.B., Chen, M., Ma, Y.Z., Xu, Z.S., Lan, J.H, 2019. Functional analysis of the soybean GmCDPK3 gene responding to drought and salt stresses. Int. J. Mol. Sci. 20, 5909.
Wang, J.P., Xu, Y.P., Munyampundu, J.P., Liu, T.Y., Cai, X.Z., 2015. Calcium-dependent protein kinase (CDPK) and CDPK-related kinase (CRK) gene families in tomato: genome-wide identification and functional analyses in disease resistance. Mol. Genet. Genom. 84, 303–315.
Wen, F., Ye, F., Xiao, Z., 2020. Genome-wide survey and expression analysis of calcium-dependent protein kinase (CDPK) in grass Brachypodium distachyon. BMC Genom. 21, 1–17.
Witte, C.P., Keinath, N., Dubiella, U., 2010. Tobacco calcium dependent protein kinases are differentially phosphorylated *in vivo* as part of a kinase cascade that regulates stress response. J. Biol. Chem. 285, 9740–9748.
Xu, X., Liu, M., Lu, L., He, M., Qu, W., Xu, Q., Qi, X., Chen, X., 2015. Genome-wide analysis and expression of the calcium-dependent protein kinase gene family in cucumber. Mol. Genet. Genom. 290, 1403–1414.
Yu, T.F., Zhao, W.Y., Fu, J.D., Liu, Y.W., Chen, M., Zhou, Y.B., Ma, Y.Z., Xu, Z.S., Xi, Y.J., 2018. Genome-wide analysis of CDPK family in foxtail millet and determination of SiCDPK24 functions in drought stress. Front. Plant Sci. 9, 651. https://doi.org/10.3389/fpls.2018.00651.
Zhang, Y., 2008. I-TASSER server for protein 3D structure prediction. BMC Bioinform. 23, 9–40.
Zhao, P., Liu, Y., Kong, W., Ji, J., Cai, T., Guo, Z., 2021. Genome-wide identification and characterization of calcium-dependent protein kinase (CDPK) and CDPK-related kinase (CRK) gene families in Medicago truncatula. Int. J. Mol. Sci. 22, 1044.
Zuo, R., Hu, R., Chai, G., Xu, M., Qi, G., Kong, Y., Zhou, G., 2013. Genome-wide identification, classification, and expression analysis of CDPK and its closely related gene families in poplar (*Populus trichocarpa*). Mol. Biol. Rep. 40, 2645–2662.

Acta Physiologiae Plantarum (2020) 42:10
https://doi.org/10.1007/s11738-019-3002-y

ORIGINAL ARTICLE

Comparison of catalase activity in different organs of the potato (*Solanum tuberosum* L.) cultivars grown under field condition and purification by three-phase partitioning

Gurpreet Kaur[1] · Shweta Sharma[1] · Niranjan Das[1]

Received: 29 March 2019 / Revised: 13 August 2019 / Accepted: 27 December 2019 / Published online: 7 January 2020
© Franciszek Górski Institute of Plant Physiology, Polish Academy of Sciences, Kraków 2020

Abstract
Catalase (CAT) (H_2O_2: H_2O_2 oxidoreductase; EC 1.11.1.6) is capable of directly dismutating moderately reactive H_2O_2 into H_2O and O_2, and is regarded as one of the major enzymatic antioxidants in plants. The CAT isozymes are known to be differentially expressed and regulated. In this study, micropropagated potato plantlets of seven cultivars were grown under field condition with uniform agricultural practices. CAT activities were measured in the crude extracts from different potato organs namely tubers, leaves and stems at different stages of their growth. Relatively higher CAT activity was noticed in the very small actively growing tubers as compared to the other tissues. Cultivar-dependent differences were noticed in terms of the CAT activities which clearly indicated variation with regard to their antioxidative capacities. pH profile, thermostability and storage stability of CAT were examined. A simple and rapid three-phase partitioning (TPP) method worked effectively with regard to purification of CAT from the crude extracts. Both denaturing and non-denaturing PAGE analyses suggested that both the tuber-type and leaf-type CAT are tetrameric in nature and varied in size, possibly referred to the distinct isoforms in potato.

Keywords Potato (*Solanum tuberosum* L.) cultivars · Field condition · Catalase (CAT) · Three-phase partitioning (TPP) · PAGE analyses

Introduction

In plants, aerobic metabolism and different types of stresses such as salinity, drought, extreme temperatures, heavy metals, pollutants, high irradiance, mechanical stress, nutrient deprivation and infection by pathogens lead to generation of the reactive oxygen species (ROS) namely singlet oxygen ($^1O_2$), superoxide anion radical ($O_2^{\cdot -}$), hydrogen peroxide (H_2O_2) and hydroxyl radical ($OH^{\cdot}$) at varying degrees depending on the cell, tissue or organ types. Quantitatively, ROS production is low under normal growth conditions (the rate of $O_2^{\cdot -}$ production is ~ 240 μM s^{-1} with a steady-state level of ~ 0.5 μM H_2O_2 in chloroplasts). However, various stresses disrupt the cellular homeostasis that trigger enhanced production of ROS (production rate of $O_2^{\cdot -}$ ranges from 240 to 720 μM s^{-1} with a steady-state level of 5–15 μM H_2O_2) which causes oxidative damage of various cellular components such as membranes, nucleic acids, proteins, lipids, resulting in cell death (Hammond-Kosack and Jones 1996; Mittler 2002). Currently, ROS are also viewed as signals and secondary messengers involved in stress response, defence and programmed cell death (PCD) (Gapper and Dolan 2006; Mittler 2017). ROS-mediated deleterious effects could be overcome by several enzymatic and non-enzymatic antioxidants. Some enzymatic antioxidants are superoxide dismutases (SODs), catalases (CATs), peroxidases (PRXs), guaiacol peroxidases (GPXs) and glutathione reductase (GR). Ascorbic acid (AA), reduced glutathione (GSH), α-tocopherol, carotenoids, phenolics, flavonoids and proline are the common examples of non-enzymatic

Communicated by P. Wojtaszek.

Electronic supplementary material The online version of this article (https://doi.org/10.1007/s11738-019-3002-y) contains supplementary material, which is available to authorized users.

✉ Niranjan Das
ndas@thapar.edu

[1] Department of Biotechnology, Thapar Institute of Engineering and Technology, Patiala, Punjab 147004, India

antioxidants (Bowler et al. 1991; Foyer and Noctor 2005; Das and Roychoudhury 2014; Choudhury et al. 2017).

Superoxide anion radical ($O_2^{\cdot-}$) is usually the first ROS to be formed in the chloroplasts and other cellular compartments as well. The moderately reactive $O_2^{\cdot-}$ is dismutated into O_2 and H_2O_2 by the metalloenzyme, SOD. H_2O_2, the most frequently occurring ROS, is produced in peroxisomes by oxidases involved in β-oxidation of fatty acids, photorespiration and purine catabolism. It is also produced in mitochondria and chloroplasts. H_2O_2 plays some crucial roles in plant cells that include signal transduction, cell wall lignification and defence against pathogens. CATs, in these organelles essentially eliminate H_2O_2 if produced in excess. Cytosol, endoplasmic reticulum and the nucleus are also the sites of H_2O_2 generation but in small quantities (Scandalios et al. 1997; Fahnenstich et al. 2008; Gill and Tuteja 2010). Due to a significantly longer half-life (~ 1 ms), H_2O_2 is capable of crossing membranes via aquaporins and traverses longer distances within the cell causing oxidative damage (Bienert et al. 2007). H_2O_2 in excess leads to the formation of harmful $OH^{\cdot}$ radicals through decomposition by fenton type of reaction (Cabiscol et al. 2000).

Hydroperoxidases (E.C. 1.11.1.x) represent ubiquitous housekeeping oxidoreductases involved in the various processes of the plant life cycle such as development, defence, ageing and senescence. They include catalases (CAT, H_2O_2: H_2O_2 oxidoreductase; EC 1.11.1.6), ascorbate peroxidase (APX, Ascorbate: H_2O_2 oxido-reductase; EC 1.11.1.1) and other peroxidases where AH_2 refers to an electron donor. Catalases are highly expressed enzymes. In tobacco (*Nicotiana plumbaginifolia)*, CAT was found to be predominantly present in peroxisomes which acted as a sink for H_2O_2 and appeared to be indispensable for stress defence in C_3 plants (Willekens et al. 1997). In *Arabidopsis,* oxidative stress caused the proliferation of peroxisomes (Lopez-Huertas et al. 2000). Most of the prokaryotic and eukaryotic CATs are monofunctional, heme-containing tetramers consisting of polypeptides of M_r ~ 50–70 kDa having very high turnover number. They catalyse very rapid decomposition of H_2O_2 by dismutation with concomitant evolution of molecular oxygen (O_2). Apart from CATs, the ascorbate–glutathione cycle and APX are also important in controlling the level of ROS in almost all the cellular compartments. CAT shows significantly lower affinity for H_2O_2 as compared to APX and other peroxidases as evident from the respective K_m values, i.e., at mM and µM range, respectively (Mittler 2002). It is now commonly agreed that APX contributes towards fine modulation of H_2O_2 level required for signalling pathways; whereas, CAT is responsible for the removal of the excess formed during stresses (Klotz and Loewen 2003; Zamocky et al. 2008; Mhamdi et al. 2010). Multiple isoforms of CAT are found in plants, they are coded by several genes as found in cucumber, *Arabidopsis*, tobacco, maize, pumpkins, cottonseed and barley (Hu et al. 2016). The catalase isoforms show distinct expression patterns under abiotic stresses suggesting their protective role in plant defence (Guan and Scandalios 1996; Zimmermann et al. 2006; Du et al. 2008; Su et al. 2014).

Potato (*Solanum tuberosum* L.) is a member of the *Solanaceae* family. Most of the potato cultivars are autotetraploid ($2n = 4x = 48$) and highly heterozygous. Therefore, it is likely that the individual genes involved in ROS metabolism have multiple forms depending on the cultivar genotype. Considerable progress has been made on CAT and other antioxidants in potato to date. Beaumont et al. (1990) isolated and purified CAT, a tetramer of 56 kDa subunits and devoid of NADPH, from peroxisomal fraction of mature potato tubers. Cyanide, azide and thiols were found to act as inhibitors of this enzyme. Cultivar-dependent differences of antioxidative capacity in terms of SOD, CAT and α-Tocopherol content under stresses were also reported in potato tubers (Spychalla and Desborough 1990). The distinct expression patterns of various antioxidant enzymes were noticed during tuber dormancy and oxidative stress due to soil drought (Rojas-Beltran et al. 2000; Boguszewska et al. 2010). These reports clearly suggest that the level of various ROS and antioxidants had influence on different stages of the potato life cycle, such as vegetative growth, tuberization, tuber dormancy and sprouting under normal and stress conditions.

There are number of high-yielding and commercially important Indian potato cultivars suitable to different agro-climatic zones of the Indian subcontinent (Kumar et al. 2014). There is no comprehensive report available to date with regard to enzymatic and non-enzymatic antioxidants in different organs of the individual cultivars at biochemical and molecular level. This study focused on the determination of CAT, a major enzymatic antioxidant, activities in the crude protein extracts of the growing and mature tubers along with other organs, namely leaf and stem grown under field condition. The purpose was to assess and compare the CAT activities between the different organs of the potato cultivars, followed by the analyses of pH profile, thermo and storage stability. Currently, three-phase partitioning (TPP) has gained considerable importance with regard to isolation, purification and concentration of protein/enzyme and other bioactive molecules from different sources without compromising the activity and yield (Özer et al. 2010; Duman and Kaya 2013; Yan et al. 2017). Keeping this in mind, the various process parameters of the TPP method were examined and adopted for purification and characterization of CAT from the crude extracts.

Materials and methods

Plant materials, growth conditions and reagents

Some of the Indian potato cultivars namely Kufri Chipsona-1 (KC-1), Kufri Chipsona-2 (KC-2), Kufri Chandramukhi (KCh), Kufri Jyoti (KJy), Kufri Ashoka (KAs) and Kufri Pukhraj (KPu) are routinely maintained in our laboratory. The former two are processing varieties. KCh and KAs are early maturing; whereas, the other cultivars are medium maturing. These high-yielding and commercially important varieties were procured earlier from Central Potato Research Institute (CPRI), Shimla, India. They vary with regard to genetic make-up, maturation time, disease resistance, tuber yield and quality. They grow under different agro-climatic conditions of the Indian subcontinent. All these cultivars along with Desiree (De), a reference cultivar, were routinely micropropagated at 25–27 °C, ~ 70% relative humidity under 16 h photoperiod with a light intensity of 40–42 mmol m^{-2} s^{-1} spectral flux photon of photo-synthetically active (460–700 nm) radiations on MS-basal medium with 2.5% sucrose at 4–5 week intervals. The potato plantlets were acclimatized prior to cultivation in the field for nearly 15 weeks (mid of November to end of February). Different organs, namely tuber, leaf and stem were collected at various stages of growth and stored at − 80 °C till further use. Chemicals and enzymes were procured from Sigma-aldrich Pvt. Ltd, SRL and HiMedia Laboratories, India.

Preparation of crude organ extracts

The crude extracts were made from different potato organs following the protocol as described earlier (Kandukuri et al. 2012; Duman and Kaya 2013). Briefly, approx. 3.0 g of tubers (peels were removed), leaves and stems of the individual potato cultivars were cut into small pieces and pulverized to fine powder in liquid nitrogen; then homogenized in 10 mL of 50 mM phosphate buffer, pH 7.0 with 8% PVP, 10 mM PMSF, 0.1 mM EDTA and 30 mM KCl into a fine paste using mortar and pestle. The homogenate was filtered through three layers of cheesecloth, and then centrifuged at 10,000 *g* for 20 min at 4 °C and the clear supernatant was collected and used for quantification of total protein, CAT assay and analyses of its thermostability, pH profile and storage stability.

Quantification of total protein

Total protein contents of the individual organ extracts were determined by Folin–Ciocalteau method (Lowry et al. 1951) using bovine serum albumin (BSA) as the standard.

Assay of catalase activity

CAT activity was determined by measuring a decrease in the absorbance of H_2O_2 at 240 nm as described earlier (Aebi 1984; Miyagawa et al. 2000). The CAT activity was measured on the basis of the difference in absorbance (ΔA_{240}) per unit of time. 30 µL of crude enzyme extract was taken in a total reaction volume of 3.0 mL having the following composition: 10 mM H_2O_2 in 50 mM phosphate buffer (pH 7.0). One unit of activity is defined as the amount of enzyme which catalyses the decomposition of 1.0 µmol of H_2O_2 per min at pH 7.0 and 25 °C as calculated from the extinction coefficient for H_2O_2 at 240 nm of 39.4 M^{-1} cm^{-1}.

pH profile, thermostability and storage stability

All these parameters related to CAT were examined using crude extract from mature tubers of the potato cultivar KC-1 along with the exotic cultivar De. To see the effect of pH on the activity, CAT assay was carried out at various pH values ranging from 3.0 to 9.0 using the following buffer systems: 50 mM sodium acetate buffer (pH 3.0, 4.0 and 5.0) and 50 mM sodium phosphate buffer (pH 6.0, 7.0, 8.0 and 9.0). Prior to CAT assay, each 30 µL aliquot of the crude extract was mixed in 1.0 mL of each buffer, kept overnight at 4 °C to determine both stability and optimum pH as well. Thermostability refers to the ability of an enzyme to resist thermal unfolding in the absence of its substrate (Özer et al. 2010). To determine the temperature dependence of CAT activity, 30 µL aliquots of the crude extract were taken in the individual reaction mixtures (pH 7.0) and incubated in water bath at different temperatures ranging from 10 to 70 °C (10, 20, 30, 40, 50, 60, and 70 °C) for 60 min. Enzyme activity was determined under the standard assay condition as described above. For storage stability, each 30 µL aliquot of the crude extract was mixed in 1.0 mL of 50 mM phosphate buffer (pH 7.0) and stored at 4 °C. CAT assay was performed every day for a week and the data were recorded.

Three-phase partitioning (TPP)

Three-phase partitioning (TPP) method was employed for purification of CAT from the crude extracts prepared from mature potato tuber and leaf organs as described by Dennison and Lovrien (1997). Prior to purification of CAT by TPP method, some of the crucial process parameters namely ammonium sulphate saturation, extract to t-butanol ratio,

temperature and pH were evaluated (data not shown). Saturation with 40% (w/v) ammonium sulphate and crude extract to t-butanol in 1:1 (v/v) ratio at 25 °C were found to be effective and applicable to different organ extracts as CAT accumulation occurred maximally only at interfacial phase. Briefly, the crude extract was saturated with 40% (w/v) ammonium sulphate at 25 °C, and vortexed gently to dissolve the salt followed by addition of t-butanol in 1:1 (v/v) ratio to the mixture, then vortexed gently and incubated at 25 °C for 60 min. The mixture was centrifuged at 4500 × *g* for 5 min at 4 °C to ensure the separation of phases. The upper t-butanol layer was removed; the middle interfacial precipitate containing CAT was collected carefully in a separate tube, then dissolved in 1.0 mL of 50 mM phosphate buffer (pH 7.0), and finally used for CAT assay and total protein content. Likewise, the lower aqueous layer i.e., bottom phase was collected and analysed.

Statistical analysis

Each of the CAT assays in different organ extracts and other biochemical experiments as described above was carried out in triplicate and the data were presented as the Mean ± SD of $n = 3$ independent experiments. Standard deviation and mean values were calculated using SPSS software of IBM. Statistical differences between the means of CAT activities in the potato organs were calculated using one-way analysis of variance (ANOVA) for a significance level of 0.05.

Denaturing and native polyacrylamide gel electrophoresis (PAGE)

Proteins in the TPP-purified extracts were resolved through both denaturing SDS-PAGE and non-denaturing native PAGE on the basis of their electrophoretic mobility (a function of length of polypeptide chain or molecular weight) using 7.5% polyacrylamide gel according to the procedures as described earlier (Laemmli 1970; Schägger and Jagow 1991). Approx. 20 µg of protein was loaded in each lane and the protein bands were visualized by staining the gel with Coomassie brilliant blue R-250 for 1 h followed by destaining using the mixture containing 40% methanol and 10% acetic acid for 2–3 h.

Results and discussion

Catalase activity in different organ tissues

ROS metabolism plays a crucial role in a plant's life cycle under both normal and stress conditions. Thorough studies on the individual components of the antioxidant machinery only can help in understanding such metabolic aspects properly. Activities of some major enzymatic antioxidants like SODs, CATs and/or PRXs along with sequestration of metal ions are crucial for maintaining the normal steady-state $O_2^{\cdot -}$:H_2O_2 ratio. Several stresses perturb such ratio causing overproduction of ROS, H_2O_2 in particular, where CATs become indispensable for detoxification (Bowler et al. 1991; Mittler 2002; Choudhury et al. 2017). Cat1-defecient tobacco plants showed enhanced sensitivity towards stresses, including cell death under certain conditions (Willekens et al. 1997). ROS play a dual role in plants. At low concentrations, H_2O_2 acts as a signal molecule; whereas, at high concentrations, it causes extensive damage to cellular components. As ROS are beneficial to plants, various antioxidative systems of the cell, including CAT, keep ROS at a basal non-toxic level (Gill and Tuteja 2010; Mittler 2017). Various non-enzymatic and enzymatic antioxidants are found in the stored potato tubers (Spychalla and Desborough 1990). Tuber development i.e., from initiation of stolons to maturation of tubers, is a complex process associated with a multitude of cellular, morphological and biochemical changes (Rojas-Beltran et al. 2000; Boguszewska et al. 2010). The specific role of ROS metabolism and signalling associated with such biological processes are yet to be clearly understood in potato and other plants. The activities of the individual antioxidants in different organs are likely to reflect their antioxidative potential to combat various stresses. This study focused on determining CAT activities in different potato organs including tubers at various stages of growth under field condition.

After acclimatization, the disease-free potato plantlets were grown under field condition in the central plain zone of Punjab, a North-Western state of India, having temperate climate and different organs were collected as shown in Fig. 1. CAT activity was measured in the tubers at different stages of growth and found to vary significantly between some of the cultivars depending on their genotypes (Table 1). In the cultivars namely KC-1 and KPu, CAT activities were found to be comparable at different stages of tuber growth i.e., from early growing to maturation; whereas, there was a gradual decrease in CAT activity in the cases of KAs and De. Actively growing very small tubers showed relatively higher CAT activity, an attribute found to be a common feature in the potato cultivars with a maximum value noticed in KAs followed by De. Higher CAT activity could be a sign of defence against ROS produced in the metabolically active early growing tubers which needs to be clearly understood. CAT activity was also determined in other potato organs, namely leaf and stem, as shown in Table 2. CAT activity was found to be lower in the leaves in comparison to the growing tubers. Young and fully-expanded mature leaves of each cultivar did not differ significantly with regard to CAT activity. It is likely that a steady CAT level is required in the leaves for active defence against ROS generated by

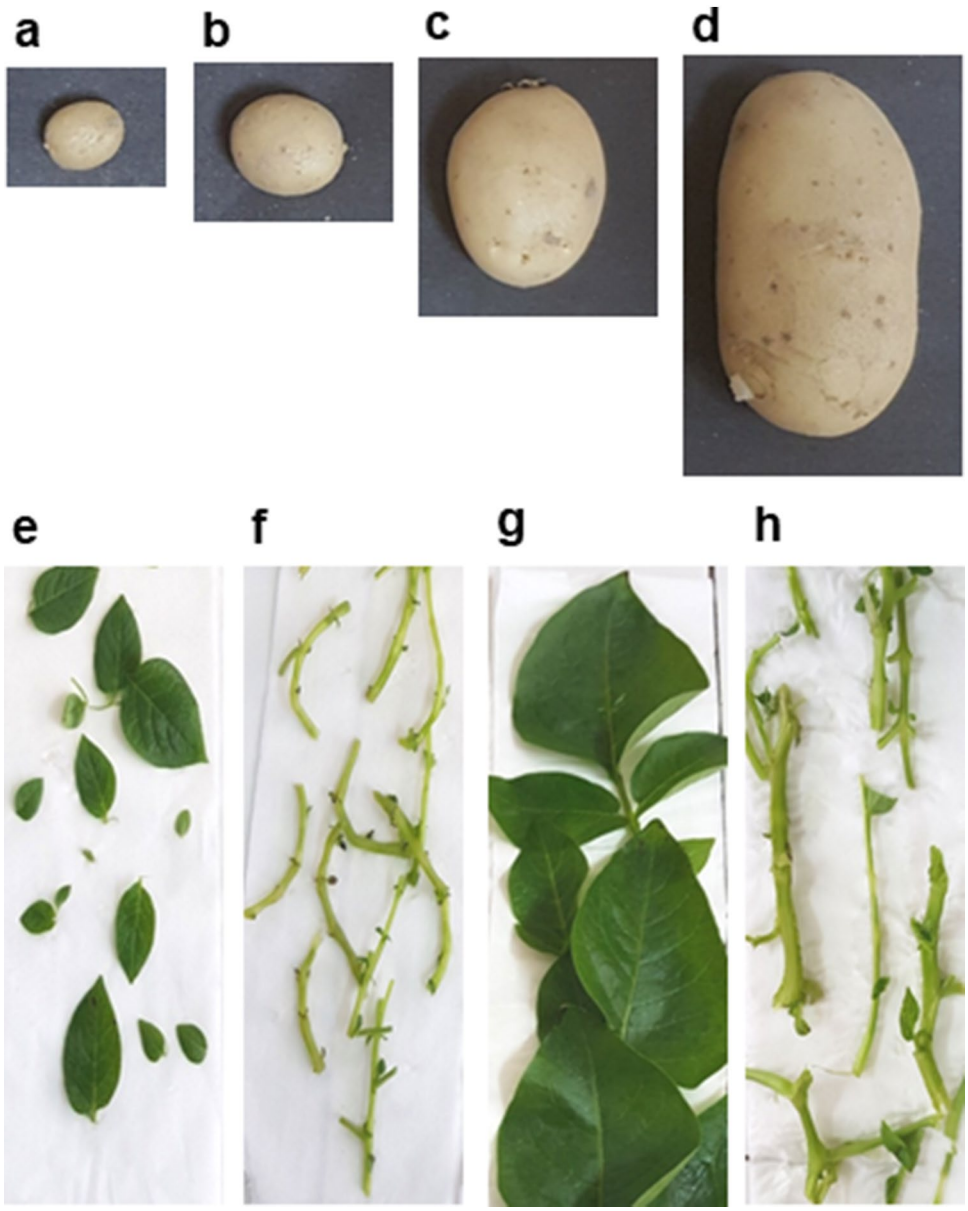

Fig. 1 Morphology of different organs of the potato cultivar KC-1 grown under field condition. Tubers at various stages of growth: **a** very small, **b** small, **c** medium, and **d** large or mature; **e** young leaf, **f** young stem, **g** fully-expanded mature leaf, **h** mature stem

Table 1 Comparison of catalase activity in the tubers of the potato cultivars at different stages of growth under field condition (the experimental data are presented as mean ± SD of $n = 3$ tuber extracts)

Potato cultivars	Catalase activity (μmol H_2O_2/min per mg protein)			
	Very small (1–3 g)	Small (4–7 g)	Medium (8–13 g)	Large (15–20 g)
Kufri Chipsona-1	921 ± 16	800 ± 18	899 ± 22	951 ± 16
Kufri Chipsona-2	593 ± 10	462 ± 20	400 ± 8	373 ± 10
Kufri Pukhraj	799 ± 26	666 ± 21	683 ± 18	709 ± 17
Kufri Chandramukhi	800 ± 9	708 ± 13	695 ± 12	601 ± 14
Kufri Jyoti	437 ± 21	293 ± 23	776 ± 10	586 ± 17
Kufri Ashoka	1577 ± 13	1399 ± 17	973 ± 15	818 ± 11
Desiree	1144 ± 21	937 ± 29	858 ± 18	758 ± 16

photorespiration and aerobic metabolism. The mature stems of the cultivars showed significantly lower CAT activity as compared to the other organs which suggested that the highly vascular and differentiated stems could be associated with lower antioxidative capacity. Differential expression patterns of several CAT isoforms were reported in tobacco,

Table 2 Comparison of catalase activity in the growing and mature leaf and stem tissues of the potato cultivars grown under field condition (the experimental data are presented as mean ± SD of $n = 3$ organ tissue extracts)

Potato cultivars	Catalase activity (μmol H_2O_2/min per mg of protein)			
	Growing organ		Mature organ	
	Leaf	Stem	Leaf	Stem
Kufri Chipsona-1	846 ± 23	254 ± 24	951 ± 22	170 ± 19
Kufri Chipsona -2	236 ± 10	137 ± 14	370 ± 16	189 ± 16
Kufri Pukhraj	220 ± 11	339 ± 21	267 ± 14	411 ± 19
Kufri Chandramukhi	504 ± 20	499 ± 16	559 ± 13	248 ± 21
Kufri Jyoti	454 ± 19	427 ± 20	586 ± 17	264 ± 16
Kufri Ashoka	311 ± 9	312 ± 16	574 ± 22	418 ± 19
Desiree	945 ± 21	439 ± 16	501 ± 14	335 ± 15

potato and other plants. Unlike other organs, stem showed mainly the expression of Class II catalases (Willekens et al. 1994; Rojas-Beltran et al. 2000). Multiple isoforms of CAT including Class II possibly contributed to higher CAT activity in the leaves and other organs in comparison to the stem.

In potato, considerable progress has been made on CAT since its purification and characterization from tuber peroxisomes (Beaumont et al. 1990). Stressful situation like prolonged storage of the tubers at low temperatures resulted in time dependent increases of SOD, CAT and α-Tocopherol contents clearly indicative of protection against enhanced ROS production. Cultivar-dependent differences were also noticed in terms of their antioxidant contents (Spychalla and Desborough 1990). Expression patterns and activity of several antioxidant enzymes including CAT during tuber dormancy were reported. Low CAT levels in the dormant tubers probably helps in gradual accumulation of H_2O_2-a prerequisite for sprouting (Rojas-Beltran et al. 2000). Tuberization in potato is a complex developmental process influenced by a number of factors such as photoperiod, temperature, nitrogen nutrition and endogenous levels of the phytohormones (Sarkar 2008). A comparative proteomic approach was adopted to monitor differentially expressed proteins during tuber development. The expression of the ROS catabolizing enzymes such as SOD, APX and CAT was significantly increased during transition from stolons to tubers which clearly indicated active cellular defence during growth and development. In other words, the developing tubers are inherently associated with active antioxidative machinery to combat stresses (Agrawal et al. 2008). Various stresses as mentioned earlier adversely affect growth, development and productivity and may even lead to huge crop loss (Lawlor 2002). Enhanced activities of some antioxidant enzymes, including CAT isozymes, were reported in potato under salt stress (Rahnama and Ebrahimzadeh 2005). Boguszewska et al. (2010) carried out experiments with some potato cultivars sensitive to soil drought and other stresses. Increased activity of antioxidative enzymes like POX, SOD and CAT was considered to play a protective role under oxidative stress and in turn prevented yield losses.

In plants, various factors like the genetic composition (G), the environment (E) and importantly the interactions between them ($G \times E$) have profound influence on their growth, development, fitness, performance, adaptation and other physiological aspects. A particular species with different genotypes respond differently by exposure to the same environmental factors (El-Soda et al. 2014). This explains why the different potato cultivars are adaptive to various agro-climatic zones and vary with regard to several attributes such as vegetative growth, maturation time, tuber yield and quality, tuber dormancy, sprouting and tolerance to various biotic and abiotic stresses depending on the genotypes (Kumar et al. 2014). Soil properties and climatic conditions influence the productivity of a crop. The potato plants under study were grown in the sandy-loam soil during mid of November to the end of February. Usually extreme cold conditions prevail during January to mid-February with a temperature range of 5–10 °C. Duration of photoperiod, fluctuations between day and night temperatures, soil moisture and nutrient contents potentially impose stresses during vegetative growth of potato (Demagante and Vander Zaag 1988; Romero et al. 2017). The cultivar-dependent differences of CAT activities of different potato organs, including tubers at various stages of growth appeared to be quite consistent with the earlier studies. The data also indicated a variation of their antioxidative potential under field condition depending on the genotypes. The potato cultivars are likely to show varying tolerance towards oxidative stress. Moreover, relatively low CAT activity was found in the freshly harvested mature tubers i.e., large tubers reflecting the state of dormancy as evident in the earlier report (Rojas-Beltran et al. 2000).

Effects of pH, temperature and storage

pH profile, thermostability and storage stability are important biochemical attributes of an enzyme. For such studies, crude enzyme extracts from the mature tubers of KC-1 and De were used. The relative activities (%) were calculated based on the ratio of the CAT activity obtained at certain condition to the maximum activity obtained at the range of same condition. The effect of pH on CAT activity was determined and is shown in Fig. 2. The optimum pH was found to be 7.0 which coincides with the biological pH. The CAT activity is drastically reduced at pH 3.0 or below and 9.0 or above. The data clearly indicated that the surrounding pH has a profound influence on the net charge of an enzyme hence its overall conformation and enzymatic performance. As evident in the literature, CAT assay is usually carried

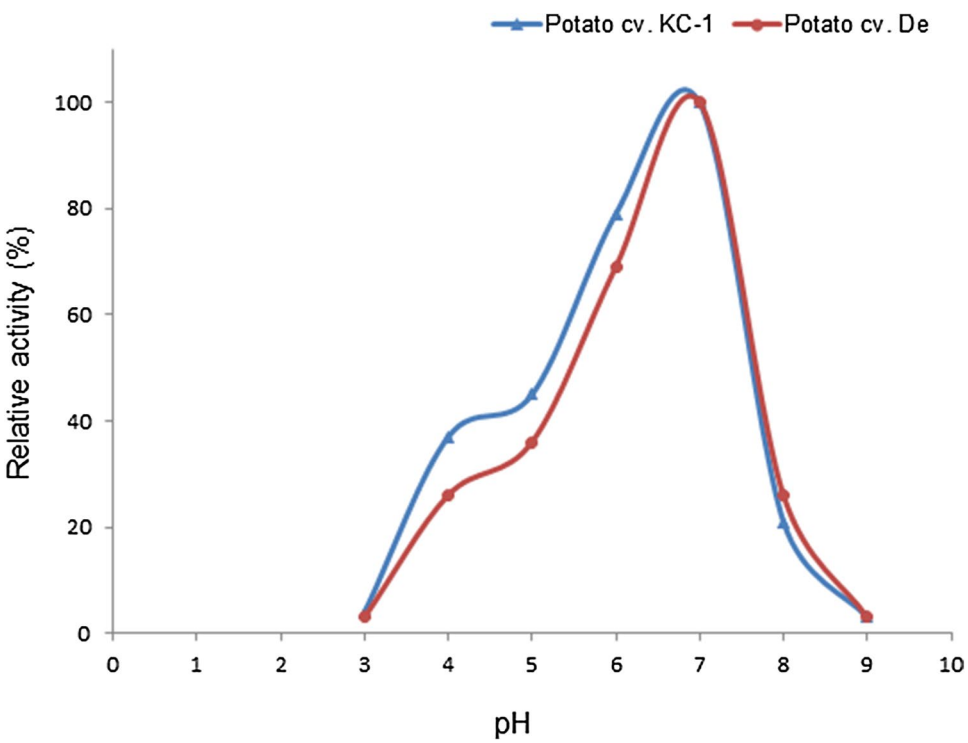

Fig. 2 Effect of pH on CAT activity in the crude tuber extracts

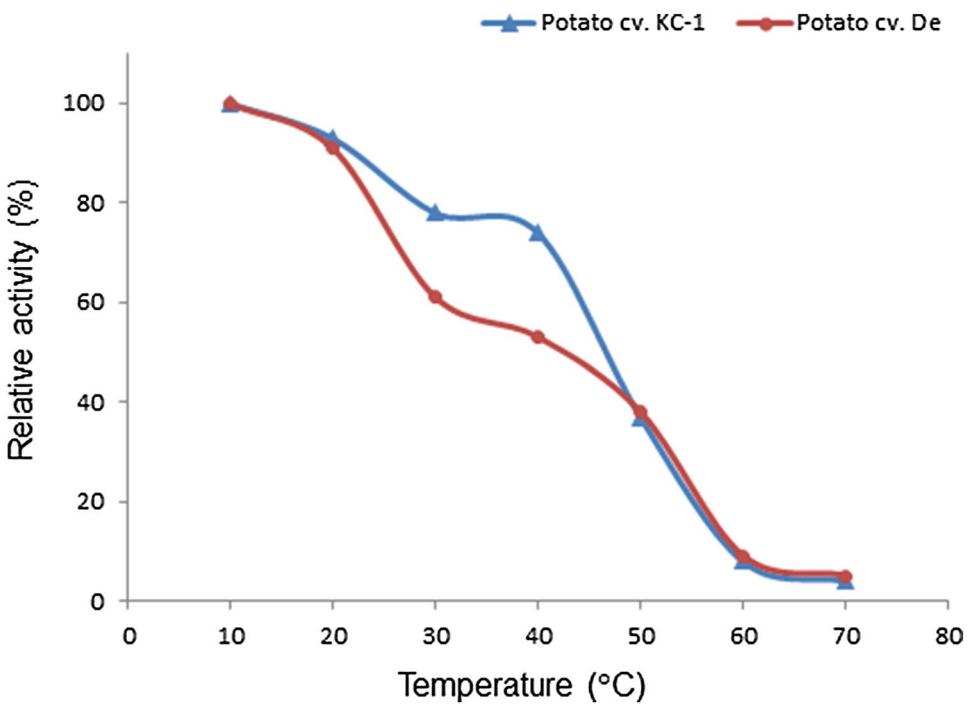

Fig. 3 Effect of temperature on CAT activity in the crude tuber extracts

out at 25–30 °C (Aebi 1984; Kawakami et al. 2000). To understand the thermostability of CAT, equal aliquots of the crude protein extract were incubated at different temperatures i.e., 10–70 °C for 1 h prior to standard assay. The results as shown in Fig. 3 clearly indicated that CAT activity remained stable at low temperature i.e., below 20 °C. The CAT activity was significantly compromised at 50 °C and above very likely due to enzyme inactivation. The surrounding temperatures have profound influence on the overall three-dimensional conformation of an enzyme and its catalytic efficiency. Loss of CAT function at higher temperatures, possibly due to deviation from its stable tetrameric

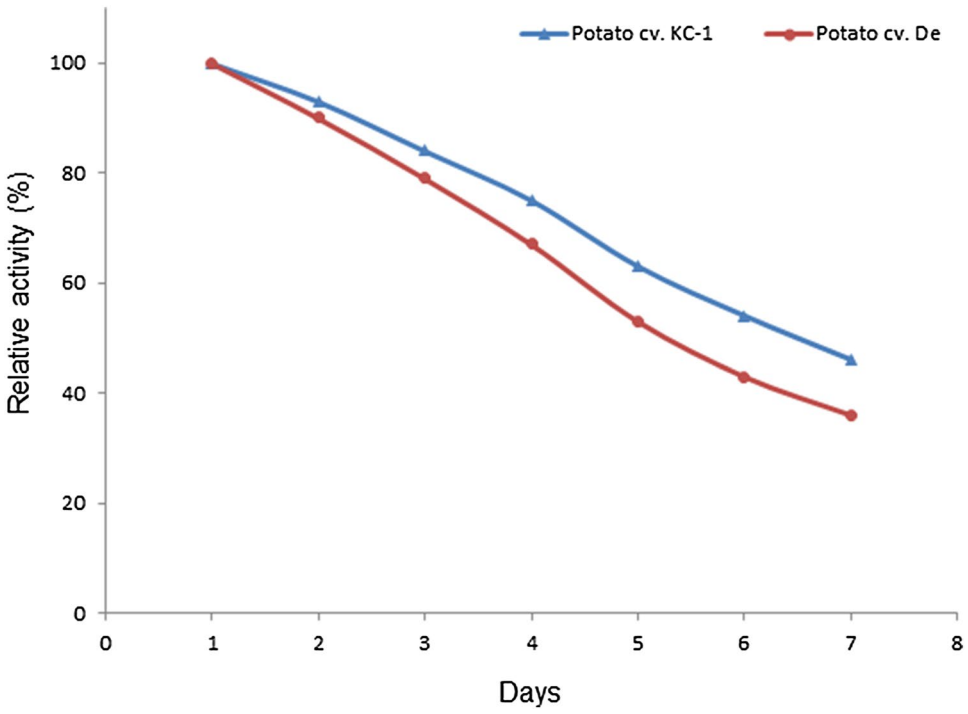

Fig. 4 Storage stability of CAT in the crude tuber extracts

structure, are found to be consistent with earlier reports (Kandukuri et al. 2012). There was no significant change of CAT activity in the crude extract if kept at 4 °C up to 3 days for both the potato cultivars suggesting considerable storage stability of this enzyme (Fig. 4).

Purification of catalase by three-phase partitioning (TPP)

TPP method relies on the principles of salting out, isoionic and cosolvent precipitation (Dennison and Lovrien 1997; Saxena et al. 2007). In this method, water soluble proteins/enzymes separate into the intermediate phase helping isolate and concentrate proteins. The TPP purification step of the crude potato organ extracts is shown in supplementary Fig. S1. Purification and recovery profile of CAT corresponding to the cultivars KC-1 and De are shown in Table 3. With regard to interfacial phase, CAT recovery up to 179% with 3.81 folds of purification was observed in the case of KC-1 leaf. Some degree of altered conformational and solvation state of the enzyme purified by this method possibly contributed to such enhanced CAT activities as proposed earlier (Kiss et al. 1998). Moreover, the data appeared to be consistent with other published reports (Özer et al. 2010; Duman and Kaya 2013) and clearly indicated that the TPP method had worked efficiently for the crude protein extracts from different potato organs which differed considerably with regard to storage biomolecules and other metabolites.

Table 3 Purification and recovery profile of catalase (CAT) from mature organs of the potato cultivars by three-phase partitioning (TPP)

Potato tissue	Step	Total activity (U)	Total protein (mg)	Specific activity (U/mg)	Purification (fold)	Recovery (%)
Tuber (KC-1)	Crude extract	566	0.71	797	1.00	100
	Interfacial phase of TPP	761	0.25	3044	3.82	134
Leaf (KC-1)	Crude extract	253	0.34	744	1.00	100
	Interfacial phase of TPP	453	0.16	2831	3.81	179
Tuber (De)	Crude extract	812	0.87	933	1.00	100
	Interfacial phase of TPP	1065	0.30	3550	3.80	131
Leaf (De)	Crude extract	312	0.33	945	1.00	100
	Interfacial phase of TPP	408	0.15	2720	2.87	131

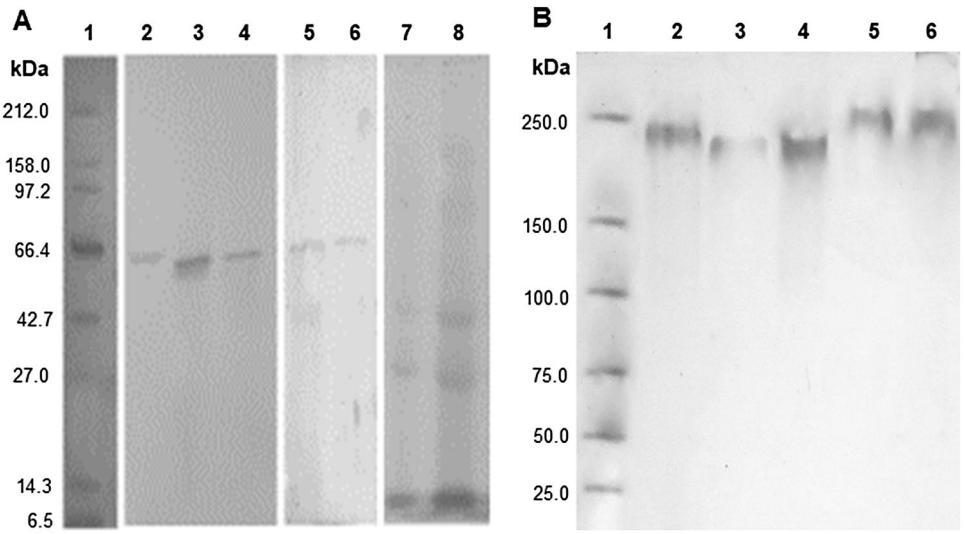

Fig. 5 Polyacrylamide gel electrophoresis of TPP-purified catalase (CAT) extract from the potato organs. **a** Denaturing SDS-PAGE; *lane 1*, protein molecular weight markers; *lane 2*, CAT from bovine liver; *lanes 3* and *4*, from the tubers of KC-1 and De, respectively; *lanes 5* and *6*; from the leaves of KC-1 and De, respectively; *lanes 7* and *8*, crude extracts from tuber and leaf of KC-1, respectively; **b** Non-denaturing PAGE; *lanes 1* to *6*, loading patterns were same as presented in **a**

Polyacrylamide gel electrophoresis (PAGE)

The TPP purified protein extracts were analysed by both denaturing SDS-PAGE and non-denaturing PAGE as shown in Fig. 5. The purified tuber extract appeared to be homogenous in SDS-PAGE with a molecular weight nearly 60 kDa, whereas the size was ~ 240 kDa as found in native PAGE suggesting it as a tetramer. This observation is consistent with the reported data on CAT from the peroxisomal fraction of mature potato tuber (Beaumont et al. 1990). As evident from the difference in mobility, the size of CAT corresponding to leaf appeared to be larger in comparison to tuber CAT. Tuber-type and leaf-type CAT as observed probably refer to the distinct isoforms in potato; their expression patterns and other attributes remain unclear.

Conclusions

In potato, soil drought and other stresses are known to adversely affect the vegetative growth, yield and quality of the tubers. In this study, a total of seven potato cultivars were allowed to grow under field condition—a situation where a growing plant had to face a multitude of stresses during its life span because of fluctuations in environmental conditions despite of the conventional and more or less uniform agricultural practices. Various antioxidants are likely to be involved to combat oxidative stress for the growth and survival of plants. Several biochemical attributes of CAT like pH profile, thermostability and storage stability as presented in this report were not available in potato earlier. Variation in CAT activities could be considered as an indicator of the cultivar-dependent differences with regard to their antioxidative capacities under field condition. Very likely, both the genotype (G) and gene-environment ($G \times E$) interactions contribute to varying stress tolerance between the individual cultivars. This could explain, at least partially, why these cultivars are suitable to different agro-climatic zones in the Indian subcontinent. Such data could be useful in developing stress-tolerant varieties through crop breeding. Purification of CAT from the crude protein extracts by TPP method to almost homogeneity is also an important aspect of this study. Tuber-type and leaf-type CAT were found to vary with regard to their size as evident from PAGE analysis.

Author contribution statement GK contributed significantly in designing and execution of the experiments, data analysis, compilation of the results and manuscript preparation; SS contributed to some of the experiments and compilation of data; ND provided scientific advice and discussions, analysed the results, corrected and revised the manuscript.

Acknowledgements We gracefully thank UGC, Government of India, for providing UGC:MAN Fellowship to G. Kaur.

Compliance with ethical standards

Conflict of interest The authors declare no conflict of interest.

Human and animal rights statement This study did not involve human participants and/or animals.

References

Aebi H (1984) Catalase in vitro. Methods Enzymol 105:121–126
Agrawal L, Chakraborty S, Jaiswal DK, Gupta S, Datta A, Chakraborty N (2008) Comparative proteomics of tuber induction, development and maturation reveal the complexity of tuberization process in potato (*Solanum tuberosum* L.). J Proteome Res 7:3803–3817

Beaumont F, Jouve H-M, Gagnon J, Gaillard J, Pelmont J (1990) Purification and properties of a catalase from potato tubers (*Solanum tuberosum*). Plant Sci 72:19–26

Bienert GP, Møller ALB, Kristiansen KA, Schulz A, Møller IM, Schjoerring JK, Jahn TP (2007) Specific aquaporins facilitate the diffusion of hydrogen peroxide across membranes. J Biol Chem 282:1183–1192

Boguszewska D, Grudkowska M, Zagdańska B (2010) Drought-responsive antioxidant enzymes in potato (*Solanum tuberosum* L.). Pot Res 53:373–382

Bowler C, Slooten L, Vandenbranden S, Rycke RD, Botterman J, Sybesma C, Montagu MV, Inzé D (1991) Manganese superoxide dismutase can reduce cellular damage mediated by oxygen radicals in transgenic plants. EMBO J 10:1723–1732

Cabiscol E, Tamarit J, Ros J (2000) Oxidative stress in bacteria and protein damage by reactive oxygen species. Int Microbiol 3:3–8

Choudhury FK, Rivero RM, Blumwald E, Mittler R (2017) Reactive oxygen species, abiotic stress and stress combination. Plant J 90:856–867

Das K, Roychoudhury A (2014) Reactive oxygen species (ROS) and response of antioxidants as ROS-scavengers during environmental stress in plants. Front Environ Sci 2:53. https://doi.org/10.3389/fenvs.2014.00053

Demagante AL, Vander Zaag P (1988) The response of potato (*Solanum* spp.) to photoperiod and light intensity under high temperatures. Pot Res 31:73–83

Dennison C, Lovrien R (1997) Three phase partitioning: concentration and purification of proteins. Protein Expres Purif 11:149–161

Du Y-Y, Wang P-C, Chen J, Song C-P (2008) Comprehensive functional analysis of the catalase gene family in *Arabidopsis thaliana*. J Integr Plant Biol 50:1318–1326

Duman YA, Kaya E (2013) Three-phase partitioning as a rapid and easy method for the purification and recovery of catalase from sweet potato tubers (*Solanum tuberosum*). Appl Biochem Biotechnol 170:1119–1126

El-Soda M, Malosetti M, Zwaan BJ, Koornneef M, Aarts MGM (2014) Genotype x environment interaction QTL mapping in plants: lessons from *Arabidopsis*. Trends Plant Sci 19:390–398

Fahnenstich H, Scarpeci TE, Valle EM, Flügge U-I, Maurino VG (2008) Generation of hydrogen peroxide in chloroplasts of Arabidopsis overexpressing glycolate oxidase as an inducible system to study oxidative stress. Plant Physiol 148:719–729

Foyer CH, Noctor G (2005) Redox homeostasis and antioxidant signaling: a metabolic interface between stress perception and physiological responses. Plant Cell 17:1866–1875

Gapper C, Dolan L (2006) Control of plant development by reactive oxygen species. Plant Physiol 141:341–345

Gill SS, Tuteja N (2010) Reactive oxygen species and antioxidant machinery in abiotic stress tolerance in crop plants. Plant Physiol Biochem 48:909–930

Guan L, Scandalios JG (1996) Molecular evolution of maize catalases and their relationship to other eukaryotic and prokaryotic catalases. J Mol Evol 42:570–579

Hammond-Kosack KE, Jones JDG (1996) Resistance gene-dependent plant defense responses. Plant Cell 8:1773–1791

Hu L, Yang Y, Jiang L, Liu S (2016) The catalase gene family in cucumber: genome-wide identification and organization. Genet Mol Biol 39:408–415

Kandukuri SS, Noor A, Ranjini SS, Vijayalakshmi MA (2012) Purification and characterization of catalase from sprouted black gram (*Vigna mungo*) seeds. J Chromatogr B 889–890:50–54

Kawakami S, Mizuno M, Tsuchida H (2000) Comparison of antioxidant enzyme activities between *Solanum tuberosum* L. cultivars Danshaku and Kitaakari during low-temperature storage. J Agric Food Chem 48:2117–2121

Kiss É, Szamos J, Tamás B, Borbás R (1998) Interfacial behavior of proteins in three-phase partitioning using salt-containing water/*tert*-butanol systems. Colloids Surf A Physicochem Eng Aspects 142:295–302

Klotz MG, Loewen PC (2003) The molecular evolution of catalatic hydroperoxidases: evidence for multiple lateral transfer of genes between prokaryota and from bacteria into eukaryota. Mol Biol Evol 20:1098–1112

Kumar V, Luthra SK, Bhardwaj V, Singh BP (2014) Indian potato varieties and their salient features. CPRI Technical Bulletin No. 78 (revised), ICAR-Central Potato Research Institute, Shimla, Himachal Pradesh, India

Laemmli UK (1970) Cleavage of structural proteins during the assembly of the head of bacteriophage T4. Nature 227:680–685

Lawlor DW (2002) Limitation to photosynthesis in water-stressed leaves: stomata vs. metabolism and the role of ATP. Ann Bot 89:871–885

Lopez-Huertas E, Charlton WL, Johnson B, Graham IA, Baker A (2000) Stress induces peroxisome biogenesis genes. EMBO J 19:6770–6777

Lowry OH, Rosebrough NJ, Farr AL, Randall RJ (1951) Protein measurement with the folin phenol reagent. J Biol Chem 193:265–275

Mhamdi A, Queval G, Chaouch S, Vanderauwera S, Breusegem FV, Noctor G (2010) Catalase function in plants: a focus on *Arabidopsis* mutants as stress-mimic models. J Expt Bot 61:4197–4220

Mittler R (2002) Oxidative stress, antioxidants and stress tolerance. Trends Plant Sci 7:405–410

Mittler R (2017) ROS are good. Trends Plant Sci 22:11–19

Miyagawa Y, Tamoi M, Shigeoka S (2000) Evaluation of the defense system in chloroplasts to photooxidative stress caused by paraquat using transgenic tobacco plants expressing catalase from *Escherichia coli*. Plant Cell Physiol 41:311–320

Özer B, Akardere E, Çelem EB, Önal S (2010) Three-phase partitioning as a rapid and efficient method for purification of invertase from tomato. Biochem Eng J 50:110–115

Rahnama H, Ebrahimzadeh H (2005) The effect of NaCl on antioxidant enzyme activities in potato seedlings. Biol Plantarum 49:93–97

Rojas-Beltran JA, Dejaeghere F, Abd Alla Kotb M, Du Jardin P (2000) Expression and activity of antioxidant enzymes during potato tuber dormancy. Pot Res 43:383–393

Romero AP, Alarcón A, Valbuena RI, Galeano CH (2017) Physiological assessment of water stress in potato using spectral information. Front Plant Sci 8:1608

Sarkar D (2008) The signal transduction pathways controlling in planta tuberization in potato: an emerging synthesis. Plant Cell Rep 27:1–8

Saxena L, Iyer BK, Ananthanarayan L (2007) Three phase partitioning as a novel method for purification of ragi (*Eleusine coracana*) bifunctional amylase/protease inhibitor. Process Biochem 42:491–495

Scandalios JG, Guan L, Polidoros AN (1997) Catalases in plants: gene structure, properties, regulation, and expression. In: Scandalios JG (ed), Oxidative stress and the molecular biology of antioxidant defenses. Cold Spring Harbor Liboratory Press pp 343–406

Schägger H, Jagow GV (1991) Blue native electrophoresis for isolation of membrane protein complexes in enzymatically active form. Anal Biochem 199:223–231

Spychalla JP, Desborough SL (1990) Superoxide dismutase, catalase, and α-tocopherol content of stored potato tubers. Plant Physiol 94:1214–1218

Su Y, Guo J, Ling H, Chen S, Wang S, Xu L, Allan AC, Que Y (2014) Isolation of a novel peroxisomal catalase gene from sugarcane, which is responsive to biotic and abiotic stresses. PLoS ONE 9:e84426. https://doi.org/10.1371/journal.pone.0084426

Tan KH, Lovrien R (1972) Enzymology in aqueous-organic cosolvent binary mixtures. J Biol Chem 247:3278–3285

Willekens H, Langebartels C, Tire C, Montagu MV, Inzé D, Camp WV (1994) Differential expression of catalase genes in *Nicotiana plumbaginifolia* (L.). Proc Natl Acad Sci USA 91:10450–10454

Willekens H, Chamnongpol S, Davey M, Schraudner M, Langebartels C, Montagu MV, Inzé D, Camp WV (1997) Catalase is a sink for H_2O_2 and is indispensable for stress defence in C-3 plants. EMBO J 16:4806–4816

Yan J-K, Wang Y-Y, Qiu W-Y, Ma H, Wang Z-B, Wu J-Y (2017) Three-phase partitioning as an elegant and versatile platform applied to non-chromatographic bioseparation processes. Crit Rev Food Sci Nutri. https://doi.org/10.1080/10408398.2017.1327418

Zamocky M, Furtmüller PG, Obinger C (2008) Evolution of catalases from bacteria to humans. Antioxid Redox Signal 10:1527–1548

Zimmermann P, Heinlein C, Orendi G, Zentgraf U (2006) Senescence-specific regulation of catalases in *Arabidopsis thaliana* (L.) Heynh. Plant Cell Environ 29:1049–1060

Publisher's Note Springer Nature remains neutral with regard to jurisdictional claims in published maps and institutional affiliations.